BOUNDARY-LAYER STABILITY ANALYSIS FOR A YAWED CONE AND A SWEPT, SLOTTED AIRFOIL

Thesis

by

JAY M. PATEL

Submitted to the Graduate and Professional School of
Texas A&M University
in partial fulfillment of the requirements for the degree of

MASTER OF SCIENCE

Co-Chairs of Committee,	Koen J. Groot
	Helen L. Reed
Committee Members,	Prabir Daripa
Head of Department,	Ivett Leyva

August 2022

Major Subject: Aerospace Engineering

ABSTRACT

Current numerical methods solving the Navier-Stokes equations such as, the subject matter of this project, the parabolized stability equations (PSE) have proven to be costly for industrial applications. In particular, improving upon cost effective numerical methods for hypersonic regimes has been a topic of interest. The Hypersonic Vehicle Simulation Institute aims to study the process of transition for hypersonic boundary layers by extending the amplification factor transport (AFT) model to these flow regimes. The work done in this paper will provide developers of the AFT model with accurate stability results calculated by LPSE for comparison and relate the growth rates of the instability to energy contributions within the system.

The geometry chosen for this study is a straight cone with an angle of incidence. The crossflow instability is identified with a max N-factor of 14.5 at an azimuthal angle of 148.6° and a wavenumber of 81.9. In its current form, the AFT model only reports instability near the leeward plane and does not capture the crossflow mechanisms in the regions reported by LPSE.

An energy-perturbation budget analysis shows large Reynolds-flux production counteracted by pressure work and dissipation for highly unstable conditions. The balancing of these energy production values results in the growth rate. The largest energy contribution factors are the Reynolds heat-flux and the temperature-perturbation dissipation. Using these two terms, the neutral point is approximated with low relative error compared to the growth rate neutral point ($\leq 10\%$ for regions of interest) as well as large linear correlation to the development of the growth rate in the streamwise direction.

Another topic of interest for aerospace engineers is the reduction of drag on commercial aircraft. The National Aeronautics and Space Administration (NASA) University Leadership Initiative (ULI) has developed an airfoil with the slotted-natural-laminar-flow concept (SNLF). Stability characteristics for the bottom side of this airfoil, which includes the slotted region, are generated using linear (LPSE) and nonlinear (NPSE) parabolized stability equations. The development of instability mechanisms described for portions upstream of the slot, near the slot entrance, and within

the slotted region of the airfoil for varying sweep angles $0^\circ \leq \Lambda \leq 35^\circ$.

The instability mechanisms are defined as the crossflow instability for swept cases and the Görtler mechanism in the concave region of the slot. Using LPSE, a large Görtler amplification is found in the slot ($N = 13$) for the steady and unsteady equivalent of the disturbance. This amplification is stabilized by the presence of crossflow within the slot. At $\Lambda = 35^\circ$, the N-factor is approximately 8.5 and 7.5 for the unsteady and steady disturbance, respectively.

For large sweep angles ($\Lambda \geq 20^\circ$) a destabilized crossflow instability is present in the upstream portion of the airfoil. This amplification is quickly dampened by the convex surface curvature resulting in a stable flow at the slot entrance indicating little to no upstream influence of the crossflow instability.

A nonlinear study indicates the highly distorted Görtler instability within the vicinity of the slot. The largest initial amplitude allowing convergence is $A_{(0,1)} = 10^{-2}$. The neutral point for the nonlinear case remains consistently at a location slightly downstream of the slot entrance regardless of sweep. A more pronounced sweep angle results in nonlinear saturation occurring further downstream. The crossflow velocity component causes a smearing effect primarily in regions where the velocity has upwelled further into the freestream.

ACKNOWLEDGMENTS

The work in this thesis would not be possible without the advisory of Dr. Koen Groot. Through his guidance and support I have developed a stronger passion for learning and grown immensely in a professional and personal capacity. My experience as a graduate student was enhanced greatly from working with Dr. Groot. In addition, I would like to thank Dr. Helen Reed and Dr. Prabir Daripa for their continued assistance throughout my career as a graduate student. I am ever grateful for the opportunity to work with professors that have such a wealth of experience and knowledge.

I am thankful to have worked with colleagues who foster an environment built around learning. I'd like to thank Ethan for the amazing guidance both with research and life. I could not have asked for better company to have during those late night crunch sessions while working on this thesis. I would like to thank Andrew for always laughing at my jokes, even the bad ones of which there were many. I would also like to thank Madeline for being someone who I can talk with about sports and acronyms. Thank you as well to Mikkel Hatem, Travis Kocian, Daniel Mullen, Sam Padge, and Jeppesen Feliciano for the great conversations and support. I will greatly cherish the time I have spent with these people and am privileged to call them my friends.

I am very fortunate to have Gail Rowe and Kendall Lackey provide administrative support. Gail has been instrumental in helping me keep up with deadlines and providing support behind the scenes.

Finally, I would like to thank my parents and my brother. Their endless support has pushed me to greater heights.

CONTRIBUTORS AND FUNDING SOURCES

Contributors

This work was supported by a thesis committee consisting of my advisor Dr. Koen Groot and co-advisor Dr. Helen Reed of the Department of Aerospace Engineering and Dr. Prabir Daripa of the Department of Mathematics.

The OVERFLOW solutions in Chapter 3 were provided by Caleb Saiyasak and Dr. James Coder of the University of Tennessee, Knoxville. The MSES solutions in Chapter 4 were also provided by Dr. James Coder. This work was also aided by my colleagues Dr. Koen Groot, Dr. Helen Reed, and Ethan Beyak.

The analyses depicted in Sections 3.3 and 4.3.1 were conducted in part by Dr. Koen Groot of the Department of Aerospace Engineering and were published in 2021 to the American Institute of Aeronautics and Astronautics. The equations found in appendix C were provided by Ethan Beyak.

All other work conducted for the thesis was completed by the student independently.

Funding Sources

Graduate study was supported as a graduate research assistant at Texas A&M University. The work presented in this thesis is supported in part by the DoD HPCMP Hypersonic Vehicle Simulation Institute under agreement FA7000-20-2-0003.

Additionally, the work is supported by the National Aeronautics and Space Administration (NASA) under the agreement award number NNX17AJ95A. The work was performed under the University Leadership Initiative (ULI) at Texas A&M University as a subcontract to the University of Tennessee, Knoxville Advanced Aerodynamic Design Center for Ultra-Efficient Commercial Vehicles.

NOMENCLATURE

VARIABLES

α	Streamwise wavenumber in the leading-edge-orthogonal direction
β	Spanwise wavenumber in the leading-edge-parallel direction
β_H	Hartree Parameter
γ	Ratio of specific heats
δ	Boundary-layer height
δ_r	Blasius length
ϵ	Small factor
θ	Azimuthal angle
κ	Coefficient of thermal conductivity
λ_v	Second viscosity coefficient
Λ	Sweep angle
μ	Dynamic viscosity coefficient
ρ	Density
ϕ	Primitive variable vector (u, v, w, T, ρ)
Φ	Norm value
ψ	Wave angle
∇	Divergence operator (s, y, z)
Ψ	Dissipation
ω	Angular frequency
χ	Slowly varying streamwise coordinate

a	Speed of sound
A	Amplitude
$\mathcal{A}$, $\mathcal{B}$, $\mathcal{C}$, and $\mathcal{D}$	Coefficient matrices (5×5) present in the disturbance equations
c	Leading-edge-normal chord length
c_p	Specific heat at constant pressure
c_v	Specific heat at constant volume
c_{ph}	Phase speed
D	Viscous energy terms
Ec	Eckert number
f	Regular frequency or period
G	Görtler number
h_1, h_2, h_3	Curvature scales in the (s, y, z) directions, respectively
H	Shape factor
k	Wavenumber multiple factor
L	Reference length
$\mathcal{L}$	Linear disturbance matrix
M	Mach number
n	Frequency multiple factor
N	Amplification factor
$\mathcal{N}$	Nonlinear forcing vector
p	Pressure
P	Pressure work
Pr	Prandtl number
Q	Resultant velocity
R	Radius of curvature

R	Reynolds-flux term
R_g	Specific gas constant
Re	Reynolds number
s, y, z	Local Cartesian coordinate system
S	Sutherland's temperature
t	Time variable
T	Temperature
u, v, w	Velocity components in (s, y, z) directions, respectively
V	Velocity vector (u, v, w)
x, Y, Z	Global Cartesian coordinate system

ACRONYMS

AOA	Angle of attack
CF	Crossflow
CST	Computational Stability and Transition
DEKAF	Digits by Ethan, Koen, Alex, and Fernando
EPIC	Euonymous Parabolized Instability Code
HVSI	Hypersonic Vehicle Simulation Institute
IATA	International Air Transport Association
LPSE	Linear parabolized stability equations
LST	Linear stability theory
MFD	Mean flow distortion
NASA	National Aeronautics and Space Administration
NLF	Natural-laminar-flow
NPSE	Nonlinear parabolized stability equations
PSE	Parabolized stability equations

SCF	Stationary crossflow
SNLF	Slotted, natural-laminar-flow
TCF	Traveling crossflow
TS	Tollmien-Schlichting
TAMU	Texas A&M University
ULI	University Leadership Initiative
UTK	University of Tennessee, Knoxville

SUBSCRIPTS

e	Edge value
i	Imaginary value
∞	Freestream quantity
(n, k)	Fourier mode
r	Real value
w	Pertaining to values at the wall

SUPERSCRIPTS

$*$	Dimensional quantity
$\dagger$	Complex conjugate
T	Matrix transpose
quad	Quadratic
cub	Cubic
(1), (2),...	Arbitrary Fourier mode number

ACCENTS

$\wedge$	Shape-function quantity
$-$	Basic state quantity

$'$	Disturbance quantity
$\sim$	Dummy variable
$\rightarrow$	Vector

TABLE OF CONTENTS

Page

ABSTRACT ii

ACKNOWLEDGMENTS iv

CONTRIBUTORS AND FUNDING SOURCES v

NOMENCLATURE vi

TABLE OF CONTENTS xi

LIST OF FIGURES xiii

1. INTRODUCTION 2

    1.1 Background 2
    1.2 Motivation 2
        1.2.1 High-Speed Project: HVSI 3
        1.2.2 Low-Speed Project: ULI 3
    1.3 Instability Mechanisms 4
        1.3.1 Crossflow 4
        1.3.2 Görtler 5

2. METHODOLOGY 6

    2.1 Governing Equations 6
    2.2 Non-Dimensionalization 7
    2.3 Stability Formulation 8
        2.3.1 Linear Stability Theory 9
        2.3.2 Linear Parabolized Stability Equations 10
        2.3.3 Nonlinear Parabolized Stability Equations 12
    2.4 Stability Solver 14
    2.5 Budget Analysis 16

3. test 20

    3.1 Geometry and Grid Structure 20
    3.2 Base-Flow 21
    3.3 Stability Results 22
    3.4 Budget Analysis 24
        3.4.1 Total-Perturbation Energy 24

3.4.2 Conservation of Energy Perturbation 28
3.4.3 Crossflow-Velocity-Perturbation Energy 29

4. test 33

4.1 Base-Flow 33
4.2 Boundary-Layer Properties 34
4.3 Stability Results 38
4.3.1 Linear Stability Results 38
4.3.2 NPSE Results 44

5. CONCLUSION 52

5.1 Cone Configuration 52
5.2 Swept-wing Configuration 53

REFERENCES 56

APPENDIX A. BUDGET ANALYSIS STABILITY EQUATIONS 60

A.1 s - Momentum 61
A.2 y - Momentum 62
A.3 z - Momentum 64
A.4 Conservation of Energy 65
A.5 Conservation of Mass Continuity 67

APPENDIX B. MOST-AMPLIFIED SWEPT WING CHARACTERISTICS 68

APPENDIX C. PARABOLIZED STABILITY EQUATIONS 71

C.1 s - Momentum 72
C.2 y - Momentum 74
C.3 z - Momentum 76
C.4 Conservation of Energy 77
C.5 Conservation of Mass Continuity 79
C.6 Quadratic Nonlinear Forcing Vector 80
C.7 Cubic Nonlinear Forcing Vector 91

LIST OF FIGURES

FIGURE Page

2.1 Visual representation of (n, k) modes. Blue dots represent modes needing to be solved for, yellow stars represent modes that can be found by conjugating known modes, and green triangles represent modes that can be found by applying spanwise symmetry conditions. (Left) Non-symmetric flow field. (Right) Spanwise symmetric flow field. 13

2.2 Individual contributions to the total energy normalization as seen on the most amplified vortex path and wavenumber. 19

3.1 test 21

3.2 test 23

3.3 test 23

3.4 test 24

3.5 Energy-budget decomposition for the total-perturbation equation, see Eq. 2.37. Black: $-\alpha_i$ as integrated along the streamwise direction representing an approximate N-factor. Red: Reynolds-flux energy production terms, R. Green: pressure work terms, P. Blue: viscous terms, D. (Left) Integrated growth at the base of the geometry with varying wavenumbers choosing the vortex path supporting the most amplified solution. (Right) Integrated growth for each vortex path at the base of the cone choosing the most amplified wavenumber. 25

3.6 Solid black line: $-\alpha_i$ as solved with LPSE. Solid grey line: approximate growth rate $-\alpha_{i,\mathrm{approx}}$ defined by sum of terms within threshold. Red line: Reynolds-flux energy production terms. Blue line: viscous terms with the largest transmission being defined with individual curves. Green line: pressure terms (combined into a single curve). The plots represent dominant terms of the total-perturbation energy which allow $-\alpha_{i,\mathrm{approx}}$ to be within $\pm 20\%$ (a), $\pm 10\%$ (b), and $\pm 5\%$ (c) of $-\alpha_i$. 27

3.7 (Left) Relative error (%) between the $-\alpha_i$ neutral point and the approximate neutral point as found by $\hat{T}^{\dagger}\left(\mathrm{R}_{\hat{T},\max} + \mathrm{D}_{\hat{T},\max}\right)$. (Right) Linear correlation coefficient between $-\alpha_i$ and $\mathrm{R}_{\hat{T},\max} + \mathrm{D}_{\hat{T},\max}$ along x. The θ-m plane consists of all azimuthal paths and each wavenumber along those paths. 28

3.8 Energy-budget decomposition for the conservation of energy disturbance equation, Eq. 3.3. Black: $-\alpha_i$ as integrated along the streamwise direction representing an approximate N-factor. Red: Reynolds-flux energy production terms, $\mathrm{R}_{\hat{T}}$. Green: pressure work terms, $\mathrm{P}_{\hat{T}}$. Blue: viscous terms, $\mathrm{D}_{\hat{T}}$. (Left) Integrated growth at the base of the geometry with varying wavenumbers choosing the vortex path supporting the most amplified solution. (Right) Integrated growth for each vortex path at the base of the cone choosing the most amplified wavenumber. 29

3.9 Solid black line: $-\alpha_i$ as solved with LPSE. Solid grey line: approximate growth rate $-\alpha_{i,\mathrm{approx}}$ defined by sum of terms within threshold. Red line: Reynolds-flux energy production terms. Blue line: viscous terms with the largest transmission being defined with individual curves. Green line: pressure terms (combined into a single curve). The plots represent dominant terms of the conservation of energy disturbance which allow $-\alpha_{i,\mathrm{approx}}$ to be within $\pm 20\%$ (a), $\pm 10\%$ (b), and $\pm 5\%$ (c) of $-\alpha_i$. 30

3.10 Energy-budget decomposition for the conservation of energy disturbance equation, Eq. 3.3. Black: $-\alpha_i$ as integrated along the streamwise direction representing an approximate N-factor. Red: Reynolds-flux energy production terms, $\mathrm{R}_{\hat{w}}$. Green: pressure work terms, $\mathrm{P}_{\hat{w}}$. Blue: viscous terms, $\mathrm{D}_{\hat{w}}$. (Left) Integrated growth at the base of the geometry with varying wavenumbers choosing the vortex path supporting the most amplified solution. (Right) Integrated growth for each vortex path at the base of the cone choosing the most amplified wavenumber. 31

3.11 Solid black line: $-\alpha_i$ as solved with LPSE. Solid grey line: approximate growth rate $-\alpha_{i,\mathrm{approx}}$ defined by sum of terms within threshold. Red line: Reynolds-flux energy production terms. Blue line: viscous terms with the largest transmission being defined with individual curves. Green line: pressure terms (combined into a single curve). The plots represent dominant terms of the spanwise-perturbation energy which allow $-\alpha_{i,\mathrm{approx}}$ to be within $\pm 20\%$ (a), $\pm 10\%$ (b), and $\pm 5\%$ (c) of $-\alpha_i$. 32

4.1 (a) The X207.LS geometry plotted with the chord along the x-axis (blue line). The slot entrance is defined with a red dot on the x-axis. (b) Pressure distributions for increasing angles of attack are shown in color for the bottom side of the fore-element for a 0° sweep angle. The gray curves represent the pressure distribution for the top side of the same element as well as the aft element [2]. 35

4.2 Streamwise development of boundary layer parameters for angle of attack 2.25°. Dashed vertical line indicates the slot entrance defined by $1/R = 0$ (red star) [2]..... 36

4.3 Crossflow parameters for $\Lambda = 5^\circ$. (Top left) Pressure coefficient. (Bottom left) Wall-normal location of the crossflow velocity inflection point. (Right) Crossflow-velocity profiles at increasing x/c stations. 37

4.4 N-factor envelopes (steady/unsteady content) versus chordwise position for increasing sweep angles. Full-chord approach initializes LPSE at the attachment line and slot-only approach initializes just upstream the slot entrance. The full-chord envelopes in the slot correspond to *unadjusted neutral points* at the entrance of the slot [2]. 42

4.5 N-factor envelopes (steady/unsteady content) versus chordwise position for increasing sweep angles. Full-chord approach initializes LPSE at the attachment line and slot-only approach initializes just upstream the slot entrance. The full-chord envelopes in the slot correspond to *updated neutral points* close to the slot entrance [2]. 43

4.6 Nonlinear disturbance amplitude for u' and associated harmonic modes and linear amplitude of fundamental mode. Solid line indicates the entrance of the slot. The dashed lines indicate: (I) the neutral point of the fundamental mode, (II) the saturation point, and (III) the location at which MFD overtakes the $(0, 1)$ mode. Sweeps 0° to 15° are presented. 45

4.7 Nonlinear disturbance amplitude for u' and associated harmonic modes and linear amplitude of fundamental mode. Solid line indicates the entrance of the slot. The dashed lines indicate: (I) the neutral point of the fundamental mode, (II) the saturation point, and (III) the location at which MFD overtakes the $(0, 1)$ mode. Sweeps 20° to 35° are presented. 46

4.8 Chordwise locations of the fundamental mode neutral point, the saturation location, and the location at which the MFD overtakes the fundamental mode for varying sweep. 47

4.9 Chordwise locations of the fundamental mode neutral point, the saturation location, and the location at which the MFD overtakes the fundamental mode for varying sweep. 48

4.10 Development of the Görtler instability within the slot as seen by the nondimensional u velocity (m/s) for $0^\circ \leq \Lambda \leq 15^\circ$. The furthest right figure indicates laminar flow at the neutral point to provide reference. The second, third and fourth figures represent x/c points at x_{sat}, x_{mfd} and the end of the domain. 50

4.11 Development of the Görtler instability within the slot as seen by the nondimensional u velocity (m/s) for $20^\circ \leq \Lambda \leq 35^\circ$. The furthest right figure indicates laminar flow at the neutral point to provide reference. The second, third and fourth figures represent x/c points at x_{sat}, x_{mfd} and the end of the domain. 51

1. INTRODUCTION

1.1 Background

Turbulent flow has several detrimental effects in terms of performance. For example, in commercial aircraft it contributes a significant portion of drag, and for re-entry vehicles it causes a high thermal loading. For this reason, laminar-to-turbulent transition has been a topic of great importance to aerospace engineers. When a laminar flow experiences a disturbance, an instability mechanism can cause it to grow. If the disturbance has a large enough amplitude, it will break down to turbulence. Understanding these instability mechanisms and how they grow or decay allows engineers to better predict transition and further reduce turbulent flow.

The equations that, ultimately, govern disturbance amplification are the Navier-Stokes equations. Several numerical methods have been developed to solve these equations. The highest fidelity method is Direct Numerical Simulation (DNS). For that reason, it is the most costly method in terms of computational resources. For industrial applications, the Reynolds-Averaged Navier-Stokes (RANS) model is commonly practiced for its lower computational-resource requirements. In contrast to DNS, RANS has a lower fidelity because turbulence is modeled instead of resolved, i.e. resolving small, turbulent eddies. For the purpose of this proposal, stability methods such as Linear Stability Theory (LST, [3, 4]) and Parabolized Stability Equations (PSE, [5, 6]) will be employed. These methods impose assumptions that exploit geometrical symmetries corresponding to the specific boundary-layer flow case (i.e. the flow over an airfoil or a cone at an angle of incidence) to simplify the Navier-Stokes equations. At a highly reduced cost compared to DNS, stability methods maintain a relatively high level of fidelity, especially in regard to the perturbation dynamics.

1.2 Motivation

This study focuses on the application of PSE on two separate projects: one at high and the other at low speed. Both projects have industrial applications and understanding how disturbances

grow in each case will provide insight to understanding boundary-layer transition.

1.2.1 High-Speed Project: HVSI

As mentioned, for hypersonic applications, e.g. re-entry vehicles, surface heating is of large concern as the material can be damaged and life cycles can be reduced. Transition to turbulence of the boundary layer on this type of vehicle can be a source of larger heat transfers so understanding the instability mechanisms at hypersonic speeds has great value. The U.S. Air Force Academy (USAFA) established the Hypersonic Vehicle Simulation Institute (HVSI) to study boundary-layer transition on high speed vehicles. One objective for the HVSI is to expand on the Amplification Factor Transport (AFT, [7, 8, 9]) model which can run in parallel to a computational fluid dynamics code and account for instabilities by switching on a turbulence model when applicable. This model is being developed by the University of Tennessee, Knoxville (UTK) and is compared against PSE results provided by Texas A&M University (TAMU). A geometry that will be considered for this specific effort is a straight cone, yawed at an angle. The PSE analysis will focus on the development of the crossflow instability. Further details on this instability mechanism will be specified later. To further assist in the overarching goal of extending the existing AFT model, an accurate depiction of instability growth is necessary. To this extent, an energy-budget-analysis tool is developed. This tool will decompose the perturbed flow into the dominant sources of energy to better understand what parameters are of greater importance. These sources can then help influence the AFT model by providing a guideline for the parameters that contribute to the instability mechanisms that cause transition.

1.2.2 Low-Speed Project: ULI

In the NASA Aeronautics Strategic Implementation Plan, NASA emphasizes the goals of the International Air Transport Association (IATA) to impose reductions in net emissions for subsonic transport aircraft. These goals include a 1.5% average annual efficiency improvement between 2010 and 2020, a reduction of 50% in net emissions by 2050 as compared to 2005, and carbon neutral growth from 2020 onward. Our contribution to this overall goal is led by the University of

Tennessee, Knoxville through the NASA University Leadership Initiative (ULI) project. The ULI project established the Advanced Aerodynamic Design Center for Ultra-Efficient Commercial Vehicles to develop more aerodynamic wings for commercial aircraft. One such wing in development is a Slotted, Natural-Laminar-Flow (SNFL, [10, 11]) airfoil which operates in a low-speed setting (up to transonic speeds). By using the Natural-Laminar-Flow concept, designers can optimize airfoil shapes to minimize transition-induced-drag. The airfoil design imposes a favorable pressure gradient over a large percentage of the chord and the addition of the slot furthers that extent. The favorable pressure gradient will stabilize the Tollmien-Schlichting (TS) instability however, can amplify crossflow perturbation development [12]. The concave region within the slot will also amplify the Görtler mechanism [13, 14, 15]. The crossflow and Görtler mechanisms play a key role in the development of transition and will be studied in detail for this proposal. In particular we study 1.) which sweep angle is permissible before the crossflow instability dominates the transition process and 2.) the amplification of Görtler disturbances and the effect of sweep thereon in order to identify their potential role in the transition process.

1.3 Instability Mechanisms

1.3.1 Crossflow

The crossflow instability can be a dominant factor in three-dimensional flows experiencing a crossflow velocity such as that over cones at non-zero angle of incidence (non-zero yaw) and swept wings. This instability can grow when surface streamlines of the inviscid flow are curved by non-zero pressure gradients. The bending of the streamline causes an imbalance in forces resulting in a perpendicular velocity component relative to the local inviscid streamline. This velocity component is called crossflow. The crossflow velocity must be zero at the wall and approach zero in the freestream. Therefore, the profile of this velocity component should display an inflection point somewhere off of the wall. This inflection point is the source for an inviscid instability. If the disturbance that this instability causes grows to a large enough amplitude, *co*-rotating vortices can develop and lead to turbulent breakdown [16, 17]. These vortices typically have a characteristic

spanwise wavelength of 4 times the boundary-layer thickness [18]. Crossflow disturbances can be either stationary, corresponding to a zero frequency and a non-zero spanwise wavenumber, or traveling with both a non-zero frequency and spanwise wavenumber. For the cases presented in this paper, the crossflow mechanism is destabilized by a strong pressure gradient and larger sweep angles. In order to counteract this instability, a convex surface curvature can be used [19, 20].

1.3.2 Görtler

The Görtler instability is a centrifugal instability that dominates on concave walls such as the slotted region of the SNLF airfoil or turbine-compressor blades in an engine. The Görtler instability grows from the satisfaction of the Rayleigh circulation criterion. This simple criterion dictates that for a geometry with radius, r, and a tangential velocity, V, if $\frac{d(rV)^2}{dr} < 0$, then there shall exist an inviscid axis-symmetric instability. For the viscous flow over a concave region, the tangential velocity is zero at the wall and increases toward the freestream. Thereby, the Rayleigh circulation criterion is automatically satisfied. This instability mechanism causes disturbances to grow and develop into *counter*-rotating vortices with a characteristic spanwise wavelength of approximately one boundary-layer thickness [18]. Saric [13] provides a qualitative study on the development of this mechanism in the streamwise direction and Floryan [21] provides an in depth review on experiments studying the Görtler vortices. Many numerical simulations have studied this mechanism as well [22, 14].

2. METHODOLOGY

2.1 Governing Equations

The dimensional equations governing the physics of the flow will be presented in the form of mass continuity, conservation of momentum, and conservation of energy in enthalpy form. The equations govern a calorically perfect gas that is compressible and cast in a Cartesian coordinate system. Per Stokes' Theorem, the bulk viscosity is $\lambda_v = -\frac{2}{3}\mu$ and the second viscosity is ignored.

$$\frac{\partial \rho^*}{\partial t^*} + \rho^* \frac{\partial u^*}{\partial s^*} + \rho^* \frac{\partial v^*}{\partial y^*} + \rho^* \frac{\partial z^*}{\partial w^*} = 0 \tag{2.1}$$

$$\begin{aligned} \rho^* \left[\frac{\partial u^*}{\partial t^*} + u^* \frac{\partial u^*}{\partial s^*} + v^* \frac{\partial u^*}{\partial y^*} + w^* \frac{\partial u^*}{\partial z^*} \right] = \frac{\partial}{\partial s^*} \left[\mu^* \frac{\partial u^*}{\partial s^*} + \mu^* \frac{\partial u^*}{\partial s^*} + \lambda_v^* \nabla^* \cdot V^* - p^* \right] + \\ \frac{\partial}{\partial y^*} \left[\mu^* \frac{\partial u^*}{\partial y^*} + \mu^* \frac{\partial v^*}{\partial s^*} \right] + \frac{\partial}{\partial z^*} \left[\mu^* \frac{\partial u^*}{\partial z^*} + \mu^* \frac{\partial w^*}{\partial s^*} \right] \end{aligned} \tag{2.2}$$

$$\begin{aligned} \rho^* \left[\frac{\partial v^*}{\partial t^*} + u^* \frac{\partial v^*}{\partial s^*} + v^* \frac{\partial v^*}{\partial y^*} + w^* \frac{\partial v^*}{\partial z^*} \right] = \frac{\partial}{\partial y^*} \left[\mu^* \frac{\partial v^*}{\partial y^*} + \mu^* \frac{\partial v^*}{\partial y^*} + \lambda_v^* \nabla^* \cdot V^* - p^* \right] + \\ \frac{\partial}{\partial z^*} \left[\mu^* \frac{\partial v^*}{\partial z^*} + \mu^* \frac{\partial w^*}{\partial y^*} \right] + \frac{\partial}{\partial s^*} \left[\mu^* \frac{\partial v^*}{\partial s^*} + \mu^* \frac{\partial u^*}{\partial y^*} \right] \end{aligned} \tag{2.3}$$

$$\begin{aligned} \rho^* \left[\frac{\partial w^*}{\partial t^*} + u^* \frac{\partial w^*}{\partial s^*} + v^* \frac{\partial w^*}{\partial y^*} + w^* \frac{\partial w^*}{\partial z^*} \right] = \frac{\partial}{\partial z^*} \left[\mu^* \frac{\partial w^*}{\partial z^*} + \mu^* \frac{\partial w^*}{\partial z^*} + \lambda_v^* \nabla^* \cdot V^* - p^* \right] + \\ \frac{\partial}{\partial s^*} \left[\mu^* \frac{\partial w^*}{\partial s^*} + \mu^* \frac{\partial u^*}{\partial z^*} \right] + \frac{\partial}{\partial y^*} \left[\mu^* \frac{\partial w^*}{\partial y^*} + \mu^* \frac{\partial v^*}{\partial z^*} \right] \end{aligned} \tag{2.4}$$

$$\rho^* c_p^* \left[\frac{\partial T^*}{\partial t^*} + (V^* \cdot \nabla^*) T^* \right] = \nabla^* \cdot (\kappa^* \nabla^* T^*) + \frac{\partial p^*}{\partial t^*} + (V^* \cdot \nabla^*) \, p^* + \Psi^* \tag{2.5}$$

The coordinate system, s, y, and z represent the streamwise, wall-normal, and spanwise directions respectively and V is the velocity vector in each direction. The following constitutive relationships

and state equation will aid in defining the remaining variables for the Navier-Stokes equations [23].

$$p = \rho R_g T; \quad c_p = \frac{\gamma R_g}{\gamma - 1}; \quad \mu = \mu_{\text{ref}} \left(\frac{T}{T_{\text{ref}}} \right)^{3/2} \frac{T_{\text{ref}} + S}{T + S}; \tag{2.6}$$

2.2 Non-Dimensionalization

To non-dimensionalize the governing equations, reference values corresponding to the wall-normal edge value is used for the state variables and a reference length L is used for the length quantities.

$$\begin{gathered} s^* = Ls; \quad y^* = Ly; \quad z^* = Lz; \quad \nabla^* = \frac{\nabla}{L} \quad t^* = \frac{L}{u_e} t \\ u^* = u_e u; \quad v^* = u_e v; \quad w^* = u_e w; \quad T^* = T_e T; \quad \rho^* = \rho_e \rho; \quad p^* = \rho_e u_e^2 p \\ \mu^* = \mu_e \mu; \quad \kappa^* = \kappa_e \kappa; \quad c_p^* = c_{p_e}; \quad c_v^* = c_{v_e} \end{gathered} \tag{2.7}$$

To represent the governing equations in terms of the primitive variables, ϕ, the equation of state, $p^* = \rho^* R_g^* T^*$, is substituted for the pressure terms. The non-dimensional gas constant is formulated by substituting dimensional and reference values as such:

$$R_g = \frac{p}{\rho T} = \frac{p^*}{\rho^* T^*} \frac{\rho_e T_e}{\rho_e u_e^2} = \frac{\gamma R_g^* T_e}{\gamma u_e^2} = \frac{1}{\gamma \mathrm{M}_e^2} \tag{2.8}$$

This gas constant will help define the equation of state in a non-dimensional form.

$$p = \frac{\rho T}{\gamma \mathrm{M}_e^2} \tag{2.9}$$

The following non-dimensional parameters are defined using the reference parameters.

$$\mathrm{Re}_e = \frac{\rho_e u_e L}{\mu_e}; \quad \mathrm{Pr}_e = \frac{\mu_e c_{p_e}}{\kappa_e}; \quad \mathrm{Ec}_e = \frac{u_e^2}{c_{p_e} T_e} \tag{2.10}$$

Substituting the relations from Eqs. 2.7 - 2.10 into the governing Eqs. 2.1 - 2.5 casts the governing equations into a non-dimensional form for use in stability formulation.

$$\frac{\partial \rho}{\partial t} + \rho \frac{\partial u}{\partial s} + \rho \frac{\partial v}{\partial y} + \rho \frac{\partial z}{\partial w} = 0 \tag{2.11}$$

$$\rho \left[\frac{\partial V}{\partial t} + (V \cdot \nabla) V \right] = -\nabla p + \nabla \left[\frac{\lambda_v}{\mathrm{Re}_e} (\nabla \cdot V) \right] + \nabla \left[\frac{\mu}{\mathrm{Re}_e} \left(\nabla V + (\nabla V)^T \right) \right] \tag{2.12}$$

$$\rho \left[\frac{\partial T}{\partial t} + (V \cdot \nabla) T \right] = \frac{1}{\mathrm{Pr}_e \mathrm{Re}_e} \nabla \cdot (\kappa \nabla T) + \mathrm{Ec}_e \left[\frac{\partial p}{\partial t} + (V \cdot \nabla) p \right] + \frac{\mathrm{Ec}_e}{\mathrm{Re}_e} \Psi \tag{2.13}$$

2.3 Stability Formulation

A system of stability equations can be derived from the governing equations. The vector of total flow variables will be depicted as $\phi = [u, v, w, T, \rho]^T$. By decomposing the flow variables into a steady, laminar base-flow, $\bar{\phi}$, with an imposed disturbance quantity, ϕ', we can accurately represent a disturbed flow.

$$\begin{aligned} \phi(s, y, z, t) &= \overline{\phi}(s, y, z) + \phi'(s, y, z, t) \\ \mu(s, y, z, t) &= \overline{\mu}(T) + \frac{d\mu}{dT} T' \\ \kappa(s, y, z, t) &= \overline{\kappa}(T) + \frac{d\kappa}{dT} T' \\ c_p(s, y, z, t) &= \overline{c}_p(T) + \frac{dc_p}{dT} T' \end{aligned} \tag{2.14}$$

The decomposed flow variables in Eq. 2.14 can then be plugged back into the governing equations, Eq. 2.1-2.5. Since the basic-state quantities found in the disturbance equations must satisfy the governing equations, they can be removed. The disturbances are grouped by their respective derivative which results in the following non-homogeneous, partial differential equation [24].

$$\begin{aligned} \mathcal{A}_1 \frac{\partial^2 \phi'}{\partial s^2} + \mathcal{A}_2 \frac{\partial^2 \phi'}{\partial y^2} + \mathcal{A}_3 \frac{\partial^2 \phi'}{\partial z^2} + \mathcal{B}_1 \frac{\partial^2 \phi'}{\partial s \partial y} + \mathcal{B}_2 \frac{\partial^2 \phi'}{\partial s \partial z} + \mathcal{B}_3 \frac{\partial^2 \phi'}{\partial y \partial z} \\ + \mathcal{C}_o \frac{\partial \phi'}{\partial t} + \mathcal{C}_1 \frac{\partial \phi'}{\partial s} + \mathcal{C}_2 \frac{\partial \phi'}{\partial y} + \mathcal{C}_3 \frac{\partial \phi'}{\partial z} + \mathcal{D} \phi' = \mathcal{N} \end{aligned} \tag{2.15}$$

The rows of the coefficient matrices correspond to each of the governing equations while the column corresponds to each of the flow variables. $\mathcal{N}$ is the forcing vector containing all nonlinear terms not associated with a disturbance derivative.

2.3.1 Linear Stability Theory

Linear Stability Theory (LST) is a widely used stability method that is relatively simple to formulate [3, 4]. LST considers a flow that has no wall-normal velocity component making the flow locally parallel to the surface of the geometry, $\overline{\phi} = \left[\overline{u}(y), 0, \overline{w}(y), \overline{T}(y), \overline{\rho}(y)\right]^T$. A normal-mode can be used as a solution to the LST disturbance model which takes form in Eq. 2.16 as a perturbation ansatz. The disturbance, ϕ', is defined as a slowly varying shape function and a quickly varying wave function. Since the disturbance quantity must be real valued, the complex conjugate is added to the quantity.

$$\phi'(s, y, z, t) = \underbrace{\hat{\phi}(y)}_{\text{shape}} \underbrace{e^{i(\alpha s + \beta z - \omega t)}}_{\text{wave}} + \text{c.c.} \tag{2.16}$$

The components, α and β, represent wavenumbers in the streamwise and spanwise directions respectively while ω is a real-valued frequency which describes the nature of the wave within the solution. For a temporal disturbance analysis, ω_r and ω_i is determined by fixing the values of α and β. For the purposes of this thesis, a spatial disturbance analysis will be performed by fixing the values of ω and β to solve for α. By choosing ω and β to be real-valued, the growth or decay of the disturbance will only be contained in the streamwise direction defined by α_i. Additional relationships are defined to describe the real quantities in the form of a wave angle, ψ, and a phase speed c_{ph}.

$$\psi = \tan^{-1}\left(\frac{\beta_r}{\alpha_r}\right) \quad \text{and} \quad c_{ph} = \frac{\omega}{\sqrt{\alpha_r^2 + \beta_r^2}} \tag{2.17}$$

By considering nonlinear and streamwise varying terms to be negligible and implementing the parallel flow assumptions, Eq. 2.15 can be reduced to a homogeneous, ordinary partial differential equation. Note the coefficient matrices contain only linear terms from the matrices in Eq. 2.15 as indicated by the superscript L. Since the wave function can be divided out of the disturbance, only the shape function remains.

$$\mathcal{A}_2^{LST}\frac{\partial^2\hat{\phi}}{\partial y^2}+\mathcal{B}_2^{LST}\frac{\partial\hat{\phi}}{\partial y}+\mathcal{D}^{LST}\hat{\phi}=0 \tag{2.18}$$

Solving the equation requires a posing the system as an eigenvalue problem. By factoring out the α values from the matrices, a nonlinear equation can be formulated in Eq. 2.19.

$$\left(C_0\alpha^2+C_1\alpha+C_2\right)\hat{\phi}=0 \tag{2.19}$$

Using the Linear Companion Matrix Method [25], the nonlinear system can be linearized by letting the solution be of the form $\hat{\Theta}=\left[\alpha\hat{\Theta},\hat{\Theta}\right]^T$.

$$\mathbf{A}\hat{\Phi}=\alpha\mathbf{B}\hat{\Phi} \tag{2.20}$$

where the matrices are defined as

$$\mathbf{A}=\begin{bmatrix}-C_1 & -C_2\\ I & 0\end{bmatrix},\ \mathbf{B}=\begin{bmatrix}C_0 & 0\\ 0 & I\end{bmatrix} \tag{2.21}$$

2.3.2 Linear Parabolized Stability Equations

Linear Parabolized Stability Equations (LPSE) is another stability analysis tool that considers small variations of the base-flow in the streamwise direction [5, 24, 26]. Similar to LST, the flow is again decomposed into a mean flow and a disturbance quantity. PSE however, does contrast from LST in its ability to handle non-parallel flows. The equations are parabolic in nature along the streamwise coordinate which allows us to march downstream from a given initial condition. The streamwise growth will now depend on the slowly varying scale, $\chi=\epsilon s$, where $\epsilon=Re^{-1}$ [24]. The resulting perturbation ansatz is reflected in Eq. 2.22.

$$\phi'(s,y,z,t)=\underbrace{\hat{\phi}(\chi,y)}_{\text{shape}}\underbrace{\exp\left[i\left(\int\alpha(\chi)d\chi+\beta z-\omega t\right)\right]}_{\text{wave}}+\text{c.c.} \tag{2.22}$$

The exponential growth is absorbed into a rapidly evolving wave function with a slow varying shape function. Again we will substitute this disturbance into the Navier-Stokes equations to result in a system of equations that can be grouped into matrices. These matrices differ from the LST solution and are updated at each marching step. The benefit of using multiple scales in the marching direction can be realized when the substitution of the following terms is performed.

$$\frac{\partial \phi'}{\partial s} = \left(\epsilon \frac{\partial \hat{\phi}}{\partial \chi} + i\epsilon\alpha\hat{\phi} \right) \exp\left[i \left(\int \alpha(\chi) d\chi + \beta z - \omega t \right) \right] \tag{2.23a}$$

$$\frac{\partial^2 \phi'}{\partial s^2} = \left(\epsilon^2 \frac{\partial^2 \hat{\phi}}{\partial \chi^2} + 2i\epsilon\alpha \frac{\partial \hat{\phi}}{\partial \chi} + i\epsilon \frac{\partial \alpha}{\partial \chi}\hat{\phi} - \alpha^2\hat{\phi} \right) \exp\left[i \left(\int \alpha(\chi) d\chi + \beta z - \omega t \right) \right] \tag{2.23b}$$

From the streamwise derivatives seen in Eq. 2.23, the dissipation term highlighted in red can be neglected (i.e., $\epsilon^2 = Re^{-2} << 1$). This permits the second derivatives in the streamwise direction to be eliminated further eliminating elliptic effects on the system. The following partial differential equation in 2.24 reflects this.

$$\mathcal{A}_2^{PSE} \frac{\partial^2 \hat{\phi}}{\partial y^2} + \mathcal{B}_1^{PSE} \frac{\partial \hat{\phi}}{\partial \chi \partial y} + \mathcal{C}_1^{PSE} \frac{\partial \hat{\phi}}{\partial \chi} + \mathcal{C}_2^{PSE} \frac{\partial \hat{\phi}}{\partial y} + \mathcal{D}^{PSE} \hat{\phi} = 0 \tag{2.24}$$

PSE is solved as an initial value problem and for our flow solving configuration, the LST solution is used as the initial condition. The PSE solution is marched downstream and when the matrices are updated, the streamwise wavenumber α is also updated using an auxiliary condition defined in Eq. 2.25.

$$\alpha^{k+1} = \alpha^k - \mathrm{i} \left(\sum_{\hat{\phi} \in \{\hat{u}, \hat{v}, \ldots, \hat{\rho}\}} \int_0^{y_{\max}} \hat{\phi}^\dagger \cdot \frac{\partial \hat{\phi}}{\partial \chi} \, \mathrm{d}y \Big/ \sum_{\hat{\phi} \in \{\hat{u}, \hat{v}, \ldots, \hat{\rho}\}} \int_0^{y_{\max}} |\hat{\phi}|^2 \, \mathrm{d}y \right) \tag{2.25}$$

2.3.3 Nonlinear Parabolized Stability Equations

While LPSE focuses on solving a single spectral "mode", the nonlinear parabolized stability equations (NPSE) will solve multiple "modes". The inclusion of additional modes allows for nonlinear disturbances to be accurately captured. The disturbance is modeled as such:

$$\phi'(s,y,z,t) = \sum_{n=-\infty}^{\infty} \sum_{k=-\infty}^{\infty} \hat{\phi}_{(n,k)}(\chi,y) A_{(n,k)}(s) \exp\left[i\left(k\beta z - n\omega t\right)\right] \tag{2.26}$$

where

$$A_{(n,k)} = \frac{A_{0_{(n,k)}}}{2} \exp\left[i \int \alpha_{(n,k)}(\chi) \mathrm{d}\chi\right] \tag{2.27}$$

Since the disturbance quantity must be real-valued, the complex conjugate can be defined with the following relations. The initial amplitude $A_0(n,k)$ is divided in half and split between the mode and its complex conjugate. Using the relations found in Eq. 2.28 the disturbance parameters for modes $(-n,-k)$ and $(-n,k)$ can be solved for. As such, only about half of the modes need to be calculated to complete a full NPSE simulation.

$$\begin{aligned} \hat{\phi}_{(n,k)} &= \hat{\phi}^{\dagger}_{(-n,-k)} \\ A_{(n,k)} &= A^{\dagger}_{(-n,-k)} \\ \alpha_{(n,k)} &= -\alpha^{\dagger}_{(-n,-k)} \end{aligned} \tag{2.28}$$

Additional symmetry conditions can be applied to the system if the laminar flow field is symmetric about the spanwise coordinate. With the additional conditions found in Eq. 2.29, fewer calculations will need to be made as only a fraction of the (n,k) mode space is solved for. A visual representation of the modes and their relations can be found in Fig. 2.1.

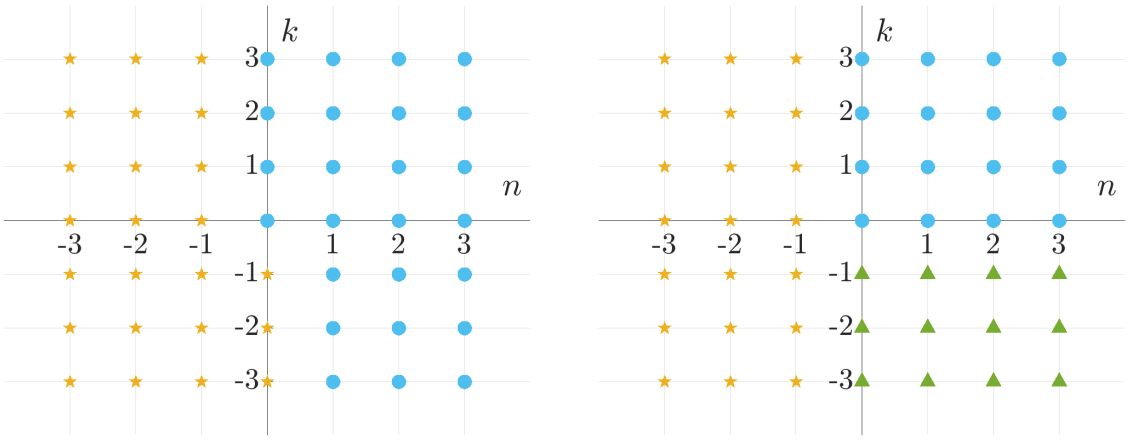

Figure 2.1: Visual representation of (n, k) modes. Blue dots represent modes needing to be solved for, yellow stars represent modes that can be found by conjugating known modes, and green triangles represent modes that can be found by applying spanwise symmetry conditions. (Left) Non-symmetric flow field. (Right) Spanwise symmetric flow field.

$$\begin{gathered}\hat{u}_{(n,k)} = \hat{u}_{(n,-k)}, \quad \hat{v}_{(n,k)} = \hat{v}_{(n,-k)}, \quad \hat{w}_{(n,k)} = -\hat{w}_{(n,-k)} \\ \hat{T}_{(n,k)} = \hat{T}_{(n,-k)}, \quad \hat{\rho}_{(n,k)} = \hat{\rho}_{(n,-k)} \\ A_{(n,k)} = A_{(n,-k)} \\ \alpha_{(n,k)} = \alpha_{(n,-k)}\end{gathered} \tag{2.29}$$

The nonlinear disturbance is substituted back into the Navier-Stokes equations and the newly found differential equation can be represented as such:

$$\mathcal{A}_2^{PSE}\frac{\partial^2\hat{\phi}}{\partial y^2} + \mathcal{B}_1^{PSE}\frac{\partial\hat{\phi}}{\partial\chi\partial y} + \mathcal{C}_1^{PSE}\frac{\partial\hat{\phi}}{\partial\chi} + \mathcal{C}_2^{PSE}\frac{\partial\hat{\phi}}{\partial y} + \mathcal{D}^{PSE}\hat{\phi} = \mathcal{N} \tag{2.30}$$

The nonlinear interactions are separated onto the right-hand side which allows a harmonic balancing between different modes. For quadratic interactions the following forcing vector is formed.

$$\mathcal{L}\left(\sum_{n_1}\sum_{k_1}\hat{\phi}_{(n_1,k_1)}A_{(n_1,k_1)}\exp\left[i\left(k_1\beta z-n_1\omega t\right)\right]\right)= \\ \mathcal{N}\left(\sum_{n_2}\sum_{k_2}\sum_{n_3}\sum_{k_3}\hat{\phi}_{(n_2,k_2)}\hat{\phi}_{(n_3,k_3)}A_{(n_2,k_2)}A_{(n_3,k_3)}\exp\left[i\left((k_2+k_3)\beta z-(n_2+n_3)\omega t\right)\right]\right) \tag{2.31}$$

Harmonic balancing consists of equating the exponents on the left- and right-hand sides which results in the following relationship between the integer scales for the wavenumber and frequency. The same process can be applied to cubic, quartic, and higher order interactions.

$$n^{(1)}=n^{(2)}+n^{(3)},\quad k^{(1)}=k^{(2)}+k^{(3)} \tag{2.32}$$

Due to the harmonic balancing, a specified mode can only interact with modes that satisfy Eq. 2.32. For example, the mode $(1,2)$ can interact with mode $(1,1)$ and $(0,1)$ for a quadratic forcing vector. A detailed breakdown of how the interacting modes are chosen can be found in [27].

The mode $(0,0)$, called the mean flow distortion (MFD) must also be considered. The MFD for a steady state is defined as the difference between the spanwise averaged transitional boundary layer and the laminar boundary layer. This mode if responsible for changes in the displacement and moment thickness. Since the MFD has no complex conjugate, a condition is imposed where $\hat{\phi}_{(0,0)}$ is real and $\alpha_{(0.0)}$ is imaginary. However, Hein [28] suggested that any non-zero $\alpha_{(0.0)}$ would be inconsistent with wall-normal boundary conditions. This assumption will be used in NPSE calculations presented in this paper as doing so has allowed further downstream convergence. A consequence of letting $\alpha_{(0.0)}=0$ is that $\hat{v}=\mathcal{O}\left(\mathrm{Re}^{-1}\right)$ as indicated by the disturbed continuity equation. The linear and nonlinear PSE can be found in appendix C.

2.4 Stability Solver

The primary program used for solving the spatial LST and PSE equations is EPIC [27, 29, 30]. EPIC is a boundary-layer disturbance solver developed by members of the Computational Stability and Transition (CST) laboratory at Texas A&M University. For EPIC, a three dimensional

boundary-layer along any arbitrary path can be considered but a uniform flow in the locally spanwise direction is imposed making this a 'quasi 3-D' assumption. Using a generalized curvilinear coordinate system, any curvatures can be accounted for in 3-D geometries and curvature can even be scaled for certain cases. For PSE calculations, it is necessary to define a vortex path to march along. The generation of these vortex paths will be outlined in the results section.

When initializing the LPSE simulation, an LST solution is generated at a user specified location and the Newton-Raphson method is used to find an approximate neutral point (the streamwise location where $\alpha_i = 0$). The LPSE solution is marched beginning at a location slightly upstream of this location to the end of the geometry. For NPSE calculations, the LST initialization and streamwise marching occurs at the user specified location. For further details on PSE implementation in EPIC, see [31].

To assist in quantifying LPSE stability results from EPIC, a parameter called the amplification factor (*N*-factor) is defined in Eq. 2.33. The *N*-factor is the accumulation of growth along a given streamwise path and is integrated from the neutral point to the end of the geometry. This growth is captured fully in α for LST. However, for PSE a small part lingers in the shape function. To properly extract the additional growth, the Chu-norm [32] is used and the equation is outlined in 2.34. The Chu-norm is used to build the foundation of the energy budget analysis outlined in the following section. The ρu perturbation mass-flux is another common method used when comparing with hot-wire measurements. A previous study within the HVSI project by Groot et al. [1] showed qualitative agreement between the current yawed-cone configuration and work done by Kocian [29], in which the ρu mass-flux was utilized.

$$N(s) = \int_{s_{\text{neut}}}^{s} -\sigma_i(\bar{s})\mathrm{d}\bar{s}, \quad \sigma(s) = \alpha - \frac{\mathrm{i}}{\Phi}\frac{\partial \Phi}{\partial s} \tag{2.33}$$

$$|\Phi(s)|^2 = \int_0^{y_{\max}} \left(\bar{\rho}(s,y)\left(|\hat{u}(s,y)|^2 + |\hat{v}|^2 + |\hat{w}|^2\right) + \frac{\bar{\rho}}{\gamma(\gamma-1)\mathrm{M}^2\bar{T}}|\hat{T}|^2 + \frac{\bar{T}}{\gamma \mathrm{M}^2 \bar{\rho}}|\hat{\rho}|^2 \right) \mathrm{d}y \tag{2.34}$$

2.5 Budget Analysis

An energy decomposition tool is necessary to quantify each of the PSE terms. The purpose is to identify terms of interest providing the AFT model information on flow conditions resulting in unstable flow. An energy analysis by Malik [19] indicated strong agreement between the secondary growth disturbance and integrated energy. In this study, Malik considers a disturbance energy equation consisting of the momentum equations with a control volume defined by a single wavelength across the boundary layer. This study will extend the disturbance equation to include the conservation of energy and mass continuity as well.

In order to properly realize the energy analysis, the scalar LPSE equations must be properly scaled and converted into energy. The process for doing so is outlined in the following steps:

1. Multiply each equation by a scaling factor consisting of a complex conjugate.

$$\begin{gathered} s\text{-momentum} \times \hat{u}^{\dagger}, \qquad y\text{-momentum} \times \hat{v}^{\dagger}, \qquad z\text{-momentum} \times \hat{w}^{\dagger}, \\ \text{energy equation} \times \frac{\hat{T}^{\dagger}}{\overline{T}}, \qquad \text{continuity equation} \times \frac{\overline{T}\hat{\rho}^{\dagger}}{\gamma \mathrm{M}^2 \overline{\rho}} \end{gathered} \tag{2.35}$$

   The LPSE equations defining the budget-analysis tool can be found in appendix A.

2. Add all linear disturbance equations. After addition, the left hand side will be defined as the

following terms:

$$\left(\omega-\alpha\frac{\overline{u}}{h_1}\right)\left(\overline{\rho}\left(|\hat{u}|^2+|\hat{v}|^2+|\hat{w}|^2\right)+\frac{\overline{\rho}}{\gamma \mathrm{Ec}\overline{T}}|\hat{T}|^2+\frac{\overline{T}}{\gamma \mathrm{M}^2\overline{\rho}}|\hat{\rho}|^2\right)$$
$$+\mathrm{i}\frac{\overline{u}}{h_1}\left(\overline{\rho}\left(\hat{u}^\dagger\frac{\partial\hat{u}}{\partial s}+\hat{v}^\dagger\frac{\partial\hat{v}}{\partial s}+\hat{w}^\dagger\frac{\partial\hat{w}}{\partial s}\right)+\frac{\overline{\rho}}{\gamma \mathrm{Ec}\overline{T}}\hat{T}^\dagger\frac{\partial\hat{T}}{\partial s}+\frac{\overline{T}}{\gamma \mathrm{M}^2\overline{\rho}}\hat{\rho}^\dagger\frac{\partial\hat{\rho}}{\partial s}\right)$$
$$=\hat{u}^\dagger\left(-\mathrm{i}\overline{\rho}\hat{v}\frac{\partial\overline{u}}{\partial y}+\mathrm{R}_{\hat{u},\mathrm{res}}+\mathrm{i}\frac{\overline{\mu}}{\mathrm{Re}}\frac{\partial^2\hat{u}}{\partial y^2}+\mathrm{D}_{\hat{u},\mathrm{res}}+\mathrm{P}_{\hat{u}}\right)+$$
$$\hat{v}^\dagger\left(\mathrm{R}_{\hat{v}}+\mathrm{D}_{\hat{v}}+\mathrm{P}_{\hat{v}}\right)+$$
$$\hat{w}^\dagger\left(-\mathrm{i}\overline{\rho}\hat{v}\frac{\partial\overline{W}}{\partial y}+\mathrm{R}_{\hat{w},\mathrm{res}}+\mathrm{i}\frac{\overline{\mu}}{\mathrm{Re}}\frac{\partial^2\hat{w}}{\partial y^2}+\mathrm{D}_{\hat{w},\mathrm{res}}+\mathrm{P}_{\hat{w}}\right)+$$
$$\hat{T}^\dagger\left(-\mathrm{i}\frac{\overline{\rho}}{\mathrm{Ec}\,\overline{T}}\hat{v}\frac{\partial\overline{T}}{\partial y}-\mathrm{i}\frac{\overline{\rho v}}{\mathrm{Ec}\,\overline{T}}\frac{\partial\hat{T}}{\partial y}-\mathrm{i}\frac{\overline{v}}{\mathrm{Ec}\,\overline{T}}\hat{\rho}\frac{\partial\overline{T}}{\partial y}+\mathrm{R}_{\hat{T},\mathrm{res}}+\mathrm{i}\frac{\kappa}{\mathrm{Ec}\,\mathrm{Pr}\,\mathrm{Re}\,\overline{T}}\frac{\partial^2\hat{T}}{\partial y^2}+\mathrm{D}_{\hat{T},\mathrm{res}}+\mathrm{P}_{\hat{T}}\right)+$$
$$\hat{\rho}^\dagger\left(-\mathrm{i}\frac{\overline{\rho}_y}{\overline{\rho}}\hat{v}+\mathrm{R}_{\hat{\rho},\mathrm{res}}+\mathrm{D}_{\hat{\rho}}+\mathrm{P}_{\hat{\rho}}\right) \tag{2.36}$$

The largest energy transfer types are Reynolds-flux production terms R (red), viscous terms D (blue), and pressure work terms P (green). Some terms within these categories have been defined individually as they produce larger transfers of energy while the rest are indicated by the subscript, 'res'. The terms are defined by which scalar Navier-Stokes equation produces the value. For example, the $\hat{T}$ subscript demonstrates terms defined in the conservation of energy equation and have been multiplied by $\hat{T}^\dagger$.

3. Now that all of the LPSE equations are combined into a single, total energy equation, the integral is taken in the y-domain:

$$\begin{aligned}
&\omega \int_0^{y_{\max}} \left(\overline{\rho} \left(|\hat{u}|^2 + |\hat{v}|^2 + |\hat{w}|^2 \right) + \frac{\overline{\rho}}{\gamma Ec \overline{T}} |\hat{T}|^2 + \frac{\overline{T}}{\gamma M^2 \overline{\rho}} |\hat{\rho}|^2 \right) \mathrm{d}y \\
&-\alpha \int_0^{y_{\max}} \frac{\overline{u}}{h_1} \left(\overline{\rho} \left(|\hat{u}|^2 + |\hat{v}|^2 + |\hat{w}|^2 \right) + \frac{\overline{\rho}}{\gamma Ec \overline{T}} |\hat{T}|^2 + \frac{\overline{T}}{\gamma M^2 \overline{\rho}} |\hat{\rho}|^2 \right) \mathrm{d}y \\
&+\mathrm{i} \int_0^{y_{\max}} \frac{\overline{u}}{h_1} \left(\overline{\rho} \left(\hat{u}^\dagger \frac{\partial \hat{u}}{\partial s} + \hat{v}^\dagger \frac{\partial \hat{v}}{\partial s} + \hat{w}^\dagger \frac{\partial \hat{w}}{\partial s} \right) + \frac{\overline{\rho}}{\gamma \mathrm{Ec} \overline{T}} \hat{T}^\dagger \frac{\partial \hat{T}}{\partial s} + \frac{\overline{T}}{\gamma \mathrm{M}^2 \overline{\rho}} \hat{\rho}^\dagger \frac{\partial \hat{\rho}}{\partial s} \right) \mathrm{d}y = \\
&\int_0^{y_{\max}} \mathrm{RHS} \ \mathrm{d}y
\end{aligned} \tag{2.37}$$

where RHS is the right-hand-side from Eq. 2.36.

4. Solve for α in the term on the left-hand side by dividing the coefficient highlighted in green from all terms in the equation. Notice that this coefficient models closely to the Chu-norm found in Eq. 2.34 with the inclusion of a factor, $\frac{\overline{u}}{h_1}$, which is a byproduct of using a curvilinear coordinate system. The modeling of this modified Chu-norm is intentional so as to model the growth rate $-\alpha_i$ while capturing how energy is generated or destroyed locally. The frequency ω will be zero since the focus of this study is on the stationary crossflow instability.

5. Optionally, integrate the resulting expression in the x-direction from a point corresponding to neutral growth, denoted by x_{neut}, up to a point of interest. The axial coordinate, x, is used for streamwise integration rather than s to allow for comparison of different paths within the same coordinate system.

Through this process, the streamwise growth of the disturbance can be quantified through the imaginary component, α_i. This process can be applied to each individual scalar LPSE equation by using the same factor defined in Eq. 2.35 resulting in a disturbance energy with only values pertaining to the related equation. The left-hand-side coefficient for α will be different which will result in a different scaling for each of the terms when dividing this quantity out. The coefficient associated with α on the left-hand-side is plotted in Fig. 2.2 for the total disturbance as well as

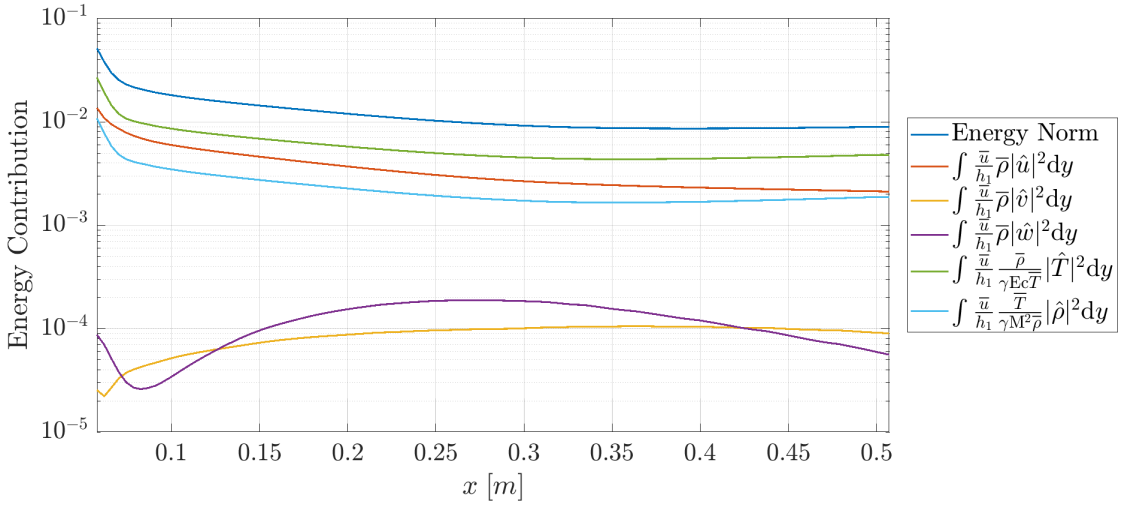

Figure 2.2: Individual contributions to the total energy normalization as seen on the most amplified vortex path and wavenumber.

each individual LPSE disturbance equation.

In addition to quantifying every energy production term, it is also possible to quantify an approximate energy production in order to satisfy a specific threshold of the total perturbation energy. This threshold is defined as a proportion of the maximum growth rate in the axial direction for the most amplified vortex path and wavenumber.

3. CONE CONFIGURATION *

3.1 Geometry and Grid Structure

The yawed-cone shape is defined as a straight cone with 7° half angle and $50\,\mu$m nose-tip radius. The current model has a length of 20 in or 0.508 m from the virtual origin to the base of the cone. A global coordinate system is defined using the x, Y, and Z axes about the virtual origin. In the global coordinate system, θ is defined as the angle about the X axis where $\theta = 0^\circ$ at the windward symmetry plane. Within this coordinate system it is necessary to define a local coordinate system that follows the path of a streamline. The coordinate s follows the streamwise path along the surface of the cone and y is the local wall-normal axis. The θ_v axis is perpendicular to the streamline and tangent to the wall and will be referred to as the spanwise component. A depiction of the yawed-cone geometry and coordinate system can be seen in Fig. 3.1.

Using Pointwise, an overset grid for the cone was created in two structured chunks with the first surrounding the nose tip and the second encompassing the rest of the geometry. Since the geometry is symmetrical, only half of the cone is generated ($0^\circ \leq \theta \leq 180^\circ$). A series of three separate grids are generated with increasing resolution. The individual grids will be dubbed *sparse*, *intermediate*, and *dense* with the naming convention indicating the grid resolution in regard to the other grids. The indices j, k, and l will indicate the axial, azimuthal, and wall-normal directions respectively. Table 3.1 indicates the resolutions for each grid.

*Material in this chapter has been reprinted with permission from "Assessment of the Amplification Factor Transport Transition Model for High-Mach Number Flows" by Koen J. Groot, Jay Patel, Caleb Saiyasak, James G. Coder, Douglas L. Stefanski and Helen L. Reed, 2021. Copyright 2021 by Koen J. Groot, Jay M. Patel, Caleb A. Saiyasak, James G. Coder, Douglas L. Stefanski & Helen L. Reed. and "Energy-Budget Analysis of the Crossflow Instability on a Hypersonic Yawed Cone" by Jay Patel, Koen Groot, Caleb Saiyasak, James Coder & Douglas Stefanski. Copyright 2021 by Koen J. Groot, Jay M. Patel, Caleb A. Saiyasak, James G. Coder, Douglas L. Stefanski & Helen L. Reed.

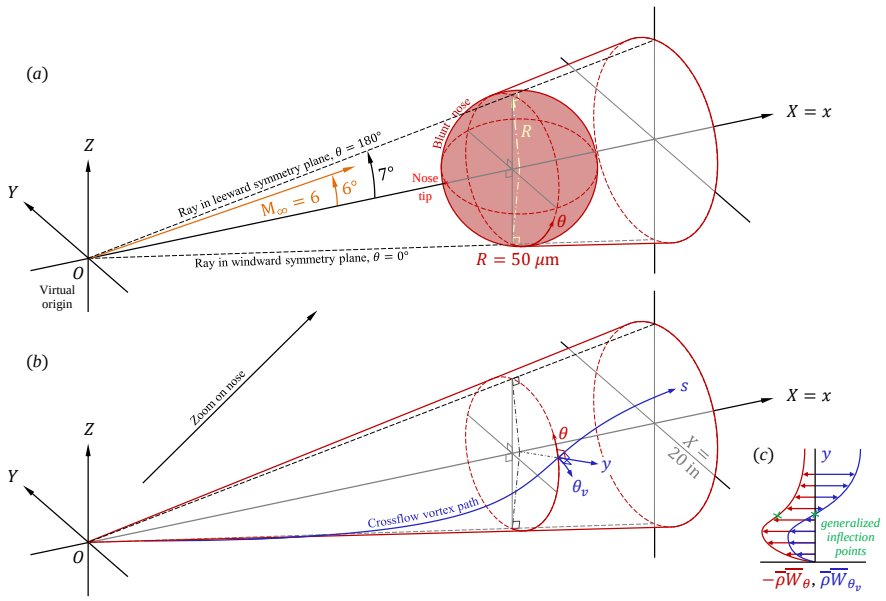

Figure 3.1: Yawed-cone geometry with zoomed in nose-tip, vortex path, and associated coordinate systems.

Grid level	Nose-cap dimensions	Body-grid dimensions	Total grid points
	$nj \times nk \times nl$	$nj \times nk \times nl$	
Sparse	$121 \times 61 \times 217$	$613 \times 271 \times 217$	$37,650,368$
Intermediate	$161 \times 81 \times 289$	$817 \times 361 \times 289$	$89,005,642$
Dense	$201 \times 101 \times 361$	$1021 \times 451 \times 361$	$173,558,692$

3.2 Base-Flow

The Mach 6.00 flow is directed at the cone with an incidence angle of $6°$ and a unit Reynolds number of 10.0×10^6 m^{-1}. The freestream temperature and pressure are $T_\infty = 53.42$ K and $p_\infty = 611.4$ Pa and the wall temperature has been defined as $T_w = 300$ K.

The laminar basic-state calculation for this geometry is generated using the NASA OVERFLOW [34, 35] Navier-Stokes solver. For this particular usage, HLLE++ fluxes along with a MUSCL-type reconstruction are used for spatial discretization [36]. This configuration allows for easier handling of non-grid-aligned shock waves without unwanted anomalies. An in-depth description for the development of the base-flow grid using OVERFLOW can be found in Ref [1].

For EPIC initialization, a vortex path must be described along the geometry. This is done by extracting the full base-flow data using Tecplot 360 then judiciously extracting a vortex path. A tool for extracting this path is developed by Travis Kocian [29] in MATLAB. This program allows for a streamlined process to quickly identify and derive multiple paths at once. These paths are defined by identifying where the spanwise velocity $\overline{W}_{theta}$ achieves an inflection point and rotating about the wall-normal axis such that the generalized inflection point has no velocity. The analytical expression for this criterion is seen in Eq. 3.1. Once a path is extracted, the spanwise wavenumber must be scaled correctly [27]. This scaling depends on paths that are neighboring the extracted path, in particular the azimuthal angle between the neighboring paths, which will help generate a local wavenumber. For this analysis a series of vortex paths were generated to encompass the entirety of the cone geometry. Due to the nature of the flow, the paths will generally start on the windward portion and travel towards the leeward portion of the cone. To avoid the effects of the nose, these paths were initialized slightly down stream of the cone origin.

$$\frac{\partial}{\partial y}\left(\overline{\rho}\frac{\partial \overline{W}_{\theta_v}}{\partial y}\right) = 0 \quad \text{where} \quad \overline{\rho}\overline{W}_{\theta_v} = 0 \quad \text{at } y = y_{\text{infl}}, \tag{3.1}$$

3.3 Stability Results

The primary instability for the yawed-cone to be studied is stationary crossflow so we set the frequency, ω to be zero. The spanwise wavenumber distribution ranges $50 \leq m \leq 400$ at an axial location $x = 0.1$ m. The discretization scheme uses 100 and 200 points in the streamwise (s) and wall-normal (y) directions. These parameters are inputted into EPIC and the following results are represented in *N*-factor curves. For the sake of this thesis the *dense* grid is further studied, however, a grid resolution study can be found in [1]. For the *dense* grid, a cluster of paths covering the majority of the geometry are plotted with the most unstable mode in Fig. 3.2. The current results have a max *N*-factor of 14.5 which compares quite well to previous computational studies [29] finding a max amplification factor of 13.7. The large amplification in the azimuthal angle range is supported by Balakumar & Owens [37] who showed that the boundary layer near

the leeward symmetry plane has been separated. Based on the nonlinear study by Moyes' [38] Fig. 5.11, using the saturation point N-factor of 11, the current LPSE studies are well within the range of transition. The N-factors for the most unstable vortex path is seen in Fig. 3.4. At the base of the cone the azimuthal angle and wavenumber are $\theta = 148.6°$ and $m = 81.9$. These values are consistent with the experimental results indicated by Craig & Saric [39].

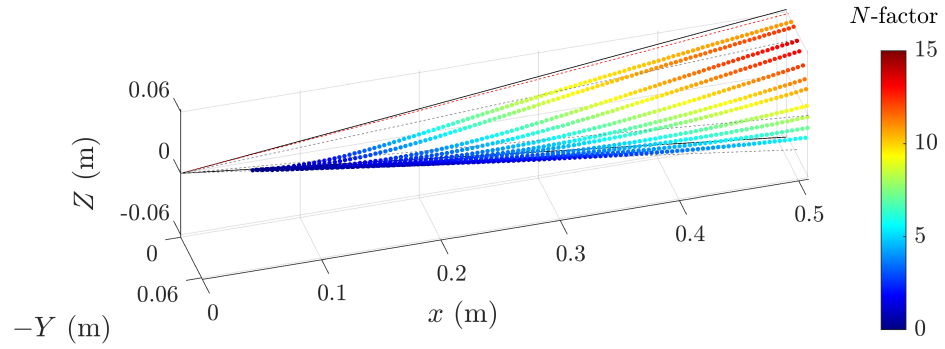

Figure 3.2: N-factor envelope for the yawed-cone configuration along the cone shape computed with LPSE for the *dense* grid.

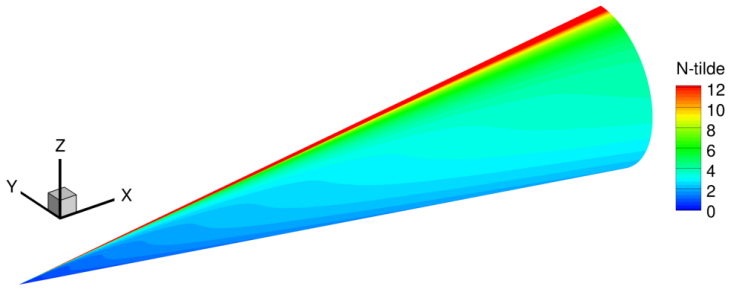

Figure 3.3: N-factor envelope for the yawed-cone configuration along the cone shape computed using the AFT model.

In comparing the current LPSE results to the AFT model found in Fig. 3.3, there is a distinct mismatch. Primarily, the AFT model only activates in the vicinity of the leeward plane and is

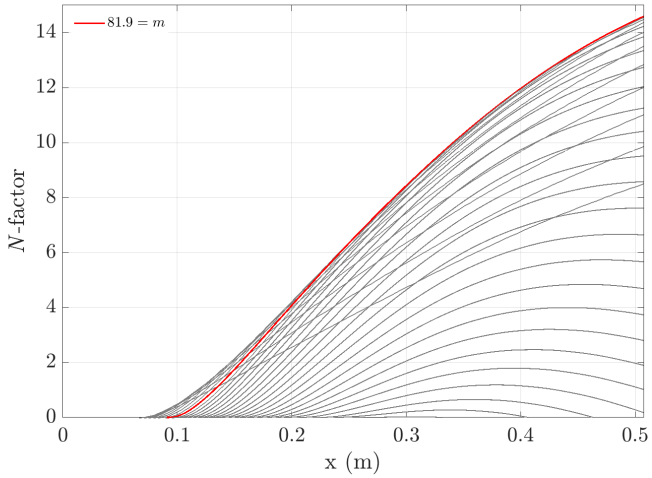

Figure 3.4: N-factors for most-amplified vortex path at varying wavenumbers with the red line indicating the most unstable curve at the base of the cone.

unable to capture the high levels of crossflow instability in the region outside of the leeward plane.

3.4 Budget Analysis

Due to the discrepancy in amplification calculations between LPSE and AFT models, a budget analysis of the energy components will be considered to assist in informing the AFT model on which energy contributions lend itself to larger instability growth. The following budget analysis will consider the entire $\theta - m$ plane at the base of the cone and a streamwise study for the most amplified vortex path and wavenumber. Disturbance energy equations for the total-perturbation, conservation of energy, and crossflow-perturbation energy will be investigated. Further analysis of the largest energy production values will focus on the location of x_{neut} as well as the linear (Pearson) correlation coefficient. The conservation of energy disturbance is studied further due to the large energy transfer seen in Fig. 2.2 and the crossflow-perturbation will be studied due to the presence of the crossflow instability.

3.4.1 Total-Perturbation Energy

The total growth rate and individual contributions are integrated in the axial direction and presented in Fig. 3.5. The individual integrated terms are the sums of the energy contributions

defined in Fig. 3.6 (c).

In the left panel of Fig. 3.5 the vortex path is confined to the path yielding the highest amplification while varying the wavenumber. The Reynolds-flux terms have the largest energy production and effectively dictate the behavior of the total growth as seen be having similar wavenumbers ($m \approx 80$ at x_{base}) for the peaks of energy production. This production term is being destroyed or transferred by the pressure work and viscous terms which remain relatively constant through the wavenumber variation. The right panel of Fig. 3.5 the azimuthal angles are varied while the wavenumber yielding the highest amplification is chosen for each path. A similar trend is found with the Reynolds-flux values dominating the growth of the instability achieving a peak near $\theta \approx 150^\circ$ while pressure work and viscous effects impose a destruction of energy rendering a more stable perturbation-energy growth.

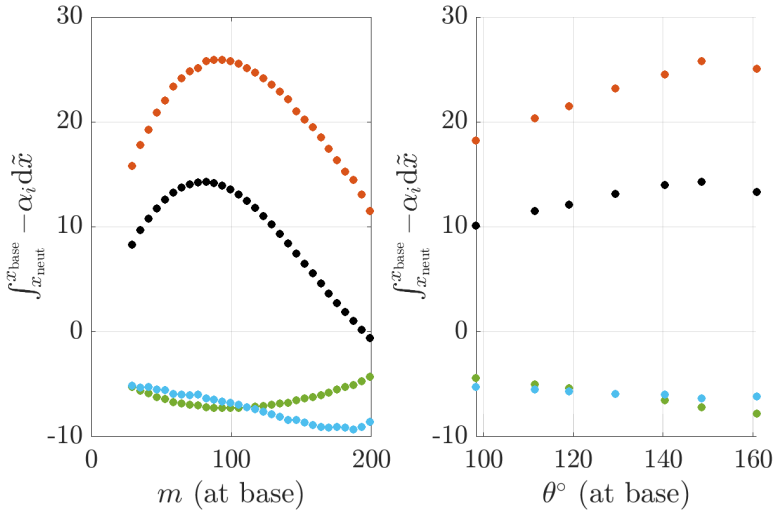

Figure 3.5: Energy-budget decomposition for the total-perturbation equation, see Eq. 2.37. Black: $-\alpha_i$ as integrated along the streamwise direction representing an approximate N-factor. Red: Reynolds-flux energy production terms, R. Green: pressure work terms, P. Blue: viscous terms, D. (Left) Integrated growth at the base of the geometry with varying wavenumbers choosing the vortex path supporting the most amplified solution. (Right) Integrated growth for each vortex path at the base of the cone choosing the most amplified wavenumber.

The values contained in the energy transfers found in Fig. 3.5 will be studied along the vortex

path and wavenumber for which the largest *N*-factor is achieved at the base of the cone. For this study the total growth, $-\alpha_i$, will be compared to an approximated growth , $-\alpha_{i,\text{approx}}$, which consists of terms summing to a percentage of the maximum growth rate. This threshold is achieved by including additional terms (in order of largest to smallest) until the desired error is produces. Fig. 3.6 indicates thresholds for 80%, 90%, and 95% of the total-perturbation growth rate. The number of terms required to achieve this threshold of growth grows from 14 in Fig. 3.6 (a) to 20 and 48 terms in 3.6 (b) and (c) respectively. This near exponential increase in required terms can be attributed to a select few terms dominating the balancing of energy while smaller valued terms play a smaller role fine tuning the exact growth rate. The primary factors in the energy balance are found to be the Reynolds-flux production and viscous-dissipation values.

From the energy-threshold evaluation, the two largest values are identified as Reynolds heat-flux and temperature-perturbation dissipation seen in Eqs. 3.2a and 3.2b respectively. Both of these terms are a product of the conservation of energy disturbance. By summing these two values, we examine how well the neutral point location can be approximated and if there exists a linear correlation to the total-perturbation growth rate.

$$\mathrm{R}_{\hat{T},\max} = -i\frac{\overline{\rho}}{\mathrm{Ec}\,\overline{T}}\hat{v}\frac{\partial\overline{T}}{\partial y} \tag{3.2a}$$

$$\mathrm{D}_{\hat{T},\max} = i\frac{\overline{\kappa}}{\mathrm{Ec}\,\mathrm{Pr}\,\mathrm{Re}\,\overline{T}}\frac{\partial^2\hat{T}}{\partial y^2} \tag{3.2b}$$

The relative error in neutral points between the growth rate $-\alpha_i$ and $\hat{T}^\dagger\left(\mathrm{R}_{\hat{T},\max} + \mathrm{D}_{\hat{T},\max}\right)$ can be found in the left panel of Fig. 3.7. An error of approximately 10% can be found for the most unstable regions for the θ-m plane. Regions of higher error can be found within the unstable portion of the θ-m plane which are manageable. Very small wavenumbers are associated with larger wavelengths in which the primary physics we aim to study may not be applicable. This is a possible reason for why there are higher relative errors for the portion of low wavenumbers. The right panel of Fig. 3.7 indicates the linear correlation coefficient for these terms along the axial coordi-

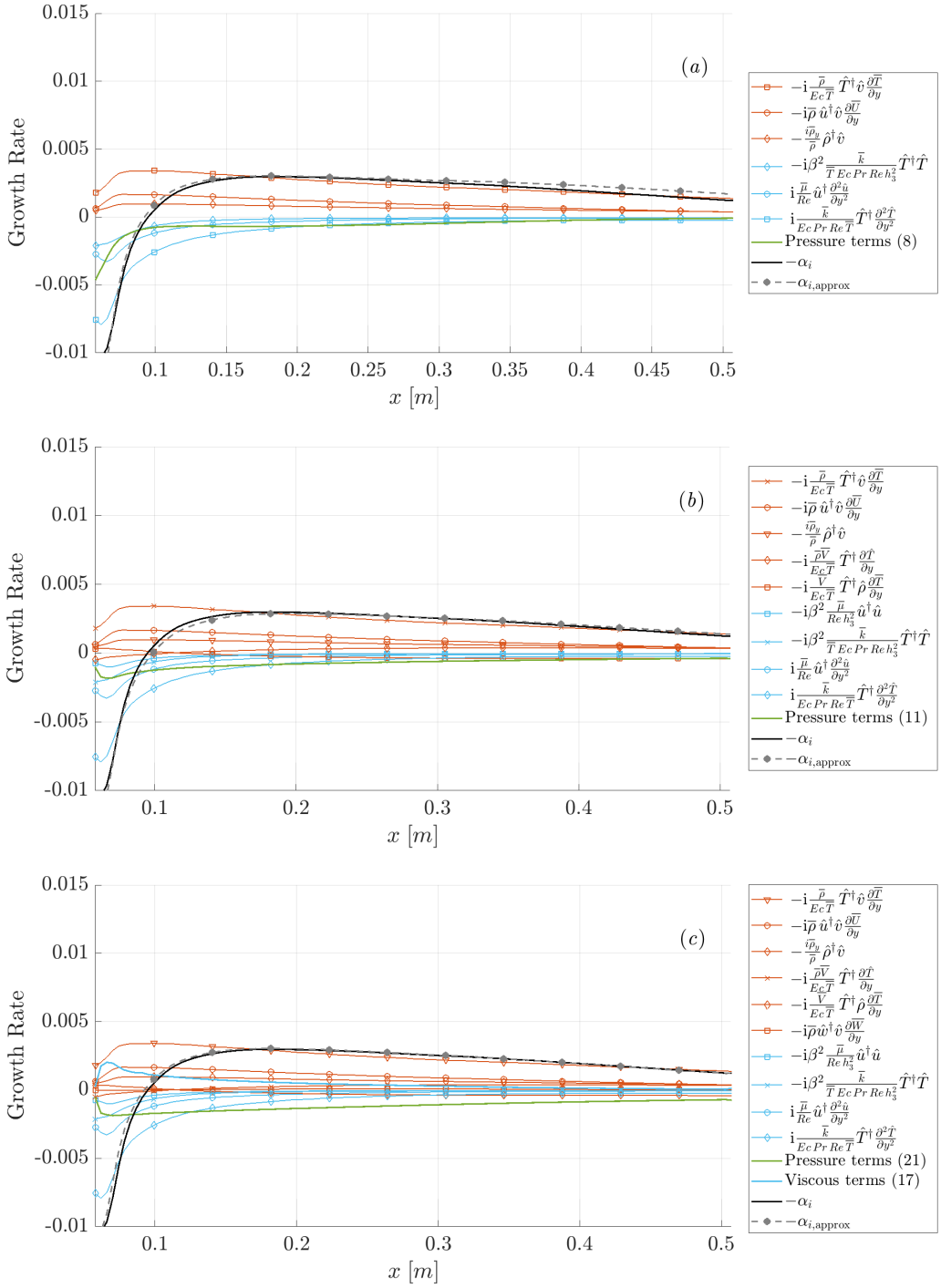

Figure 3.6: Solid black line: $-\alpha_i$ as solved with LPSE. Solid grey line: approximate growth rate $-\alpha_{i,\text{approx}}$ defined by sum of terms within threshold. Red line: Reynolds-flux energy production terms. Blue line: viscous terms with the largest transmission being defined with individual curves. Green line: pressure terms (combined into a single curve). The plots represent dominant terms of the total-perturbation energy which allow $-\alpha_{i,\text{approx}}$ to be within $\pm 20\%$ (a), $\pm 10\%$ (b), and $\pm 5\%$ (c) of $-\alpha_i$.

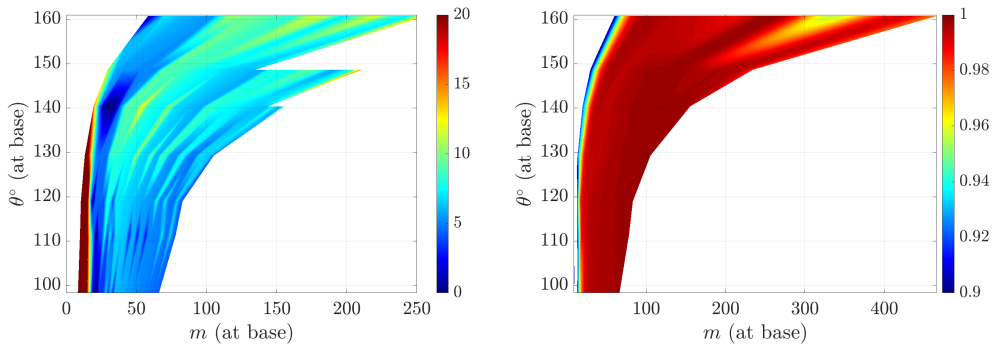

Figure 3.7: (Left) Relative error (%) between the $-\alpha_i$ neutral point and the approximate neutral point as found by $\hat{T}^\dagger \left(\mathrm{R}_{\hat{T},\max} + \mathrm{D}_{\hat{T},\max} \right)$. (Right) Linear correlation coefficient between $-\alpha_i$ and $\mathrm{R}_{\hat{T},\max} + \mathrm{D}_{\hat{T},\max}$ along x. The θ-m plane consists of all azimuthal paths and each wavenumber along those paths.

nate x. We see a high correlation (> 0.95) for the leading terms in the energy-disturbance against the growth rate. Similar to the neutral point error, this trend breaks down for small wavenumbers.

3.4.2 Conservation of Energy Perturbation

As indicated previously, a similar energy-budget analysis will be performed by defining the disturbance energy with the conservation of energy equation as reflected in Eq. 3.3. The development of these quantities along the axial direction will be studied for the most unstable scenario. In a similar fashion to the previous section, the quantities will also be integrated from the axial neutral point to the base of the cone.

$$\left(\omega - \alpha\frac{\overline{u}}{h_1}\right)\left(\frac{\overline{\rho}}{\gamma \mathrm{Ec}\overline{T}}|\hat{T}|^2\right) + \mathrm{i}\frac{\overline{u}}{h_1}\left(\frac{\overline{\rho}}{\gamma \mathrm{Ec}\overline{T}}\hat{T}^\dagger\frac{\partial \hat{T}}{\partial s}\right)$$
$$= \hat{T}^\dagger\left(-\mathrm{i}\frac{\overline{\rho}}{\mathrm{Ec}\,\overline{T}}\hat{v}\frac{\partial \overline{T}}{\partial y} - \mathrm{i}\frac{\overline{\rho}\,\overline{v}}{\mathrm{Ec}\,\overline{T}}\frac{\partial \hat{T}}{\partial y} - \mathrm{i}\frac{\overline{v}}{\mathrm{Ec}\,\overline{T}}\hat{\rho}\frac{\partial \overline{T}}{\partial y} + \mathrm{R}_{\hat{T},\mathrm{res}} + \mathrm{i}\frac{\overline{\kappa}}{\mathrm{Ec}\,\mathrm{Pr}\,\mathrm{Re}\,\overline{T}}\frac{\partial^2 \hat{T}}{\partial y^2} + \mathrm{D}_{\hat{T},\mathrm{res}} + \mathrm{P}_{\hat{T}}\right) \tag{3.3}$$

Fig. 3.8 indicates a consistent trend to Fig. 3.5 with large production caused by Reynolds-flux being destroyed by pressure work or viscous effects. This is to be expected as the dominant terms of the total-perturbation energy were developed within the conservation of energy. The terms used

in the formulation of each energy production type are defined in the legend of Fig. 3.9 (c).

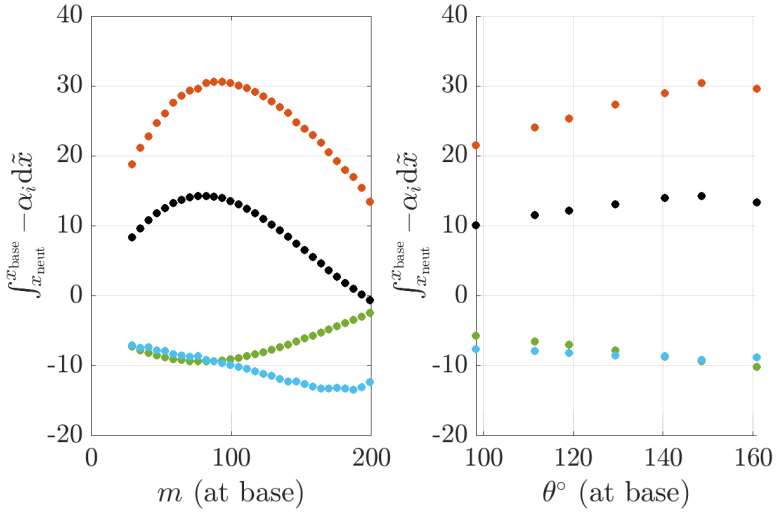

Figure 3.8: Energy-budget decomposition for the conservation of energy disturbance equation, Eq. 3.3. Black: $-\alpha_i$ as integrated along the streamwise direction representing an approximate N-factor. Red: Reynolds-flux energy production terms, $\mathrm{R}_{\hat{T}}$. Green: pressure work terms, $\mathrm{P}_{\hat{T}}$. Blue: viscous terms, $\mathrm{D}_{\hat{T}}$. (Left) Integrated growth at the base of the geometry with varying wavenumbers choosing the vortex path supporting the most amplified solution. (Right) Integrated growth for each vortex path at the base of the cone choosing the most amplified wavenumber.

An energy threshold variation study is performed in Fig. 3.9. The quantities, $\mathrm{R}_{\hat{T},\max}$ and $\mathrm{D}_{\hat{T},\max}$, again dominate the energy transference along with additional values defined in the legends for each error level.

3.4.3 Crossflow-Velocity-Perturbation Energy

With the crossflow instability being the mechanism of interest for the yawed-cone geometry, it would be expected that energy production related to the crossflow-velocity component would play a larger role in the total-perturbation energy equation. It is nevertheless valuable to analyze the kinetic energy relating to the spanwise momentum equation as seen in Eq. 3.4.

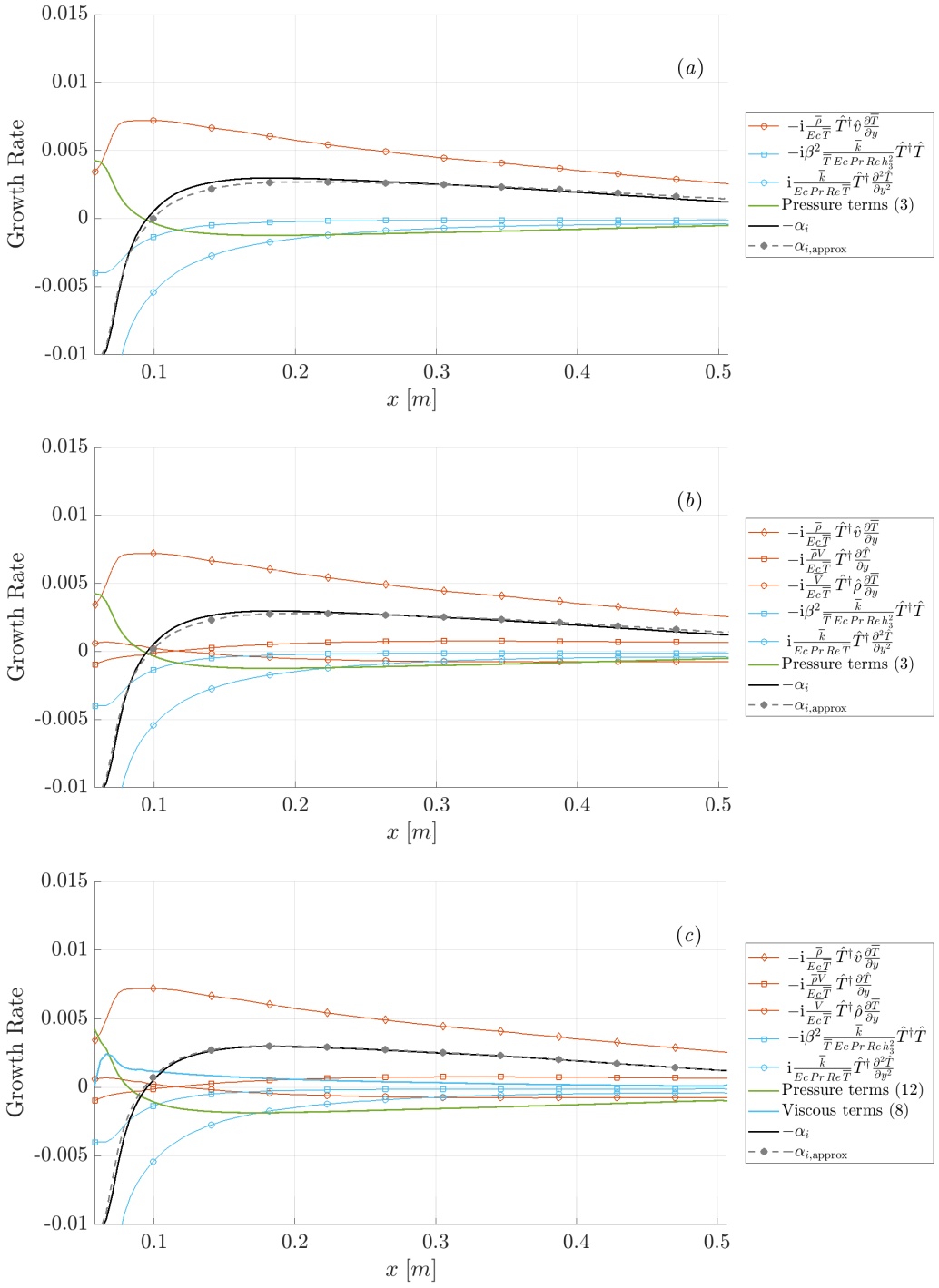

Figure 3.9: Solid black line: $-\alpha_i$ as solved with LPSE. Solid grey line: approximate growth rate $-\alpha_{i,\mathrm{approx}}$ defined by sum of terms within threshold. Red line: Reynolds-flux energy production terms. Blue line: viscous terms with the largest transmission being defined with individual curves. Green line: pressure terms (combined into a single curve). The plots represent dominant terms of the conservation of energy disturbance which allow $-\alpha_{i,\mathrm{approx}}$ to be within $\pm 20\%$ (a), $\pm 10\%$ (b), and $\pm 5\%$ (c) of $-\alpha_i$.

$$\left(\omega - \alpha\frac{\overline{u}}{h_1}\right)\left(\overline{\rho}|\hat{w}|^2\right) + \mathrm{i}\frac{\overline{u}}{h_1}\left(\overline{\rho}\hat{w}^\dagger\frac{\partial\hat{w}}{\partial s}\right)$$
$$= \hat{w}^\dagger\left(-\mathrm{i}\overline{\rho}\hat{v}\frac{\partial\overline{W}}{\partial y} + \mathrm{R}_{\hat{w},\mathrm{res}} + \mathrm{i}\frac{\overline{\mu}}{\mathrm{Re}}\frac{\partial^2\hat{w}}{\partial y^2} + \mathrm{D}_{\hat{w},\mathrm{res}} + \mathrm{P}_{\hat{w}}\right) + \tag{3.4}$$

Integrated growth rates for the most amplified quantities are found in Fig. 3.10. A slightly different trend is found in the development of energy. While the Reynolds-flux term still drives the instability growth, the pressure work has an increased hand in energy reduction. Due to this increased pressure work, the maximum growth rate does not align with the same wavenumber as $\mathrm{R}_{\hat{w}}$ as seen in previous cases. The energy threshold variation in Fig. 3.11 also reflects the larger pressure work developed on the most unstable path. The pressure work does start as an unstable value upstream of the neutral point but quickly stabilizes itself and nearly mirrors the growth of $\mathrm{R}_{\hat{w}}$.

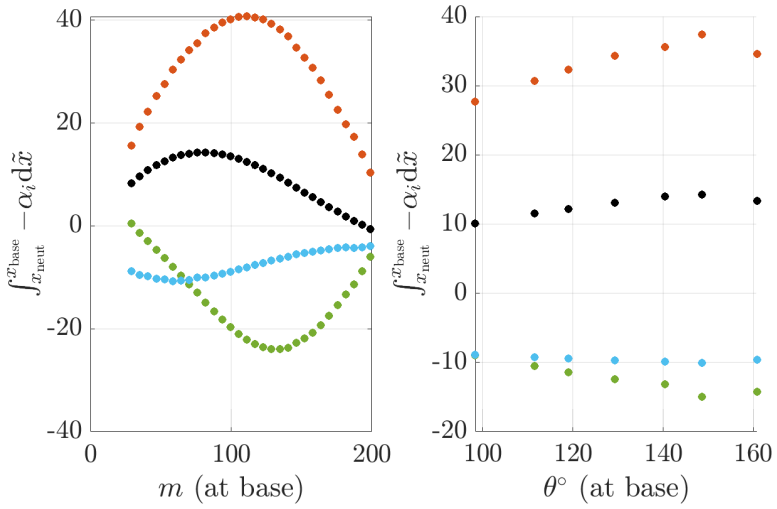

Figure 3.10: Energy-budget decomposition for the conservation of energy disturbance equation, Eq. 3.3. Black: $-\alpha_i$ as integrated along the streamwise direction representing an approximate N-factor. Red: Reynolds-flux energy production terms, $\mathrm{R}_{\hat{w}}$. Green: pressure work terms, $\mathrm{P}_{\hat{w}}$. Blue: viscous terms, $\mathrm{D}_{\hat{w}}$. (Left) Integrated growth at the base of the geometry with varying wavenumbers choosing the vortex path supporting the most amplified solution. (Right) Integrated growth for each vortex path at the base of the cone choosing the most amplified wavenumber.

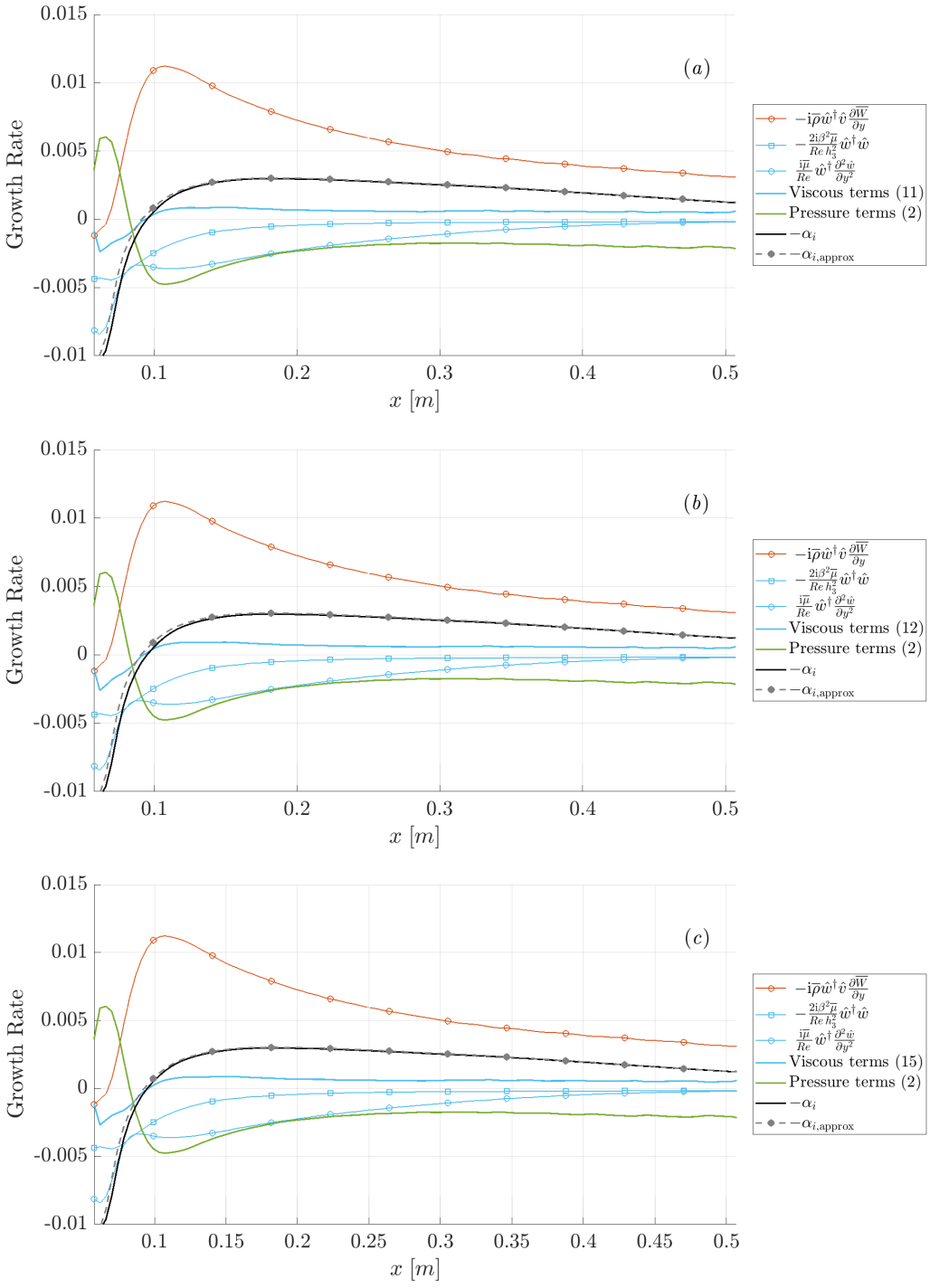

Figure 3.11: Solid black line: $-\alpha_i$ as solved with LPSE. Solid grey line: approximate growth rate $-\alpha_{i,\text{approx}}$ defined by sum of terms within threshold. Red line: Reynolds-flux energy production terms. Blue line: viscous terms with the largest transmission being defined with individual curves. Green line: pressure terms (combined into a single curve). The plots represent dominant terms of the spanwise-perturbation energy which allow $-\alpha_{i,\text{approx}}$ to be within $\pm 20\%$ (a), $\pm 10\%$ (b), and $\pm 5\%$ (c) of $-\alpha_i$.

4. SWEPT-WING CONFIGURATION*

4.1 Base-Flow

The airfoil for this study is an SNLF airfoil called the X207.LS seen in Fig. 4.1 (a). The airfoil mimics the pressure gradient found in the S207 airfoil but operates at a lower speed (hence the LS in X207.LS). The computational parameters for the base flow are based off of the near incompressible conditions defined in Klebanoff-Saric Wind Tunnel (KSWT) at Texas A&M University. The airfoil itself serves as a risk-reduction experiment to validate the computational tool's ability in predicting conditions which support laminar flow. However, the analysis will focus on the bottom surface of the fore-element for which experimental results have not been produced. The slotted region on the bottom side of the airfoil is of great significance for the following analysis.

Two coordinate systems will be defined. The first is the global system x, Y, and Z in which x is defined as the chordwise dimension perpendicular to the leading edge. The freestream quantities $\overline{u}_\infty$, $\overline{v}_\infty$, and $\overline{w}_\infty$, are defined in this frame. The local coordinate system is defined as s, y, and z where s is the dimension following the surface of the geometry, y is the wall normal component, and z is the leading-edge parallel dimension. The airfoil has a reference or chord length of 30.15 in or 0.76581 m as defined in the chord wise direction. The entrance of the slot is defined at $x/c = 0.643$. Pressure distributions are generated by MSES [40] as seen in Fig. 4.1 (b). For this study an angle of attack is chosen as 2.25° due to the generation of a strong favorable pressure gradient along the entirety of the chord. This will assist in damping Tollmein-Schlichting waves while inciting the crossflow instability [12]. A sweep variation study is performed for $0^\circ \leq \Lambda \leq 35^\circ$ at 5° increments. The sweep angle and angle of attack are defined by the freestream quantities in Eqs. 4.1 and 4.2 respectively.

*Material in this chapter has been reprinted from "Görtler Instability on a Variably Swept, Slotted, Natural-Laminar-Flow Airfoil" by Koen J. Groot, Jay Patel, Ethan S. Beyak, James G. Coder and Helen L. Reed 2021. Copyright 2021 by Koen J. Groot, Jay Patel, Ethan S. Beyak, James G. Coder and Helen L. Reed.

$$\Lambda = \arctan\left(\frac{\overline{w}_\infty}{\sqrt{\overline{u}_\infty^2 + \overline{v}_\infty^2}}\right) \tag{4.1}$$

$$\alpha = \arctan\left(\frac{\overline{v}_\infty}{\overline{u}_\infty}\right) \tag{4.2}$$

The stability calculations will employ a fixed $\mathrm{Re}_{|\overline{V}|_\infty} = c\rho_\infty|\overline{V}|_\infty/\mu_\infty$ where $|\overline{V}|_\infty$ is the freestream resultant velocity of $\overline{u}_\infty$, $\overline{v}_\infty$, and $\overline{w}_\infty$. This Reynolds number is 1.0×10^6. The Mach number defined by MSES relates to the leading-edge-orthogonal direction ($M = \sqrt{\overline{u}_\infty^2 + \overline{v}_\infty^2}/\overline{a}_\infty = 0.06$) causing a discrepancy with the KSWT Mach number and Reynolds number which is based on the total velocity component. The details on how this discrepancy is resolved can be found in [41]. Additional parameters are defined relating the properties of the air. These are $R_g = 291.171$ J/(kg K), $\gamma = 1.4$ and $\mathrm{Pr} = 0.72$. Parameters relating to Sutherland's law are $\mu_{\mathrm{ref}} = 1.716 \times 10^{-5}$ kg/(m s), $T_{\mathrm{ref}} = 273$ K and $S = 111$ K.

Using the pressure coefficients, DEKAF employed to generate a base-flow solution. DEKAF is a spectrally accurate boundary-layer solver developed by the CST Lab. The basic state will contain 2000 streamwise nodes and 250 wall normal nodes. A Malik mapping is used for clustering grid points in the wall normal direction. GICM is used to interpolate DEKAF profiles [42, 43].

4.2 Boundary-Layer Properties

The streamwise development of boundary-layer parameters are plotted in Fig. 4.2 for all considered sweep angles. These parameters are defined as the Hartree parameter, β_H, boundary-layer thickness, δ_{99}, the shape factor, H, the non-dimensional curvature, c/R, and the Görtler number, G [13] as seen if Eq. 4.3

$$G = \frac{\overline{Q}_r \delta_r \overline{\rho}_\infty}{\overline{\mu}_\infty}\sqrt{\frac{\delta_r}{R}} \tag{4.3}$$

where $\delta_r = \sqrt{\frac{\overline{\mu}_\infty s}{\overline{\rho}_\infty \overline{Q}_r}}$ is the Blasius length and $\overline{Q}_r = \sqrt{\overline{u}_\infty^2 + \overline{v}_\infty^2}$. The non-dimensional wavelength-parameter is also defined as

$$\lambda_G = \frac{\lambda_z \overline{\rho}_\infty \overline{Q}_r}{\overline{\mu}_\infty}\sqrt{\frac{\lambda_z}{R}} \tag{4.4}$$

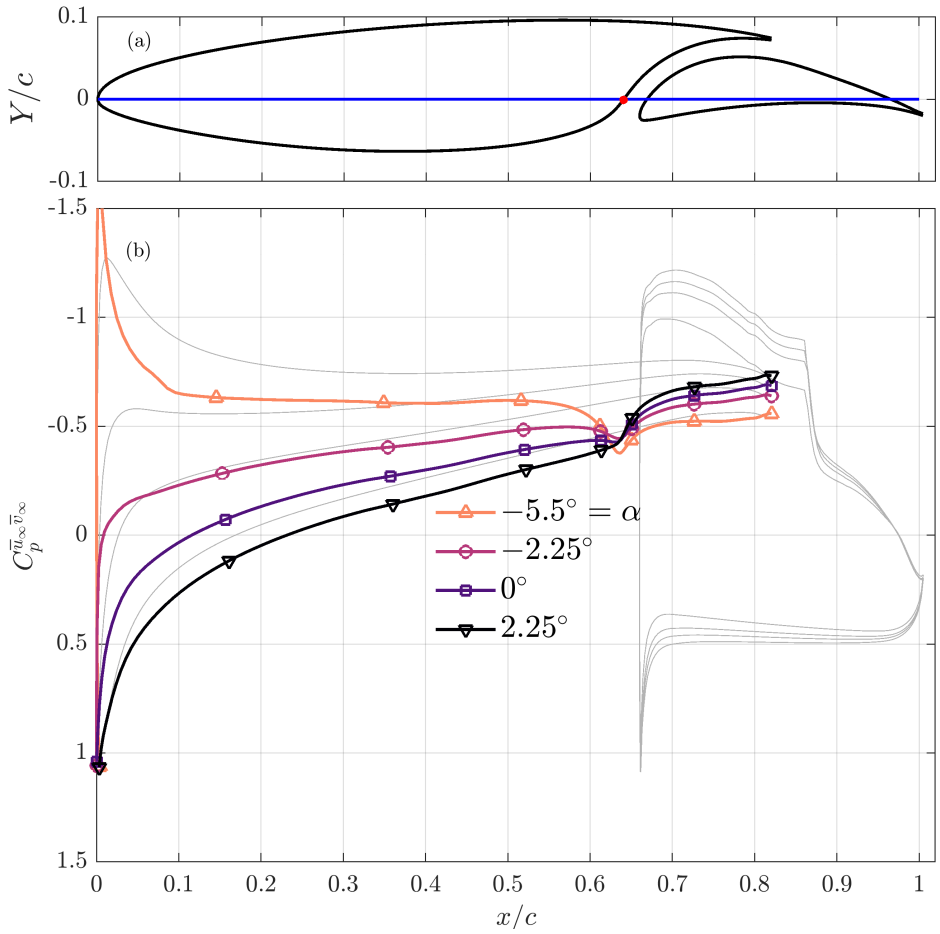

Figure 4.1: (a) The X207.LS geometry plotted with the chord along the x-axis (blue line). The slot entrance is defined with a red dot on the x-axis. (b) Pressure distributions for increasing angles of attack are shown in color for the bottom side of the fore-element for a $0°$ sweep angle. The gray curves represent the pressure distribution for the top side of the same element as well as the aft element [2].

The plot of curvature in Fig. 4.2 indicates that for positive values a convex surface curvature is present while a negative value indicates concave curvature. The location of the slot entrance was defined by the transition from a convex to concave surface geometry, $c/R = 0$. The implications of the slot can be seen strikingly on the Hartree parameter which represents the self-similar pressure gradient. The spike implies a highly favorable pressure gradient in the region of the slot. The shift in pressure gradient is also reflected in the boundary layer, which experiences a slight shrinking in size and the shape factor dipping, which results in a more full boundary layer. Qualitatively,

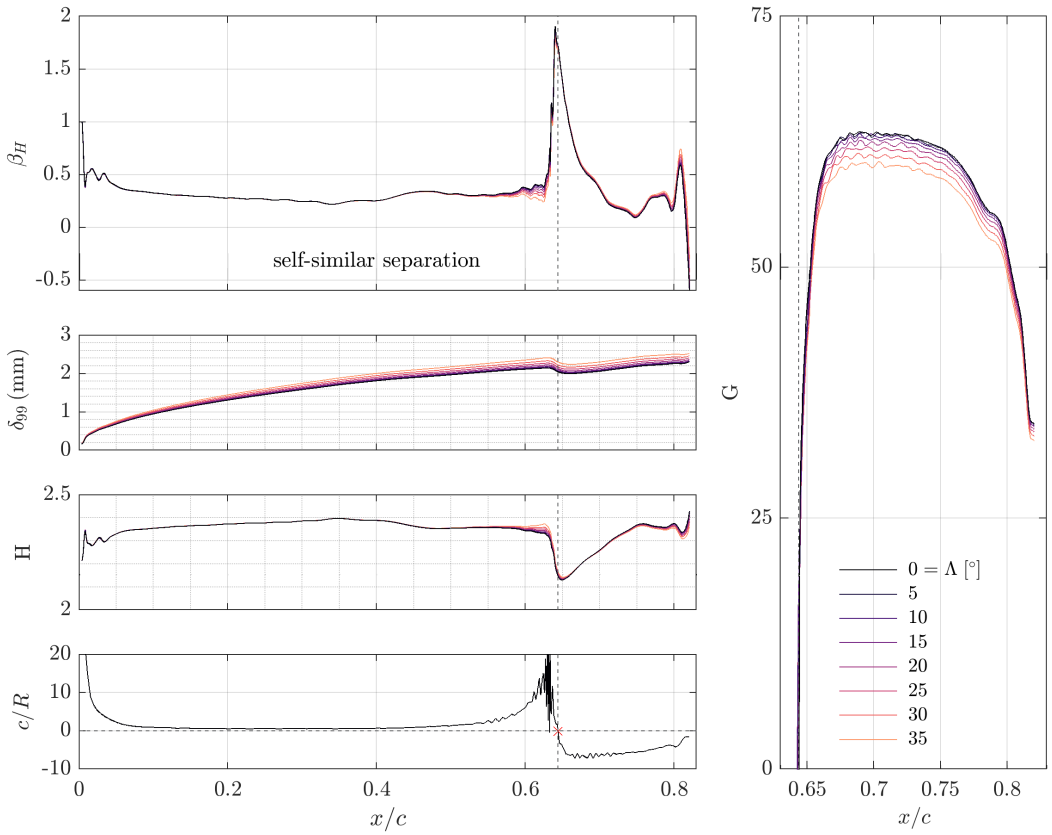

Figure 4.2: Streamwise development of boundary layer parameters for angle of attack $2.25°$. Dashed vertical line indicates the slot entrance defined by $1/R = 0$ (red star) [2].

the increase in sweep does not have a substantial impact on the development of these parameters within the vicinity of the slot.

The Görtler number, G, defines the control parameter for the the Görtler mechanism [44]. As seen in Fig. 4.2, G decreases slightly as the sweep is increased alluding to a stabilizing effect of sweep. However, the variation in the Görtler number is too small as changes in order of magnitude typically indicate a difference in the growth of the Görtler disturbance.

An additional feature of the boundary layer is the presence of a crossflow velocity for cases of non-zero sweep. The crossflow velocity corresponds to the velocity aligned about leading-edge parallel direction, z. The velocity profiles are demonstrated in Fig. 4.3 for x/c stations along the

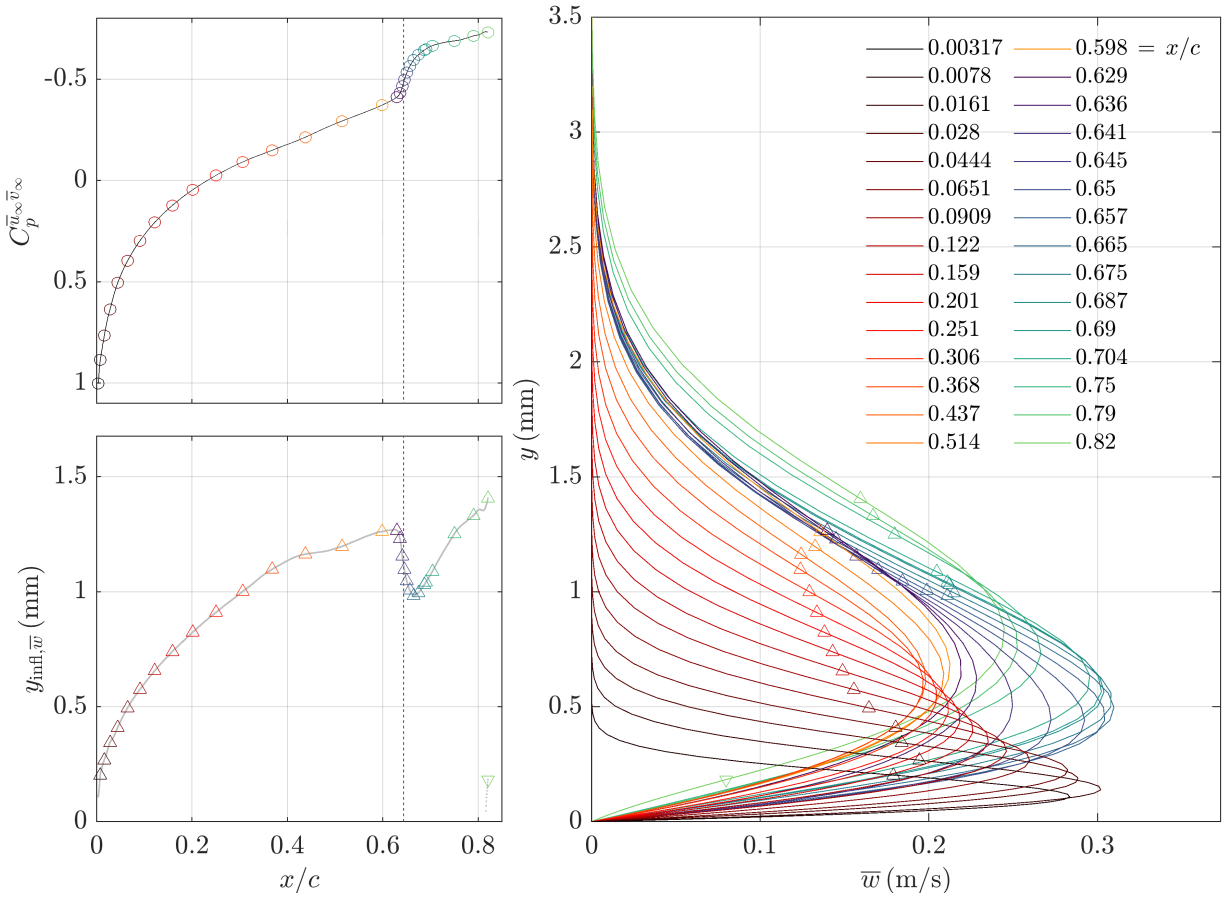

Figure 4.3: Crossflow parameters for $\Lambda = 5°$. (Top left) Pressure coefficient. (Bottom left) Wall-normal location of the crossflow velocity inflection point. (Right) Crossflow-velocity profiles at increasing x/c stations.

entirety of the chord. The crossflow component decreases upstream of the slot due to the convex curvature stifling the pressure gradient. As the flow enters the slot, the pressure gradient becomes more favorable accompanied by a rapid growth in velocity. On the crossflow profile also exists an inflection point which signals the presence of the crossflow instability. The evolution of the inflection point is akin to the boundary-layer heights as the slot has a stabilizing effect on the flow. Near the trailing edge of the airfoil, an additional inflection point emerges; however, it will be neglected as its presence does not affect the stability characteristics of the flow.

4.3 Stability Results

In the following sections, linear and nonlinear stability results for the X207.LS will be presented. In order to isolate specific instability mechanisms two approaches are taken in the initialization of the PSE problem.

Slot-only approach This approach initializes the LST eigenvalue problem at a location just upstream of the slot location. The computational grid consists of 150 streamwise points and 200 wall-normal points. This approach will consider the usage of different initial LST eigenmodes as well. The eigenmodes are defined as *fundamental* and *harmonic* and were chosen by the number of maxima within the $\hat{v}$ LST eigenvector.

Full-chord approach The full chord approach initializes the LST eigenvalue problem near the attachment line of the airfoil. The computational grid will have 750 streamwise points to secure a similar step size with the slot-only approach and 200 wall-normal points.

The following perturbation boundary conditions are imposed at the wall and the freestream defined in Eq. 4.5. The boundary condition for $\hat{\rho}_w$ is defined by the y-momentum equation.

$$\hat{q}_\infty = 0 \tag{4.5a}$$

$$\hat{u}_w = \hat{v}_w = \hat{v}_w = \hat{T}_w = 0 \tag{4.5b}$$

A first-order backwards discretization is used for the streamwise derivatives and a fourth-order central difference is used for the wall-normal derivative.

4.3.1 Linear Stability Results

The LPSE analysis allows for a relatively quick generation of stability characteristics for a broad range of initial frequencies and wavelengths. The frequency in this scenario is the regular frequency or period as defined by $f = 2\pi/\omega$ and the wavelength is defined as $\lambda_z = 2\pi/\beta$, which corresponds to the wavelength in the spanwise direction. Separate frequency and wavelength ranges are considered for slot-only and full-only approaches. These ranges and increments

are indicated in Eqs. 4.6 and 4.7. The parameter range is chosen such that the *N*-factor envelope is captured and the smaller increments indicate a span of higher instability requiring a more resolved parameter sweep. In order to capture unsteady (traveling) disturbance propagation in the positive and negative z-directions, additional simulations are ran with negative values of λ.

$$\mathrm{I\,(Hz)} : 0 \leq f \leq 600 \quad \Delta f = 25; \quad \begin{cases} \mathrm{I\,(mm)} : 0.5 \leq \lambda_z \leq 3.0 & \Delta\lambda_z = 0.25 \\ \mathrm{II\,(mm)} : 3.0 \leq \lambda_z \leq 9.0 & \Delta\lambda_z = 0.5 \end{cases} \tag{4.6}$$

$$\begin{cases} \mathrm{I\,(Hz)} : 0 \leq f \leq 200 & \Delta f = 25 \\ \mathrm{II\,(Hz)} : 200 \leq f \leq 400 & \Delta f = 50 \end{cases}; \quad \mathrm{I\,(mm)} : 2.0 \leq \lambda_z \leq 14.0 \quad \Delta\lambda_z = 1.0 \tag{4.7}$$

The wavelengths for the full-chord approach encompass a larger span due to the presence of crossflow and as indicated previously, crossflow vortex wavelengths are $4\delta_{99}$ as compared to the Görtler vortices at $1\delta_{99}$ [18]. Due to the overlaps in wavelength for the full-chord and slot-only approach, the Görtler mechanism wavelengths are maintained for each case.

An overview of the LPSE results can be found in Fig. 4.4. For these plots, only the *N*-factor envelopes are shown for each sweep case. The red curves indicate an unsteady ($f > 0\,\mathrm{Hz}$) disturbance while the blue curves are steady ($f = 0\,\mathrm{Hz}$). The solid line represents a full-chord solution while the dotted and dashed lines represent slot-only solutions using different initial LST eigenmodes. The full-chord approach was only applied to cases where $\Lambda \geq 20^\circ$ as the boundary layer was not unstable enough to be captured by EPIC. The instability parameters supporting the largest amplifications for the disturbance are presented in appendix B. Parameters not mentioned in the previous analysis include the total wavelength, $\lambda = 2\pi/\sqrt{\alpha_r^2 + \beta^2}$, the non-dimensional wavelength, λ_G, the phase speed scaled about the absolute maximum of the crossflow velocity, $c_{ph}/|\overline{w}_{\max}|$, the wave angle, ψ, and difference between the wave angle and the angle of the inviscid

streamline, $\psi - \psi_s$. The overview figure will answer the following questions:

- How does the presence of a crossflow velocity effect the Görtler mechanism within the slot?
- How does the crossflow disturbance develop upstream of the slot?
- What impact does the upstream presence of crossflow have on the Görtler mechanism within the slotted region?

To answer the first question, the instabilities of the slot-only approach are considered such that only the effect of sweep and the resulting crossflow is in question. Other sweep dependent parameters of the base flow can also be called into question such as the leading-edge orthogonal Reynolds number and the boundary layer; however these effects are deemed inconsequential for the present analysis. For $\Lambda = 0^\circ$ it is undeniable that only the Görtler mechanism is destabilized. This is due to the lack of sweep resulting in no crossflow, a stabilization of the Tollmien-Schlichting mechanism from the favorable pressure gradient [12], and large amplification only in the region of concave curvature. The instability of unsteady disturbances are found to be more amplified. In using different initial eigenmodes, the fundamental mode is found to be either slightly more or just as amplified as its harmonic mode counterpart. With the focus on the increase of crossflow velocity for the slot-only approach, we see that an increase in sweep results in a more stable boundary layer. This is indicated by the consistent decrease in max amplitude for both steady and unsteady disturbances as well as the fundamental and harmonic initializations.

The crossflow disturbance upstream of the slot is plotted as the solid lines in cases which $20^\circ \leq \Lambda \leq 35^\circ$. Although we have shown the presence of the crossflow instability for $\Lambda = 5^\circ$ and the relation to the strong favorable pressure gradient, the convex curvature has a stabilizing effect on the crossflow instability [45] and is considered stable enough to not carry influence into the slotted disturbance ($N \ll 1$). In studying the linearly amplified crossflow disturbances found in highly swept cases, the local maxima of the disturbance upstream of the slot increases consistently. The unsteady disturbance has a larger escalation for the amplitude compared to the steady disturbance.

A sharp stabilization occurs after the maxima is achieved by the crossflow instability. The increase in convex surface curvature is the likely culprit of this occurrence, see Fig. 4.2. This steep decline results in a relatively stable flow field within the vicinity of the slot entrance.

In answering the third bullet point from above, comparisons are made between the slot-only approach and full-chord approach. For the unsteady disturbance a very clear reproduction of the instability is achieved by the full-chord case. This includes the monotonic decrease in amplification due to sweep. A slight discrepancy between the steady envelopes are found, primarily for $\Lambda = 25^\circ$ and $\Lambda = 35^\circ$. The steady full-chord envelopes in Fig. 4.4 suggests a possible destabilization due to sweep.

Do to the low amplification of the full-chord envelopes at the entrance of the slot a shift is performed. This shift will align the neutral point within the region of the slot to be zero and shift ***only the N-factor curves from the secondary neutral point onwards***. Nothing about the stability parameters themselves will be changed. The updated neutral point envelopes are plotted in Fig. 4.5. The unsteady envelopes of the full-chord approach correspond quite well with the slot-only approach. The same cannot be said for the steady case; however, there is a more consistent trend in the initialization approach. The full-chord approach is consistently more amplified by an N-factor of 1 and the monotonic decrease in amplification due to sweep is recovered.

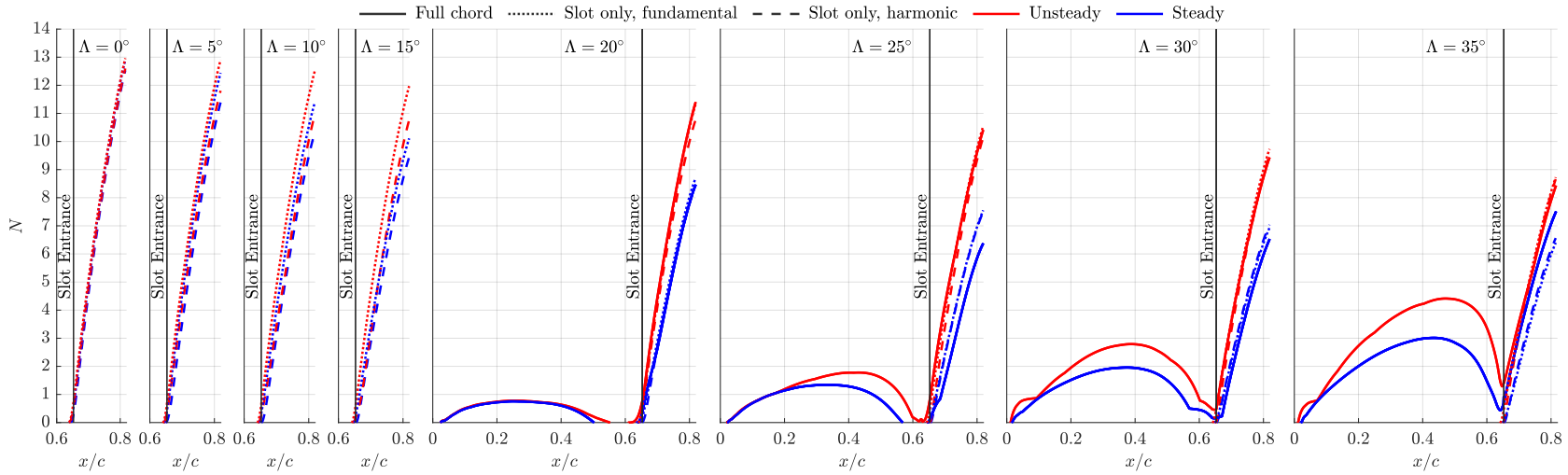

Figure 4.4: N-factor envelopes (steady/unsteady content) versus chordwise position for increasing sweep angles. Full-chord approach initializes LPSE at the attachment line and slot-only approach initializes just upstream the slot entrance. The full-chord envelopes in the slot correspond to *unadjusted neutral points* at the entrance of the slot [2].

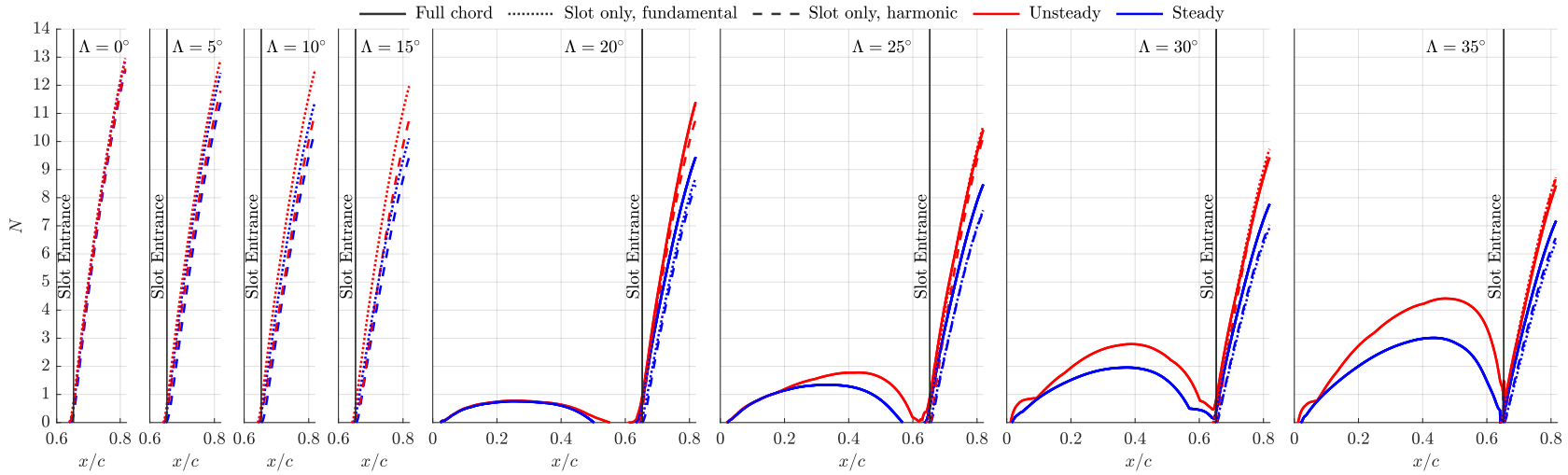

Figure 4.5: N-factor envelopes (steady/unsteady content) versus chordwise position for increasing sweep angles. Full-chord approach initializes LPSE at the attachment line and slot-only approach initializes just upstream the slot entrance. The full-chord envelopes in the slot correspond to *updated neutral points* close to the slot entrance [2].

4.3.2 NPSE Results

Nonlinear stability parameters are produced for the slotted region of the airfoil at 0° sweep. The simulation will study the steady Görtler disturbance by defining 7 harmonics, i.e. $n = 0$ and $1 \leq k \leq 7$, as well as the mean flow distortion, $(n, k) = (0, 0)$. The spanwise wavelength achieving the most amplified linear disturbance within the slow is chosen, see appendix B. As suggested previously, $\alpha_{i,(0.0)} = 0$ for this study to improve convergence of the MFD. The nonlinear forcing vector will allow up to cubic interactions. An initial amplitude for the $(0, 1)$ mode is chosen as 10^{-2} as this amplitude captured the neutral-point such that the entirety of the disturbance growth can be modeled. In the previous LPSE study, the initial location is decided a Newton-Raphson method applied to the LST eigenmode to find the neutral-point location and march from just upstream this point. In the following NPSE analysis, all LST initializations occur at the same location, $x/c = 0.629$. The computational convergence of the NPSE analysis was found to be quite sensitive to the initial LST eigenmode. The spanwise wavelength is chosen from the most amplified N-factor at the end of the domain as found by the LPSE study.

The disturbance amplitudes are presented in Figs. 4.6 and 4.7 for all considered sweep angles. The linear disturbance for the fundamental mode is also superimposed onto the plot as a dashed curve. Three chordwise positions of interest are defined. The first is the neutral point of the fundamental mode, the second is the point of saturation in which the linear disturbance deviates from the nonlinear disturbance, and third is the location at which the MFD overtakes the fundamental mode. Note, in the previous section, the fundamental mode defined the initial LST eigenmode while here it will be used more properly as the $(0, 1)$ mode. Subsequent harmonics are based off of this fundamental mode. The $\Lambda = 0^\circ$ case is most comparable to previous computational results and qualitative matches can be found with Benmalek [14] and Li & Malik [22].

A curious observation is how these points of interest develop as sweep is increased. Fig. 4.8 indicates the position of the neutral point location, saturation point, and location of MFD overtake. The neutral point varies quite little as sweep is increased implying the neutral point is not affected by the increase in crossflow. Interestingly enough, the neutral point also lies slightly downstream

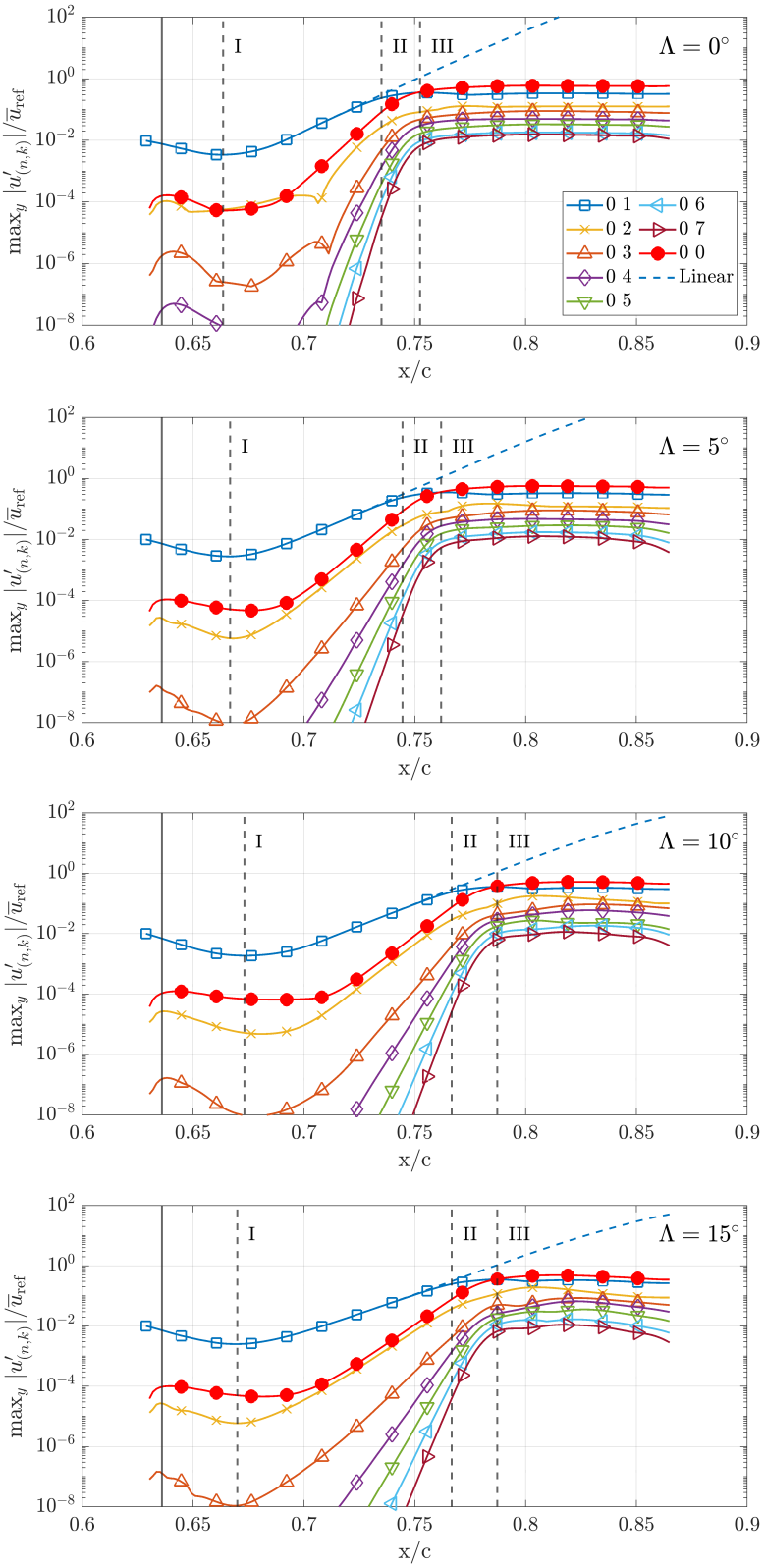

Figure 4.6: Nonlinear disturbance amplitude for u' and associated harmonic modes and linear amplitude of fundamental mode. Solid line indicates the entrance of the slot. The dashed lines indicate: (I) the neutral point of the fundamental mode, (II) the saturation point, and (III) the location at which MFD overtakes the $(0, 1)$ mode. Sweeps $0°$ to $15°$ are presented.

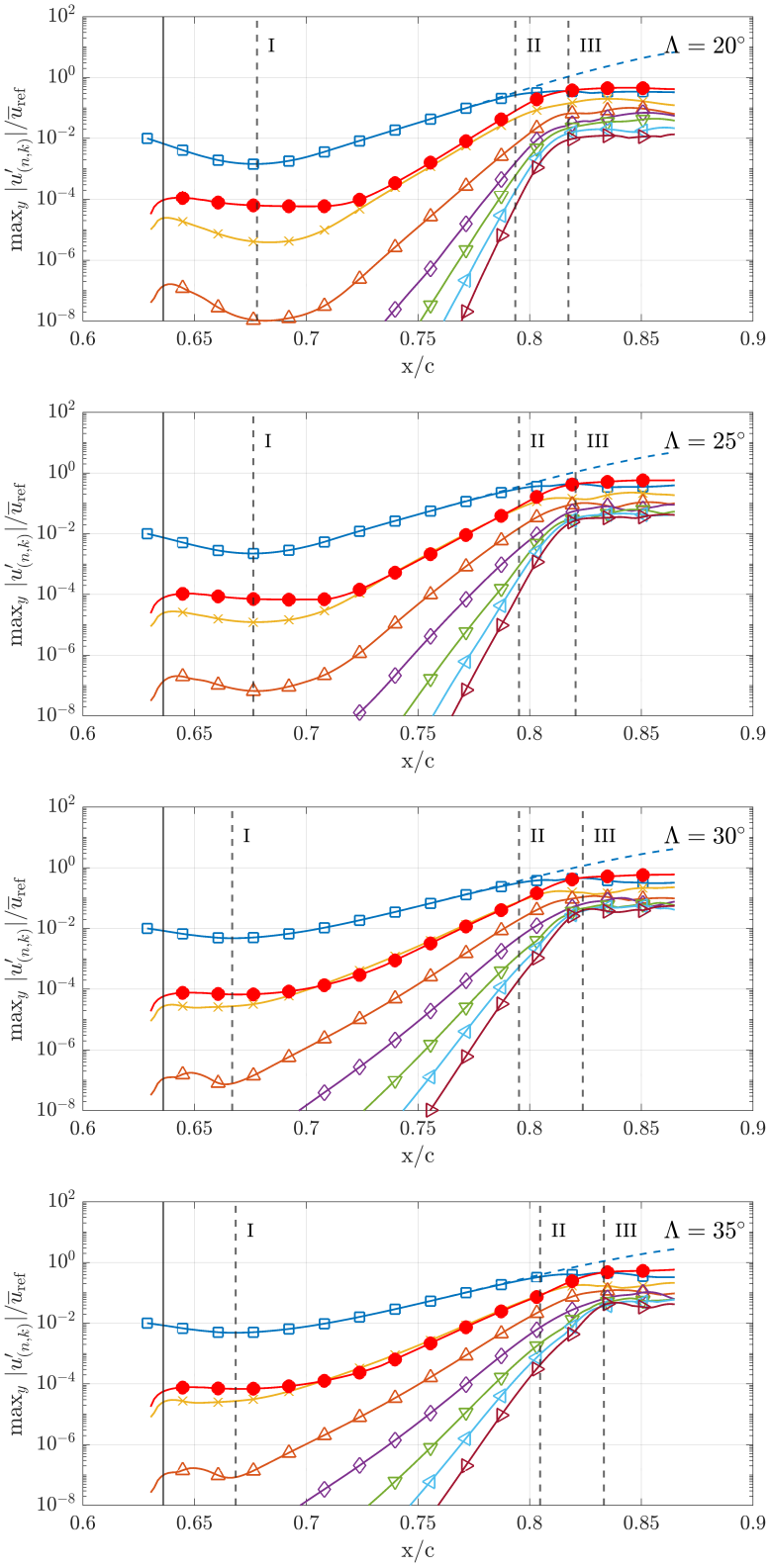

Figure 4.7: Nonlinear disturbance amplitude for u' and associated harmonic modes and linear amplitude of fundamental mode. Solid line indicates the entrance of the slot. The dashed lines indicate: (I) the neutral point of the fundamental mode, (II) the saturation point, and (III) the location at which MFD overtakes the $(0, 1)$ mode. Sweeps $20°$ to $35°$ are presented.

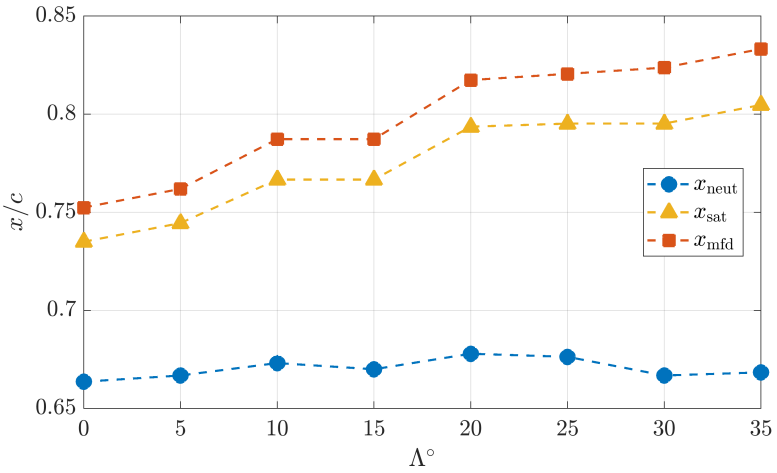

Figure 4.8: Chordwise locations of the fundamental mode neutral point, the saturation location, and the location at which the MFD overtakes the fundamental mode for varying sweep.

of the slot entrance. This differs from the LPSE analysis which indicated a neutral point near or slightly ahead of the slot entrance. The saturation point, which is calculated when the difference between the linear and nonlinear disturbance exceeds 5%, and the MFD overtake exhibit a very similar behavior. The presence of sweep forces nonlinear distortion to occur further downstream. Li & Malik also suggest that a longer wavelength will allow the MFD to overtake the fundamental mode further downstream for the Görtler instability [22]. The LPSE study in the previous section supports this as the most amplified wavelength grows for increasing sweep angles.

Fig. 4.9 illustrates the maximum amplitudes for the fundamental, MFD, and $(0, 2)$ modes. The MFD starts at a high amplitude and gradually decreases until $\Lambda = 25°$ when a large jump in amplitude occurs. A similar trend is seen for the fundamental mode except the amplitude remains constant until the jump at the same sweep angle. There currently is no explanation for the behavior of these two modes. The $(0, 2)$ mode gradually increases in size as sweep is increased.

The streamwise development of the Görtler instability can be seen in Figs. 4.10 and 4.11. The total nondimensional streamwise flow component, $u = \overline{u} + u'$, is mapped out along for increasing sweep angles at various chordwise locations using iso-velocity contours. These chordwise locations correspond to the locations of interest shown previously along with the chordwise position at

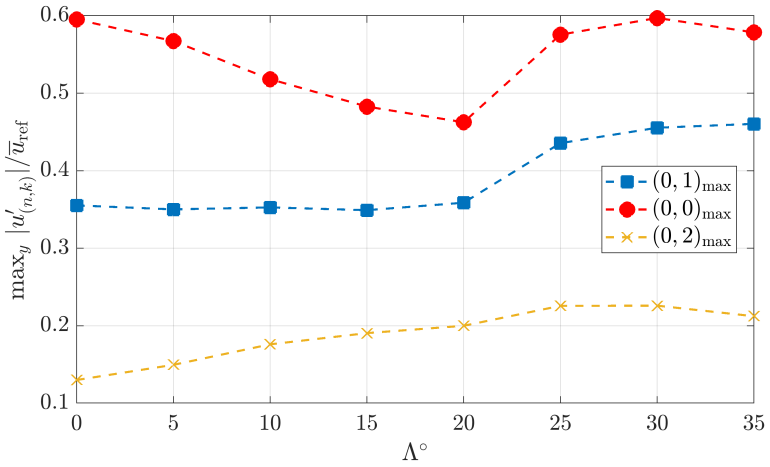

Figure 4.9: Chordwise locations of the fundamental mode neutral point, the saturation location, and the location at which the MFD overtakes the fundamental mode for varying sweep.

the end of the domain.

Focusing on the zero-degree sweep case, the characteristic behavior of the Görtler instability is seen. The second panel from the left shows a linearly disturbed amplification growing and the third panel from the left shows a nonlinearly distorted behavior. This nonlinear distortion is very indicative of the unique 'mushroom' behavior generated by the counter-rotating vortices. These vortices create regions of upwelling and squeezing in the velocity profile. In the region of upwelling flow, the fluid will impart a lower shear stress on the surface while larger shear stresses can be found when the iso-contours are squeezed. The large distortion is a product of large variation in the streamwise momentum. The spanwise wavelength was chosen to be $\lambda = 1.75\mathrm{mm}$ which compares closely to the boundary-layer thickness $\delta \approx 2.5\mathrm{mm}$. This is consistent with previous experimental studies indicating that the Görtler instability wavelength matches closely to the boundary layer thickness [18]. This shape has been well documented in experiments by Peerhossaini [44, 46] using dye injection in a water tunnel. Traveling further downstream to the end of the domain yields more upwelling suggesting a stronger influence of the Görtler mechanism resulting in distorted flow entering further in the free stream.

The sweep angles following zero sweep now include a crossflow component. The addition of

the of crossflow velocity creates a smearing effect on the linear and nonlinear disturbances. Note, due to the analysis of the bottom side of the airfoil, the axes are flipped such that the positive z coordinate moves towards the root of the wing. To resolve this discrepancy, a negative sweep angle must be considered such that the crossflow velocity component is in the direction of the wing tip. This mismatch has no effect on the physics of the flow and is only pointed out to explain why this smearing effect pushes the instability towards $z = 0$. As sweep is increased, this effect becomes more pronounced in the linear and nonlinear regions. In the nonlinearly distorted region, the smear is more distinctly seen when the velocity has upwelled while closer to the wall, the flow maintains a behavior more reminiscent of the case with zero sweep.

Since the saturation of the Görtler mechanism occurs further downstream as sweep is increased, the boundary-layer is allowed to grow for a longer chordwise distance before the nonlinear distortion occurs. However, when nonlinear effects do take hold they do so at this larger boundary-layer thickness.

Upon reaching the end of the domain, the flow is experiencing a highly distorted perturbation that has jettisoned further into the freestream. Within this region, it is difficult to say what mechanisms are dominating the flow as physics undetermined within this thesis may take hold. Swearingen & Blackwelder [47] indicate that the structure of these vortices break down very quickly leading to the onset of turbulence.

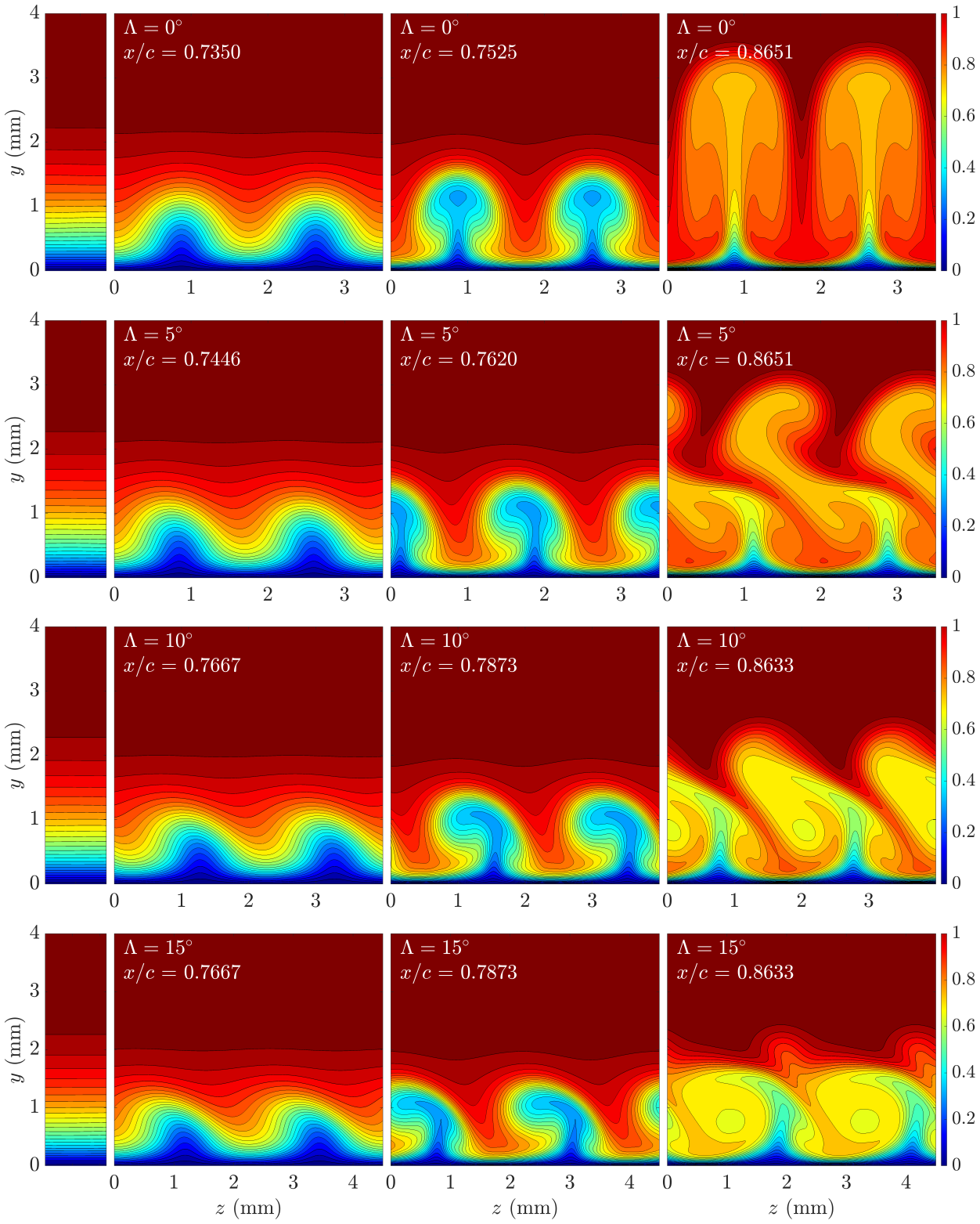

Figure 4.10: Development of the Görtler instability within the slot as seen by the nondimensional u velocity (m/s) for $0° \leq \Lambda \leq 15°$. The furthest right figure indicates laminar flow at the neutral point to provide reference. The second, third and fourth figures represent x/c points at x_{sat}, x_{mfd} and the end of the domain.

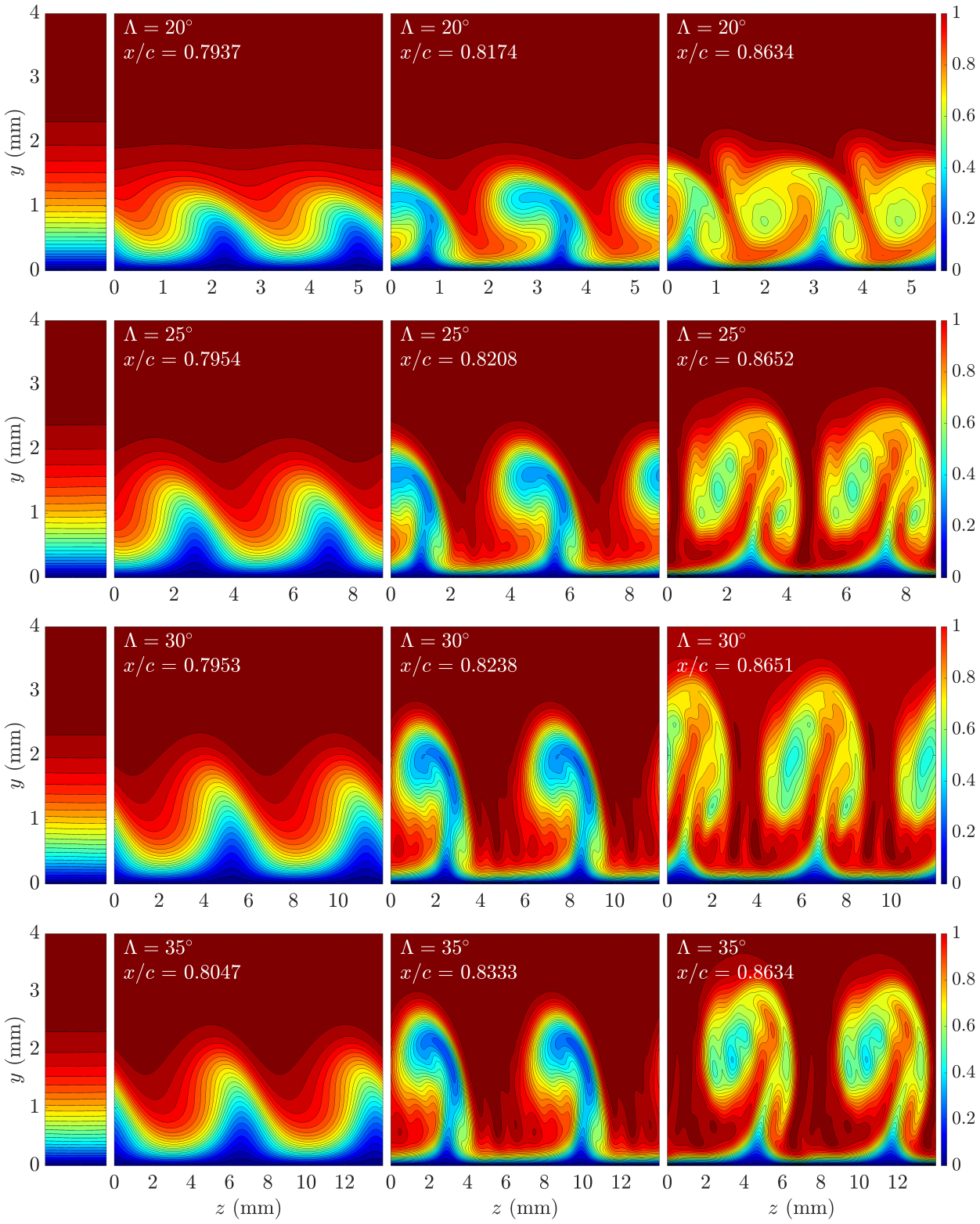

Figure 4.11: Development of the Görtler instability within the slot as seen by the nondimensional u velocity (m/s) for $20° \leq \Lambda \leq 35°$. The furthest right figure indicates laminar flow at the neutral point to provide reference. The second, third and fourth figures represent x/c points at x_{sat}, x_{mfd} and the end of the domain.

5. CONCLUSION

5.1 Cone Configuration

The primary goal of this project is to extend the AFT model into the hypersonic regime. The work of this thesis contributes to this goal by providing a stability solution using the LPSE model to compare performance. Since the AFT model activates turbulence modeling through the use of surrogate indicators, parameters assisting in the development of instability will be identified. An energy-perturbation budget analysis will be performed to assess the behavior of these relevant terms and their relation to the stability parameters as found by LPSE.

For the following stability analysis, a laminar basic state is produced using OVERFLOW. Due to symmetry conditions only half of the cone geometry is necessary to model. Along the span of the cone, multiple streamwise vortex paths are identified and initialized at a location downstream of the blunt nose. Due to the non-zero yaw, the crossflow disturbance is expected to dominate the process of transition. In particular, the stationary crossflow instability has been studied in this thesis.

Using the LPSE analysis, the azimuthal angle and wavenumber combinations leading to the most amplified boundary-layer are identified. An N-factor of 14.5 at the base of the cone has been achieved which was proven to be well within the requirements for transition. This maximum occurs for an azimuthal angle of 148.6° and a wavenumber of 81.9. In contrast, the AFT model only predicts an unstable flow in the vicinity of the leeward plane. It is quite clear that the AFT model, in its current iteration, is unable to predict unstable flow for the crossflow instability in a hypersonic regime.

In order for the AFT model to activate its turbulence modeling, additional information pertaining to the instability is needed. However, the model is unable to calculate stability characteristics such as the ones found by LPSE. Instead, properties of the boundary layer will assist in the activation of the AFT model. With this in mind, budget analysis studies are performed with different

energy-disturbance equations.

When considering the total-perturbation energy, the relation of the energy contributions to the growth rate is characterized by a large Reynolds-flux energy transfer which is destroyed or redistributed by pressure work and dissipation. By quantifying individual terms of the energy budget, a select few terms were found to dominate the flow. In particular, the Reynolds heat-flux term and the temperature-perturbation dissipation values were the largest in magnitude. In considering only these two terms for energy contribution in the streamwise direction, a good approximation of the neutral point can be predicted. The combination of these two terms also results in an approximate growth rate with a high linear correlation to the growth rate defined by LPSE.

The largest terms found in the total-perturbation were terms derived in the conservation of energy. Performing an energy-budget analysis on this disturbance equation proved to be quite trivial for this reason as similar trends to the total-perturbation energy were found.

As this study focuses on the crossflow instability itself, an analysis of the z-momentum equation is performed. In the context of this disturbance, a large Reynolds-flux contribution is found which is balanced strongly by the pressure work contribution.

The current analysis found relations of the stability characteristics to quantities of energy transfer. Of course, this relationship still depends on the stability parameters themselves so the AFT model cannot yet apply these relations. However, in being able to identify large energy contributions, future studies could relate these terms back to the base-flow parameters. Additional possibilities include finding correlations between the disturbance characteristics and the integral parameters that are only base-flow dependent.

5.2 Swept-wing Configuration

As more efficient aircraft are developed, an emphasis on drag reduction encourages a study into mechanisms of transition. To this point, the X207.LS airfoil is developed using the SNLF concept to reduce drag by supporting laminar flow over a substantial portion of the chord. The goal of this project is to assess regions of unstable flow on the bottom side of this airfoil which contains the slotted feature. In defining regions of unstable flow, the mechanisms and disturbance parameters

resulting in unstable flow will be interpreted.

Using MSES pressure distributions and the DEKAF boundary-layer solver, a base flow is generated for increasing sweep at a fixed angle of attack. The angle of attack supports a favorable pressure gradient through the entirety of the bottom side. This angle of attack along with an analysis of the boundary-layer properties, establishes the primary instability mechanisms. For the case with no sweep, the Görtler mechanism is expected to dominate the instability within the slotted region. Considering non-zero sweep introduces a crossflow velocity and more importantly an inflection point of the crossflow profile which can induce the crossflow instability.

Initializing LPSE upstream of the slot allows for an isolation of the crossflow velocity component. Within the neighborhood of the slot, an N-factor of 13 is found for $\Lambda = 0^\circ$ indicating a large Görtler disturbance due to the concave surface curvature without any complications due to crossflow. As sweep is introduced, the instabilities experience a stabilizing effect due to the gradual increase in the crossflow-velocity component.

It is found that from the leading edge to the slot entrance, the crossflow instability is noticeable unstable for higher sweep cases only ($\Lambda \geq 20^\circ$). The destabilization is caused by the strong favorable pressure gradient. However, the convex surface curvature suppresses the growth resulting in a very stable flow field at the entrance of the slot. This stable flow suggests that little to no upstream influence is imparted on the instability mechanisms within the slot. This claim is further supported by the matching of unsteady disturbances from the full-chord approach to the slot-only approach. The steady disturbance comparison still carries some discrepancies, but a qualitative match can still be assessed.

The slot-only, steady instability will be further examined through a nonlinear scope. The LPSE analysis will define the most unstable spanwise wavelength each sweep case. The modal analysis will define the subharmonics as $n = 0$ and $1 \leq k \leq 7$. The largest initial amplitude that captured the neutral point is $A_{(0,1)} = 10^{-2}$. The neutral point remains relatively constant for all sweep angles ($x_{\text{neut}} \approx 0.66$). This location is however further downstream than originally indicated by LPSE. The location at which saturation occurs is documented with the chordwise position for saturation

being pushed further downstream as shown for the case $\Lambda = 0^\circ$ in which saturation occurs at $x/c = 0.74$ while at $\Lambda = 35^\circ$ saturation occurs at $x/c = 0.80$.

A visualization of the flow at various streamwise locations indicates stable, linear, and nonlinear characteristics of the disturbance. The characteristic 'mushroom' shaped instability is a feature caused by the counter-rotating nature of the Görtler vortices. This distortion of flow can lead to regions of higher and lower shear stress possibly characterized by the MFD. Further analysis on the behavior of shear stress on the wall can assist in designating regions of higher drag. Introducing a sweeping feature creates a smearing effect on the velocity distortions which becomes more drastic for larger crossflow velocities. The boundary layer also grows much larger due to the linear instabilities having more chordwise growth before nonlinear saturation occurs for increased sweep angles. At the end of the fore-element, the flow has become highly distorted exhibiting behavior unstudied in this thesis. It is likely that the breakdown in discernible structure implies the onset of transition.

REFERENCES

[1] K. J. Groot, J. Patel, C. Saiyasak, J. G. Coder, D. L. Stefanski, and H. L. Reed, "Assessment of the amplification factor transport transition model for high-mach number flows," in *AIAA AVIATION 2021 FORUM*, p. 2830, 2021.

[2] K. J. Groot, J. Patel, E. S. Beyak, J. G. Coder, and H. L. Reed, "Görtler instability on a variably swept, slotted, natural-laminar-flow airfoil," in *AIAA AVIATION 2021 FORUM*, p. 2590, 2021.

[3] L. M. Mack, "Transition prediction and linear stability theory," *In AGARD Laminar-Turbulent Transition 22 p (SEE N78-14316 05-34*, 1977.

[4] L. M. Mack, "Boundary-layer linear stability theory," tech. rep., California Inst of Tech Pasadena Jet Propulsion Lab, 1984.

[5] T. Herbert, "Parabolized stability equations," *Annual Review of Fluid Mechanics*, vol. 29, no. 1, pp. 245–283, 1997.

[6] F. P. Bertolotti, T. Herbert, and P. Spalart, "Linear and nonlinear stability of the blasius boundary layer," *Journal of fluid mechanics*, vol. 242, pp. 441–474, 1992.

[7] J. G. Coder and M. D. Maughmer, "Computational fluid dynamics compatible transition modeling using an amplification factor transport equation," *AIAA Journal*, Vol. 52, No. 11, 2014, pp. 2506-2512.

[8] J. G. Coder, "Enhancement of the amplification factor transport transition modeling framework," *55th AIAA Aerospace Sciences Meeting*, AIAA Paper 2017-1709, Grapevine, TX, January 2017.

[9] J. G. Coder, "Further development of the amplification factor transport transition model for aerodynamic flows," *AIAA SciTech 2019 Forum*, AIAA Paper 2019-0039, San Diego, CA, January 2019.

[10] D. M. Somers, *Design of a Slotted, Natural-laminar-flow Airfoil for a Transport Aircraft*. National Aeronautics and Space Administration, Langley Research Center, 2019.

[11] J. G. Coder and D. M. Somers, "Design of a slotted, natural-laminar-flow airfoil for commercial transport applications," *Aerospace Science and Technology*, vol. 106, p. 106217, 2020.

[12] R. D. Joslin, "Aircraft laminar flow control," *Annual review of fluid mechanics*, vol. 30, no. 1, pp. 1–29, 1998.

[13] W. S. Saric, "Görtler vortices," *Annual Review of Fluid Mechanics*, vol. 26, no. 1, pp. 379–409, 1994.

[14] A. Benmalek, *Nonlinear development of Görtler vortices over variable curvature walls*. PhD thesis, Arizona State University, 1993.

[15] J. M. Floryan and W. S. Saric, "Stability of gortler vortices in boundary layers," *AIAA journal*, vol. 20, no. 3, pp. 316–324, 1982.

[16] H. L. Reed and W. S. Saric, "Stability of three-dimensional boundary layers," *Annual Review of Fluid Mechanics*, vol. 21, no. 1, pp. 235–284, 1989.

[17] W. S. Saric, H. L. Reed, and E. B. White, "Stability and transition of three-dimensional boundary layers," *Annual review of fluid mechanics*, vol. 35, no. 1, pp. 413–440, 2003.

[18] D. Arnal, "Prediction based on linear theory, in progress in transition modeling," *AGARD Report No. 793*, pp. 2–1, 1993.

[19] M. R. Malik, F. Li, M. M. Choudhari, and C.-L. Chang, "Secondary instability of crossflow vortices and swept-wing boundary-layer transition," *Journal of Fluid Mechanics*, vol. 399, pp. 85–115, 1999.

[20] T. S. Kocian, A. J. Moyes, H. L. Reed, S. A. Craig, W. S. Saric, S. P. Schneider, and J. B. Edelman, "Hypersonic crossflow instability," *Journal of Spacecraft and Rockets*, vol. 56, no. 2, pp. 432–446, 2019.

[21] J. Floryan, "On the görtler instability of boundary layers," *Progress in Aerospace Sciences*, vol. 28, no. 3, pp. 235–271, 1991.

[22] F. Li and M. R. Malik, "Fundamental and subharmonic secondary instabilities of görtler vortices," *Journal of Fluid Mechanics*, vol. 297, pp. 77–100, 1995.

[23] F. M. White and J. Majdalani, *Viscous fluid flow*, vol. 3. McGraw-Hill New York, 2006.

[24] T. S. Haynes, *Nonlinear stability and saturation of crossflow vortices in swept-wing boundary layers*. Arizona State University, 1996.

[25] T. Bridges and P. J. Morris, "Differential eigenvalue problems in which the parameter appears nonlinearly," *Journal of Computational Physics*, vol. 55, no. 3, pp. 437–460, 1984.

[26] L. Zanus, *Numerical study of chemically reacting hypersonic boundary layers by means of non-linear parabolized stability equations*. PhD thesis, 11 2021.

[27] N. B. Oliviero, *EPIC: A new and advanced nonlinear parabolized stability equation solver*. PhD thesis, 2015.

[28] S. Hein, *Nonlinear nonlocal transition analysis*. PhD thesis, 2005.

[29] T. S. Kocian, *Computational hypersonic boundary-layer stability and the validation and verification of EPIC*. PhD thesis, 2018.

[30] A. Moyes, T. S. Kocian, D. Mullen, and H. L. Reed, "Effects of initial disturbance amplitude on hypersonic crossflow instability," in *2018 AIAA Aerospace Sciences Meeting*, p. 1820, 2018.

[31] E. S. Beyak, *Transition Physics and Boundary-Layer Stability: Computational Modeling in Compressible Flow*. Ph.D. Dissertation, Texas A&M University, 2022.

[32] B.-T. Chu, "On the energy transfer to small disturbances in fluid flow (part i)," *Acta Mechanica*, vol. 1, no. 3, pp. 215–234, 1965.

[33] J. Patel, K. J. Groot, C. Saiyasak, J. G. Coder, and D. L. Stefanski, "Energy-budget analysis of the crossflow instability on a hypersonic yawed cone," p. 2830, XXXX.

[34] R. Nichols, R. Tramel, and P. Buning, "Solver and turbulence model upgrades to overflow 2 for unsteady and high-speed applications," in *24th AIAA Applied Aerodynamics Conference*, p. 2824, 2006.

[35] R. H. Nichols and P. G. Buning, "User's manual for overflow 2.1," *University of Alabama at Birmingham, Birmingham, AL*, 2008.

[36] R. Tramel, R. Nichols, and P. Buning, "Addition of improved shock-capturing schemes to overflow 2.1," in *19th AIAA Computational Fluid Dynamics*, p. 3988, 2009.

[37] P. Balakumar and L. Owens, "Stability of hypersonic boundary layers on a cone at an angle of attack," in *40th Fluid Dynamics Conference and Exhibit*, p. 4718, 2010.

[38] A. J. Moyes, *Computational Laminar-to-Turbulent Transition Physics of Complex Three-Dimensional Hypersonic Flow Fields*. PhD thesis, 2019.

[39] S. A. Craig and W. S. Saric, "Crossflow instability in a hypersonic boundary layer," *Journal of Fluid Mechanics*, vol. 808, pp. 224–244, 2016.

[40] M. Drela, "A user's guide to mses 3.05," *Massachusetts Institute of Technology (MIT), Cambridge*, 2007.

[41] E. S. Beyak, K. J. Groot, and H. L. Reed, "Computational stability analysis of a variably swept, slotted natural-laminar-flow airfoil," in *AIAA Scitech 2021 Forum*, p. 0946, 2021.

[42] K. J. Groot, F. Miró Miró, E. S. Beyak, A. Moyes, F. Pinna, and H. L. Reed, "Dekaf: spectral multi-regime basic-state solver for boundary layer stability," in *2018 Fluid Dynamics Conference*, p. 3380, 2018.

[43] M. Malik and S. Orszag, "Efficient computation of the stability of three-dimensional compressible boundary layers," in *14th Fluid and Plasma Dynamics Conference*, p. 1277, 1981.

[44] H. Peerhossaini and J. Wesfreid, "On the inner structure of streamwise görtler rolls," *International journal of heat and fluid flow*, vol. 9, no. 1, pp. 12–18, 1988.

[45] M. Malik and D. Poll, "Effect of curvature on three-dimensional boundary-layer stability," *AIAA journal*, vol. 23, no. 9, pp. 1362–1369, 1985.

[46] H. Peerhossaini, *L'instabilite d'une couche limite sur une paroi concave: les tourbillons de gortler*. PhD thesis, Paris 6, 1987.

[47] J. D. Swearingen and R. F. Blackwelder, "The growth and breakdown of streamwise vortices in the presence of a wall," *Journal of Fluid Mechanics*, vol. 182, pp. 255–290, 1987.

APPENDIX A

BUDGET ANALYSIS STABILITY EQUATIONS

The following set of equations represent the LST and LPSE equations in scalar form. The equations are in order of s-, y-, z-, momentum, conservation of energy, and continuity. The black terms represent terms found in both LST and LPSE. The green terms represent quantities found only in LPSE formulation. The conservation of energy is presented in terms of total enthalpy. The equations are shown in non-dimensional form and have been modified to accommodate the budget analysis tool. In particular, the material derivatives are represented on the left hand side of the equations and scaling factors have been applied to each of the equations such that the coefficient corresponding to the α term on the left hand side is real valued.

A.1 s - Momentum

$$
\begin{aligned}
&\omega\,\overline{\rho}\,\hat{u} - \frac{\alpha\,\overline{\rho}\,\overline{u}\,\hat{u}}{h_1} + \frac{i\,\overline{\rho}\,\overline{u}\,\hat{u}_s}{h_1} = \\
&\frac{\beta\,\overline{\rho}\,\hat{u}\,\overline{w}}{h_3} - i\,\hat{\rho}\,\overline{u}_y\,\overline{v} - i\,\overline{\rho}\,\hat{u}_y\,\overline{v} - i\,\overline{\rho}\,\overline{u}_y\,\hat{v} - \frac{i\,\hat{\rho}\,\overline{u}\,\overline{u}_s}{h_1} - \frac{i\,\overline{\rho}\,\overline{u}_s\,\hat{u}}{h_1} - \frac{i\,h_{1,y}\,\overline{\rho}\,\overline{u}\,\hat{v}}{h_1} + \frac{2\,i\,h_{3,s}\,\overline{\rho}\,\overline{w}\,\hat{w}}{h_1\,h_3} \\
&+\frac{i\,h_{3,s}\,\hat{\rho}\,\overline{w}^2}{h_1\,h_3} - \frac{i\,h_{1,y}\,\overline{\rho}\,\hat{u}\,\overline{v}}{h_1} - \frac{i\,h_{1,y}\,\hat{\rho}\,\overline{u}\,\overline{v}}{h_1} + \frac{\overline{T}\,\alpha\,\hat{\rho}}{\mathrm{M}_e^2\,\gamma_e\,h_1} + \frac{\hat{T}\,\alpha\,\overline{\rho}}{\mathrm{M}_e^2\,\gamma_e\,h_1} - \frac{i\,\Omega_p\,\overline{T}\,\hat{\rho}_s}{\mathrm{M}_e^2\,\gamma_e\,h_1} - \frac{i\,\Omega_p\,\overline{T}_s\,\hat{\rho}}{\mathrm{M}_e^2\,\gamma_e\,h_1} \\
&-\frac{i\,\Omega_p\,\hat{T}\,\overline{\rho}_s}{\mathrm{M}_e^2\,\gamma_e\,h_1} - \frac{i\,\Omega_p\,\hat{T}_s\,\overline{\rho}}{\mathrm{M}_e^2\,\gamma_e\,h_1} - \frac{\Omega_{\mathrm{Re}}\,\hat{T}\,\beta\,\overline{\mu}_{\overline{T}}\,\overline{w}_s}{\mathrm{Re}_e\,h_1\,h_3} - \frac{\Omega_{\mathrm{Re}}\,\hat{T}\,\alpha\,\overline{\lambda}_{\overline{T}}\,\overline{v}_y}{\mathrm{Re}_e\,h_1} + \frac{i\,\hat{T}\,\overline{\mu}_{\overline{T}}\,\overline{u}_{y\,y}}{\mathrm{Re}_e} + \frac{i\,\overline{T}_y\,\hat{T}\,\overline{\mu}_{\overline{T}\,\overline{T}}\,\overline{u}_y}{\mathrm{Re}_e} \\
&+\frac{i\,\hat{T}\,h_{1,y}\,\overline{\mu}_{\overline{T}}\,\overline{u}_y}{\mathrm{Re}_e\,h_1} + \frac{i\,\hat{T}_y\,\overline{\mu}_{\overline{T}}\,\overline{u}_y}{\mathrm{Re}_e} - \frac{2\,\Omega_{\mathrm{Re}}\,\hat{T}\,\alpha\,\overline{\mu}_{\overline{T}}\,\overline{u}_s}{\mathrm{Re}_e\,h_1^2} - \frac{\Omega_{\mathrm{Re}}\,\hat{T}\,\alpha\,\overline{\lambda}_{\overline{T}}\,\overline{u}_s}{\mathrm{Re}_e\,h_1^2} - \frac{i\,\overline{T}_y\,\hat{T}\,h_{1,y}\,\overline{\mu}_{\overline{T}\,\overline{T}}\,\overline{u}}{\mathrm{Re}_e\,h_1} \\
&-\frac{i\,\hat{T}_y\,h_{1,y}\,\overline{\mu}_{\overline{T}}\,\overline{u}}{\mathrm{Re}_e\,h_1} - \frac{i\,\overline{T}_y\,h_{1,y}\,\overline{\mu}_{\overline{T}}\,\hat{u}}{\mathrm{Re}_e\,h_1} + \frac{i\,\Omega_{\mathrm{Re}}\,\overline{T}_y\,\overline{\mu}_{\overline{T}}\,\hat{v}_s}{\mathrm{Re}_e\,h_1} - \frac{\overline{T}_y\,\alpha\,\overline{\mu}_{\overline{T}}\,\hat{v}}{\mathrm{Re}_e\,h_1} + \frac{i\,\overline{T}_y\,\overline{\mu}_{\overline{T}}\,\hat{u}_y}{\mathrm{Re}_e} - \frac{2\,\Omega_{\mathrm{Re}}\,\overline{T}_s\,\alpha\,\overline{\mu}_{\overline{T}}\,\hat{u}}{\mathrm{Re}_e\,h_1^2} \\
&-\frac{\Omega_{\mathrm{Re}}\,\overline{T}_s\,\beta\,\overline{\lambda}_{\overline{T}}\,\hat{w}}{\mathrm{Re}_e\,h_1\,h_3} + \frac{i\,\Omega_{\mathrm{Re}}\,\overline{T}_s\,\overline{\lambda}_{\overline{T}}\,\hat{v}_y}{\mathrm{Re}_e\,h_1} - \frac{\Omega_{\mathrm{Re}}\,\overline{T}_s\,\alpha\,\overline{\lambda}_{\overline{T}}\,\hat{u}}{\mathrm{Re}_e\,h_1^2} - \frac{3\,\alpha\,h_{1,y}\,\overline{\mu}\,\hat{v}}{\mathrm{Re}_e\,h_1^2} + \frac{i\,h_{1,y}\,\overline{\mu}\,\hat{u}_y}{\mathrm{Re}_e\,h_1} - \frac{\Omega_{\mathrm{Re}}\,\beta\,\overline{\mu}\,\hat{w}_s}{\mathrm{Re}_e\,h_1\,h_3} \\
&-\frac{i\,\alpha\,\beta\,\overline{\mu}\,\hat{w}}{\mathrm{Re}_e\,h_1\,h_3} - \frac{\alpha\,\overline{\mu}\,\hat{v}_y}{\mathrm{Re}_e\,h_1} + \frac{i\,\Omega_{\mathrm{Re}}\,\overline{\mu}\,\hat{v}_{s\,y}}{\mathrm{Re}_e\,h_1} + \frac{i\,\overline{\mu}\,\hat{u}_{y\,y}}{\mathrm{Re}_e} - \frac{4\,\Omega_{\mathrm{Re}}\,\alpha\,\overline{\mu}\,\hat{u}_s}{\mathrm{Re}_e\,h_1^2} - \frac{i\,\beta^2\,\overline{\mu}\,\hat{u}}{\mathrm{Re}_e\,h_3^2} - \frac{2\,\Omega_{\mathrm{Re}}\,\alpha_s\,\overline{\mu}\,\hat{u}}{\mathrm{Re}_e\,h_1^2} \\
&-\frac{2\,i\,\alpha^2\,\overline{\mu}\,\hat{u}}{\mathrm{Re}_e\,h_1^2} - \frac{\alpha\,h_{1,y}\,\overline{\lambda}\,\hat{v}}{\mathrm{Re}_e\,h_1^2} - \frac{\Omega_{\mathrm{Re}}\,\beta\,\overline{\lambda}\,\hat{w}_s}{\mathrm{Re}_e\,h_1\,h_3} - \frac{i\,\alpha\,\beta\,\overline{\lambda}\,\hat{w}}{\mathrm{Re}_e\,h_1\,h_3} - \frac{\alpha\,\overline{\lambda}\,\hat{v}_y}{\mathrm{Re}_e\,h_1} + \frac{i\,\Omega_{\mathrm{Re}}\,\overline{\lambda}\,\hat{v}_{s\,y}}{\mathrm{Re}_e\,h_1} - \frac{2\,\Omega_{\mathrm{Re}}\,\alpha\,\overline{\lambda}\,\hat{u}_s}{\mathrm{Re}_e\,h_1^2} \\
&-\frac{\Omega_{\mathrm{Re}}\,\alpha_s\,\overline{\lambda}\,\hat{u}}{\mathrm{Re}_e\,h_1^2} - \frac{i\,\alpha^2\,\overline{\lambda}\,\hat{u}}{\mathrm{Re}_e\,h_1^2} + \frac{3\,\Omega_{\mathrm{Re}}\,\beta\,h_{3,s}\,\overline{\mu}\,\hat{w}}{\mathrm{Re}_e\,h_1\,h_3^2} + \frac{\Omega_{\mathrm{Re}}\,\beta\,h_{3,s}\,\overline{\lambda}\,\hat{w}}{\mathrm{Re}_e\,h_1\,h_3^2} + \frac{\Omega_{\mathrm{Re}}\,\hat{T}\,\beta\,h_{3,s}\,\overline{\mu}_{\overline{T}}\,\overline{w}}{\mathrm{Re}_e\,h_1\,h_3^2} \\
&+\frac{i\,\Omega_{\mathrm{Re}}\,h_{3,y}\,\overline{\mu}\,\hat{v}_s}{\mathrm{Re}_e\,h_1\,h_3} + \frac{3\,i\,\Omega_{\mathrm{Re}}\,h_{1,y}\,\overline{\mu}\,\hat{v}_s}{\mathrm{Re}_e\,h_1^2} + \frac{i\,\Omega_{\mathrm{Re}}\,h_{3,y}\,\overline{\lambda}\,\hat{v}_s}{\mathrm{Re}_e\,h_1\,h_3} + \frac{i\,\Omega_{\mathrm{Re}}\,h_{1,y}\,\overline{\lambda}\,\hat{v}_s}{\mathrm{Re}_e\,h_1^2} + \frac{2\,i\,\Omega_{\mathrm{Re}}\,\overline{T}_s\,h_{1,y}\,\overline{\mu}_{\overline{T}}\,\hat{v}}{\mathrm{Re}_e\,h_1^2} \\
&-\frac{2\,i\,\Omega_{\mathrm{Re}}\,h_{3,s}\,h_{3,y}\,\overline{\mu}\,\hat{v}}{\mathrm{Re}_e\,h_1\,h_3^2} + \frac{2\,i\,\Omega_{\mathrm{Re}}\,h_{1,y}\,h_{3,s}\,\overline{\mu}\,\hat{v}}{\mathrm{Re}_e\,h_1^2\,h_3} - \frac{2\,i\,\Omega_{\mathrm{Re}}\,h_{1,s}\,h_{1,y}\,\overline{\mu}\,\hat{v}}{\mathrm{Re}_e\,h_1^3} - \frac{\alpha\,h_{3,y}\,\overline{\mu}\,\hat{v}}{\mathrm{Re}_e\,h_1\,h_3} + \frac{2\,i\,\Omega_{\mathrm{Re}}\,h_{1,s\,y}\,\overline{\mu}\,\hat{v}}{\mathrm{Re}_e\,h_1^2} \\
&+\frac{i\,\Omega_{\mathrm{Re}}\,\overline{T}_s\,h_{3,y}\,\overline{\lambda}_{\overline{T}}\,\hat{v}}{\mathrm{Re}_e\,h_1\,h_3} + \frac{i\,\Omega_{\mathrm{Re}}\,\overline{T}_s\,h_{1,y}\,\overline{\lambda}_{\overline{T}}\,\hat{v}}{\mathrm{Re}_e\,h_1^2} - \frac{i\,\Omega_{\mathrm{Re}}\,h_{3,s}\,h_{3,y}\,\overline{\lambda}\,\hat{v}}{\mathrm{Re}_e\,h_1\,h_3^2} + \frac{i\,\Omega_{\mathrm{Re}}\,h_{3,s\,y}\,\overline{\lambda}\,\hat{v}}{\mathrm{Re}_e\,h_1\,h_3} \\
&-\frac{i\,\Omega_{\mathrm{Re}}\,h_{1,s}\,h_{1,y}\,\overline{\lambda}\,\hat{v}}{\mathrm{Re}_e\,h_1^3} - \frac{\alpha\,h_{3,y}\,\overline{\lambda}\,\hat{v}}{\mathrm{Re}_e\,h_1\,h_3} + \frac{i\,\Omega_{\mathrm{Re}}\,h_{1,s\,y}\,\overline{\lambda}\,\hat{v}}{\mathrm{Re}_e\,h_1^2} - \frac{2\,\Omega_{\mathrm{Re}}\,\hat{T}\,\alpha\,h_{1,y}\,\overline{\mu}_{\overline{T}}\,\overline{v}}{\mathrm{Re}_e\,h_1^2} - \frac{\Omega_{\mathrm{Re}}\,\hat{T}\,\alpha\,h_{3,y}\,\overline{\lambda}_{\overline{T}}\,\overline{v}}{\mathrm{Re}_e\,h_1\,h_3} \\
&+\frac{i\,h_{3,y}\,\overline{\mu}\,\hat{u}_y}{\mathrm{Re}_e\,h_3} - \frac{\Omega_{\mathrm{Re}}\,\hat{T}\,\alpha\,h_{1,y}\,\overline{\lambda}_{\overline{T}}\,\overline{v}}{\mathrm{Re}_e\,h_1^2} - \frac{i\,h_{1,y}\,h_{3,y}\,\overline{\mu}\,\hat{u}}{\mathrm{Re}_e\,h_1\,h_3} - \frac{2\,\Omega_{\mathrm{Re}}\,\alpha\,h_{3,s}\,\overline{\mu}\,\hat{u}}{\mathrm{Re}_e\,h_1^2\,h_3} - \frac{i\,h_{1,y\,y}\,\overline{\mu}\,\hat{u}}{\mathrm{Re}_e\,h_1} - \frac{i\,\left(h_{1,y}\right)^2\,\overline{\mu}\,\hat{u}}{\mathrm{Re}_e\,h_1^2} \\
&+\frac{2\,\Omega_{\mathrm{Re}}\,\alpha\,h_{1,s}\,\overline{\mu}\,\hat{u}}{\mathrm{Re}_e\,h_1^3} - \frac{\Omega_{\mathrm{Re}}\,\alpha\,h_{3,s}\,\overline{\lambda}\,\hat{u}}{\mathrm{Re}_e\,h_1^2\,h_3} + \frac{\Omega_{\mathrm{Re}}\,\alpha\,h_{1,s}\,\overline{\lambda}\,\hat{u}}{\mathrm{Re}_e\,h_1^3} + \frac{i\,\hat{T}\,h_{3,y}\,\overline{\mu}_{\overline{T}}\,\overline{u}_y}{\mathrm{Re}_e\,h_3} - \frac{i\,\hat{T}\,h_{1,y}\,h_{3,y}\,\overline{\mu}_{\overline{T}}\,\overline{u}}{\mathrm{Re}_e\,h_1\,h_3} \\
&-\frac{i\,\hat{T}\,h_{1,y\,y}\,\overline{\mu}_{\overline{T}}\,\overline{u}}{\mathrm{Re}_e\,h_1} - \frac{i\,\hat{T}\,\left(h_{1,y}\right)^2\,\overline{\mu}_{\overline{T}}\,\overline{u}}{\mathrm{Re}_e\,h_1^2} - \frac{\Omega_{\mathrm{Re}}\,\hat{T}\,\alpha\,h_{3,s}\,\overline{\lambda}_{\overline{T}}\,\overline{u}}{\mathrm{Re}_e\,h_1^2\,h_3}
\end{aligned}
$$

A.2 y - Momentum

$$
\begin{aligned}
&\omega\,\overline{\rho}\,\hat{v} - \frac{\alpha\,\overline{\rho}\,\overline{u}\,\hat{v}}{h_1} + \frac{i\,\overline{\rho}\,\overline{u}\,\hat{v}_s}{h_1} = \\
&+\frac{2\,i\,h_{3,y}\,\overline{\rho}\,\overline{w}\,\hat{w}}{h_3} + \frac{i\,h_{3,y}\,\hat{\rho}\,\overline{w}^2}{h_3} + \frac{\beta\,\overline{\rho}\,\hat{v}\,\overline{w}}{h_3} - i\,\overline{\rho}\,\overline{v}_y\,\hat{v} - i\,\overline{\rho}\,\overline{v}\,\hat{v}_y + \frac{i\,h_{1,y}\,\hat{\rho}\,\overline{u}^2}{h_1} + \frac{2\,i\,h_{1,y}\,\overline{\rho}\,\overline{u}\,\hat{u}}{h_1} \\
&-\frac{i\,\overline{T}\,\hat{\rho}_y}{\mathrm{M}_e^2\,\gamma_e} - \frac{i\,\overline{T}_y\,\hat{\rho}}{\mathrm{M}_e^2\,\gamma_e} - \frac{i\,\hat{T}\,\overline{\rho}_y}{\mathrm{M}_e^2\,\gamma_e} - \frac{i\,\hat{T}_y\,\overline{\rho}}{\mathrm{M}_e^2\,\gamma_e} - \frac{\hat{T}\,\beta\,\overline{\mu}_{\overline{T}}\,\overline{w}_y}{\mathrm{Re}_e\,h_3} + \frac{2\,i\,\Omega_{\mathrm{Re}}\,\hat{T}\,\overline{\mu}_{\overline{T}}\,\overline{v}_{y\,y}}{\mathrm{Re}_e} + \frac{i\,\Omega_{\mathrm{Re}}\,\hat{T}\,\overline{\lambda}_{\overline{T}}\,\overline{v}_{y\,y}}{\mathrm{Re}_e} \\
&+\frac{2\,i\,\Omega_{\mathrm{Re}}\,\overline{T}_y\,\hat{T}\,\overline{\mu}_{\overline{T}\,\overline{T}}\,\overline{v}_y}{\mathrm{Re}_e} + \frac{i\,\Omega_{\mathrm{Re}}\,\overline{T}_y\,\hat{T}\,\overline{\lambda}_{\overline{T}\,\overline{T}}\,\overline{v}_y}{\mathrm{Re}_e} + \frac{2\,i\,\Omega_{\mathrm{Re}}\,\hat{T}_y\,\overline{\mu}_{\overline{T}}\,\overline{v}_y}{\mathrm{Re}_e} + \frac{i\,\Omega_{\mathrm{Re}}\,\hat{T}_y\,\overline{\lambda}_{\overline{T}}\,\overline{v}_y}{\mathrm{Re}_e} \\
&+\frac{i\,\Omega_{\mathrm{Re}}\,\overline{T}_s\,\hat{T}\,\overline{\mu}_{\overline{T}\,\overline{T}}\,\overline{u}_y}{\mathrm{Re}_e\,h_1} + \frac{i\,\Omega_{\mathrm{Re}}\,\hat{T}_s\,\overline{\mu}_{\overline{T}}\,\overline{u}_y}{\mathrm{Re}_e\,h_1} - \frac{\hat{T}\,\alpha\,\overline{\mu}_{\overline{T}}\,\overline{u}_y}{\mathrm{Re}_e\,h_1} + \frac{i\,\Omega_{\mathrm{Re}}\,\hat{T}\,\overline{\mu}_{\overline{T}}\,\overline{u}_{s\,y}}{\mathrm{Re}_e\,h_1} + \frac{i\,\Omega_{\mathrm{Re}}\,\hat{T}\,\overline{\lambda}_{\overline{T}}\,\overline{u}_{s\,y}}{\mathrm{Re}_e\,h_1} \\
&+\frac{i\,\Omega_{\mathrm{Re}}\,\overline{T}_y\,\hat{T}\,\overline{\lambda}_{\overline{T}\,\overline{T}}\,\overline{u}_s}{\mathrm{Re}_e\,h_1} + \frac{i\,\Omega_{\mathrm{Re}}\,\hat{T}_y\,\overline{\lambda}_{\overline{T}}\,\overline{u}_s}{\mathrm{Re}_e\,h_1} + \frac{\hat{T}\,\alpha\,h_{1,y}\,\overline{\mu}_{\overline{T}}\,\overline{u}}{\mathrm{Re}_e\,h_1^2} + \frac{2\,i\,\overline{T}_y\,\overline{\mu}_{\overline{T}}\,\hat{v}_y}{\mathrm{Re}_e} + \frac{i\,\overline{T}_y\,h_{1,y}\,\overline{\lambda}_{\overline{T}}\,\hat{v}}{\mathrm{Re}_e\,h_1} \\
&-\frac{\overline{T}_y\,\beta\,\overline{\lambda}_{\overline{T}}\,\hat{w}}{\mathrm{Re}_e\,h_3} + \frac{i\,\overline{T}_y\,\overline{\lambda}_{\overline{T}}\,\hat{v}_y}{\mathrm{Re}_e} + \frac{i\,\Omega_{\mathrm{Re}}\,\overline{T}_y\,\overline{\lambda}_{\overline{T}}\,\hat{u}_s}{\mathrm{Re}_e\,h_1} - \frac{\overline{T}_y\,\alpha\,\overline{\lambda}_{\overline{T}}\,\hat{u}}{\mathrm{Re}_e\,h_1} - \frac{\Omega_{\mathrm{Re}}\,\overline{T}_s\,\alpha\,\overline{\mu}_{\overline{T}}\,\hat{v}}{\mathrm{Re}_e\,h_1^2} + \frac{i\,\Omega_{\mathrm{Re}}\,\overline{T}_s\,\overline{\mu}_{\overline{T}}\,\hat{u}_y}{\mathrm{Re}_e\,h_1} \\
&+\frac{2\,i\,h_{1,y}\,\overline{\mu}\,\hat{v}_y}{\mathrm{Re}_e\,h_1} + \frac{3\,\alpha\,h_{1,y}\,\overline{\mu}\,\hat{u}}{\mathrm{Re}_e\,h_1^2} - \frac{\beta\,\overline{\mu}\,\hat{w}_y}{\mathrm{Re}_e\,h_3} + \frac{2\,i\,\overline{\mu}\,\hat{v}_{y\,y}}{\mathrm{Re}_e} - \frac{2\,\Omega_{\mathrm{Re}}\,\alpha\,\overline{\mu}\,\hat{v}_s}{\mathrm{Re}_e\,h_1^2} - \frac{i\,\beta^2\,\overline{\mu}\,\hat{v}}{\mathrm{Re}_e\,h_3^2} - \frac{\Omega_{\mathrm{Re}}\,\alpha_s\,\overline{\mu}\,\hat{v}}{\mathrm{Re}_e\,h_1^2} \\
&-\frac{i\,\alpha^2\,\overline{\mu}\,\hat{v}}{\mathrm{Re}_e\,h_1^2} - \frac{\alpha\,\overline{\mu}\,\hat{u}_y}{\mathrm{Re}_e\,h_1} + \frac{i\,\Omega_{\mathrm{Re}}\,\overline{\mu}\,\hat{u}_{s\,y}}{\mathrm{Re}_e\,h_1} + \frac{i\,h_{1,y}\,\overline{\lambda}\,\hat{v}_y}{\mathrm{Re}_e\,h_1} + \frac{\alpha\,h_{1,y}\,\overline{\lambda}\,\hat{u}}{\mathrm{Re}_e\,h_1^2} - \frac{\beta\,\overline{\lambda}\,\hat{w}_y}{\mathrm{Re}_e\,h_3} + \frac{i\,\overline{\lambda}\,\hat{v}_{y\,y}}{\mathrm{Re}_e} - \frac{\alpha\,\overline{\lambda}\,\hat{u}_y}{\mathrm{Re}_e\,h_1} \\
&+\frac{i\,\Omega_{\mathrm{Re}}\,\overline{\lambda}\,\hat{u}_{s\,y}}{\mathrm{Re}_e\,h_1} + \frac{3\,\beta\,h_{3,y}\,\overline{\mu}\,\hat{w}}{\mathrm{Re}_e\,h_3^2} + \frac{\beta\,h_{3,y}\,\overline{\lambda}\,\hat{w}}{\mathrm{Re}_e\,h_3^2} + \frac{\hat{T}\,\beta\,h_{3,y}\,\overline{\mu}_{\overline{T}}\,\overline{w}}{\mathrm{Re}_e\,h_3^2} + \frac{2\,i\,h_{3,y}\,\overline{\mu}\,\hat{v}_y}{\mathrm{Re}_e\,h_3} + \frac{i\,h_{3,y}\,\overline{\lambda}\,\hat{v}_y}{\mathrm{Re}_e\,h_3} \\
&-\frac{2\,i\,\left(h_{3,y}\right)^2\,\overline{\mu}\,\hat{v}}{\mathrm{Re}_e\,h_3^2} - \frac{\Omega_{\mathrm{Re}}\,\alpha\,h_{3,s}\,\overline{\mu}\,\hat{v}}{\mathrm{Re}_e\,h_1^2\,h_3} - \frac{2\,i\,\left(h_{1,y}\right)^2\,\overline{\mu}\,\hat{v}}{\mathrm{Re}_e\,h_1^2} + \frac{\Omega_{\mathrm{Re}}\,\alpha\,h_{1,s}\,\overline{\mu}\,\hat{v}}{\mathrm{Re}_e\,h_1^3} + \frac{i\,\overline{T}_y\,h_{3,y}\,\overline{\lambda}_{\overline{T}}\,\hat{v}}{\mathrm{Re}_e\,h_3} + \frac{i\,h_{3,y\,y}\,\overline{\lambda}\,\hat{v}}{\mathrm{Re}_e\,h_3} \\
&-\frac{i\,\left(h_{3,y}\right)^2\,\overline{\lambda}\,\hat{v}}{\mathrm{Re}_e\,h_3^2} + \frac{i\,h_{1,y\,y}\,\overline{\lambda}\,\hat{v}}{\mathrm{Re}_e\,h_1} - \frac{i\,\left(h_{1,y}\right)^2\,\overline{\lambda}\,\hat{v}}{\mathrm{Re}_e\,h_1^2} + \frac{2\,i\,\Omega_{\mathrm{Re}}\,\hat{T}\,h_{3,y}\,\overline{\mu}_{\overline{T}}\,\overline{v}_y}{\mathrm{Re}_e\,h_3} + \frac{2\,i\,\Omega_{\mathrm{Re}}\,\hat{T}\,h_{1,y}\,\overline{\mu}_{\overline{T}}\,\overline{v}_y}{\mathrm{Re}_e\,h_1} \\
&+\frac{i\,\Omega_{\mathrm{Re}}\,\hat{T}\,h_{3,y}\,\overline{\lambda}_{\overline{T}}\,\overline{v}_y}{\mathrm{Re}_e\,h_3} + \frac{i\,\Omega_{\mathrm{Re}}\,\hat{T}\,h_{1,y}\,\overline{\lambda}_{\overline{T}}\,\overline{v}_y}{\mathrm{Re}_e\,h_1} - \frac{2\,i\,\Omega_{\mathrm{Re}}\,\hat{T}\,\left(h_{3,y}\right)^2\,\overline{\mu}_{\overline{T}}\,\overline{v}}{\mathrm{Re}_e\,h_3^2} - \frac{2\,i\,\Omega_{\mathrm{Re}}\,\hat{T}\,\left(h_{1,y}\right)^2\,\overline{\mu}_{\overline{T}}\,\overline{v}}{\mathrm{Re}_e\,h_1^2} \\
&+\frac{i\,\Omega_{\mathrm{Re}}\,\overline{T}_y\,\hat{T}\,h_{3,y}\,\overline{\lambda}_{\overline{T}\,\overline{T}}\,\overline{v}}{\mathrm{Re}_e\,h_3} + \frac{i\,\Omega_{\mathrm{Re}}\,\overline{T}_y\,\hat{T}\,h_{1,y}\,\overline{\lambda}_{\overline{T}\,\overline{T}}\,\overline{v}}{\mathrm{Re}_e\,h_1} + \frac{i\,\Omega_{\mathrm{Re}}\,\hat{T}\,h_{3,y\,y}\,\overline{\lambda}_{\overline{T}}\,\overline{v}}{\mathrm{Re}_e\,h_3} - \frac{i\,\Omega_{\mathrm{Re}}\,\hat{T}\,\left(h_{3,y}\right)^2\,\overline{\lambda}_{\overline{T}}\,\overline{v}}{\mathrm{Re}_e\,h_3^2} \\
&+\frac{i\,\Omega_{\mathrm{Re}}\,\hat{T}_y\,h_{3,y}\,\overline{\lambda}_{\overline{T}}\,\overline{v}}{\mathrm{Re}_e\,h_3} + \frac{i\,\Omega_{\mathrm{Re}}\,\hat{T}\,h_{1,y\,y}\,\overline{\lambda}_{\overline{T}}\,\overline{v}}{\mathrm{Re}_e\,h_1} - \frac{i\,\Omega_{\mathrm{Re}}\,\hat{T}\,\left(h_{1,y}\right)^2\,\overline{\lambda}_{\overline{T}}\,\overline{v}}{\mathrm{Re}_e\,h_1^2} + \frac{i\,\Omega_{\mathrm{Re}}\,\hat{T}_y\,h_{1,y}\,\overline{\lambda}_{\overline{T}}\,\overline{v}}{\mathrm{Re}_e\,h_1} \\
&+\frac{i\,\Omega_{\mathrm{Re}}\,h_{3,s}\,\overline{\mu}\,\hat{u}_y}{\mathrm{Re}_e\,h_1\,h_3} + \frac{i\,\Omega_{\mathrm{Re}}\,h_{3,s}\,\overline{\lambda}\,\hat{u}_y}{\mathrm{Re}_e\,h_1\,h_3} - \frac{3\,i\,\Omega_{\mathrm{Re}}\,h_{1,y}\,\overline{\mu}\,\hat{u}_s}{\mathrm{Re}_e\,h_1^2} - \frac{i\,\Omega_{\mathrm{Re}}\,h_{1,y}\,\overline{\lambda}\,\hat{u}_s}{\mathrm{Re}_e\,h_1^2} \\
&-\frac{i\,\Omega_{\mathrm{Re}}\,\overline{T}_s\,h_{1,y}\,\overline{\mu}_{\overline{T}}\,\hat{u}}{\mathrm{Re}_e\,h_1^2} - \frac{2\,i\,\Omega_{\mathrm{Re}}\,h_{3,s}\,h_{3,y}\,\overline{\mu}\,\hat{u}}{\mathrm{Re}_e\,h_1\,h_3^2} - \frac{i\,\Omega_{\mathrm{Re}}\,h_{1,y}\,h_{3,s}\,\overline{\mu}\,\hat{u}}{\mathrm{Re}_e\,h_1^2\,h_3} + \frac{i\,\Omega_{\mathrm{Re}}\,h_{1,s}\,h_{1,y}\,\overline{\mu}\,\hat{u}}{\mathrm{Re}_e\,h_1^3}
\end{aligned}
$$

$$-\frac{i\,\Omega_{\mathrm{Re}}\,h_{1,s\,y}\,\overline{\mu}\,\hat{u}}{\mathrm{Re}_e\,h_1^2}+\frac{i\,\Omega_{\mathrm{Re}}\,\overline{T}_y\,h_{3,s}\,\overline{\lambda}_{\overline{T}}\,\hat{u}}{\mathrm{Re}_e\,h_1\,h_3}-\frac{i\,\Omega_{\mathrm{Re}}\,h_{3,s}\,h_{3,y}\,\overline{\lambda}\,\hat{u}}{\mathrm{Re}_e\,h_1\,h_3^2}+\frac{i\,\Omega_{\mathrm{Re}}\,h_{3,s\,y}\,\overline{\lambda}\,\hat{u}}{\mathrm{Re}_e\,h_1\,h_3}$$
$$-\frac{i\,\Omega_{\mathrm{Re}}\,h_{1,y}\,h_{3,s}\,\overline{\lambda}\,\hat{u}}{\mathrm{Re}_e\,h_1^2\,h_3}+\frac{i\,\Omega_{\mathrm{Re}}\,\hat{T}\,h_{3,s}\,\overline{\mu}_{\overline{T}}\,\overline{u}_y}{\mathrm{Re}_e\,h_1\,h_3}+\frac{i\,\Omega_{\mathrm{Re}}\,\hat{T}\,h_{3,s}\,\overline{\lambda}_{\overline{T}}\,\overline{u}_y}{\mathrm{Re}_e\,h_1\,h_3}-\frac{3\,i\,\Omega_{\mathrm{Re}}\,\hat{T}\,h_{1,y}\,\overline{\mu}_{\overline{T}}\,\overline{u}_s}{\mathrm{Re}_e\,h_1^2}$$
$$-\frac{i\,\Omega_{\mathrm{Re}}\,\hat{T}\,h_{1,y}\,\overline{\lambda}_{\overline{T}}\,\overline{u}_s}{\mathrm{Re}_e\,h_1^2}-\frac{i\,\Omega_{\mathrm{Re}}\,\overline{T}_s\,\hat{T}\,h_{1,y}\,\overline{\mu}_{\overline{T}\,\overline{T}}\,\overline{u}}{\mathrm{Re}_e\,h_1^2}-\frac{2\,i\,\Omega_{\mathrm{Re}}\,\hat{T}\,h_{3,s}\,h_{3,y}\,\overline{\mu}_{\overline{T}}\,\overline{u}}{\mathrm{Re}_e\,h_1\,h_3^2}-\frac{i\,\Omega_{\mathrm{Re}}\,\hat{T}\,h_{1,y}\,h_{3,s}\,\overline{\mu}_{\overline{T}}\,\overline{u}}{\mathrm{Re}_e\,h_1^2\,h_3}$$
$$+\frac{i\,\Omega_{\mathrm{Re}}\,\hat{T}\,h_{1,s}\,h_{1,y}\,\overline{\mu}_{\overline{T}}\,\overline{u}}{\mathrm{Re}_e\,h_1^3}-\frac{i\,\Omega_{\mathrm{Re}}\,\hat{T}_s\,h_{1,y}\,\overline{\mu}_{\overline{T}}\,\overline{u}}{\mathrm{Re}_e\,h_1^2}-\frac{i\,\Omega_{\mathrm{Re}}\,\hat{T}\,h_{1,s\,y}\,\overline{\mu}_{\overline{T}}\,\overline{u}}{\mathrm{Re}_e\,h_1^2}+\frac{i\,\Omega_{\mathrm{Re}}\,\overline{T}_y\,\hat{T}\,h_{3,s}\,\overline{\lambda}_{\overline{T}\,\overline{T}}\,\overline{u}}{\mathrm{Re}_e\,h_1\,h_3}$$
$$-\frac{i\,\Omega_{\mathrm{Re}}\,\hat{T}\,h_{3,s}\,h_{3,y}\,\overline{\lambda}_{\overline{T}}\,\overline{u}}{\mathrm{Re}_e\,h_1\,h_3^2}+\frac{i\,\Omega_{\mathrm{Re}}\,\hat{T}\,h_{3,s\,y}\,\overline{\lambda}_{\overline{T}}\,\overline{u}}{\mathrm{Re}_e\,h_1\,h_3}-\frac{i\,\Omega_{\mathrm{Re}}\,\hat{T}\,h_{1,y}\,h_{3,s}\,\overline{\lambda}_{\overline{T}}\,\overline{u}}{\mathrm{Re}_e\,h_1^2\,h_3}+\frac{i\,\Omega_{\mathrm{Re}}\,\hat{T}_y\,h_{3,s}\,\overline{\lambda}_{\overline{T}}\,\overline{u}}{\mathrm{Re}_e\,h_1\,h_3}$$

A.3 z - Momentum

$$
\begin{aligned}
&\omega\,\overline{\rho}\,\hat{w} - \frac{\alpha\,\overline{\rho}\,\overline{u}\,\hat{w}}{h_1} + \frac{i\,\overline{\rho}\,\overline{u}\,\hat{w}_s}{h_1} = \\
&-i\,\hat{\rho}\,\overline{v}\,\overline{w}_y - i\,\overline{\rho}\,\hat{v}\,\overline{w}_y - i\,\overline{\rho}\,\overline{v}\,\hat{w}_y - \frac{i\,\hat{\rho}\,\overline{u}\,\overline{w}_s}{h_1} - \frac{i\,\overline{\rho}\,\hat{u}\,\overline{w}_s}{h_1} + \frac{\beta\,\overline{\rho}\,\overline{w}\,\hat{w}}{h_3} - \frac{i\,h_{3,y}\,\overline{\rho}\,\overline{v}\,\hat{w}}{h_3} - \frac{i\,h_{3,y}\,\overline{\rho}\,\hat{v}\,\overline{w}}{h_3} \\
&- \frac{i\,h_{3,y}\,\hat{\rho}\,\overline{v}\,\overline{w}}{h_3} - \frac{i\,h_{3,s}\,\overline{\rho}\,\overline{u}\,\hat{w}}{h_1\,h_3} - \frac{i\,h_{3,s}\,\overline{\rho}\,\hat{u}\,\overline{w}}{h_1\,h_3} - \frac{i\,h_{3,s}\,\hat{\rho}\,\overline{u}\,\overline{w}}{h_1\,h_3} + \frac{\overline{T}\,\beta\,\hat{\rho}}{\mathrm{M}_e^2\,\gamma_e\,h_3} + \frac{\hat{T}\,\beta\,\overline{\rho}}{\mathrm{M}_e^2\,\gamma_e\,h_3} \\
&+ \frac{i\,\hat{T}\,\overline{\mu}_{\overline{T}}\,\overline{w}_{yy}}{\mathrm{Re}_e} + \frac{i\,\overline{T}_y\,\hat{T}\,\overline{\mu}_{\overline{T}\,\overline{T}}\,\overline{w}_y}{\mathrm{Re}_e} + \frac{i\,\hat{T}\,h_{3,y}\,\overline{\mu}_{\overline{T}}\,\overline{w}_y}{\mathrm{Re}_e\,h_3} + \frac{i\,\hat{T}\,h_{1,y}\,\overline{\mu}_{\overline{T}}\,\overline{w}_y}{\mathrm{Re}_e\,h_1} - \frac{\Omega_{\mathrm{Re}}\,\hat{T}\,\alpha\,\overline{\mu}_{\overline{T}}\,\overline{w}_s}{\mathrm{Re}_e\,h_1^2} - \frac{i\,\alpha^2\,\overline{\mu}\,\hat{w}}{\mathrm{Re}_e\,h_1^2} \\
&- \frac{\Omega_{\mathrm{Re}}\,\beta\,\overline{\mu}\,\hat{u}_s}{\mathrm{Re}_e\,h_1\,h_3} - \frac{\Omega_{\mathrm{Re}}\,\hat{T}\,\beta\,\overline{\lambda}_{\overline{T}}\,\overline{u}_s}{\mathrm{Re}_e\,h_1\,h_3} - \frac{\Omega_{\mathrm{Re}}\,\hat{T}\,\beta\,\overline{\lambda}_{\overline{T}}\,\overline{v}_y}{\mathrm{Re}_e\,h_3} - \frac{\beta\,\overline{\mu}\,\hat{v}_y}{\mathrm{Re}_e\,h_3} + \frac{i\,\overline{\mu}\,\hat{w}_{yy}}{\mathrm{Re}_e} + \frac{i\,\overline{T}_y\,\overline{\mu}_{\overline{T}}\,\hat{w}_y}{\mathrm{Re}_e} - \frac{\overline{T}_y\,\beta\,\overline{\mu}_{\overline{T}}\,\hat{v}}{\mathrm{Re}_e\,h_3} \\
&- \frac{\Omega_{\mathrm{Re}}\,\overline{T}_s\,\alpha\,\overline{\mu}_{\overline{T}}\,\hat{w}}{\mathrm{Re}_e\,h_1^2} - \frac{\Omega_{\mathrm{Re}}\,\overline{T}_s\,\beta\,\overline{\mu}_{\overline{T}}\,\hat{u}}{\mathrm{Re}_e\,h_1\,h_3} + \frac{i\,h_{1,y}\,\overline{\mu}\,\hat{w}_y}{\mathrm{Re}_e\,h_1} + \frac{i\,\beta\,h_{1,y}\,\overline{\mu}\,\hat{v}}{\mathrm{Re}_e\,h_1\,h_3} - \frac{2\,\Omega_{\mathrm{Re}}\,\alpha\,\overline{\mu}\,\hat{w}_s}{\mathrm{Re}_e\,h_1^2} - \frac{2\,i\,\beta^2\,\overline{\mu}\,\hat{w}}{\mathrm{Re}_e\,h_3^2} \\
&- \frac{\Omega_{\mathrm{Re}}\,\alpha_s\,\overline{\mu}\,\hat{w}}{\mathrm{Re}_e\,h_1^2} - \frac{i\,\alpha\,\beta\,\overline{\mu}\,\hat{u}}{\mathrm{Re}_e\,h_1\,h_3} - \frac{\beta\,h_{1,y}\,\overline{\lambda}\,\hat{v}}{\mathrm{Re}_e\,h_1\,h_3} - \frac{i\,\beta^2\,\overline{\lambda}\,\hat{w}}{\mathrm{Re}_e\,h_3^2} - \frac{\beta\,\overline{\lambda}\,\hat{v}_y}{\mathrm{Re}_e\,h_3} - \frac{\Omega_{\mathrm{Re}}\,\beta\,\overline{\lambda}\,\hat{u}_s}{\mathrm{Re}_e\,h_1\,h_3} \\
&- \frac{i\,\alpha\,\beta\,\overline{\lambda}\,\hat{u}}{\mathrm{Re}_e\,h_1\,h_3} + \frac{i\,h_{3,y}\,\overline{\mu}\,\hat{w}_y}{\mathrm{Re}_e\,h_3} - \frac{i\,\overline{T}_y\,h_{3,y}\,\overline{\mu}_{\overline{T}}\,\hat{w}}{\mathrm{Re}_e\,h_3} - \frac{i\,h_{3,yy}\,\overline{\mu}\,\hat{w}}{\mathrm{Re}_e\,h_3} - \frac{i\,(h_{3,y})^2\,\overline{\mu}\,\hat{w}}{\mathrm{Re}_e\,h_3^2} - \frac{i\,h_{1,y}\,h_{3,y}\,\overline{\mu}\,\hat{w}}{\mathrm{Re}_e\,h_1\,h_3} \\
&- \frac{\Omega_{\mathrm{Re}}\,\alpha\,h_{3,s}\,\overline{\mu}\,\hat{w}}{\mathrm{Re}_e\,h_1^2\,h_3} + \frac{\Omega_{\mathrm{Re}}\,\alpha\,h_{1,s}\,\overline{\mu}\,\hat{w}}{\mathrm{Re}_e\,h_1^3} + \frac{i\,\hat{T}_y\,\overline{\mu}_{\overline{T}}\,\overline{w}_y}{\mathrm{Re}_e} - \frac{i\,\overline{T}_y\,\hat{T}\,h_{3,y}\,\overline{\mu}_{\overline{T}\,\overline{T}}\,\overline{w}}{\mathrm{Re}_e\,h_3} - \frac{i\,\hat{T}\,h_{3,yy}\,\overline{\mu}_{\overline{T}}\,\overline{w}}{\mathrm{Re}_e\,h_3} \\
&- \frac{i\,\hat{T}\,(h_{3,y})^2\,\overline{\mu}_{\overline{T}}\,\overline{w}}{\mathrm{Re}_e\,h_3^2} - \frac{i\,\hat{T}\,h_{1,y}\,h_{3,y}\,\overline{\mu}_{\overline{T}}\,\overline{w}}{\mathrm{Re}_e\,h_1\,h_3} - \frac{i\,\hat{T}_y\,h_{3,y}\,\overline{\mu}_{\overline{T}}\,\overline{w}}{\mathrm{Re}_e\,h_3} + \frac{\Omega_{\mathrm{Re}}\,\hat{T}\,\alpha\,h_{3,s}\,\overline{\mu}_{\overline{T}}\,\overline{w}}{\mathrm{Re}_e\,h_1^2\,h_3} - \frac{3\,\beta\,h_{3,y}\,\overline{\mu}\,\hat{v}}{\mathrm{Re}_e\,h_3^2} \\
&- \frac{\beta\,h_{3,y}\,\overline{\lambda}\,\hat{v}}{\mathrm{Re}_e\,h_3^2} - \frac{2\,\Omega_{\mathrm{Re}}\,\hat{T}\,\beta\,h_{3,y}\,\overline{\mu}_{\overline{T}}\,\overline{v}}{\mathrm{Re}_e\,h_3^2} - \frac{\Omega_{\mathrm{Re}}\,\hat{T}\,\beta\,h_{3,y}\,\overline{\lambda}_{\overline{T}}\,\overline{v}}{\mathrm{Re}_e\,h_3^2} - \frac{\Omega_{\mathrm{Re}}\,\hat{T}\,\beta\,h_{1,y}\,\overline{\lambda}_{\overline{T}}\,\overline{v}}{\mathrm{Re}_e\,h_1\,h_3} - \frac{3\,\Omega_{\mathrm{Re}}\,\beta\,h_{3,s}\,\overline{\mu}\,\hat{u}}{\mathrm{Re}_e\,h_1\,h_3^2} \\
&- \frac{\Omega_{\mathrm{Re}}\,\beta\,h_{3,s}\,\overline{\lambda}\,\hat{u}}{\mathrm{Re}_e\,h_1\,h_3^2} - \frac{2\,\Omega_{\mathrm{Re}}\,\hat{T}\,\beta\,h_{3,s}\,\overline{\mu}_{\overline{T}}\,\overline{u}}{\mathrm{Re}_e\,h_1\,h_3^2} - \frac{\Omega_{\mathrm{Re}}\,\hat{T}\,\beta\,h_{3,s}\,\overline{\lambda}_{\overline{T}}\,\overline{u}}{\mathrm{Re}_e\,h_1\,h_3^2}
\end{aligned}
$$

A.4 Conservation of Energy

$$
\begin{aligned}
&\frac{\hat{T}\,\omega\,\overline{\rho}}{\gamma_e\,\mathrm{Ec}_e\,\overline{T}}-\frac{\hat{T}\,\alpha\,\overline{\rho}\,\overline{u}}{\gamma_e\,\mathrm{Ec}_e\,h_1\,\overline{T}}+\frac{i\,\hat{T}_s\,\overline{\rho}\,\overline{u}}{\gamma_e\,\mathrm{Ec}_e\,h_1\,\overline{T}}=\\
&\frac{\hat{T}\,\beta\,\overline{\rho}\,\overline{w}}{\mathrm{Ec}_e\,h_3\,\overline{T}}-\frac{i\,\overline{T}_y\,\hat{\rho}\,\overline{v}}{\mathrm{Ec}_e\,\overline{T}}-\frac{i\,\hat{T}_y\,\overline{\rho}\,\overline{v}}{\mathrm{Ec}_e\,\overline{T}}-\frac{i\,\overline{T}_s\,\hat{\rho}\,\overline{u}}{\mathrm{Ec}_e\,h_1\,\overline{T}}-\frac{i\,\overline{T}_y\,\overline{\rho}\,\hat{v}}{\mathrm{Ec}_e\,\overline{T}}-\frac{i\,\overline{T}_s\,\overline{\rho}\,\hat{u}}{\mathrm{Ec}_e\,h_1\,\overline{T}}+\frac{i\,\Omega_p\,\hat{\rho}_s\,\overline{u}}{\gamma_e\,\mathrm{M}_e^2\,h_1}+\frac{i\,\Omega_p\,\overline{T}_s\,\hat{\rho}\,\overline{u}}{\gamma_e\,\mathrm{M}_e^2\,h_1\,\overline{T}}\\
&+\frac{i\,\Omega_p\,\hat{T}\,\overline{\rho}_s\,\overline{u}}{\gamma_e\,\mathrm{M}_e^2\,h_1\,\overline{T}}-\frac{\alpha\,\hat{\rho}\,\overline{u}}{\gamma_e\,\mathrm{M}_e^2\,h_1}+\frac{\omega\,\hat{\rho}}{\gamma_e\,\mathrm{M}_e^2}-\frac{\beta\,\hat{\rho}\,\overline{w}}{\gamma_e\,\mathrm{M}_e^2\,h_3}-\frac{\hat{T}\,\beta\,\overline{\rho}\,\overline{w}}{\gamma_e\,\mathrm{M}_e^2\,h_3\,\overline{T}}+\frac{i\,\hat{\rho}_y\,\overline{v}}{\gamma_e\,\mathrm{M}_e^2}+\frac{i\,\overline{T}_y\,\hat{\rho}\,\overline{v}}{\gamma_e\,\mathrm{M}_e^2\,\overline{T}}+\frac{i\,\hat{T}\,\overline{\rho}_y\,\overline{v}}{\gamma_e\,\mathrm{M}_e^2\,\overline{T}}\\
&+\frac{i\,\hat{T}_y\,\overline{\rho}\,\overline{v}}{\gamma_e\,\mathrm{M}_e^2\,\overline{T}}+\frac{i\,\overline{\rho}_y\,\hat{v}}{\gamma_e\,\mathrm{M}_e^2}+\frac{i\,\overline{T}_y\,\overline{\rho}\,\hat{v}}{\gamma_e\,\mathrm{M}_e^2\,\overline{T}}+\frac{i\,\Omega_p\,\overline{\rho}_s\,\hat{u}}{\gamma_e\,\mathrm{M}_e^2\,h_1}+\frac{i\,\Omega_p\,\overline{T}_s\,\overline{\rho}\,\hat{u}}{\gamma_e\,\mathrm{M}_e^2\,h_1\,\overline{T}}+\frac{i\,\hat{T}\,\overline{\mu}_{\overline{T}}\,(\overline{w}_y)^2}{\mathrm{Re}_e\,\overline{T}}+\frac{2\,i\,\overline{\mu}\,\overline{w}_y\,\hat{w}_y}{\mathrm{Re}_e\,\overline{T}}\\
&-\frac{2\,\beta\,\overline{\mu}\,\hat{v}\,\overline{w}_y}{\mathrm{Re}_e\,h_3\,\overline{T}}-\frac{2\,\Omega_{\mathrm{Re}}\,\alpha\,\overline{\mu}\,\overline{w}_s\,\hat{w}}{\mathrm{Re}_e\,h_1^2\,\overline{T}}-\frac{2\,i\,h_{1,y}\,\overline{\mu}\,\overline{u}\,\hat{u}_y}{\mathrm{Re}_e\,h_1\,\overline{T}}+\frac{2\,\alpha\,h_{1,y}\,\overline{\mu}\,\overline{u}\,\hat{v}}{\mathrm{Re}_e\,h_1^2\,\overline{T}}+\frac{i\,\hat{T}_y\,h_{1,y}\,\overline{\kappa}}{\mathrm{Ec}_e\,\mathrm{Pr}_e\,\mathrm{Re}_e\,h_1\,\overline{T}}\\
&+\frac{i\,\overline{T}_y\,\hat{T}\,h_{1,y}\,\overline{\kappa}_{\overline{T}}}{\mathrm{Ec}_e\,\mathrm{Pr}_e\,\mathrm{Re}_e\,h_1\,\overline{T}}-\frac{2\,\Omega_{\mathrm{Re}}\,\beta\,\overline{\mu}\,\hat{u}\,\overline{w}_s}{\mathrm{Re}_e\,h_1\,h_3\,\overline{T}}+\frac{4\,i\,\Omega_{\mathrm{Re}}\,\overline{\mu}\,\overline{v}_y\,\hat{v}_y}{\mathrm{Re}_e\,\overline{T}}-\frac{2\,\Omega_{\mathrm{Re}}\,\beta\,\overline{\lambda}\,\overline{v}_y\,\hat{w}}{\mathrm{Re}_e\,h_3\,\overline{T}}+\frac{2\,i\,\Omega_{\mathrm{Re}}\,\overline{\lambda}\,\overline{v}_y\,\hat{v}_y}{\mathrm{Re}_e\,\overline{T}}\\
&-\frac{2\,\Omega_{\mathrm{Re}}\,\alpha\,\overline{\lambda}\,\hat{u}\,\overline{v}_y}{\mathrm{Re}_e\,h_1\,\overline{T}}+\frac{i\,\hat{T}\,\overline{\mu}_{\overline{T}}\,(\overline{u}_y)^2}{\mathrm{Re}_e\,\overline{T}}-\frac{2\,i\,\hat{T}\,h_{1,y}\,\overline{\mu}_{\overline{T}}\,\overline{u}\,\overline{u}_y}{\mathrm{Re}_e\,h_1\,\overline{T}}-\frac{2\,i\,h_{1,y}\,\overline{\mu}\,\overline{u}_y\,\hat{u}}{\mathrm{Re}_e\,h_1\,\overline{T}}+\frac{2\,i\,\Omega_{\mathrm{Re}}\,\overline{\mu}\,\overline{u}_y\,\hat{v}_s}{\mathrm{Re}_e\,h_1\,\overline{T}}\\
&-\frac{2\,\alpha\,\overline{\mu}\,\overline{u}_y\,\hat{v}}{\mathrm{Re}_e\,h_1\,\overline{T}}-\frac{2\,\Omega_{\mathrm{Re}}\,\beta\,\overline{\lambda}\,\overline{u}_s\,\hat{w}}{\mathrm{Re}_e\,h_1\,h_3\,\overline{T}}+\frac{2\,i\,\Omega_{\mathrm{Re}}\,\overline{\lambda}\,\overline{u}_s\,\hat{v}_y}{\mathrm{Re}_e\,h_1\,\overline{T}}-\frac{2\,\Omega_{\mathrm{Re}}\,\alpha\,\overline{\lambda}\,\overline{u}_s\,\hat{u}}{\mathrm{Re}_e\,h_1^2\,\overline{T}}-\frac{4\,\Omega_{\mathrm{Re}}\,\alpha\,\overline{\mu}\,\overline{u}_s\,\hat{u}}{\mathrm{Re}_e\,h_1^2\,\overline{T}}\\
&+\frac{i\,\overline{T}_{yy}\,\hat{T}\,\overline{\kappa}_{\overline{T}}}{\mathrm{Ec}_e\,\mathrm{Pr}_e\,\mathrm{Re}_e\,\overline{T}}+\frac{2\,i\,\overline{\mu}\,\overline{u}_y\,\hat{u}_y}{\mathrm{Re}_e\,\overline{T}}+\frac{i\,\hat{T}_{yy}\,\overline{\kappa}}{\mathrm{Ec}_e\,\mathrm{Pr}_e\,\mathrm{Re}_e\,\overline{T}}+\frac{i\,\left(\overline{T}_y\right)^2\,\hat{T}\,\overline{\kappa}_{\overline{T}\,\overline{T}}}{\mathrm{Ec}_e\,\mathrm{Pr}_e\,\mathrm{Re}_e\,\overline{T}}+\frac{2\,i\,\overline{T}_y\,\hat{T}_y\,\overline{\kappa}_{\overline{T}}}{\mathrm{Ec}_e\,\mathrm{Pr}_e\,\mathrm{Re}_e\,\overline{T}}\\
&-\frac{2\,\Omega_{\mathrm{Re}}\,\overline{T}_s\,\hat{T}\,\alpha\,\overline{\kappa}_{\overline{T}}}{\mathrm{Ec}_e\,\mathrm{Pr}_e\,\mathrm{Re}_e\,h_1^2\,\overline{T}}-\frac{2\,\Omega_{\mathrm{Re}}\,\hat{T}_s\,\alpha\,\overline{\kappa}}{\mathrm{Ec}_e\,\mathrm{Pr}_e\,\mathrm{Re}_e\,h_1^2\,\overline{T}}-\frac{i\,\hat{T}\,\beta^2\,\overline{\kappa}}{\mathrm{Ec}_e\,\mathrm{Pr}_e\,\mathrm{Re}_e\,h_3^2\,\overline{T}}\\
&-\frac{\Omega_{\mathrm{Re}}\,\hat{T}\,\alpha_s\,\overline{\kappa}}{\mathrm{Ec}_e\,\mathrm{Pr}_e\,\mathrm{Re}_e\,h_1^2\,\overline{T}}-\frac{i\,\hat{T}\,\alpha^2\,\overline{\kappa}}{\mathrm{Ec}_e\,\mathrm{Pr}_e\,\mathrm{Re}_e\,h_1^2\,\overline{T}}-\frac{2\,i\,h_{3,y}\,\overline{\mu}\,\overline{w}\,\hat{w}_y}{\mathrm{Re}_e\,h_3\,\overline{T}}-\frac{2\,i\,h_{3,y}\,\overline{\mu}\,\overline{w}_y\,\hat{w}}{\mathrm{Re}_e\,h_3\,\overline{T}}+\frac{2\,i\,\left(h_{3,y}\right)^2\,\overline{\mu}\,\overline{w}\,\hat{w}}{\mathrm{Re}_e\,h_3^2\,\overline{T}}\\
&+\frac{2\,\Omega_{\mathrm{Re}}\,\alpha\,h_{3,s}\,\overline{\mu}\,\overline{w}\,\hat{w}}{\mathrm{Re}_e\,h_1^2\,h_3\,\overline{T}}-\frac{4\,\Omega_{\mathrm{Re}}\,\beta\,h_{3,y}\,\overline{\mu}\,\overline{v}\,\hat{w}}{\mathrm{Re}_e\,h_3^2\,\overline{T}}-\frac{2\,\Omega_{\mathrm{Re}}\,\beta\,h_{3,y}\,\overline{\lambda}\,\overline{v}\,\hat{w}}{\mathrm{Re}_e\,h_3^2\,\overline{T}}-\frac{2\,\Omega_{\mathrm{Re}}\,\beta\,h_{1,y}\,\overline{\lambda}\,\overline{v}\,\hat{w}}{\mathrm{Re}_e\,h_1\,h_3\,\overline{T}}\\
&-\frac{4\,\Omega_{\mathrm{Re}}\,\beta\,h_{3,s}\,\overline{\mu}\,\overline{u}\,\hat{w}}{\mathrm{Re}_e\,h_1\,h_3^2\,\overline{T}}-\frac{2\,\Omega_{\mathrm{Re}}\,\beta\,h_{3,s}\,\overline{\lambda}\,\overline{u}\,\hat{w}}{\mathrm{Re}_e\,h_1\,h_3^2\,\overline{T}}-\frac{2\,i\,\hat{T}\,h_{3,y}\,\overline{\mu}_{\overline{T}}\,\overline{w}\,\overline{w}_y}{\mathrm{Re}_e\,h_3\,\overline{T}}+\frac{i\,\hat{T}\,\left(h_{3,y}\right)^2\,\overline{\mu}_{\overline{T}}\,\overline{w}^2}{\mathrm{Re}_e\,h_3^2\,\overline{T}}\\
&+\frac{2\,\beta\,h_{3,y}\,\overline{\mu}\,\hat{v}\,\overline{w}}{\mathrm{Re}_e\,h_3^2\,\overline{T}}+\frac{2\,\Omega_{\mathrm{Re}}\,\beta\,h_{3,s}\,\overline{\mu}\,\hat{u}\,\overline{w}}{\mathrm{Re}_e\,h_1\,h_3^2\,\overline{T}}+\frac{2\,i\,\Omega_{\mathrm{Re}}\,h_{3,y}\,\overline{\lambda}\,\overline{v}\,\hat{v}_y}{\mathrm{Re}_e\,h_3\,\overline{T}}+\frac{2\,i\,\Omega_{\mathrm{Re}}\,h_{1,y}\,\overline{\lambda}\,\overline{v}\,\hat{v}_y}{\mathrm{Re}_e\,h_1\,\overline{T}}
\end{aligned}
$$

$$+\frac{2\,i\,\Omega_{\mathrm{Re}}\,h_{3,s}\,\overline{\lambda}\,\overline{u}\,\hat{v}_y}{\mathrm{Re}_e\,h_1\,h_3\,\overline{T}}-\frac{2\,i\,\Omega_{\mathrm{Re}}\,h_{1,y}\,\overline{\mu}\,\overline{u}\,\hat{v}_s}{\mathrm{Re}_e\,h_1^2\,\overline{T}}+\frac{2\,i\,\Omega_{\mathrm{Re}}\,h_{3,y}\,\overline{\lambda}\,\overline{v}_y\,\hat{v}}{\mathrm{Re}_e\,h_3\,\overline{T}}+\frac{2\,i\,\Omega_{\mathrm{Re}}\,h_{1,y}\,\overline{\lambda}\,\overline{v}_y\,\hat{v}}{\mathrm{Re}_e\,h_1\,\overline{T}}$$
$$+\frac{4\,i\,\Omega_{\mathrm{Re}}\,\left(h_{3,y}\right)^2\,\overline{\mu}\,\overline{v}\,\hat{v}}{\mathrm{Re}_e\,h_3^2\,\overline{T}}+\frac{4\,i\,\Omega_{\mathrm{Re}}\,\left(h_{1,y}\right)^2\,\overline{\mu}\,\overline{v}\,\hat{v}}{\mathrm{Re}_e\,h_1^2\,\overline{T}}+\frac{2\,i\,\Omega_{\mathrm{Re}}\,\left(h_{3,y}\right)^2\,\overline{\lambda}\,\overline{v}\,\hat{v}}{\mathrm{Re}_e\,h_3^2\,\overline{T}}+\frac{4\,i\,\Omega_{\mathrm{Re}}\,h_{1,y}\,h_{3,y}\,\overline{\lambda}\,\overline{v}\,\hat{v}}{\mathrm{Re}_e\,h_1\,h_3\,\overline{T}}$$
$$+\frac{2\,i\,\Omega_{\mathrm{Re}}\,\left(h_{1,y}\right)^2\,\overline{\lambda}\,\overline{v}\,\hat{v}}{\mathrm{Re}_e\,h_1^2\,\overline{T}}+\frac{4\,i\,\Omega_{\mathrm{Re}}\,h_{1,y}\,\overline{\mu}\,\overline{u}_s\,\hat{v}}{\mathrm{Re}_e\,h_1^2\,\overline{T}}+\frac{2\,i\,\Omega_{\mathrm{Re}}\,h_{3,y}\,\overline{\lambda}\,\overline{u}_s\,\hat{v}}{\mathrm{Re}_e\,h_1\,h_3\,\overline{T}}+\frac{2\,i\,\Omega_{\mathrm{Re}}\,h_{1,y}\,\overline{\lambda}\,\overline{u}_s\,\hat{v}}{\mathrm{Re}_e\,h_1^2\,\overline{T}}$$
$$+\frac{4\,i\,\Omega_{\mathrm{Re}}\,h_{3,s}\,h_{3,y}\,\overline{\mu}\,\overline{u}\,\hat{v}}{\mathrm{Re}_e\,h_1\,h_3^2\,\overline{T}}+\frac{2\,i\,\Omega_{\mathrm{Re}}\,h_{3,s}\,h_{3,y}\,\overline{\lambda}\,\overline{u}\,\hat{v}}{\mathrm{Re}_e\,h_1\,h_3^2\,\overline{T}}+\frac{2\,i\,\Omega_{\mathrm{Re}}\,h_{1,y}\,h_{3,s}\,\overline{\lambda}\,\overline{u}\,\hat{v}}{\mathrm{Re}_e\,h_1^2\,h_3\,\overline{T}}-\frac{4\,\Omega_{\mathrm{Re}}\,\alpha\,h_{1,y}\,\overline{\mu}\,\hat{u}\,\overline{v}}{\mathrm{Re}_e\,h_1^2\,\overline{T}}$$
$$-\frac{2\,\Omega_{\mathrm{Re}}\,\alpha\,h_{3,y}\,\overline{\lambda}\,\hat{u}\,\overline{v}}{\mathrm{Re}_e\,h_1\,h_3\,\overline{T}}-\frac{2\,\Omega_{\mathrm{Re}}\,\alpha\,h_{1,y}\,\overline{\lambda}\,\hat{u}\,\overline{v}}{\mathrm{Re}_e\,h_1^2\,\overline{T}}+\frac{2\,i\,\left(h_{1,y}\right)^2\,\overline{\mu}\,\overline{u}\,\hat{u}}{\mathrm{Re}_e\,h_1^2\,\overline{T}}-\frac{2\,\Omega_{\mathrm{Re}}\,\alpha\,h_{3,s}\,\overline{\lambda}\,\overline{u}\,\hat{u}}{\mathrm{Re}_e\,h_1^2\,h_3\,\overline{T}}$$
$$+\frac{i\,\hat{T}\,\left(h_{1,y}\right)^2\,\overline{\mu}_{\overline{T}}\,\overline{u}^2}{\mathrm{Re}_e\,h_1^2\,\overline{T}}+\frac{i\,\overline{T}_y\,\hat{T}\,h_{3,y}\,\overline{\kappa}_{\overline{T}}}{\mathrm{Ec}_e\,\mathrm{Pr}_e\,\mathrm{Re}_e\,h_3\,\overline{T}}+\frac{i\,\hat{T}_y\,h_{3,y}\,\overline{\kappa}}{\mathrm{Ec}_e\,\mathrm{Pr}_e\,\mathrm{Re}_e\,h_3\,\overline{T}}$$
$$-\frac{\Omega_{\mathrm{Re}}\,\hat{T}\,\alpha\,h_{3,s}\,\overline{\kappa}}{\mathrm{Ec}_e\,\mathrm{Pr}_e\,\mathrm{Re}_e\,h_1^2\,h_3\,\overline{T}}+\frac{\Omega_{\mathrm{Re}}\,\hat{T}\,\alpha\,h_{1,s}\,\overline{\kappa}}{\mathrm{Ec}_e\,\mathrm{Pr}_e\,\mathrm{Re}_e\,h_1^3\,\overline{T}}$$

A.5 Conservation of Mass Continuity

$$\frac{\omega\hat{\rho}}{\overline{\rho}} - \frac{\alpha\hat{\rho}\overline{u}}{h_1\overline{\rho}} + \frac{i\,\hat{\rho}_s\overline{u}}{h_1\overline{\rho}} =$$
$$\frac{\beta\hat{\rho}\overline{w}}{h_3\overline{\rho}} - \frac{i\hat{\rho}\overline{v}_y}{\overline{\rho}} - \frac{i\hat{\rho}_y\overline{v}}{\overline{\rho}} - \frac{i\hat{\rho}\overline{u}_s}{h_1\overline{\rho}} - \frac{i\overline{\rho}_y\hat{v}}{\overline{\rho}} - \frac{i\overline{\rho}_s\hat{u}}{h_1\overline{\rho}} - \frac{ih_{1,y}\hat{v}}{h_1} + \frac{\beta\hat{w}}{h_3}$$
$$-i\hat{v}_y - \frac{i\hat{u}_s}{h_1} + \frac{\alpha\hat{u}}{h_1} - \frac{ih_{3,y}\hat{v}}{h_3} - \frac{ih_{3,y}\hat{\rho}\overline{v}}{h_3\overline{\rho}} - \frac{ih_{1,y}\hat{\rho}\overline{v}}{h_1\overline{\rho}} - \frac{ih_{3,s}\hat{u}}{h_1h_3} - \frac{ih_{3,s}\hat{\rho}\overline{u}}{h_1h_3\overline{\rho}}$$

APPENDIX B

MOST-AMPLIFIED SWEPT WING CHARACTERISTICS

The following tables indicate stability characteristics for most amplified N-factor curve for different sweeps, regions of the airfoil, steady and unsteady cases, and initialization approach. These values were generated originally in [2].

Λ [°]	x/c [%]	f [Hz]	approach	N	δ_{99} [mm]	λ [mm]	λ_z [mm]	λ_{G}	$\frac{c_{\mathrm{ph}}}{\lvert\overline{w}_{s,\max}\rvert}$	ψ_w [°]	$\psi_w - \psi_s$ [°]
0	82	0	slot only, fundamental	13.1	2.31	1.75	1.75	133	0/0	+90.0	+90.0
		0	slot only, harmonic	12.7	2.31	1.75	1.75	133	0/0	+90.0	+90.0
		25	slot only, fundamental	13.2	2.31	1.75	−1.75	133	∞	−89.8	−89.8
		50	slot only, harmonic	12.8	2.31	1.75	1.75	133	∞	+89.5	+89.5
5	82	0	slot only, fundamental	12.5	2.32	1.75	1.75	132	0	+87.1	+90.9
		0	slot only, harmonic	11.5	2.32	1.75	1.75	132	0	+87.1	+90.9
		100	slot only, fundamental	13.0	2.32	1.75	1.75	132	0.8	+86.2	+89.9
		125	slot only, harmonic	11.9	2.32	1.75	1.75	132	0.9	+85.9	+89.7
10	82	0	slot only, fundamental	11.5	2.33	1.99	2.00	159	0	+84.1	+91.7
		0	slot only, harmonic	10.4	2.33	1.99	2.00	159	0	+84.1	+91.7
		175	slot only, fundamental	12.6	2.33	1.74	1.75	131	0.7	+82.5	+90.1
		125	slot only, harmonic	11.0	2.33	1.74	1.75	131	0.5	+83.0	+90.5
15	82	0	slot only, fundamental	10.2	2.35	2.22	2.25	187	0	+81.1	+92.5
		0	slot only, harmonic	9.5	2.35	2.47	2.50	219	0	+81.1	+92.4
		225	slot only, fundamental	12.0	2.35	1.96	2.00	156	0.7	+78.8	+90.2
		175	slot only, harmonic	10.8	2.35	1.97	2.00	156	0.5	+79.3	+90.7

Λ [°]	x/c [%]	f [Hz]	approach	N	δ_{99} [mm]	λ [mm]	λ_z [mm]	λ_{G}	$\frac{c_{\mathrm{ph}}}{\lvert\overline{w}_{s,\max}\rvert}$	ψ_w [°]	$\psi_w - \psi_s$ [°]
20	25	0	full chord	0.8	1.51	8.60	9.00	998	0	+72.8	+92.3
	27	25	full chord	0.8	1.55	9.52	10.00	1138	0.3	+72.1	+91.5
	82	0	slot only, fundamental	8.7	2.38	2.69	2.75	245	0	+77.9	+93.2
		0	slot only, harmonic	8.5	2.38	2.93	3.00	279	0	+77.8	+93.1
		0	full chord, updated n.p.	9.5	2.38	3.90	4.00	430	0	+77.5	+92.7
		0	full chord, unadjusted n.p.	8.5	2.38	2.45	2.50	213	0	+78.0	+93.3
		300	slot only, fundamental	11.4	2.38	1.93	2.00	152	0.7	+75.0	+90.3
		350	slot only, harmonic	10.8	2.38	1.45	1.50	99	0.6	+75.5	+90.8
		300	full chord, updated n.p.	11.4	2.38	1.93	2.00	152	0.7	+75.0	+90.3
		300	full chord, unadjusted n.p.	11.4	2.38	1.93	2.00	152	0.7	+75.0	+90.3
25	33	0	full chord	1.3	1.75	9.32	10.00	1155	0	+68.7	+92.3
	43	100	full chord	1.8	1.97	7.61	−8.00	878	0.9	−108.1	−85.3
	82	0	slot only, fundamental	7.6	2.42	4.32	4.50	495	0	+73.9	+93.2
		0	slot only, harmonic	7.5	2.42	4.32	4.50	495	0	+73.9	+93.2
		0	full chord, updated n.p.	8.5	2.42	4.80	5.00	580	0	+73.7	+93.1
		0	full chord, unadjusted n.p.	6.4	2.42	2.89	3.00	270	0	+74.7	+94.0
		325	slot only, fundamental	10.6	2.42	2.13	2.25	175	0.6	+71.1	+90.4
		300	slot only, harmonic	10.2	2.42	2.13	2.25	175	0.6	+71.4	+90.7
		300	full chord, updated n.p.	10.5	2.42	2.13	2.25	175	0.6	+71.4	+90.7
		300	full chord, unadjusted n.p.	10.5	2.42	2.13	2.25	175	0.6	+71.4	+90.7

Λ [°]	x/c [%]	f [Hz]	approach	N	δ_{99} [mm]	λ [mm]	λ_z [mm]	λ_{G}	$\frac{c_{\mathrm{ph}}}{\lvert\overline{w}_{s,\max}\rvert}$	ψ_w [°]	$\psi_w - \psi_s$ [°]
30	37	0	full chord	2.0	1.90	5.38	6.00	509	0	+63.7	+91.7
	39	125	full chord	2.8	1.93	5.51	−6.00	518	0.7	−113.3	−85.4
	82	0	slot only, fundamental	7.0	2.47	5.63	6.00	729	0	+69.8	+93.3
		0	slot only, harmonic	7.1	2.47	5.17	5.50	639	0	+69.9	+93.4
		0	full chord, updated n.p.	7.8	2.47	5.63	6.00	729	0	+69.8	+93.2
		0	full chord, unadjusted n.p.	6.6	2.47	5.63	6.00	729	0	+69.8	+93.2
		375	slot only, fundamental	9.8	2.47	2.08	2.25	167	0.6	+67.3	+90.8
		350	slot only, harmonic	9.6	2.47	2.08	2.25	167	0.6	+67.6	+91.0
		350	full chord, updated n.p.	9.5	2.47	2.74	3.00	258	0.8	+66.2	+89.6
		350	full chord, unadjusted n.p.	9.5	2.47	2.74	3.00	258	0.8	+66.2	+89.6
35	43	0	full chord	3.0	2.08	6.04	7.00	653	0	+59.6	+91.8
	47	150	full chord	4.4	2.13	7.24	−8.00	960	1.0	−115.1	−83.3
	82	0	slot only, fundamental	6.5	2.53	6.38	7.00	869	0	+65.6	+93.4
		0	slot only, harmonic	6.7	2.53	5.93	6.50	777	0	+65.7	+93.5
		0	full chord, updated n.p.	7.3	2.53	6.38	7.00	869	0	+65.6	+93.4
		0	full chord, unadjusted n.p.	7.6	2.53	7.28	8.00	1061	0	+65.5	+93.2
		400	slot only, fundamental	8.9	2.53	2.23	2.50	185	0.6	+63.1	+90.9
		375	slot only, harmonic	8.8	2.53	2.23	2.50	185	0.6	+63.3	+91.1
		350	full chord, updated n.p.	8.6	2.53	3.08	3.50	307	0.8	+61.8	+89.6
		350	full chord, unadjusted n.p.	8.6	2.53	3.08	3.50	307	0.8	+61.8	+89.6

APPENDIX C

PARABOLIZED STABILITY EQUATIONS

The parabolized stability equations for a curvilinear coordinate system are represented below. This representation is what is used for PSE calculations in the EPIC code. The equations are formatted using a program called DERIVE which is a symbolic algebra manipulator rooted in Mathematica. For further details on DERIVE see chapter 4 in Beyak's disseration [31].

The left-hand side of each of the equations consider a single mode, $\phi^{(1)}$, while the right-hand side may contain no nonlinear interaction, quadratic interaction, or cubic interaction. The level of complexity is defined by the nonlinear forcing vector, $\mathcal{N}$. If $\mathcal{N} = 0$ the LPSE is modeled, if $\mathcal{N} = \mathcal{N}^{\mathrm{quad}}$ then quadratic interactions are allowed and if $\mathcal{N} = \mathcal{N}^{\mathrm{quad}} + \mathcal{N}^{\mathrm{cub}}$, then cubic interactions are allowed.

The assumptions which separate the LST, LPSE, and NPSE analysis are defined in detail in chapter 2. The LST distinction has not been made in this appendix as they have been previously identified in appendix A.

C.1 s - Momentum

$$
-\frac{i\,\Omega_{\mathrm{Re}}\,\beta\,\overline{\mu}\,\hat{w}_s}{\mathrm{Re}_e\,h_1\,h_3}-\frac{i\,\Omega_{\mathrm{Re}}\,\beta\,\overline{\lambda}_v\,\hat{w}_s}{\mathrm{Re}_e\,h_1\,h_3}-\frac{2\,h_{3,s}\,\overline{\rho}\,\overline{w}\,\hat{w}}{h_1\,h_3}+\frac{3\,i\,\Omega_{\mathrm{Re}}\,\beta\,h_{3,s}\,\overline{\mu}\,\hat{w}}{\mathrm{Re}_e\,h_1\,h_3^2}+\frac{\alpha\,\beta\,\overline{\mu}\,\hat{w}}{\mathrm{Re}_e\,h_1\,h_3}
$$

$$
-\frac{i\,\Omega_{\mathrm{Re}}\,\overline{T}_s\,\beta\,\overline{\lambda}_{v\overline{T}}\,\hat{w}}{\mathrm{Re}_e\,h_1\,h_3}+\frac{i\,\Omega_{\mathrm{Re}}\,\beta\,h_{3,s}\,\overline{\lambda}_v\,\hat{w}}{\mathrm{Re}_e\,h_1\,h_3^2}+\frac{\alpha\,\beta\,\overline{\lambda}_v\,\hat{w}}{\mathrm{Re}_e\,h_1\,h_3}-\frac{i\,\Omega_{\mathrm{Re}}\,\hat{T}\,\beta\,\overline{\mu}_{\overline{T}}\,\overline{w}_s}{\mathrm{Re}_e\,h_1\,h_3}-\frac{h_{3,s}\,\hat{\rho}\,\overline{w}^2}{h_1\,h_3}
$$

$$
+\frac{i\,\beta\,\overline{\rho}\,\hat{u}\,\overline{w}}{h_3}+\frac{i\,\Omega_{\mathrm{Re}}\,\hat{T}\,\beta\,h_{3,s}\,\overline{\mu}_{\overline{T}}\,\overline{w}}{\mathrm{Re}_e\,h_1\,h_3^2}-\frac{i\,\alpha\,\overline{\mu}\,\hat{v}_y}{\mathrm{Re}_e\,h_1}-\frac{\Omega_{\mathrm{Re}}\,\overline{T}_s\,\overline{\lambda}_{v\overline{T}}\,\hat{v}_y}{\mathrm{Re}_e\,h_1}-\frac{i\,\alpha\,\overline{\lambda}_v\,\hat{v}_y}{\mathrm{Re}_e\,h_1}-\frac{\Omega_{\mathrm{Re}}\,\overline{\mu}\,\hat{v}_{s\,y}}{\mathrm{Re}_e\,h_1}
$$

$$
-\frac{\Omega_{\mathrm{Re}}\,\overline{\lambda}_v\,\hat{v}_{s\,y}}{\mathrm{Re}_e\,h_1}-\frac{\Omega_{\mathrm{Re}}\,\overline{T}_y\,\overline{\mu}_{\overline{T}}\,\hat{v}_s}{\mathrm{Re}_e\,h_1}-\frac{\Omega_{\mathrm{Re}}\,h_{3,y}\,\overline{\mu}\,\hat{v}_s}{\mathrm{Re}_e\,h_1\,h_3}-\frac{3\,\Omega_{\mathrm{Re}}\,h_{1,y}\,\overline{\mu}\,\hat{v}_s}{\mathrm{Re}_e\,h_1^2}-\frac{\Omega_{\mathrm{Re}}\,h_{3,y}\,\overline{\lambda}_v\,\hat{v}_s}{\mathrm{Re}_e\,h_1\,h_3}-\frac{\Omega_{\mathrm{Re}}\,h_{1,y}\,\overline{\lambda}_v\,\hat{v}_s}{\mathrm{Re}_e\,h_1^2}
$$

$$
+\overline{\rho}\,\overline{u}_y\,\hat{v}+\frac{h_{1,y}\,\overline{\rho}\,\overline{u}\,\hat{v}}{h_1}-\frac{2\,\Omega_{\mathrm{Re}}\,\overline{T}_s\,h_{1,y}\,\overline{\mu}_{\overline{T}}\,\hat{v}}{\mathrm{Re}_e\,h_1^2}-\frac{i\,\overline{T}_y\,\alpha\,\overline{\mu}_{\overline{T}}\,\hat{v}}{\mathrm{Re}_e\,h_1}+\frac{2\,\Omega_{\mathrm{Re}}\,h_{3,s}\,h_{3,y}\,\overline{\mu}\,\hat{v}}{\mathrm{Re}_e\,h_1\,h_3^2}
$$

$$
-\frac{i\,\alpha\,h_{3,y}\,\overline{\mu}\,\hat{v}}{\mathrm{Re}_e\,h_1\,h_3}-\frac{2\,\Omega_{\mathrm{Re}}\,h_{1,y}\,h_{3,s}\,\overline{\mu}\,\hat{v}}{\mathrm{Re}_e\,h_1^2\,h_3}+\frac{2\,\Omega_{\mathrm{Re}}\,h_{1,s}\,h_{1,y}\,\overline{\mu}\,\hat{v}}{\mathrm{Re}_e\,h_1^3}-\frac{3\,i\,\alpha\,h_{1,y}\,\overline{\mu}\,\hat{v}}{\mathrm{Re}_e\,h_1^2}-\frac{2\,\Omega_{\mathrm{Re}}\,h_{1,s\,y}\,\overline{\mu}\,\hat{v}}{\mathrm{Re}_e\,h_1^2}
$$

$$
-\frac{\Omega_{\mathrm{Re}}\,\overline{T}_s\,h_{3,y}\,\overline{\lambda}_{v\overline{T}}\,\hat{v}}{\mathrm{Re}_e\,h_1\,h_3}-\frac{\Omega_{\mathrm{Re}}\,\overline{T}_s\,h_{1,y}\,\overline{\lambda}_{v\overline{T}}\,\hat{v}}{\mathrm{Re}_e\,h_1^2}+\frac{\Omega_{\mathrm{Re}}\,h_{3,s}\,h_{3,y}\,\overline{\lambda}_v\,\hat{v}}{\mathrm{Re}_e\,h_1\,h_3^2}-\frac{i\,\alpha\,h_{3,y}\,\overline{\lambda}_v\,\hat{v}}{\mathrm{Re}_e\,h_1\,h_3}-\frac{\Omega_{\mathrm{Re}}\,h_{3,s\,y}\,\overline{\lambda}_v\,\hat{v}}{\mathrm{Re}_e\,h_1\,h_3}
$$

$$
+\frac{\Omega_{\mathrm{Re}}\,h_{1,s}\,h_{1,y}\,\overline{\lambda}_v\,\hat{v}}{\mathrm{Re}_e\,h_1^3}-\frac{i\,\alpha\,h_{1,y}\,\overline{\lambda}_v\,\hat{v}}{\mathrm{Re}_e\,h_1^2}-\frac{\Omega_{\mathrm{Re}}\,h_{1,s\,y}\,\overline{\lambda}_v\,\hat{v}}{\mathrm{Re}_e\,h_1^2}-\frac{i\,\Omega_{\mathrm{Re}}\,\hat{T}\,\alpha\,\overline{\lambda}_{v\overline{T}}\,\overline{v}_y}{\mathrm{Re}_e\,h_1}
$$

$$
+\overline{\rho}\,\hat{u}_y\,\overline{v}+\frac{h_{1,y}\,\overline{\rho}\,\hat{u}\,\overline{v}}{h_1}+\hat{\rho}\,\overline{u}_y\,\overline{v}+\frac{h_{1,y}\,\hat{\rho}\,\overline{u}\,\overline{v}}{h_1}-\frac{2\,i\,\Omega_{\mathrm{Re}}\,\hat{T}\,\alpha\,h_{1,y}\,\overline{\mu}_{\overline{T}}\,\overline{v}}{\mathrm{Re}_e\,h_1^2}-\frac{i\,\Omega_{\mathrm{Re}}\,\hat{T}\,\alpha\,h_{3,y}\,\overline{\lambda}_{v\overline{T}}\,\overline{v}}{\mathrm{Re}_e\,h_1\,h_3}
$$

$$
-\frac{i\,\Omega_{\mathrm{Re}}\,\hat{T}\,\alpha\,h_{1,y}\,\overline{\lambda}_{v\overline{T}}\,\overline{v}}{\mathrm{Re}_e\,h_1^2}-\frac{\overline{\mu}\,\hat{u}_{y\,y}}{\mathrm{Re}_e}-\frac{\overline{T}_y\,\overline{\mu}_{\overline{T}}\,\hat{u}_y}{\mathrm{Re}_e}-\frac{h_{3,y}\,\overline{\mu}\,\hat{u}_y}{\mathrm{Re}_e\,h_3}-\frac{h_{1,y}\,\overline{\mu}\,\hat{u}_y}{\mathrm{Re}_e\,h_1}+\frac{\overline{\rho}\,\overline{u}\,\hat{u}_s}{h_1}
$$

$$
-\frac{4\,i\,\Omega_{\mathrm{Re}}\,\alpha\,\overline{\mu}\,\hat{u}_s}{\mathrm{Re}_e\,h_1^2}-\frac{2\,i\,\Omega_{\mathrm{Re}}\,\alpha\,\overline{\lambda}_v\,\hat{u}_s}{\mathrm{Re}_e\,h_1^2}+\frac{\overline{\rho}\,\overline{u}_s\,\hat{u}}{h_1}+\frac{i\,\alpha\,\overline{\rho}\,\overline{u}\,\hat{u}}{h_1}-i\,\omega\,\overline{\rho}\,\hat{u}+\frac{\overline{T}_y\,h_{1,y}\,\overline{\mu}_{\overline{T}}\,\hat{u}}{\mathrm{Re}_e\,h_1}
$$

$$
-\frac{2\,i\,\Omega_{\mathrm{Re}}\,\overline{T}_s\,\alpha\,\overline{\mu}_{\overline{T}}\,\hat{u}}{\mathrm{Re}_e\,h_1^2}+\frac{h_{1,y}\,h_{3,y}\,\overline{\mu}\,\hat{u}}{\mathrm{Re}_e\,h_1\,h_3}-\frac{2\,i\,\Omega_{\mathrm{Re}}\,\alpha\,h_{3,s}\,\overline{\mu}\,\hat{u}}{\mathrm{Re}_e\,h_1^2\,h_3}+\frac{\beta^2\,\overline{\mu}\,\hat{u}}{\mathrm{Re}_e\,h_3^2}+\frac{h_{1,y\,y}\,\overline{\mu}\,\hat{u}}{\mathrm{Re}_e\,h_1}+\frac{(h_{1,y})^2\,\overline{\mu}\,\hat{u}}{\mathrm{Re}_e\,h_1^2}
$$

$$
+\frac{2\,i\,\Omega_{\mathrm{Re}}\,\alpha\,h_{1,s}\,\overline{\mu}\,\hat{u}}{\mathrm{Re}_e\,h_1^3}-\frac{2\,i\,\Omega_{\mathrm{Re}}\,\alpha_s\,\overline{\mu}\,\hat{u}}{\mathrm{Re}_e\,h_1^2}+\frac{2\,\alpha^2\,\overline{\mu}\,\hat{u}}{\mathrm{Re}_e\,h_1^2}-\frac{i\,\Omega_{\mathrm{Re}}\,\overline{T}_s\,\alpha\,\overline{\lambda}_{v\overline{T}}\,\hat{u}}{\mathrm{Re}_e\,h_1^2}-\frac{i\,\Omega_{\mathrm{Re}}\,\alpha\,h_{3,s}\,\overline{\lambda}_v\,\hat{u}}{\mathrm{Re}_e\,h_1^2\,h_3}
$$

$$
+\frac{i\,\Omega_{\mathrm{Re}}\,\alpha\,h_{1,s}\,\overline{\lambda}_v\,\hat{u}}{\mathrm{Re}_e\,h_1^3}-\frac{i\,\Omega_{\mathrm{Re}}\,\alpha_s\,\overline{\lambda}_v\,\hat{u}}{\mathrm{Re}_e\,h_1^2}+\frac{\alpha^2\,\overline{\lambda}_v\,\hat{u}}{\mathrm{Re}_e\,h_1^2}-\frac{\hat{T}\,\overline{\mu}_{\overline{T}}\,\overline{u}_{y\,y}}{\mathrm{Re}_e}-\frac{\overline{T}_y\,\hat{T}\,\overline{\mu}_{\overline{T}\,\overline{T}}\,\overline{u}_y}{\mathrm{Re}_e}-\frac{\hat{T}\,h_{3,y}\,\overline{\mu}_{\overline{T}}\,\overline{u}_y}{\mathrm{Re}_e\,h_3}
$$

$$-\frac{\hat{T}\,h_{1,y}\,\overline{\mu}_{\overline{T}}\,\overline{u}_y}{\mathrm{Re}_e\,h_1}-\frac{\hat{T}_y\,\overline{\mu}_{\overline{T}}\,\overline{u}_y}{\mathrm{Re}_e}+\frac{\hat{\rho}\,\overline{u}\,\overline{u}_s}{h_1}-\frac{2\,i\,\Omega_{\mathrm{Re}}\,\hat{T}\,\alpha\,\overline{\mu}_{\overline{T}}\,\overline{u}_s}{\mathrm{Re}_e\,h_1^2}-\frac{i\,\Omega_{\mathrm{Re}}\,\hat{T}\,\alpha\,\overline{\lambda}_{v\overline{T}}\,\overline{u}_s}{\mathrm{Re}_e\,h_1^2}$$
$$+\frac{\overline{T}_y\,\hat{T}\,h_{1,y}\,\overline{\mu}_{\overline{T}\,\overline{T}}\,\overline{u}}{\mathrm{Re}_e\,h_1}+\frac{\hat{T}\,h_{1,y}\,h_{3,y}\,\overline{\mu}_{\overline{T}}\,\overline{u}}{\mathrm{Re}_e\,h_1\,h_3}+\frac{\hat{T}\,h_{1,y\,y}\,\overline{\mu}_{\overline{T}}\,\overline{u}}{\mathrm{Re}_e\,h_1}+\frac{\hat{T}\,\left(h_{1,y}\right)^2\,\overline{\mu}_{\overline{T}}\,\overline{u}}{\mathrm{Re}_e\,h_1^2}+\frac{\hat{T}_y\,h_{1,y}\,\overline{\mu}_{\overline{T}}\,\overline{u}}{\mathrm{Re}_e\,h_1}$$
$$-\frac{i\,\Omega_{\mathrm{Re}}\,\hat{T}\,\alpha\,h_{3,s}\,\overline{\lambda}_{v\overline{T}}\,\overline{u}}{\mathrm{Re}_e\,h_1^2\,h_3}+\frac{\Omega_p\,\overline{T}\,\hat{\rho}_s}{{\mathrm{M}_e}^2\,\gamma_e\,h_1}+\frac{i\,\overline{T}\,\alpha\,\hat{\rho}}{{\mathrm{M}_e}^2\,\gamma_e\,h_1}+\frac{\Omega_p\,\overline{T}_s\,\hat{\rho}}{{\mathrm{M}_e}^2\,\gamma_e\,h_1}+\frac{\Omega_p\,\hat{T}\,\overline{\rho}_s}{{\mathrm{M}_e}^2\,\gamma_e\,h_1}$$
$$+\frac{i\,\hat{T}\,\alpha\,\overline{\rho}}{{\mathrm{M}_e}^2\,\gamma_e\,h_1}+\frac{\Omega_p\,\hat{T}_s\,\overline{\rho}}{{\mathrm{M}_e}^2\,\gamma_e\,h_1}=\mathcal{N}(1)$$

C.2 y - Momentum

$$
-\frac{i\,\beta\,\overline{\mu}\,\hat{w}_y}{\mathrm{Re}_e\,h_3}-\frac{i\,\beta\,\overline{\lambda}_v\,\hat{w}_y}{\mathrm{Re}_e\,h_3}-\frac{2\,h_{3,y}\,\overline{\rho}\,\overline{w}\,\hat{w}}{h_3}+\frac{3\,i\,\beta\,h_{3,y}\,\overline{\mu}\,\hat{w}}{\mathrm{Re}_e\,h_3^2}-\frac{i\,\overline{T}_y\,\beta\,\overline{\lambda}_{v\overline{T}}\,\hat{w}}{\mathrm{Re}_e\,h_3}+\frac{i\,\beta\,h_{3,y}\,\overline{\lambda}_v\,\hat{w}}{\mathrm{Re}_e\,h_3^2}
$$

$$
-\frac{i\,\hat{T}\,\beta\,\overline{\mu}_{\overline{T}}\,\overline{w}_y}{\mathrm{Re}_e\,h_3}-\frac{h_{3,y}\,\hat{\rho}\,\overline{w}^2}{h_3}+\frac{i\,\beta\,\overline{\rho}\,\hat{v}\,\overline{w}}{h_3}+\frac{i\,\hat{T}\,\beta\,h_{3,y}\,\overline{\mu}_{\overline{T}}\,\overline{w}}{\mathrm{Re}_e\,h_3^2}-\frac{2\,\overline{\mu}\,\hat{v}_{y\,y}}{\mathrm{Re}_e}-\frac{\overline{\lambda}_v\,\hat{v}_{y\,y}}{\mathrm{Re}_e}
$$

$$
+\overline{\rho}\,\overline{v}\,\hat{v}_y-\frac{2\,\overline{T}_y\,\overline{\mu}_{\overline{T}}\,\hat{v}_y}{\mathrm{Re}_e}-\frac{2\,h_{3,y}\,\overline{\mu}\,\hat{v}_y}{\mathrm{Re}_e\,h_3}-\frac{2\,h_{1,y}\,\overline{\mu}\,\hat{v}_y}{\mathrm{Re}_e\,h_1}-\frac{\overline{T}_y\,\overline{\lambda}_{v\overline{T}}\,\hat{v}_y}{\mathrm{Re}_e}-\frac{h_{3,y}\,\overline{\lambda}_v\,\hat{v}_y}{\mathrm{Re}_e\,h_3}
$$

$$
-\frac{h_{1,y}\,\overline{\lambda}_v\,\hat{v}_y}{\mathrm{Re}_e\,h_1}+\frac{\overline{\rho}\,\overline{u}\,\hat{v}_s}{h_1}-\frac{2\,i\,\Omega_{\mathrm{Re}}\,\alpha\,\overline{\mu}\,\hat{v}_s}{\mathrm{Re}_e\,h_1^2}+\overline{\rho}\,\overline{v}_y\,\hat{v}+\frac{i\,\alpha\,\overline{\rho}\,\overline{u}\,\hat{v}}{h_1}-i\,\omega\,\overline{\rho}\,\hat{v}-\frac{i\,\Omega_{\mathrm{Re}}\,\overline{T}_s\,\alpha\,\overline{\mu}_{\overline{T}}\,\hat{v}}{\mathrm{Re}_e\,h_1^2}
$$

$$
+\frac{2\,\left(h_{3,y}\right)^2\,\overline{\mu}\,\hat{v}}{\mathrm{Re}_e\,h_3^2}-\frac{i\,\Omega_{\mathrm{Re}}\,\alpha\,h_{3,s}\,\overline{\mu}\,\hat{v}}{\mathrm{Re}_e\,h_1^2\,h_3}+\frac{\beta^2\,\overline{\mu}\,\hat{v}}{\mathrm{Re}_e\,h_3^2}+\frac{2\,\left(h_{1,y}\right)^2\,\overline{\mu}\,\hat{v}}{\mathrm{Re}_e\,h_1^2}+\frac{i\,\Omega_{\mathrm{Re}}\,\alpha\,h_{1,s}\,\overline{\mu}\,\hat{v}}{\mathrm{Re}_e\,h_1^3}-\frac{i\,\Omega_{\mathrm{Re}}\,\alpha_s\,\overline{\mu}\,\hat{v}}{\mathrm{Re}_e\,h_1^2}
$$

$$
+\frac{\alpha^2\,\overline{\mu}\,\hat{v}}{\mathrm{Re}_e\,h_1^2}-\frac{\overline{T}_y\,h_{3,y}\,\overline{\lambda}_{v\overline{T}}\,\hat{v}}{\mathrm{Re}_e\,h_3}-\frac{\overline{T}_y\,h_{1,y}\,\overline{\lambda}_{v\overline{T}}\,\hat{v}}{\mathrm{Re}_e\,h_1}-\frac{h_{3,y\,y}\,\overline{\lambda}_v\,\hat{v}}{\mathrm{Re}_e\,h_3}+\frac{\left(h_{3,y}\right)^2\,\overline{\lambda}_v\,\hat{v}}{\mathrm{Re}_e\,h_3^2}-\frac{h_{1,y\,y}\,\overline{\lambda}_v\,\hat{v}}{\mathrm{Re}_e\,h_1}
$$

$$
+\frac{\left(h_{1,y}\right)^2\,\overline{\lambda}_v\,\hat{v}}{\mathrm{Re}_e\,h_1^2}-\frac{2\,\Omega_{\mathrm{Re}}\,\hat{T}\,\overline{\mu}_{\overline{T}}\,\overline{v}_{y\,y}}{\mathrm{Re}_e}-\frac{\Omega_{\mathrm{Re}}\,\hat{T}\,\overline{\lambda}_{v\overline{T}}\,\overline{v}_{y\,y}}{\mathrm{Re}_e}-\frac{2\,\Omega_{\mathrm{Re}}\,\overline{T}_y\,\hat{T}\,\overline{\mu}_{\overline{T}\,\overline{T}}\,\overline{v}_y}{\mathrm{Re}_e}-\frac{2\,\Omega_{\mathrm{Re}}\,\hat{T}\,h_{3,y}\,\overline{\mu}_{\overline{T}}\,\overline{v}_y}{\mathrm{Re}_e\,h_3}
$$

$$
-\frac{2\,\Omega_{\mathrm{Re}}\,\hat{T}\,h_{1,y}\,\overline{\mu}_{\overline{T}}\,\overline{v}_y}{\mathrm{Re}_e\,h_1}-\frac{2\,\Omega_{\mathrm{Re}}\,\hat{T}_y\,\overline{\mu}_{\overline{T}}\,\overline{v}_y}{\mathrm{Re}_e}-\frac{\Omega_{\mathrm{Re}}\,\overline{T}_y\,\hat{T}\,\overline{\lambda}_{v\overline{T}\,\overline{T}}\,\overline{v}_y}{\mathrm{Re}_e}-\frac{\Omega_{\mathrm{Re}}\,\hat{T}\,h_{3,y}\,\overline{\lambda}_{v\overline{T}}\,\overline{v}_y}{\mathrm{Re}_e\,h_3}
$$

$$
-\frac{\Omega_{\mathrm{Re}}\,\hat{T}\,h_{1,y}\,\overline{\lambda}_{v\overline{T}}\,\overline{v}_y}{\mathrm{Re}_e\,h_1}-\frac{\Omega_{\mathrm{Re}}\,\hat{T}_y\,\overline{\lambda}_{v\overline{T}}\,\overline{v}_y}{\mathrm{Re}_e}+\frac{2\,\Omega_{\mathrm{Re}}\,\hat{T}\,\left(h_{3,y}\right)^2\,\overline{\mu}_{\overline{T}}\,\overline{v}}{\mathrm{Re}_e\,h_3^2}+\frac{2\,\Omega_{\mathrm{Re}}\,\hat{T}\,\left(h_{1,y}\right)^2\,\overline{\mu}_{\overline{T}}\,\overline{v}}{\mathrm{Re}_e\,h_1^2}
$$

$$
-\frac{\Omega_{\mathrm{Re}}\,\overline{T}_y\,\hat{T}\,h_{3,y}\,\overline{\lambda}_{v\overline{T}\,\overline{T}}\,\overline{v}}{\mathrm{Re}_e\,h_3}-\frac{\Omega_{\mathrm{Re}}\,\overline{T}_y\,\hat{T}\,h_{1,y}\,\overline{\lambda}_{v\overline{T}\,\overline{T}}\,\overline{v}}{\mathrm{Re}_e\,h_1}-\frac{\Omega_{\mathrm{Re}}\,\hat{T}\,h_{3,y\,y}\,\overline{\lambda}_{v\overline{T}}\,\overline{v}}{\mathrm{Re}_e\,h_3}+\frac{\Omega_{\mathrm{Re}}\,\hat{T}\,\left(h_{3,y}\right)^2\,\overline{\lambda}_{v\overline{T}}\,\overline{v}}{\mathrm{Re}_e\,h_3^2}
$$

$$
-\frac{\Omega_{\mathrm{Re}}\,\hat{T}_y\,h_{3,y}\,\overline{\lambda}_{v\overline{T}}\,\overline{v}}{\mathrm{Re}_e\,h_3}-\frac{\Omega_{\mathrm{Re}}\,\hat{T}\,h_{1,y\,y}\,\overline{\lambda}_{v\overline{T}}\,\overline{v}}{\mathrm{Re}_e\,h_1}+\frac{\Omega_{\mathrm{Re}}\,\hat{T}\,\left(h_{1,y}\right)^2\,\overline{\lambda}_{v\overline{T}}\,\overline{v}}{\mathrm{Re}_e\,h_1^2}-\frac{\Omega_{\mathrm{Re}}\,\hat{T}_y\,h_{1,y}\,\overline{\lambda}_{v\overline{T}}\,\overline{v}}{\mathrm{Re}_e\,h_1}
$$

$$
-\frac{\Omega_{\mathrm{Re}}\,\overline{T}_s\,\overline{\mu}_{\overline{T}}\,\hat{u}_y}{\mathrm{Re}_e\,h_1}-\frac{\Omega_{\mathrm{Re}}\,h_{3,s}\,\overline{\mu}\,\hat{u}_y}{\mathrm{Re}_e\,h_1\,h_3}-\frac{i\,\alpha\,\overline{\mu}\,\hat{u}_y}{\mathrm{Re}_e\,h_1}-\frac{\Omega_{\mathrm{Re}}\,h_{3,s}\,\overline{\lambda}_v\,\hat{u}_y}{\mathrm{Re}_e\,h_1\,h_3}-\frac{i\,\alpha\,\overline{\lambda}_v\,\hat{u}_y}{\mathrm{Re}_e\,h_1}-\frac{\Omega_{\mathrm{Re}}\,\overline{\mu}\,\hat{u}_{s\,y}}{\mathrm{Re}_e\,h_1}
$$

$$
-\frac{\Omega_{\mathrm{Re}}\,\overline{\lambda}_v\,\hat{u}_{s\,y}}{\mathrm{Re}_e\,h_1}+\frac{3\,\Omega_{\mathrm{Re}}\,h_{1,y}\,\overline{\mu}\,\hat{u}_s}{\mathrm{Re}_e\,h_1^2}-\frac{\Omega_{\mathrm{Re}}\,\overline{T}_y\,\overline{\lambda}_{v\overline{T}}\,\hat{u}_s}{\mathrm{Re}_e\,h_1}+\frac{\Omega_{\mathrm{Re}}\,h_{1,y}\,\overline{\lambda}_v\,\hat{u}_s}{\mathrm{Re}_e\,h_1^2}-\frac{2\,h_{1,y}\,\overline{\rho}\,\overline{u}\,\hat{u}}{h_1}
$$

$$
+\frac{\Omega_{\mathrm{Re}}\,\overline{T}_s\,h_{1,y}\,\overline{\mu}_{\overline{T}}\,\hat{u}}{\mathrm{Re}_e\,h_1^2}+\frac{2\,\Omega_{\mathrm{Re}}\,h_{3,s}\,h_{3,y}\,\overline{\mu}\,\hat{u}}{\mathrm{Re}_e\,h_1\,h_3^2}+\frac{\Omega_{\mathrm{Re}}\,h_{1,y}\,h_{3,s}\,\overline{\mu}\,\hat{u}}{\mathrm{Re}_e\,h_1^2\,h_3}-\frac{\Omega_{\mathrm{Re}}\,h_{1,s}\,h_{1,y}\,\overline{\mu}\,\hat{u}}{\mathrm{Re}_e\,h_1^3}+\frac{3\,i\,\alpha\,h_{1,y}\,\overline{\mu}\,\hat{u}}{\mathrm{Re}_e\,h_1^2}
$$

$$
+\frac{\Omega_{\mathrm{Re}}\,h_{1,s\,y}\,\overline{\mu}\,\hat{u}}{\mathrm{Re}_e\,h_1^2}-\frac{\Omega_{\mathrm{Re}}\,\overline{T}_y\,h_{3,s}\,\overline{\lambda}_{v\overline{T}}\,\hat{u}}{\mathrm{Re}_e\,h_1\,h_3}-\frac{i\,\overline{T}_y\,\alpha\,\overline{\lambda}_{v\overline{T}}\,\hat{u}}{\mathrm{Re}_e\,h_1}+\frac{\Omega_{\mathrm{Re}}\,h_{3,s}\,h_{3,y}\,\overline{\lambda}_v\,\hat{u}}{\mathrm{Re}_e\,h_1\,h_3^2}-\frac{\Omega_{\mathrm{Re}}\,h_{3,s\,y}\,\overline{\lambda}_v\,\hat{u}}{\mathrm{Re}_e\,h_1\,h_3}
$$

$$
+\frac{\Omega_{\mathrm{Re}}\,h_{1,y}\,h_{3,s}\,\overline{\lambda}_v\,\hat{u}}{\mathrm{Re}_e\,h_1^2\,h_3}+\frac{i\,\alpha\,h_{1,y}\,\overline{\lambda}_v\,\hat{u}}{\mathrm{Re}_e\,h_1^2}-\frac{\Omega_{\mathrm{Re}}\,\overline{T}_s\,\hat{T}\,\overline{\mu}_{\overline{T}\,\overline{T}}\,\overline{u}_y}{\mathrm{Re}_e\,h_1}-\frac{\Omega_{\mathrm{Re}}\,\hat{T}\,h_{3,s}\,\overline{\mu}_{\overline{T}}\,\overline{u}_y}{\mathrm{Re}_e\,h_1\,h_3}
$$

$$-\frac{i\,\hat{T}\,\alpha\,\overline{\mu}_{\overline{T}}\,\overline{u}_y}{\mathrm{Re}_e\,h_1}-\frac{\Omega_{\mathrm{Re}}\,\hat{T}_s\,\overline{\mu}_{\overline{T}}\,\overline{u}_y}{\mathrm{Re}_e\,h_1}-\frac{\Omega_{\mathrm{Re}}\,\hat{T}\,h_{3,s}\,\overline{\lambda}_{v\overline{T}}\,\overline{u}_y}{\mathrm{Re}_e\,h_1\,h_3}-\frac{\Omega_{\mathrm{Re}}\,\hat{T}\,\overline{\mu}_{\overline{T}}\,\overline{u}_{s\,y}}{\mathrm{Re}_e\,h_1}-\frac{\Omega_{\mathrm{Re}}\,\hat{T}\,\overline{\lambda}_{v\overline{T}}\,\overline{u}_{s\,y}}{\mathrm{Re}_e\,h_1}$$
$$+\frac{3\,\Omega_{\mathrm{Re}}\,\hat{T}\,h_{1,y}\,\overline{\mu}_{\overline{T}}\,\overline{u}_s}{\mathrm{Re}_e\,h_1^2}-\frac{\Omega_{\mathrm{Re}}\,\overline{T}_y\,\hat{T}\,\overline{\lambda}_{v\overline{T}\,\overline{T}}\,\overline{u}_s}{\mathrm{Re}_e\,h_1}+\frac{\Omega_{\mathrm{Re}}\,\hat{T}\,h_{1,y}\,\overline{\lambda}_{v\overline{T}}\,\overline{u}_s}{\mathrm{Re}_e\,h_1^2}-\frac{\Omega_{\mathrm{Re}}\,\hat{T}_y\,\overline{\lambda}_{v\overline{T}}\,\overline{u}_s}{\mathrm{Re}_e\,h_1}-\frac{h_{1,y}\,\hat{\rho}\,\overline{u}^2}{h_1}$$
$$+\frac{\Omega_{\mathrm{Re}}\,\overline{T}_s\,\hat{T}\,h_{1,y}\,\overline{\mu}_{\overline{T}\,\overline{T}}\,\overline{u}}{\mathrm{Re}_e\,h_1^2}+\frac{2\,\Omega_{\mathrm{Re}}\,\hat{T}\,h_{3,s}\,h_{3,y}\,\overline{\mu}_{\overline{T}}\,\overline{u}}{\mathrm{Re}_e\,h_1\,h_3^2}+\frac{\Omega_{\mathrm{Re}}\,\hat{T}\,h_{1,y}\,h_{3,s}\,\overline{\mu}_{\overline{T}}\,\overline{u}}{\mathrm{Re}_e\,h_1^2\,h_3}-\frac{\Omega_{\mathrm{Re}}\,\hat{T}\,h_{1,s}\,h_{1,y}\,\overline{\mu}_{\overline{T}}\,\overline{u}}{\mathrm{Re}_e\,h_1^3}$$
$$+\frac{i\,\hat{T}\,\alpha\,h_{1,y}\,\overline{\mu}_{\overline{T}}\,\overline{u}}{\mathrm{Re}_e\,h_1^2}+\frac{\Omega_{\mathrm{Re}}\,\hat{T}_s\,h_{1,y}\,\overline{\mu}_{\overline{T}}\,\overline{u}}{\mathrm{Re}_e\,h_1^2}+\frac{\Omega_{\mathrm{Re}}\,\hat{T}\,h_{1,s\,y}\,\overline{\mu}_{\overline{T}}\,\overline{u}}{\mathrm{Re}_e\,h_1^2}-\frac{\Omega_{\mathrm{Re}}\,\overline{T}_y\,\hat{T}\,h_{3,s}\,\overline{\lambda}_{v\overline{T}\,\overline{T}}\,\overline{u}}{\mathrm{Re}_e\,h_1\,h_3}$$
$$+\frac{\Omega_{\mathrm{Re}}\,\hat{T}\,h_{3,s}\,h_{3,y}\,\overline{\lambda}_{v\overline{T}}\,\overline{u}}{\mathrm{Re}_e\,h_1\,h_3^2}-\frac{\Omega_{\mathrm{Re}}\,\hat{T}\,h_{3,s\,y}\,\overline{\lambda}_{v\overline{T}}\,\overline{u}}{\mathrm{Re}_e\,h_1\,h_3}+\frac{\Omega_{\mathrm{Re}}\,\hat{T}\,h_{1,y}\,h_{3,s}\,\overline{\lambda}_{v\overline{T}}\,\overline{u}}{\mathrm{Re}_e\,h_1^2\,h_3}-\frac{\Omega_{\mathrm{Re}}\,\hat{T}_y\,h_{3,s}\,\overline{\lambda}_{v\overline{T}}\,\overline{u}}{\mathrm{Re}_e\,h_1\,h_3}$$
$$+\frac{\overline{T}\,\hat{\rho}_y}{\mathrm{M}_e{}^2\,\gamma_e}+\frac{\overline{T}_y\,\hat{\rho}}{\mathrm{M}_e{}^2\,\gamma_e}+\frac{\hat{T}\,\overline{\rho}_y}{\mathrm{M}_e{}^2\,\gamma_e}+\frac{\hat{T}_y\,\overline{\rho}}{\mathrm{M}_e{}^2\,\gamma_e}=\mathcal{N}(2)$$

C.3 z - Momentum

$$
\begin{aligned}
&-\frac{\overline{\mu}\,\hat{w}_{y\,y}}{\mathrm{Re}_e}+\overline{\rho}\,\overline{v}\,\hat{w}_y-\frac{\overline{T}_y\,\overline{\mu}_{\overline{T}}\,\hat{w}_y}{\mathrm{Re}_e}-\frac{h_{3,y}\,\overline{\mu}\,\hat{w}_y}{\mathrm{Re}_e\,h_3}-\frac{h_{1,y}\,\overline{\mu}\,\hat{w}_y}{\mathrm{Re}_e\,h_1}+\frac{\overline{\rho}\,\overline{u}\,\hat{w}_s}{h_1}-\frac{2\,i\,\Omega_{\mathrm{Re}}\,\alpha\,\overline{\mu}\,\hat{w}_s}{\mathrm{Re}_e\,h_1^2}\\
&+\frac{i\,\beta\,\overline{\rho}\,\overline{w}\,\hat{w}}{h_3}+\frac{h_{3,y}\,\overline{\rho}\,\overline{v}\,\hat{w}}{h_3}+\frac{h_{3,s}\,\overline{\rho}\,\overline{u}\,\hat{w}}{h_1\,h_3}+\frac{i\,\alpha\,\overline{\rho}\,\overline{u}\,\hat{w}}{h_1}-i\,\omega\,\overline{\rho}\,\hat{w}+\frac{\overline{T}_y\,h_{3,y}\,\overline{\mu}_{\overline{T}}\,\hat{w}}{\mathrm{Re}_e\,h_3}\\
&-\frac{i\,\Omega_{\mathrm{Re}}\,\overline{T}_s\,\alpha\,\overline{\mu}_{\overline{T}}\,\hat{w}}{\mathrm{Re}_e\,h_1^2}+\frac{h_{3,y\,y}\,\overline{\mu}\,\hat{w}}{\mathrm{Re}_e\,h_3}+\frac{(h_{3,y})^2\,\overline{\mu}\,\hat{w}}{\mathrm{Re}_e\,h_3^2}+\frac{h_{1,y}\,h_{3,y}\,\overline{\mu}\,\hat{w}}{\mathrm{Re}_e\,h_1\,h_3}-\frac{i\,\Omega_{\mathrm{Re}}\,\alpha\,h_{3,s}\,\overline{\mu}\,\hat{w}}{\mathrm{Re}_e\,h_1^2\,h_3}+\frac{2\,\beta^2\,\overline{\mu}\,\hat{w}}{\mathrm{Re}_e\,h_3^2}\\
&+\frac{i\,\Omega_{\mathrm{Re}}\,\alpha\,h_{1,s}\,\overline{\mu}\,\hat{w}}{\mathrm{Re}_e\,h_1^3}-\frac{i\,\Omega_{\mathrm{Re}}\,\alpha_s\,\overline{\mu}\,\hat{w}}{\mathrm{Re}_e\,h_1^2}+\frac{\alpha^2\,\overline{\mu}\,\hat{w}}{\mathrm{Re}_e\,h_1^2}+\frac{\beta^2\,\overline{\lambda}_v\,\hat{w}}{\mathrm{Re}_e\,h_3^2}-\frac{\hat{T}\,\overline{\mu}_{\overline{T}}\,\overline{w}_{y\,y}}{\mathrm{Re}_e}+\overline{\rho}\,\hat{v}\,\overline{w}_y\\
&+\hat{\rho}\,\overline{v}\,\overline{w}_y-\frac{\overline{T}_y\,\hat{T}\,\overline{\mu}_{\overline{T}\,\overline{T}}\,\overline{w}_y}{\mathrm{Re}_e}-\frac{\hat{T}\,h_{3,y}\,\overline{\mu}_{\overline{T}}\,\overline{w}_y}{\mathrm{Re}_e\,h_3}-\frac{\hat{T}\,h_{1,y}\,\overline{\mu}_{\overline{T}}\,\overline{w}_y}{\mathrm{Re}_e\,h_1}-\frac{\hat{T}_y\,\overline{\mu}_{\overline{T}}\,\overline{w}_y}{\mathrm{Re}_e}+\frac{\overline{\rho}\,\hat{u}\,\overline{w}_s}{h_1}+\frac{\hat{\rho}\,\overline{u}\,\overline{w}_s}{h_1}\\
&-\frac{i\,\Omega_{\mathrm{Re}}\,\hat{T}\,\alpha\,\overline{\mu}_{\overline{T}}\,\overline{w}_s}{\mathrm{Re}_e\,h_1^2}+\frac{h_{3,y}\,\overline{\rho}\,\hat{v}\,\overline{w}}{h_3}+\frac{h_{3,y}\,\hat{\rho}\,\overline{v}\,\overline{w}}{h_3}+\frac{h_{3,s}\,\overline{\rho}\,\hat{u}\,\overline{w}}{h_1\,h_3}+\frac{h_{3,s}\,\hat{\rho}\,\overline{u}\,\overline{w}}{h_1\,h_3}+\frac{\overline{T}_y\,\hat{T}\,h_{3,y}\,\overline{\mu}_{\overline{T}\,\overline{T}}\,\overline{w}}{\mathrm{Re}_e\,h_3}\\
&+\frac{\hat{T}\,h_{3,y\,y}\,\overline{\mu}_{\overline{T}}\,\overline{w}}{\mathrm{Re}_e\,h_3}+\frac{\hat{T}\,(h_{3,y})^2\,\overline{\mu}_{\overline{T}}\,\overline{w}}{\mathrm{Re}_e\,h_3^2}+\frac{\hat{T}\,h_{1,y}\,h_{3,y}\,\overline{\mu}_{\overline{T}}\,\overline{w}}{\mathrm{Re}_e\,h_1\,h_3}+\frac{\hat{T}_y\,h_{3,y}\,\overline{\mu}_{\overline{T}}\,\overline{w}}{\mathrm{Re}_e\,h_3}+\frac{i\,\Omega_{\mathrm{Re}}\,\hat{T}\,\alpha\,h_{3,s}\,\overline{\mu}_{\overline{T}}\,\overline{w}}{\mathrm{Re}_e\,h_1^2\,h_3}\\
&-\frac{i\,\beta\,\overline{\mu}\,\hat{v}_y}{\mathrm{Re}_e\,h_3}-\frac{i\,\beta\,\overline{\lambda}_v\,\hat{v}_y}{\mathrm{Re}_e\,h_3}-\frac{i\,\overline{T}_y\,\beta\,\overline{\mu}_{\overline{T}}\,\hat{v}}{\mathrm{Re}_e\,h_3}-\frac{3\,i\,\beta\,h_{3,y}\,\overline{\mu}\,\hat{v}}{\mathrm{Re}_e\,h_3^2}-\frac{i\,\beta\,h_{1,y}\,\overline{\mu}\,\hat{v}}{\mathrm{Re}_e\,h_1\,h_3}-\frac{i\,\beta\,h_{3,y}\,\overline{\lambda}_v\,\hat{v}}{\mathrm{Re}_e\,h_3^2}\\
&-\frac{i\,\beta\,h_{1,y}\,\overline{\lambda}_v\,\hat{v}}{\mathrm{Re}_e\,h_1\,h_3}-\frac{i\,\Omega_{\mathrm{Re}}\,\hat{T}\,\beta\,\overline{\lambda}_{v\overline{T}}\,\overline{v}_y}{\mathrm{Re}_e\,h_3}-\frac{2\,i\,\Omega_{\mathrm{Re}}\,\hat{T}\,\beta\,h_{3,y}\,\overline{\mu}_{\overline{T}}\,\overline{v}}{\mathrm{Re}_e\,h_3^2}-\frac{i\,\Omega_{\mathrm{Re}}\,\hat{T}\,\beta\,h_{3,y}\,\overline{\lambda}_{v\overline{T}}\,\overline{v}}{\mathrm{Re}_e\,h_3^2}\\
&-\frac{i\,\Omega_{\mathrm{Re}}\,\hat{T}\,\beta\,h_{1,y}\,\overline{\lambda}_{v\overline{T}}\,\overline{v}}{\mathrm{Re}_e\,h_1\,h_3}-\frac{i\,\Omega_{\mathrm{Re}}\,\beta\,\overline{\mu}\,\hat{u}_s}{\mathrm{Re}_e\,h_1\,h_3}-\frac{i\,\Omega_{\mathrm{Re}}\,\beta\,\overline{\lambda}_v\,\hat{u}_s}{\mathrm{Re}_e\,h_1\,h_3}-\frac{i\,\Omega_{\mathrm{Re}}\,\overline{T}_s\,\beta\,\overline{\mu}_{\overline{T}}\,\hat{u}}{\mathrm{Re}_e\,h_1\,h_3}-\frac{3\,i\,\Omega_{\mathrm{Re}}\,\beta\,h_{3,s}\,\overline{\mu}\,\hat{u}}{\mathrm{Re}_e\,h_1\,h_3^2}\\
&+\frac{\alpha\,\beta\,\overline{\mu}\,\hat{u}}{\mathrm{Re}_e\,h_1\,h_3}-\frac{i\,\Omega_{\mathrm{Re}}\,\beta\,h_{3,s}\,\overline{\lambda}_v\,\hat{u}}{\mathrm{Re}_e\,h_1\,h_3^2}+\frac{\alpha\,\beta\,\overline{\lambda}_v\,\hat{u}}{\mathrm{Re}_e\,h_1\,h_3}-\frac{i\,\Omega_{\mathrm{Re}}\,\hat{T}\,\beta\,\overline{\lambda}_{v\overline{T}}\,\overline{u}_s}{\mathrm{Re}_e\,h_1\,h_3}-\frac{2\,i\,\Omega_{\mathrm{Re}}\,\hat{T}\,\beta\,h_{3,s}\,\overline{\mu}_{\overline{T}}\,\overline{u}}{\mathrm{Re}_e\,h_1\,h_3^2}\\
&-\frac{i\,\Omega_{\mathrm{Re}}\,\hat{T}\,\beta\,h_{3,s}\,\overline{\lambda}_{v\overline{T}}\,\overline{u}}{\mathrm{Re}_e\,h_1\,h_3^2}+\frac{i\,\overline{T}\,\beta\,\hat{\rho}}{{\mathrm{M}_e}^2\,\gamma_e\,h_3}+\frac{i\,\hat{T}\,\beta\,\overline{\rho}}{{\mathrm{M}_e}^2\,\gamma_e\,h_3}=\mathcal{N}(3)
\end{aligned}
$$

C.4 Conservation of Energy

$$
-\frac{2\,\mathrm{Ec}_e\,\overline{\mu}\,\overline{w}_y\,\hat{w}_y}{\mathrm{Re}_e}+\frac{2\,\mathrm{Ec}_e\,h_{3,y}\,\overline{\mu}\,\overline{w}\,\hat{w}_y}{\mathrm{Re}_e\,h_3}+\frac{2\,\mathrm{Ec}_e\,h_{3,y}\,\overline{\mu}\,\overline{w}_y\,\hat{w}}{\mathrm{Re}_e\,h_3}-\frac{2\,i\,\mathrm{Ec}_e\,\Omega_{\mathrm{Re}}\,\alpha\,\overline{\mu}\,\overline{w}_s\,\hat{w}}{\mathrm{Re}_e\,h_1^2}
$$

$$
-\frac{2\,\mathrm{Ec}_e\,\left(h_{3,y}\right)^2\,\overline{\mu}\,\overline{w}\,\hat{w}}{\mathrm{Re}_e\,h_3^2}+\frac{2\,i\,\mathrm{Ec}_e\,\Omega_{\mathrm{Re}}\,\alpha\,h_{3,s}\,\overline{\mu}\,\overline{w}\,\hat{w}}{\mathrm{Re}_e\,h_1^2\,h_3}-\frac{2\,i\,\mathrm{Ec}_e\,\Omega_{\mathrm{Re}}\,\beta\,\overline{\lambda}_v\,\overline{v}_y\,\hat{w}}{\mathrm{Re}_e\,h_3}
$$

$$
-\frac{4\,i\,\mathrm{Ec}_e\,\Omega_{\mathrm{Re}}\,\beta\,h_{3,y}\,\overline{\mu}\,\overline{v}\,\hat{w}}{\mathrm{Re}_e\,h_3^2}-\frac{2\,i\,\mathrm{Ec}_e\,\Omega_{\mathrm{Re}}\,\beta\,h_{3,y}\,\overline{\lambda}_v\,\overline{v}\,\hat{w}}{\mathrm{Re}_e\,h_3^2}-\frac{2\,i\,\mathrm{Ec}_e\,\Omega_{\mathrm{Re}}\,\beta\,h_{1,y}\,\overline{\lambda}_v\,\overline{v}\,\hat{w}}{\mathrm{Re}_e\,h_1\,h_3}
$$

$$
-\frac{2\,i\,\mathrm{Ec}_e\,\Omega_{\mathrm{Re}}\,\beta\,\overline{\lambda}_v\,\overline{u}_s\,\hat{w}}{\mathrm{Re}_e\,h_1\,h_3}-\frac{4\,i\,\mathrm{Ec}_e\,\Omega_{\mathrm{Re}}\,\beta\,h_{3,s}\,\overline{\mu}\,\overline{u}\,\hat{w}}{\mathrm{Re}_e\,h_1\,h_3^2}-\frac{2\,i\,\mathrm{Ec}_e\,\Omega_{\mathrm{Re}}\,\beta\,h_{3,s}\,\overline{\lambda}_v\,\overline{u}\,\hat{w}}{\mathrm{Re}_e\,h_1\,h_3^2}
$$

$$
-\frac{\mathrm{Ec}_e\,\hat{T}\,\overline{\mu}_{\overline{T}}\,\left(\overline{w}_y\right)^2}{\mathrm{Re}_e}+\frac{2\,\mathrm{Ec}_e\,\hat{T}\,h_{3,y}\,\overline{\mu}_{\overline{T}}\,\overline{w}\,\overline{w}_y}{\mathrm{Re}_e\,h_3}-\frac{2\,i\,\mathrm{Ec}_e\,\beta\,\overline{\mu}\,\hat{v}\,\overline{w}_y}{\mathrm{Re}_e\,h_3}-\frac{2\,i\,\mathrm{Ec}_e\,\Omega_{\mathrm{Re}}\,\beta\,\overline{\mu}\,\hat{u}\,\overline{w}_s}{\mathrm{Re}_e\,h_1\,h_3}
$$

$$
-\frac{\mathrm{Ec}_e\,\hat{T}\,\left(h_{3,y}\right)^2\,\overline{\mu}_{\overline{T}}\,\overline{w}^2}{\mathrm{Re}_e\,h_3^2}+\frac{2\,i\,\mathrm{Ec}_e\,\beta\,h_{3,y}\,\overline{\mu}\,\hat{v}\,\overline{w}}{\mathrm{Re}_e\,h_3^2}+\frac{2\,i\,\mathrm{Ec}_e\,\Omega_{\mathrm{Re}}\,\beta\,h_{3,s}\,\overline{\mu}\,\hat{u}\,\overline{w}}{\mathrm{Re}_e\,h_1\,h_3^2}-\frac{i\,\mathrm{Ec}_e\,\overline{T}\,\beta\,\hat{\rho}\,\overline{w}}{{\mathrm{M}_e}^2\,\gamma_e\,h_3}
$$

$$
-\frac{i\,\mathrm{Ec}_e\,\hat{T}\,\beta\,\overline{\rho}\,\overline{w}}{{\mathrm{M}_e}^2\,\gamma_e\,h_3}+\frac{i\,\hat{T}\,\beta\,\overline{\rho}\,\overline{w}}{h_3}-\frac{4\,\mathrm{Ec}_e\,\Omega_{\mathrm{Re}}\,\overline{\mu}\,\overline{v}_y\,\hat{v}_y}{\mathrm{Re}_e}-\frac{2\,\mathrm{Ec}_e\,\Omega_{\mathrm{Re}}\,\overline{\lambda}_v\,\overline{v}_y\,\hat{v}_y}{\mathrm{Re}_e}
$$

$$
-\frac{2\,\mathrm{Ec}_e\,\Omega_{\mathrm{Re}}\,h_{3,y}\,\overline{\lambda}_v\,\overline{v}\,\hat{v}_y}{\mathrm{Re}_e\,h_3}-\frac{2\,\mathrm{Ec}_e\,\Omega_{\mathrm{Re}}\,h_{1,y}\,\overline{\lambda}_v\,\overline{v}\,\hat{v}_y}{\mathrm{Re}_e\,h_1}-\frac{2\,\mathrm{Ec}_e\,\Omega_{\mathrm{Re}}\,\overline{\lambda}_v\,\overline{u}_s\,\hat{v}_y}{\mathrm{Re}_e\,h_1}-\frac{2\,\mathrm{Ec}_e\,\Omega_{\mathrm{Re}}\,h_{3,s}\,\overline{\lambda}_v\,\overline{u}\,\hat{v}_y}{\mathrm{Re}_e\,h_1\,h_3}
$$

$$
-\frac{2\,\mathrm{Ec}_e\,\Omega_{\mathrm{Re}}\,\overline{\mu}\,\overline{u}_y\,\hat{v}_s}{\mathrm{Re}_e\,h_1}+\frac{2\,\mathrm{Ec}_e\,\Omega_{\mathrm{Re}}\,h_{1,y}\,\overline{\mu}\,\overline{u}\,\hat{v}_s}{\mathrm{Re}_e\,h_1^2}-\frac{2\,\mathrm{Ec}_e\,\Omega_{\mathrm{Re}}\,h_{3,y}\,\overline{\lambda}_v\,\overline{v}_y\,\hat{v}}{\mathrm{Re}_e\,h_3}-\frac{2\,\mathrm{Ec}_e\,\Omega_{\mathrm{Re}}\,h_{1,y}\,\overline{\lambda}_v\,\overline{v}_y\,\hat{v}}{\mathrm{Re}_e\,h_1}
$$

$$
-\frac{4\,\mathrm{Ec}_e\,\Omega_{\mathrm{Re}}\,\left(h_{3,y}\right)^2\,\overline{\mu}\,\overline{v}\,\hat{v}}{\mathrm{Re}_e\,h_3^2}-\frac{4\,\mathrm{Ec}_e\,\Omega_{\mathrm{Re}}\,\left(h_{1,y}\right)^2\,\overline{\mu}\,\overline{v}\,\hat{v}}{\mathrm{Re}_e\,h_1^2}-\frac{2\,\mathrm{Ec}_e\,\Omega_{\mathrm{Re}}\,\left(h_{3,y}\right)^2\,\overline{\lambda}_v\,\overline{v}\,\hat{v}}{\mathrm{Re}_e\,h_3^2}
$$

$$
-\frac{4\,\mathrm{Ec}_e\,\Omega_{\mathrm{Re}}\,h_{1,y}\,h_{3,y}\,\overline{\lambda}_v\,\overline{v}\,\hat{v}}{\mathrm{Re}_e\,h_1\,h_3}-\frac{2\,\mathrm{Ec}_e\,\Omega_{\mathrm{Re}}\,\left(h_{1,y}\right)^2\,\overline{\lambda}_v\,\overline{v}\,\hat{v}}{\mathrm{Re}_e\,h_1^2}-\frac{2\,i\,\mathrm{Ec}_e\,\alpha\,\overline{\mu}\,\overline{u}_y\,\hat{v}}{\mathrm{Re}_e\,h_1}
$$

$$
-\frac{4\,\mathrm{Ec}_e\,\Omega_{\mathrm{Re}}\,h_{1,y}\,\overline{\mu}\,\overline{u}_s\,\hat{v}}{\mathrm{Re}_e\,h_1^2}-\frac{2\,\mathrm{Ec}_e\,\Omega_{\mathrm{Re}}\,h_{3,y}\,\overline{\lambda}_v\,\overline{u}_s\,\hat{v}}{\mathrm{Re}_e\,h_1\,h_3}-\frac{2\,\mathrm{Ec}_e\,\Omega_{\mathrm{Re}}\,h_{1,y}\,\overline{\lambda}_v\,\overline{u}_s\,\hat{v}}{\mathrm{Re}_e\,h_1^2}
$$

$$
-\frac{4\,\mathrm{Ec}_e\,\Omega_{\mathrm{Re}}\,h_{3,s}\,h_{3,y}\,\overline{\mu}\,\overline{u}\,\hat{v}}{\mathrm{Re}_e\,h_1\,h_3^2}+\frac{2\,i\,\mathrm{Ec}_e\,\alpha\,h_{1,y}\,\overline{\mu}\,\overline{u}\,\hat{v}}{\mathrm{Re}_e\,h_1^2}-\frac{2\,\mathrm{Ec}_e\,\Omega_{\mathrm{Re}}\,h_{3,s}\,h_{3,y}\,\overline{\lambda}_v\,\overline{u}\,\hat{v}}{\mathrm{Re}_e\,h_1\,h_3^2}
$$

$$
-\frac{2\,\mathrm{Ec}_e\,\Omega_{\mathrm{Re}}\,h_{1,y}\,h_{3,s}\,\overline{\lambda}_v\,\overline{u}\,\hat{v}}{\mathrm{Re}_e\,h_1^2\,h_3}-\frac{\mathrm{Ec}_e\,\overline{T}\,\overline{\rho}_y\,\hat{v}}{{\mathrm{M}_e}^2\,\gamma_e}-\frac{\mathrm{Ec}_e\,\overline{T}_y\,\overline{\rho}\,\hat{v}}{{\mathrm{M}_e}^2\,\gamma_e}+\overline{T}_y\,\overline{\rho}\,\hat{v}
$$

$$
-\frac{2\,i\,\mathrm{Ec}_e\,\Omega_{\mathrm{Re}}\,\alpha\,\overline{\lambda}_v\,\hat{u}\,\overline{v}_y}{\mathrm{Re}_e\,h_1}-\frac{4\,i\,\mathrm{Ec}_e\,\Omega_{\mathrm{Re}}\,\alpha\,h_{1,y}\,\overline{\mu}\,\hat{u}\,\overline{v}}{\mathrm{Re}_e\,h_1^2}-\frac{2\,i\,\mathrm{Ec}_e\,\Omega_{\mathrm{Re}}\,\alpha\,h_{3,y}\,\overline{\lambda}_v\,\hat{u}\,\overline{v}}{\mathrm{Re}_e\,h_1\,h_3}
$$

$$
-\frac{2\,i\,\mathrm{Ec}_e\,\Omega_{\mathrm{Re}}\,\alpha\,h_{1,y}\,\overline{\lambda}_v\,\hat{u}\,\overline{v}}{\mathrm{Re}_e\,h_1^2}-\frac{\mathrm{Ec}_e\,\overline{T}\,\hat{\rho}_y\,\overline{v}}{{\mathrm{M}_e}^2\,\gamma_e}-\frac{\mathrm{Ec}_e\,\overline{T}_y\,\hat{\rho}\,\overline{v}}{{\mathrm{M}_e}^2\,\gamma_e}+\overline{T}_y\,\hat{\rho}\,\overline{v}-\frac{\mathrm{Ec}_e\,\hat{T}\,\overline{\rho}_y\,\overline{v}}{{\mathrm{M}_e}^2\,\gamma_e}
$$

$$
-\frac{\mathrm{Ec}_e\,\hat{T}_y\,\overline{\rho}\,\overline{v}}{{\mathrm{M}_e}^2\,\gamma_e}+\hat{T}_y\,\overline{\rho}\,\overline{v}-\frac{2\,\mathrm{Ec}_e\,\overline{\mu}\,\overline{u}_y\,\hat{u}_y}{\mathrm{Re}_e}+\frac{2\,\mathrm{Ec}_e\,h_{1,y}\,\overline{\mu}\,\overline{u}\,\hat{u}_y}{\mathrm{Re}_e\,h_1}+\frac{2\,\mathrm{Ec}_e\,h_{1,y}\,\overline{\mu}\,\overline{u}_y\,\hat{u}}{\mathrm{Re}_e\,h_1}
$$

$$-\frac{4\,i\,\mathrm{Ec}_e\,\Omega_{\mathrm{Re}}\,\alpha\,\overline{\mu}\,\overline{u}_s\,\hat{u}}{\mathrm{Re}_e\,h_1^2}-\frac{2\,i\,\mathrm{Ec}_e\,\Omega_{\mathrm{Re}}\,\alpha\,\overline{\lambda}_v\,\overline{u}_s\,\hat{u}}{\mathrm{Re}_e\,h_1^2}-\frac{2\,\mathrm{Ec}_e\,\left(h_{1,y}\right)^2\,\overline{\mu}\,\overline{u}\,\hat{u}}{\mathrm{Re}_e\,h_1^2}-\frac{2\,i\,\mathrm{Ec}_e\,\Omega_{\mathrm{Re}}\,\alpha\,h_{3,s}\,\overline{\lambda}_v\,\overline{u}\,\hat{u}}{\mathrm{Re}_e\,h_1^2\,h_3}$$
$$-\frac{\mathrm{Ec}_e\,\overline{T}\,\overline{\rho}_s\,\hat{u}}{{\mathrm{M}_e}^2\,\gamma_e\,h_1}-\frac{\mathrm{Ec}_e\,\overline{T}_s\,\overline{\rho}\,\hat{u}}{{\mathrm{M}_e}^2\,\gamma_e\,h_1}+\frac{\overline{T}_s\,\overline{\rho}\,\hat{u}}{h_1}-\frac{\mathrm{Ec}_e\,\hat{T}\,\overline{\mu}_{\overline{T}}\,\left(\overline{u}_y\right)^2}{\mathrm{Re}_e}+\frac{2\,\mathrm{Ec}_e\,\hat{T}\,h_{1,y}\,\overline{\mu}_{\overline{T}}\,\overline{u}\,\overline{u}_y}{\mathrm{Re}_e\,h_1}$$
$$-\frac{\mathrm{Ec}_e\,\hat{T}\,\left(h_{1,y}\right)^2\,\overline{\mu}_{\overline{T}}\,\overline{u}^2}{\mathrm{Re}_e\,h_1^2}-\frac{\mathrm{Ec}_e\,\Omega_p\,\overline{T}\,\hat{\rho}_s\,\overline{u}}{{\mathrm{M}_e}^2\,\gamma_e\,h_1}-\frac{i\,\mathrm{Ec}_e\,\overline{T}\,\alpha\,\hat{\rho}\,\overline{u}}{{\mathrm{M}_e}^2\,\gamma_e\,h_1}-\frac{\mathrm{Ec}_e\,\Omega_p\,\overline{T}_s\,\hat{\rho}\,\overline{u}}{{\mathrm{M}_e}^2\,\gamma_e\,h_1}+\frac{\overline{T}_s\,\hat{\rho}\,\overline{u}}{h_1}$$
$$-\frac{\mathrm{Ec}_e\,\Omega_p\,\hat{T}\,\overline{\rho}_s\,\overline{u}}{{\mathrm{M}_e}^2\,\gamma_e\,h_1}-\frac{i\,\mathrm{Ec}_e\,\hat{T}\,\alpha\,\overline{\rho}\,\overline{u}}{{\mathrm{M}_e}^2\,\gamma_e\,h_1}-\frac{\mathrm{Ec}_e\,\Omega_p\,\hat{T}_s\,\overline{\rho}\,\overline{u}}{{\mathrm{M}_e}^2\,\gamma_e\,h_1}+\frac{i\,\hat{T}\,\alpha\,\overline{\rho}\,\overline{u}}{h_1}+\frac{\hat{T}_s\,\overline{\rho}\,\overline{u}}{h_1}+\frac{i\,\mathrm{Ec}_e\,\overline{T}\,\omega\,\hat{\rho}}{{\mathrm{M}_e}^2\,\gamma_e}$$
$$+\frac{i\,\mathrm{Ec}_e\,\hat{T}\,\omega\,\overline{\rho}}{{\mathrm{M}_e}^2\,\gamma_e}-i\,\hat{T}\,\omega\,\overline{\rho}-\frac{\left(\overline{T}_y\right)^2\,\hat{T}\,\overline{\kappa}_{\overline{T}\,\overline{T}}}{\mathrm{Pr}_e\,\mathrm{Re}_e}-\frac{\overline{T}_y\,\hat{T}\,h_{3,y}\,\overline{\kappa}_{\overline{T}}}{\mathrm{Pr}_e\,\mathrm{Re}_e\,h_3}-\frac{\overline{T}_y\,\hat{T}\,h_{1,y}\,\overline{\kappa}_{\overline{T}}}{\mathrm{Pr}_e\,\mathrm{Re}_e\,h_1}$$
$$-\frac{2\,i\,\Omega_{\mathrm{Re}}\,\overline{T}_s\,\hat{T}\,\alpha\,\overline{\kappa}_{\overline{T}}}{\mathrm{Pr}_e\,\mathrm{Re}_e\,h_1^2}-\frac{2\,\overline{T}_y\,\hat{T}_y\,\overline{\kappa}_{\overline{T}}}{\mathrm{Pr}_e\,\mathrm{Re}_e}-\frac{\overline{T}_{y\,y}\,\hat{T}\,\overline{\kappa}_{\overline{T}}}{\mathrm{Pr}_e\,\mathrm{Re}_e}-\frac{\hat{T}_y\,h_{3,y}\,\overline{\kappa}}{\mathrm{Pr}_e\,\mathrm{Re}_e\,h_3}-\frac{i\,\Omega_{\mathrm{Re}}\,\hat{T}\,\alpha\,h_{3,s}\,\overline{\kappa}}{\mathrm{Pr}_e\,\mathrm{Re}_e\,h_1^2\,h_3}$$
$$+\frac{\hat{T}\,\beta^2\,\overline{\kappa}}{\mathrm{Pr}_e\,\mathrm{Re}_e\,h_3^2}-\frac{\hat{T}_y\,h_{1,y}\,\overline{\kappa}}{\mathrm{Pr}_e\,\mathrm{Re}_e\,h_1}+\frac{i\,\Omega_{\mathrm{Re}}\,\hat{T}\,\alpha\,h_{1,s}\,\overline{\kappa}}{\mathrm{Pr}_e\,\mathrm{Re}_e\,h_1^3}-\frac{i\,\Omega_{\mathrm{Re}}\,\hat{T}\,\alpha_s\,\overline{\kappa}}{\mathrm{Pr}_e\,\mathrm{Re}_e\,h_1^2}+\frac{\hat{T}\,\alpha^2\,\overline{\kappa}}{\mathrm{Pr}_e\,\mathrm{Re}_e\,h_1^2}$$
$$-\frac{2\,i\,\Omega_{\mathrm{Re}}\,\hat{T}_s\,\alpha\,\overline{\kappa}}{\mathrm{Pr}_e\,\mathrm{Re}_e\,h_1^2}-\frac{\hat{T}_{y\,y}\,\overline{\kappa}}{\mathrm{Pr}_e\,\mathrm{Re}_e}=\mathcal{N}(4)$$

C.5 Conservation of Mass Continuity

$$\frac{i\,\beta\,\overline{\rho}\,\hat{w}}{h_3}+\frac{i\,\beta\,\hat{\rho}\,\overline{w}}{h_3}+\overline{\rho}\,\hat{v}_y+\overline{\rho}_y\,\hat{v}+\frac{h_{3,y}\,\overline{\rho}\,\hat{v}}{h_3}+\frac{h_{1,y}\,\overline{\rho}\,\hat{v}}{h_1}+\hat{\rho}\,\overline{v}_y$$
$$+\hat{\rho}_y\,\overline{v}+\frac{h_{3,y}\,\hat{\rho}\,\overline{v}}{h_3}+\frac{h_{1,y}\,\hat{\rho}\,\overline{v}}{h_1}+\frac{\overline{\rho}\,\hat{u}_s}{h_1}+\frac{\overline{\rho}_s\,\hat{u}}{h_1}+\frac{h_{3,s}\,\overline{\rho}\,\hat{u}}{h_1\,h_3}+\frac{i\,\alpha\,\overline{\rho}\,\hat{u}}{h_1}$$
$$+\frac{\hat{\rho}\,\overline{u}_s}{h_1}+\frac{\hat{\rho}_s\,\overline{u}}{h_1}+\frac{h_{3,s}\,\hat{\rho}\,\overline{u}}{h_1\,h_3}+\frac{i\,\alpha\,\hat{\rho}\,\overline{u}}{h_1}-i\,\omega\,\hat{\rho}=\mathcal{N}(5)$$

C.6 Quadratic Nonlinear Forcing Vector

$$
\begin{aligned}
\frac{\mathcal{N}^{\text{quad}}(1)}{A^{(1)}\,A^{(2)}} = &-\frac{i\,\Omega_{\text{Re}}\,\hat{T}^{(1)}\,\beta_0\,k^{(2)}\,\overline{\mu}_{\overline{T}}\,\hat{w}_s^{(2)}}{\text{Re}_e\,h_1\,h_3} - \frac{i\,\Omega_{\text{Re}}\,\hat{T}^{(1)}\,\beta_0\,k^{(1)}\,\overline{\mu}_{\overline{T}}\,\hat{w}_s^{(2)}}{\text{Re}_e\,h_1\,h_3} - \frac{i\,\Omega_{\text{Re}}\,\hat{T}^{(1)}\,\beta_0\,k^{(2)}\,\overline{\lambda}_{v\overline{T}}\,\hat{w}_s^{(2)}}{\text{Re}_e\,h_1\,h_3} \\
&-\frac{h_{3,s}\,\overline{\rho}\,\hat{w}^{(1)}\,\hat{w}^{(2)}}{h_1\,h_3} - \frac{2\,h_{3,s}\,\hat{\rho}^{(1)}\,\overline{w}\,\hat{w}^{(2)}}{h_1\,h_3} + \frac{i\,\beta_0\,k^{(1)}\,\overline{\rho}\,\hat{u}^{(1)}\,\hat{w}^{(2)}}{h_3} + \frac{3\,i\,\Omega_{\text{Re}}\,\hat{T}^{(1)}\,\beta_0\,h_{3,s}\,k^{(2)}\,\overline{\mu}_{\overline{T}}\,\hat{w}^{(2)}}{\text{Re}_e\,h_1\,h_3^2} \\
&+\frac{\hat{T}^{(1)}\,\alpha^{(2)}\,\beta_0\,k^{(2)}\,\overline{\mu}_{\overline{T}}\,\hat{w}^{(2)}}{\text{Re}_e\,h_1\,h_3} + \frac{i\,\Omega_{\text{Re}}\,\hat{T}^{(1)}\,\beta_0\,h_{3,s}\,k^{(1)}\,\overline{\mu}_{\overline{T}}\,\hat{w}^{(2)}}{\text{Re}_e\,h_1\,h_3^2} + \frac{\hat{T}^{(1)}\,\alpha^{(2)}\,\beta_0\,k^{(1)}\,\overline{\mu}_{\overline{T}}\,\hat{w}^{(2)}}{\text{Re}_e\,h_1\,h_3} \\
&-\frac{i\,\Omega_{\text{Re}}\,\overline{T}_s\,\hat{T}^{(1)}\,\beta_0\,k^{(2)}\,\overline{\lambda}_{v\overline{T}\,\overline{T}}\,\hat{w}^{(2)}}{\text{Re}_e\,h_1\,h_3} + \frac{i\,\Omega_{\text{Re}}\,\hat{T}^{(1)}\,\beta_0\,h_{3,s}\,k^{(2)}\,\overline{\lambda}_{v\overline{T}}\,\hat{w}^{(2)}}{\text{Re}_e\,h_1\,h_3^2} + \frac{\hat{T}^{(1)}\,\alpha^{(2)}\,\beta_0\,k^{(2)}\,\overline{\lambda}_{v\overline{T}}\,\hat{w}^{(2)}}{\text{Re}_e\,h_1\,h_3} \\
&+\frac{\hat{T}^{(1)}\,\alpha^{(1)}\,\beta_0\,k^{(2)}\,\overline{\lambda}_{v\overline{T}}\,\hat{w}^{(2)}}{\text{Re}_e\,h_1\,h_3} - \frac{i\,\Omega_{\text{Re}}\,\hat{T}_s^{(1)}\,\beta_0\,k^{(2)}\,\overline{\lambda}_{v\overline{T}}\,\hat{w}^{(2)}}{\text{Re}_e\,h_1\,h_3} + \frac{i\,\beta_0\,k^{(2)}\,\hat{\rho}^{(1)}\,\hat{u}^{(2)}\,\overline{w}}{h_3} \\
&-\frac{i\,\hat{T}^{(1)}\,\alpha^{(2)}\,\overline{\mu}_{\overline{T}}\,\hat{v}_y^{(2)}}{\text{Re}_e\,h_1} - \frac{\Omega_{\text{Re}}\,\overline{T}_s\,\hat{T}^{(1)}\,\overline{\lambda}_{v\overline{T}\,\overline{T}}\,\hat{v}_y^{(2)}}{\text{Re}_e\,h_1} - \frac{i\,\hat{T}^{(1)}\,\alpha^{(2)}\,\overline{\lambda}_{v\overline{T}}\,\hat{v}_y^{(2)}}{\text{Re}_e\,h_1} - \frac{i\,\hat{T}^{(1)}\,\alpha^{(1)}\,\overline{\lambda}_{v\overline{T}}\,\hat{v}_y^{(2)}}{\text{Re}_e\,h_1} \\
&-\frac{\Omega_{\text{Re}}\,\hat{T}_s^{(1)}\,\overline{\lambda}_{v\overline{T}}\,\hat{v}_y^{(2)}}{\text{Re}_e\,h_1} - \frac{\Omega_{\text{Re}}\,\hat{T}^{(1)}\,\overline{\mu}_{\overline{T}}\,\hat{v}_{sy}^{(2)}}{\text{Re}_e\,h_1} - \frac{\Omega_{\text{Re}}\,\hat{T}^{(1)}\,\overline{\lambda}_{v\overline{T}}\,\hat{v}_{sy}^{(2)}}{\text{Re}_e\,h_1} - \frac{\Omega_{\text{Re}}\,\overline{T}_y\,\hat{T}^{(1)}\,\overline{\mu}_{\overline{T}\,\overline{T}}\,\hat{v}_s^{(2)}}{\text{Re}_e\,h_1} \\
&-\frac{\Omega_{\text{Re}}\,\hat{T}^{(1)}\,h_{3,y}\,\overline{\mu}_{\overline{T}}\,\hat{v}_s^{(2)}}{\text{Re}_e\,h_1\,h_3} - \frac{3\,\Omega_{\text{Re}}\,\hat{T}^{(1)}\,h_{1,y}\,\overline{\mu}_{\overline{T}}\,\hat{v}_s^{(2)}}{\text{Re}_e\,h_1^2} - \frac{\Omega_{\text{Re}}\,\hat{T}_y^{(1)}\,\overline{\mu}_{\overline{T}}\,\hat{v}_s^{(2)}}{\text{Re}_e\,h_1} - \frac{\Omega_{\text{Re}}\,\hat{T}^{(1)}\,h_{3,y}\,\overline{\lambda}_{v\overline{T}}\,\hat{v}_s^{(2)}}{\text{Re}_e\,h_1\,h_3} \\
&-\frac{\Omega_{\text{Re}}\,\hat{T}^{(1)}\,h_{1,y}\,\overline{\lambda}_{v\overline{T}}\,\hat{v}_s^{(2)}}{\text{Re}_e\,h_1^2} + \overline{\rho}\,\hat{u}_y^{(1)}\,\hat{v}^{(2)} + \frac{h_{1,y}\,\overline{\rho}\,\hat{u}^{(1)}\,\hat{v}^{(2)}}{h_1} + \hat{\rho}^{(1)}\,\overline{u}_y\,\hat{v}^{(2)} + \frac{h_{1,y}\,\hat{\rho}^{(1)}\,\overline{u}\,\hat{v}^{(2)}}{h_1} \\
&-\frac{2\,\Omega_{\text{Re}}\,\overline{T}_s\,\hat{T}^{(1)}\,h_{1,y}\,\overline{\mu}_{\overline{T}\,\overline{T}}\,\hat{v}^{(2)}}{\text{Re}_e\,h_1^2} - \frac{i\,\overline{T}_y\,\hat{T}^{(1)}\,\alpha^{(2)}\,\overline{\mu}_{\overline{T}\,\overline{T}}\,\hat{v}^{(2)}}{\text{Re}_e\,h_1} + \frac{2\,\Omega_{\text{Re}}\,\hat{T}^{(1)}\,h_{3,s}\,h_{3,y}\,\overline{\mu}_{\overline{T}}\,\hat{v}^{(2)}}{\text{Re}_e\,h_1\,h_3^2} \\
&-\frac{i\,\hat{T}^{(1)}\,\alpha^{(2)}\,h_{3,y}\,\overline{\mu}_{\overline{T}}\,\hat{v}^{(2)}}{\text{Re}_e\,h_1\,h_3} - \frac{2\,\Omega_{\text{Re}}\,\hat{T}^{(1)}\,h_{1,y}\,h_{3,s}\,\overline{\mu}_{\overline{T}}\,\hat{v}^{(2)}}{\text{Re}_e\,h_1^2\,h_3} + \frac{2\,\Omega_{\text{Re}}\,\hat{T}^{(1)}\,h_{1,s}\,h_{1,y}\,\overline{\mu}_{\overline{T}}\,\hat{v}^{(2)}}{\text{Re}_e\,h_1^3} \\
&-\frac{3\,i\,\hat{T}^{(1)}\,\alpha^{(2)}\,h_{1,y}\,\overline{\mu}_{\overline{T}}\,\hat{v}^{(2)}}{\text{Re}_e\,h_1^2} - \frac{2\,i\,\hat{T}^{(1)}\,\alpha^{(1)}\,h_{1,y}\,\overline{\mu}_{\overline{T}}\,\hat{v}^{(2)}}{\text{Re}_e\,h_1^2} - \frac{2\,\Omega_{\text{Re}}\,\hat{T}_s^{(1)}\,h_{1,y}\,\overline{\mu}_{\overline{T}}\,\hat{v}^{(2)}}{\text{Re}_e\,h_1^2} \\
&-\frac{2\,\Omega_{\text{Re}}\,\hat{T}^{(1)}\,h_{1,s\,y}\,\overline{\mu}_{\overline{T}}\,\hat{v}^{(2)}}{\text{Re}_e\,h_1^2} - \frac{i\,\hat{T}_y^{(1)}\,\alpha^{(2)}\,\overline{\mu}_{\overline{T}}\,\hat{v}^{(2)}}{\text{Re}_e\,h_1} - \frac{\Omega_{\text{Re}}\,\overline{T}_s\,\hat{T}^{(1)}\,h_{3,y}\,\overline{\lambda}_{v\overline{T}\,\overline{T}}\,\hat{v}^{(2)}}{\text{Re}_e\,h_1\,h_3} \\
&-\frac{\Omega_{\text{Re}}\,\overline{T}_s\,\hat{T}^{(1)}\,h_{1,y}\,\overline{\lambda}_{v\overline{T}\,\overline{T}}\,\hat{v}^{(2)}}{\text{Re}_e\,h_1^2} + \frac{\Omega_{\text{Re}}\,\hat{T}^{(1)}\,h_{3,s}\,h_{3,y}\,\overline{\lambda}_{v\overline{T}}\,\hat{v}^{(2)}}{\text{Re}_e\,h_1\,h_3^2} - \frac{i\,\hat{T}^{(1)}\,\alpha^{(2)}\,h_{3,y}\,\overline{\lambda}_{v\overline{T}}\,\hat{v}^{(2)}}{\text{Re}_e\,h_1\,h_3} \\
&-\frac{i\,\hat{T}^{(1)}\,\alpha^{(1)}\,h_{3,y}\,\overline{\lambda}_{v\overline{T}}\,\hat{v}^{(2)}}{\text{Re}_e\,h_1\,h_3} - \frac{\Omega_{\text{Re}}\,\hat{T}_s^{(1)}\,h_{3,y}\,\overline{\lambda}_{v\overline{T}}\,\hat{v}^{(2)}}{\text{Re}_e\,h_1\,h_3} - \frac{\Omega_{\text{Re}}\,\hat{T}^{(1)}\,h_{3,s\,y}\,\overline{\lambda}_{v\overline{T}}\,\hat{v}^{(2)}}{\text{Re}_e\,h_1\,h_3} \\
&+\frac{\Omega_{\text{Re}}\,\hat{T}^{(1)}\,h_{1,s}\,h_{1,y}\,\overline{\lambda}_{v\overline{T}}\,\hat{v}^{(2)}}{\text{Re}_e\,h_1^3} - \frac{i\,\hat{T}^{(1)}\,\alpha^{(2)}\,h_{1,y}\,\overline{\lambda}_{v\overline{T}}\,\hat{v}^{(2)}}{\text{Re}_e\,h_1^2} - \frac{i\,\hat{T}^{(1)}\,\alpha^{(1)}\,h_{1,y}\,\overline{\lambda}_{v\overline{T}}\,\hat{v}^{(2)}}{\text{Re}_e\,h_1^2}
\end{aligned}
$$

$$-\frac{\Omega_{\mathrm{Re}}\,\hat{T}_s^{(1)}\,h_{1,y}\,\overline{\lambda}_{v\overline{T}}\,\hat{v}^{(2)}}{\mathrm{Re}_e\,h_1^2}-\frac{\Omega_{\mathrm{Re}}\,\hat{T}^{(1)}\,h_{1,s\,y}\,\overline{\lambda}_{v\overline{T}}\,\hat{v}^{(2)}}{\mathrm{Re}_e\,h_1^2}+\hat{\rho}^{(1)}\,\hat{u}_y^{(2)}\,\overline{v}+\frac{h_{1,y}\,\hat{\rho}^{(1)}\,\hat{u}^{(2)}\,\overline{v}}{h_1}$$
$$-\frac{\hat{T}^{(1)}\,\overline{\mu}_{\overline{T}}\,\hat{u}_{y\,y}^{(2)}}{\mathrm{Re}_e}-\frac{\overline{T}_y\,\hat{T}^{(1)}\,\overline{\mu}_{\overline{T}\,\overline{T}}\,\hat{u}_y^{(2)}}{\mathrm{Re}_e}-\frac{\hat{T}^{(1)}\,h_{3,y}\,\overline{\mu}_{\overline{T}}\,\hat{u}_y^{(2)}}{\mathrm{Re}_e\,h_3}-\frac{\hat{T}^{(1)}\,h_{1,y}\,\overline{\mu}_{\overline{T}}\,\hat{u}_y^{(2)}}{\mathrm{Re}_e\,h_1}$$
$$-\frac{\hat{T}_y^{(1)}\,\overline{\mu}_{\overline{T}}\,\hat{u}_y^{(2)}}{\mathrm{Re}_e}+\frac{\overline{\rho}\,\hat{u}^{(1)}\,\hat{u}_s^{(2)}}{h_1}+\frac{\hat{\rho}^{(1)}\,\overline{u}\,\hat{u}_s^{(2)}}{h_1}-\frac{4\,i\,\Omega_{\mathrm{Re}}\,\hat{T}^{(1)}\,\alpha^{(2)}\,\overline{\mu}_{\overline{T}}\,\hat{u}_s^{(2)}}{\mathrm{Re}_e\,h_1^2}$$
$$-\frac{2\,i\,\Omega_{\mathrm{Re}}\,\hat{T}^{(1)}\,\alpha^{(1)}\,\overline{\mu}_{\overline{T}}\,\hat{u}_s^{(2)}}{\mathrm{Re}_e\,h_1^2}-\frac{2\,i\,\Omega_{\mathrm{Re}}\,\hat{T}^{(1)}\,\alpha^{(2)}\,\overline{\lambda}_{v\overline{T}}\,\hat{u}_s^{(2)}}{\mathrm{Re}_e\,h_1^2}-\frac{i\,\Omega_{\mathrm{Re}}\,\hat{T}^{(1)}\,\alpha^{(1)}\,\overline{\lambda}_{v\overline{T}}\,\hat{u}_s^{(2)}}{\mathrm{Re}_e\,h_1^2}$$
$$+\frac{i\,\alpha^{(2)}\,\overline{\rho}\,\hat{u}^{(1)}\,\hat{u}^{(2)}}{h_1}+\frac{\hat{\rho}^{(1)}\,\overline{u}_s\,\hat{u}^{(2)}}{h_1}+\frac{i\,\alpha^{(2)}\,\hat{\rho}^{(1)}\,\overline{u}\,\hat{u}^{(2)}}{h_1}$$
$$-i\,n^{(2)}\,\omega_0\,\hat{\rho}^{(1)}\,\hat{u}^{(2)}+\frac{\overline{T}_y\,\hat{T}^{(1)}\,h_{1,y}\,\overline{\mu}_{\overline{T}\,\overline{T}}\,\hat{u}^{(2)}}{\mathrm{Re}_e\,h_1}-\frac{2\,i\,\Omega_{\mathrm{Re}}\,\overline{T}_s\,\hat{T}^{(1)}\,\alpha^{(2)}\,\overline{\mu}_{\overline{T}\,\overline{T}}\,\hat{u}^{(2)}}{\mathrm{Re}_e\,h_1^2}$$
$$+\frac{\hat{T}^{(1)}\,\left(\beta_0\,k^{(2)}\right)^2\,\overline{\mu}_{\overline{T}}\,\hat{u}^{(2)}}{\mathrm{Re}_e\,h_3^2}+\frac{\hat{T}^{(1)}\,{\beta_0}^2\,k^{(1)}\,k^{(2)}\,\overline{\mu}_{\overline{T}}\,\hat{u}^{(2)}}{\mathrm{Re}_e\,h_3^2}+\frac{\hat{T}^{(1)}\,h_{1,y}\,h_{3,y}\,\overline{\mu}_{\overline{T}}\,\hat{u}^{(2)}}{\mathrm{Re}_e\,h_1\,h_3}$$
$$-\frac{2\,i\,\Omega_{\mathrm{Re}}\,\hat{T}^{(1)}\,\alpha^{(2)}\,h_{3,s}\,\overline{\mu}_{\overline{T}}\,\hat{u}^{(2)}}{\mathrm{Re}_e\,h_1^2\,h_3}+\frac{\hat{T}^{(1)}\,h_{1,y\,y}\,\overline{\mu}_{\overline{T}}\,\hat{u}^{(2)}}{\mathrm{Re}_e\,h_1}+\frac{\hat{T}^{(1)}\,\left(h_{1,y}\right)^2\,\overline{\mu}_{\overline{T}}\,\hat{u}^{(2)}}{\mathrm{Re}_e\,h_1^2}$$
$$+\frac{\hat{T}_y^{(1)}\,h_{1,y}\,\overline{\mu}_{\overline{T}}\,\hat{u}^{(2)}}{\mathrm{Re}_e\,h_1}+\frac{2\,i\,\Omega_{\mathrm{Re}}\,\hat{T}^{(1)}\,\alpha^{(2)}\,h_{1,s}\,\overline{\mu}_{\overline{T}}\,\hat{u}^{(2)}}{\mathrm{Re}_e\,h_1^3}-\frac{2\,i\,\Omega_{\mathrm{Re}}\,\hat{T}^{(1)}\,\alpha_s^{(2)}\,\overline{\mu}_{\overline{T}}\,\hat{u}^{(2)}}{\mathrm{Re}_e\,h_1^2}$$
$$+\frac{2\,\hat{T}^{(1)}\,\left(\alpha^{(2)}\right)^2\,\overline{\mu}_{\overline{T}}\,\hat{u}^{(2)}}{\mathrm{Re}_e\,h_1^2}+\frac{2\,\hat{T}^{(1)}\,\alpha^{(1)}\,\alpha^{(2)}\,\overline{\mu}_{\overline{T}}\,\hat{u}^{(2)}}{\mathrm{Re}_e\,h_1^2}-\frac{2\,i\,\Omega_{\mathrm{Re}}\,\hat{T}_s^{(1)}\,\alpha^{(2)}\,\overline{\mu}_{\overline{T}}\,\hat{u}^{(2)}}{\mathrm{Re}_e\,h_1^2}$$
$$-\frac{i\,\Omega_{\mathrm{Re}}\,\overline{T}_s\,\hat{T}^{(1)}\,\alpha^{(2)}\,\overline{\lambda}_{v\overline{T}\,\overline{T}}\,\hat{u}^{(2)}}{\mathrm{Re}_e\,h_1^2}-\frac{i\,\Omega_{\mathrm{Re}}\,\hat{T}^{(1)}\,\alpha^{(2)}\,h_{3,s}\,\overline{\lambda}_{v\overline{T}}\,\hat{u}^{(2)}}{\mathrm{Re}_e\,h_1^2\,h_3}-\frac{i\,\Omega_{\mathrm{Re}}\,\hat{T}^{(1)}\,\alpha^{(1)}\,h_{3,s}\,\overline{\lambda}_{v\overline{T}}\,\hat{u}^{(2)}}{\mathrm{Re}_e\,h_1^2\,h_3}$$
$$+\frac{i\,\Omega_{\mathrm{Re}}\,\hat{T}^{(1)}\,\alpha^{(2)}\,h_{1,s}\,\overline{\lambda}_{v\overline{T}}\,\hat{u}^{(2)}}{\mathrm{Re}_e\,h_1^3}-\frac{i\,\Omega_{\mathrm{Re}}\,\hat{T}^{(1)}\,\alpha_s^{(2)}\,\overline{\lambda}_{v\overline{T}}\,\hat{u}^{(2)}}{\mathrm{Re}_e\,h_1^2}+\frac{\hat{T}^{(1)}\,\left(\alpha^{(2)}\right)^2\,\overline{\lambda}_{v\overline{T}}\,\hat{u}^{(2)}}{\mathrm{Re}_e\,h_1^2}$$
$$+\frac{\hat{T}^{(1)}\,\alpha^{(1)}\,\alpha^{(2)}\,\overline{\lambda}_{v\overline{T}}\,\hat{u}^{(2)}}{\mathrm{Re}_e\,h_1^2}-\frac{i\,\Omega_{\mathrm{Re}}\,\hat{T}_s^{(1)}\,\alpha^{(2)}\,\overline{\lambda}_{v\overline{T}}\,\hat{u}^{(2)}}{\mathrm{Re}_e\,h_1^2}+\frac{\hat{T}^{(1)}\,\hat{\rho}_s^{(2)}}{{\mathrm{M}_e}^2\,\gamma_e\,h_1}$$
$$+\frac{i\,\hat{T}^{(1)}\,\alpha^{(2)}\,\hat{\rho}^{(2)}}{{\mathrm{M}_e}^2\,\gamma_e\,h_1}+\frac{i\,\hat{T}^{(1)}\,\alpha^{(1)}\,\hat{\rho}^{(2)}}{{\mathrm{M}_e}^2\,\gamma_e\,h_1}+\frac{\hat{T}_s^{(1)}\,\hat{\rho}^{(2)}}{{\mathrm{M}_e}^2\,\gamma_e\,h_1}$$

$$\frac{\mathcal{N}^{\mathrm{quad}}(2)}{A^{(1)}\,A^{(2)}} = -\frac{i\,\hat{T}^{(1)}\,\beta_0\,k^{(2)}\,\overline{\mu}_{\overline{T}}\,\hat{w}_y^{(2)}}{\mathrm{Re}_e\,h_3} - \frac{i\,\hat{T}^{(1)}\,\beta_0\,k^{(1)}\,\overline{\mu}_{\overline{T}}\,\hat{w}_y^{(2)}}{\mathrm{Re}_e\,h_3} - \frac{i\,\hat{T}^{(1)}\,\beta_0\,k^{(2)}\,\overline{\lambda}_{v\overline{T}}\,\hat{w}_y^{(2)}}{\mathrm{Re}_e\,h_3}$$
$$-\frac{h_{3,y}\,\overline{\rho}\,\hat{w}^{(1)}\,\hat{w}^{(2)}}{h_3} - \frac{2\,h_{3,y}\,\hat{\rho}^{(1)}\,\overline{w}\,\hat{w}^{(2)}}{h_3} + \frac{i\,\beta_0\,k^{(1)}\,\overline{\rho}\,\hat{v}^{(1)}\,\hat{w}^{(2)}}{h_3} + \frac{3\,i\,\hat{T}^{(1)}\,\beta_0\,h_{3,y}\,k^{(2)}\,\overline{\mu}_{\overline{T}}\,\hat{w}^{(2)}}{\mathrm{Re}_e\,h_3^2}$$
$$+\frac{i\,\hat{T}^{(1)}\,\beta_0\,h_{3,y}\,k^{(1)}\,\overline{\mu}_{\overline{T}}\,\hat{w}^{(2)}}{\mathrm{Re}_e\,h_3^2} - \frac{i\,\overline{T}_y\,\hat{T}^{(1)}\,\beta_0\,k^{(2)}\,\overline{\lambda}_{v\overline{T}\,\overline{T}}\,\hat{w}^{(2)}}{\mathrm{Re}_e\,h_3} + \frac{i\,\hat{T}^{(1)}\,\beta_0\,h_{3,y}\,k^{(2)}\,\overline{\lambda}_{v\overline{T}}\,\hat{w}^{(2)}}{\mathrm{Re}_e\,h_3^2}$$
$$-\frac{i\,\hat{T}_y^{(1)}\,\beta_0\,k^{(2)}\,\overline{\lambda}_{v\overline{T}}\,\hat{w}^{(2)}}{\mathrm{Re}_e\,h_3} + \frac{i\,\beta_0\,k^{(2)}\,\hat{\rho}^{(1)}\,\hat{v}^{(2)}\,\overline{w}}{h_3} - \frac{2\,\hat{T}^{(1)}\,\overline{\mu}_{\overline{T}}\,\hat{v}_{yy}^{(2)}}{\mathrm{Re}_e} - \frac{\hat{T}^{(1)}\,\overline{\lambda}_{v\overline{T}}\,\hat{v}_{yy}^{(2)}}{\mathrm{Re}_e} + \overline{\rho}\,\hat{v}^{(1)}\,\hat{v}_y^{(2)}$$
$$+\hat{\rho}^{(1)}\,\overline{v}\,\hat{v}_y^{(2)} - \frac{2\,\overline{T}_y\,\hat{T}^{(1)}\,\overline{\mu}_{\overline{T}\,\overline{T}}\,\hat{v}_y^{(2)}}{\mathrm{Re}_e} - \frac{2\,\hat{T}^{(1)}\,h_{3,y}\,\overline{\mu}_{\overline{T}}\,\hat{v}_y^{(2)}}{\mathrm{Re}_e\,h_3} - \frac{2\,\hat{T}^{(1)}\,h_{1,y}\,\overline{\mu}_{\overline{T}}\,\hat{v}_y^{(2)}}{\mathrm{Re}_e\,h_1} - \frac{2\,\hat{T}_y^{(1)}\,\overline{\mu}_{\overline{T}}\,\hat{v}_y^{(2)}}{\mathrm{Re}_e}$$
$$-\frac{\overline{T}_y\,\hat{T}^{(1)}\,\overline{\lambda}_{v\overline{T}\,\overline{T}}\,\hat{v}_y^{(2)}}{\mathrm{Re}_e} - \frac{\hat{T}^{(1)}\,h_{3,y}\,\overline{\lambda}_{v\overline{T}}\,\hat{v}_y^{(2)}}{\mathrm{Re}_e\,h_3} - \frac{\hat{T}^{(1)}\,h_{1,y}\,\overline{\lambda}_{v\overline{T}}\,\hat{v}_y^{(2)}}{\mathrm{Re}_e\,h_1} - \frac{\hat{T}_y^{(1)}\,\overline{\lambda}_{v\overline{T}}\,\hat{v}_y^{(2)}}{\mathrm{Re}_e}$$
$$+\frac{\overline{\rho}\,\hat{u}^{(1)}\,\hat{v}_s^{(2)}}{h_1} + \frac{\hat{\rho}^{(1)}\,\overline{u}\,\hat{v}_s^{(2)}}{h_1} - \frac{2\,i\,\Omega_{\mathrm{Re}}\,\hat{T}^{(1)}\,\alpha^{(2)}\,\overline{\mu}_{\overline{T}}\,\hat{v}_s^{(2)}}{\mathrm{Re}_e\,h_1^2} - \frac{i\,\Omega_{\mathrm{Re}}\,\hat{T}^{(1)}\,\alpha^{(1)}\,\overline{\mu}_{\overline{T}}\,\hat{v}_s^{(2)}}{\mathrm{Re}_e\,h_1^2} + \hat{\rho}^{(1)}\,\overline{v}_y\,\hat{v}^{(2)}$$
$$+\frac{i\,\alpha^{(2)}\,\overline{\rho}\,\hat{u}^{(1)}\,\hat{v}^{(2)}}{h_1} + \frac{i\,\alpha^{(2)}\,\hat{\rho}^{(1)}\,\overline{u}\,\hat{v}^{(2)}}{h_1} - i\,n^{(2)}\,\omega_0\,\hat{\rho}^{(1)}\,\hat{v}^{(2)} - \frac{i\,\Omega_{\mathrm{Re}}\,\overline{T}_s\,\hat{T}^{(1)}\,\alpha^{(2)}\,\overline{\mu}_{\overline{T}\,\overline{T}}\,\hat{v}^{(2)}}{\mathrm{Re}_e\,h_1^2}$$
$$+\frac{\hat{T}^{(1)}\,\left(\beta_0\,k^{(2)}\right)^2\,\overline{\mu}_{\overline{T}}\,\hat{v}^{(2)}}{\mathrm{Re}_e\,h_3^2} + \frac{\hat{T}^{(1)}\,{\beta_0}^2\,k^{(1)}\,k^{(2)}\,\overline{\mu}_{\overline{T}}\,\hat{v}^{(2)}}{\mathrm{Re}_e\,h_3^2} + \frac{2\,\hat{T}^{(1)}\,\left(h_{3,y}\right)^2\,\overline{\mu}_{\overline{T}}\,\hat{v}^{(2)}}{\mathrm{Re}_e\,h_3^2}$$
$$-\frac{i\,\Omega_{\mathrm{Re}}\,\hat{T}^{(1)}\,\alpha^{(2)}\,h_{3,s}\,\overline{\mu}_{\overline{T}}\,\hat{v}^{(2)}}{\mathrm{Re}_e\,h_1^2\,h_3} + \frac{2\,\hat{T}^{(1)}\,\left(h_{1,y}\right)^2\,\overline{\mu}_{\overline{T}}\,\hat{v}^{(2)}}{\mathrm{Re}_e\,h_1^2} + \frac{i\,\Omega_{\mathrm{Re}}\,\hat{T}^{(1)}\,\alpha^{(2)}\,h_{1,s}\,\overline{\mu}_{\overline{T}}\,\hat{v}^{(2)}}{\mathrm{Re}_e\,h_1^3}$$
$$-\frac{i\,\Omega_{\mathrm{Re}}\,\hat{T}^{(1)}\,\alpha_s^{(2)}\,\overline{\mu}_{\overline{T}}\,\hat{v}^{(2)}}{\mathrm{Re}_e\,h_1^2} + \frac{\hat{T}^{(1)}\,\left(\alpha^{(2)}\right)^2\,\overline{\mu}_{\overline{T}}\,\hat{v}^{(2)}}{\mathrm{Re}_e\,h_1^2} + \frac{\hat{T}^{(1)}\,\alpha^{(1)}\,\alpha^{(2)}\,\overline{\mu}_{\overline{T}}\,\hat{v}^{(2)}}{\mathrm{Re}_e\,h_1^2}$$
$$-\frac{i\,\Omega_{\mathrm{Re}}\,\hat{T}_s^{(1)}\,\alpha^{(2)}\,\overline{\mu}_{\overline{T}}\,\hat{v}^{(2)}}{\mathrm{Re}_e\,h_1^2} - \frac{\overline{T}_y\,\hat{T}^{(1)}\,h_{3,y}\,\overline{\lambda}_{v\overline{T}\,\overline{T}}\,\hat{v}^{(2)}}{\mathrm{Re}_e\,h_3} - \frac{\overline{T}_y\,\hat{T}^{(1)}\,h_{1,y}\,\overline{\lambda}_{v\overline{T}\,\overline{T}}\,\hat{v}^{(2)}}{\mathrm{Re}_e\,h_1}$$
$$-\frac{\hat{T}^{(1)}\,h_{3,y\,y}\,\overline{\lambda}_{v\overline{T}}\,\hat{v}^{(2)}}{\mathrm{Re}_e\,h_3} + \frac{\hat{T}^{(1)}\,\left(h_{3,y}\right)^2\,\overline{\lambda}_{v\overline{T}}\,\hat{v}^{(2)}}{\mathrm{Re}_e\,h_3^2} - \frac{\hat{T}_y^{(1)}\,h_{3,y}\,\overline{\lambda}_{v\overline{T}}\,\hat{v}^{(2)}}{\mathrm{Re}_e\,h_3}$$
$$-\frac{\hat{T}^{(1)}\,h_{1,y\,y}\,\overline{\lambda}_{v\overline{T}}\,\hat{v}^{(2)}}{\mathrm{Re}_e\,h_1} + \frac{\hat{T}^{(1)}\,\left(h_{1,y}\right)^2\,\overline{\lambda}_{v\overline{T}}\,\hat{v}^{(2)}}{\mathrm{Re}_e\,h_1^2} - \frac{\hat{T}_y^{(1)}\,h_{1,y}\,\overline{\lambda}_{v\overline{T}}\,\hat{v}^{(2)}}{\mathrm{Re}_e\,h_1}$$
$$-\frac{\Omega_{\mathrm{Re}}\,\overline{T}_s\,\hat{T}^{(1)}\,\overline{\mu}_{\overline{T}\,\overline{T}}\,\hat{u}_y^{(2)}}{\mathrm{Re}_e\,h_1} - \frac{\Omega_{\mathrm{Re}}\,\hat{T}^{(1)}\,h_{3,s}\,\overline{\mu}_{\overline{T}}\,\hat{u}_y^{(2)}}{\mathrm{Re}_e\,h_1\,h_3} - \frac{i\,\hat{T}^{(1)}\,\alpha^{(2)}\,\overline{\mu}_{\overline{T}}\,\hat{u}_y^{(2)}}{\mathrm{Re}_e\,h_1} - \frac{i\,\hat{T}^{(1)}\,\alpha^{(1)}\,\overline{\mu}_{\overline{T}}\,\hat{u}_y^{(2)}}{\mathrm{Re}_e\,h_1}$$
$$-\frac{\Omega_{\mathrm{Re}}\,\hat{T}_s^{(1)}\,\overline{\mu}_{\overline{T}}\,\hat{u}_y^{(2)}}{\mathrm{Re}_e\,h_1} - \frac{\Omega_{\mathrm{Re}}\,\hat{T}^{(1)}\,h_{3,s}\,\overline{\lambda}_{v\overline{T}}\,\hat{u}_y^{(2)}}{\mathrm{Re}_e\,h_1\,h_3} - \frac{i\,\hat{T}^{(1)}\,\alpha^{(2)}\,\overline{\lambda}_{v\overline{T}}\,\hat{u}_y^{(2)}}{\mathrm{Re}_e\,h_1} - \frac{\Omega_{\mathrm{Re}}\,\hat{T}^{(1)}\,\overline{\mu}_{\overline{T}}\,\hat{u}_{s\,y}^{(2)}}{\mathrm{Re}_e\,h_1}$$
$$-\frac{\Omega_{\mathrm{Re}}\,\hat{T}^{(1)}\,\overline{\lambda}_{v\overline{T}}\,\hat{u}_{s\,y}^{(2)}}{\mathrm{Re}_e\,h_1} + \frac{3\,\Omega_{\mathrm{Re}}\,\hat{T}^{(1)}\,h_{1,y}\,\overline{\mu}_{\overline{T}}\,\hat{u}_s^{(2)}}{\mathrm{Re}_e\,h_1^2} - \frac{\Omega_{\mathrm{Re}}\,\overline{T}_y\,\hat{T}^{(1)}\,\overline{\lambda}_{v\overline{T}\,\overline{T}}\,\hat{u}_s^{(2)}}{\mathrm{Re}_e\,h_1} + \frac{\Omega_{\mathrm{Re}}\,\hat{T}^{(1)}\,h_{1,y}\,\overline{\lambda}_{v\overline{T}}\,\hat{u}_s^{(2)}}{\mathrm{Re}_e\,h_1^2}$$

$$
\begin{aligned}
&-\frac{\Omega_{\mathrm{Re}}\,\hat{T}_y^{(1)}\,\overline{\lambda}_{v\overline{T}}\,\hat{u}_s^{(2)}}{\mathrm{Re}_e\,h_1}-\frac{h_{1,y}\,\overline{\rho}\,\hat{u}^{(1)}\,\hat{u}^{(2)}}{h_1}-\frac{2\,h_{1,y}\,\hat{\rho}^{(1)}\,\overline{u}\,\hat{u}^{(2)}}{h_1}+\frac{\Omega_{\mathrm{Re}}\,\overline{T}_s\,\hat{T}^{(1)}\,h_{1,y}\,\overline{\mu}_{\overline{T}\,\overline{T}}\,\hat{u}^{(2)}}{\mathrm{Re}_e\,h_1^2}\\
&+\frac{2\,\Omega_{\mathrm{Re}}\,\hat{T}^{(1)}\,h_{3,s}\,h_{3,y}\,\overline{\mu}_{\overline{T}}\,\hat{u}^{(2)}}{\mathrm{Re}_e\,h_1\,h_3^2}+\frac{\Omega_{\mathrm{Re}}\,\hat{T}^{(1)}\,h_{1,y}\,h_{3,s}\,\overline{\mu}_{\overline{T}}\,\hat{u}^{(2)}}{\mathrm{Re}_e\,h_1^2\,h_3}-\frac{\Omega_{\mathrm{Re}}\,\hat{T}^{(1)}\,h_{1,s}\,h_{1,y}\,\overline{\mu}_{\overline{T}}\,\hat{u}^{(2)}}{\mathrm{Re}_e\,h_1^3}\\
&+\frac{3\,i\,\hat{T}^{(1)}\,\alpha^{(2)}\,h_{1,y}\,\overline{\mu}_{\overline{T}}\,\hat{u}^{(2)}}{\mathrm{Re}_e\,h_1^2}+\frac{i\,\hat{T}^{(1)}\,\alpha^{(1)}\,h_{1,y}\,\overline{\mu}_{\overline{T}}\,\hat{u}^{(2)}}{\mathrm{Re}_e\,h_1^2}+\frac{\Omega_{\mathrm{Re}}\,\hat{T}_s^{(1)}\,h_{1,y}\,\overline{\mu}_{\overline{T}}\,\hat{u}^{(2)}}{\mathrm{Re}_e\,h_1^2}\\
&+\frac{\Omega_{\mathrm{Re}}\,\hat{T}^{(1)}\,h_{1,s\,y}\,\overline{\mu}_{\overline{T}}\,\hat{u}^{(2)}}{\mathrm{Re}_e\,h_1^2}-\frac{\Omega_{\mathrm{Re}}\,\overline{T}_y\,\hat{T}^{(1)}\,h_{3,s}\,\overline{\lambda}_{v\overline{T}\,\overline{T}}\,\hat{u}^{(2)}}{\mathrm{Re}_e\,h_1\,h_3}-\frac{i\,\overline{T}_y\,\hat{T}^{(1)}\,\alpha^{(2)}\,\overline{\lambda}_{v\overline{T}\,\overline{T}}\,\hat{u}^{(2)}}{\mathrm{Re}_e\,h_1}\\
&+\frac{\Omega_{\mathrm{Re}}\,\hat{T}^{(1)}\,h_{3,s}\,h_{3,y}\,\overline{\lambda}_{v\overline{T}}\,\hat{u}^{(2)}}{\mathrm{Re}_e\,h_1\,h_3^2}-\frac{\Omega_{\mathrm{Re}}\,\hat{T}^{(1)}\,h_{3,s\,y}\,\overline{\lambda}_{v\overline{T}}\,\hat{u}^{(2)}}{\mathrm{Re}_e\,h_1\,h_3}+\frac{\Omega_{\mathrm{Re}}\,\hat{T}^{(1)}\,h_{1,y}\,h_{3,s}\,\overline{\lambda}_{v\overline{T}}\,\hat{u}^{(2)}}{\mathrm{Re}_e\,h_1^2\,h_3}\\
&-\frac{\Omega_{\mathrm{Re}}\,\hat{T}_y^{(1)}\,h_{3,s}\,\overline{\lambda}_{v\overline{T}}\,\hat{u}^{(2)}}{\mathrm{Re}_e\,h_1\,h_3}+\frac{i\,\hat{T}^{(1)}\,\alpha^{(2)}\,h_{1,y}\,\overline{\lambda}_{v\overline{T}}\,\hat{u}^{(2)}}{\mathrm{Re}_e\,h_1^2}-\frac{i\,\hat{T}_y^{(1)}\,\alpha^{(2)}\,\overline{\lambda}_{v\overline{T}}\,\hat{u}^{(2)}}{\mathrm{Re}_e\,h_1}\\
&+\frac{\hat{T}^{(1)}\,\hat{\rho}_y^{(2)}}{{\mathrm{M}_e}^2\,\gamma_e}+\frac{\hat{T}_y^{(1)}\,\hat{\rho}^{(2)}}{{\mathrm{M}_e}^2\,\gamma_e}
\end{aligned}
$$

$$\frac{\mathcal{N}^{\mathrm{quad}}(3)}{A^{(1)}\,A^{(2)}} = -\frac{\hat{T}^{(1)}\,\overline{\mu}_{\overline{T}}\,\hat{w}_{y}^{(2)}}{\mathrm{Re}_e} + \overline{\rho}\,\hat{v}^{(1)}\,\hat{w}_{y}^{(2)} + \hat{\rho}^{(1)}\,\overline{v}\,\hat{w}_{y}^{(2)} - \frac{\overline{T}_{y}\,\hat{T}^{(1)}\,\overline{\mu}_{\overline{T}\,\overline{T}}\,\hat{w}_{y}^{(2)}}{\mathrm{Re}_e} - \frac{\hat{T}^{(1)}\,h_{3,y}\,\overline{\mu}_{\overline{T}}\,\hat{w}_{y}^{(2)}}{\mathrm{Re}_e\,h_3}$$
$$-\frac{\hat{T}^{(1)}\,h_{1,y}\,\overline{\mu}_{\overline{T}}\,\hat{w}_{y}^{(2)}}{\mathrm{Re}_e\,h_1} - \frac{\hat{T}_{y}^{(1)}\,\overline{\mu}_{\overline{T}}\,\hat{w}_{y}^{(2)}}{\mathrm{Re}_e} + \frac{\overline{\rho}\,\hat{u}^{(1)}\,\hat{w}_{s}^{(2)}}{h_1} + \frac{\hat{\rho}^{(1)}\,\overline{u}\,\hat{w}_{s}^{(2)}}{h_1} - \frac{2\,i\,\Omega_{\mathrm{Re}}\,\hat{T}^{(1)}\,\alpha^{(2)}\,\overline{\mu}_{\overline{T}}\,\hat{w}_{s}^{(2)}}{\mathrm{Re}_e\,h_1^2}$$
$$-\frac{i\,\Omega_{\mathrm{Re}}\,\hat{T}^{(1)}\,\alpha^{(1)}\,\overline{\mu}_{\overline{T}}\,\hat{w}_{s}^{(2)}}{\mathrm{Re}_e\,h_1^2} + \frac{i\,\beta_0\,k^{(2)}\,\overline{\rho}\,\hat{w}^{(1)}\,\hat{w}^{(2)}}{h_3} + \frac{i\,\beta_0\,k^{(2)}\,\hat{\rho}^{(1)}\,\overline{w}\,\hat{w}^{(2)}}{h_3} + \frac{h_{3,y}\,\overline{\rho}\,\hat{v}^{(1)}\,\hat{w}^{(2)}}{h_3}$$
$$+\frac{h_{3,y}\,\hat{\rho}^{(1)}\,\overline{v}\,\hat{w}^{(2)}}{h_3} + \frac{h_{3,s}\,\overline{\rho}\,\hat{u}^{(1)}\,\hat{w}^{(2)}}{h_1\,h_3} + \frac{i\,\alpha^{(2)}\,\overline{\rho}\,\hat{u}^{(1)}\,\hat{w}^{(2)}}{h_1} + \frac{h_{3,s}\,\hat{\rho}^{(1)}\,\overline{u}\,\hat{w}^{(2)}}{h_1\,h_3}$$
$$+\frac{i\,\alpha^{(2)}\,\hat{\rho}^{(1)}\,\overline{u}\,\hat{w}^{(2)}}{h_1} - i\,n^{(2)}\,\omega_0\,\hat{\rho}^{(1)}\,\hat{w}^{(2)} + \frac{\overline{T}_{y}\,\hat{T}^{(1)}\,h_{3,y}\,\overline{\mu}_{\overline{T}\,\overline{T}}\,\hat{w}^{(2)}}{\mathrm{Re}_e\,h_3} - \frac{i\,\Omega_{\mathrm{Re}}\,\overline{T}_{s}\,\hat{T}^{(1)}\,\alpha^{(2)}\,\overline{\mu}_{\overline{T}\,\overline{T}}\,\hat{w}^{(2)}}{\mathrm{Re}_e\,h_1^2}$$
$$+\frac{2\,\hat{T}^{(1)}\,\left(\beta_0\,k^{(2)}\right)^2\,\overline{\mu}_{\overline{T}}\,\hat{w}^{(2)}}{\mathrm{Re}_e\,h_3^2} + \frac{2\,\hat{T}^{(1)}\,{\beta_0}^2\,k^{(1)}\,k^{(2)}\,\overline{\mu}_{\overline{T}}\,\hat{w}^{(2)}}{\mathrm{Re}_e\,h_3^2} + \frac{\hat{T}^{(1)}\,h_{3,y\,y}\,\overline{\mu}_{\overline{T}}\,\hat{w}^{(2)}}{\mathrm{Re}_e\,h_3}$$
$$+\frac{\hat{T}^{(1)}\,\left(h_{3,y}\right)^2\,\overline{\mu}_{\overline{T}}\,\hat{w}^{(2)}}{\mathrm{Re}_e\,h_3^2} + \frac{\hat{T}^{(1)}\,h_{1,y}\,h_{3,y}\,\overline{\mu}_{\overline{T}}\,\hat{w}^{(2)}}{\mathrm{Re}_e\,h_1\,h_3} + \frac{\hat{T}_{y}^{(1)}\,h_{3,y}\,\overline{\mu}_{\overline{T}}\,\hat{w}^{(2)}}{\mathrm{Re}_e\,h_3} - \frac{i\,\Omega_{\mathrm{Re}}\,\hat{T}^{(1)}\,\alpha^{(2)}\,h_{3,s}\,\overline{\mu}_{\overline{T}}\,\hat{w}^{(2)}}{\mathrm{Re}_e\,h_1^2\,h_3}$$
$$+\frac{i\,\Omega_{\mathrm{Re}}\,\hat{T}^{(1)}\,\alpha^{(1)}\,h_{3,s}\,\overline{\mu}_{\overline{T}}\,\hat{w}^{(2)}}{\mathrm{Re}_e\,h_1^2\,h_3} + \frac{i\,\Omega_{\mathrm{Re}}\,\hat{T}^{(1)}\,\alpha^{(2)}\,h_{1,s}\,\overline{\mu}_{\overline{T}}\,\hat{w}^{(2)}}{\mathrm{Re}_e\,h_1^3} - \frac{i\,\Omega_{\mathrm{Re}}\,\hat{T}^{(1)}\,\alpha_{s}^{(2)}\,\overline{\mu}_{\overline{T}}\,\hat{w}^{(2)}}{\mathrm{Re}_e\,h_1^2}$$
$$+\frac{\hat{T}^{(1)}\,\left(\alpha^{(2)}\right)^2\,\overline{\mu}_{\overline{T}}\,\hat{w}^{(2)}}{\mathrm{Re}_e\,h_1^2} + \frac{\hat{T}^{(1)}\,\alpha^{(1)}\,\alpha^{(2)}\,\overline{\mu}_{\overline{T}}\,\hat{w}^{(2)}}{\mathrm{Re}_e\,h_1^2} - \frac{i\,\Omega_{\mathrm{Re}}\,\hat{T}_{s}^{(1)}\,\alpha^{(2)}\,\overline{\mu}_{\overline{T}}\,\hat{w}^{(2)}}{\mathrm{Re}_e\,h_1^2}$$
$$+\frac{\hat{T}^{(1)}\,\left(\beta_0\,k^{(2)}\right)^2\,\overline{\lambda}_{v\overline{T}}\,\hat{w}^{(2)}}{\mathrm{Re}_e\,h_3^2} + \frac{\hat{T}^{(1)}\,{\beta_0}^2\,k^{(1)}\,k^{(2)}\,\overline{\lambda}_{v\overline{T}}\,\hat{w}^{(2)}}{\mathrm{Re}_e\,h_3^2} + \hat{\rho}^{(1)}\,\hat{v}^{(2)}\,\overline{w}_{y} + \frac{\hat{\rho}^{(1)}\,\hat{u}^{(2)}\,\overline{w}_{s}}{h_1}$$
$$+\frac{h_{3,y}\,\hat{\rho}^{(1)}\,\hat{v}^{(2)}\,\overline{w}}{h_3} + \frac{h_{3,s}\,\hat{\rho}^{(1)}\,\hat{u}^{(2)}\,\overline{w}}{h_1\,h_3} - \frac{i\,\hat{T}^{(1)}\,\beta_0\,k^{(2)}\,\overline{\mu}_{\overline{T}}\,\hat{v}_{y}^{(2)}}{\mathrm{Re}_e\,h_3} - \frac{i\,\hat{T}^{(1)}\,\beta_0\,k^{(2)}\,\overline{\lambda}_{v\overline{T}}\,\hat{v}_{y}^{(2)}}{\mathrm{Re}_e\,h_3}$$
$$-\frac{i\,\hat{T}^{(1)}\,\beta_0\,k^{(1)}\,\overline{\lambda}_{v\overline{T}}\,\hat{v}_{y}^{(2)}}{\mathrm{Re}_e\,h_3} - \frac{i\,\overline{T}_{y}\,\hat{T}^{(1)}\,\beta_0\,k^{(2)}\,\overline{\mu}_{\overline{T}\,\overline{T}}\,\hat{v}^{(2)}}{\mathrm{Re}_e\,h_3} - \frac{3\,i\,\hat{T}^{(1)}\,\beta_0\,h_{3,y}\,k^{(2)}\,\overline{\mu}_{\overline{T}}\,\hat{v}^{(2)}}{\mathrm{Re}_e\,h_3^2}$$
$$-\frac{i\,\hat{T}^{(1)}\,\beta_0\,h_{1,y}\,k^{(2)}\,\overline{\mu}_{\overline{T}}\,\hat{v}^{(2)}}{\mathrm{Re}_e\,h_1\,h_3} - \frac{i\,\hat{T}_{y}^{(1)}\,\beta_0\,k^{(2)}\,\overline{\mu}_{\overline{T}}\,\hat{v}^{(2)}}{\mathrm{Re}_e\,h_3} - \frac{2\,i\,\hat{T}^{(1)}\,\beta_0\,h_{3,y}\,k^{(1)}\,\overline{\mu}_{\overline{T}}\,\hat{v}^{(2)}}{\mathrm{Re}_e\,h_3^2}$$
$$-\frac{i\,\hat{T}^{(1)}\,\beta_0\,h_{3,y}\,k^{(2)}\,\overline{\lambda}_{v\overline{T}}\,\hat{v}^{(2)}}{\mathrm{Re}_e\,h_3^2} - \frac{i\,\hat{T}^{(1)}\,\beta_0\,h_{1,y}\,k^{(2)}\,\overline{\lambda}_{v\overline{T}}\,\hat{v}^{(2)}}{\mathrm{Re}_e\,h_1\,h_3} - \frac{i\,\hat{T}^{(1)}\,\beta_0\,h_{3,y}\,k^{(1)}\,\overline{\lambda}_{v\overline{T}}\,\hat{v}^{(2)}}{\mathrm{Re}_e\,h_3^2}$$
$$-\frac{i\,\hat{T}^{(1)}\,\beta_0\,h_{1,y}\,k^{(1)}\,\overline{\lambda}_{v\overline{T}}\,\hat{v}^{(2)}}{\mathrm{Re}_e\,h_1\,h_3} - \frac{i\,\Omega_{\mathrm{Re}}\,\hat{T}^{(1)}\,\beta_0\,k^{(2)}\,\overline{\mu}_{\overline{T}}\,\hat{u}_{s}^{(2)}}{\mathrm{Re}_e\,h_1\,h_3} - \frac{i\,\Omega_{\mathrm{Re}}\,\hat{T}^{(1)}\,\beta_0\,k^{(2)}\,\overline{\lambda}_{v\overline{T}}\,\hat{u}_{s}^{(2)}}{\mathrm{Re}_e\,h_1\,h_3}$$
$$-\frac{i\,\Omega_{\mathrm{Re}}\,\hat{T}^{(1)}\,\beta_0\,k^{(1)}\,\overline{\lambda}_{v\overline{T}}\,\hat{u}_{s}^{(2)}}{\mathrm{Re}_e\,h_1\,h_3} - \frac{i\,\Omega_{\mathrm{Re}}\,\overline{T}_{s}\,\hat{T}^{(1)}\,\beta_0\,k^{(2)}\,\overline{\mu}_{\overline{T}\,\overline{T}}\,\hat{u}^{(2)}}{\mathrm{Re}_e\,h_1\,h_3} - \frac{3\,i\,\Omega_{\mathrm{Re}}\,\hat{T}^{(1)}\,\beta_0\,h_{3,s}\,k^{(2)}\,\overline{\mu}_{\overline{T}}\,\hat{u}^{(2)}}{\mathrm{Re}_e\,h_1\,h_3^2}$$
$$+\frac{\hat{T}^{(1)}\,\alpha^{(2)}\,\beta_0\,k^{(2)}\,\overline{\mu}_{\overline{T}}\,\hat{u}^{(2)}}{\mathrm{Re}_e\,h_1\,h_3} + \frac{\hat{T}^{(1)}\,\alpha^{(1)}\,\beta_0\,k^{(2)}\,\overline{\mu}_{\overline{T}}\,\hat{u}^{(2)}}{\mathrm{Re}_e\,h_1\,h_3} - \frac{i\,\Omega_{\mathrm{Re}}\,\hat{T}_{s}^{(1)}\,\beta_0\,k^{(2)}\,\overline{\mu}_{\overline{T}}\,\hat{u}^{(2)}}{\mathrm{Re}_e\,h_1\,h_3}$$

$$-\frac{2\,i\,\Omega_{\mathrm{Re}}\,\hat{T}^{(1)}\,\beta_0\,h_{3,s}\,k^{(1)}\,\overline{\mu}_{\overline{T}}\,\hat{u}^{(2)}}{\mathrm{Re}_e\,h_1\,h_3^2}-\frac{i\,\Omega_{\mathrm{Re}}\,\hat{T}^{(1)}\,\beta_0\,h_{3,s}\,k^{(2)}\,\overline{\lambda}_{v\overline{T}}\,\hat{u}^{(2)}}{\mathrm{Re}_e\,h_1\,h_3^2}$$
$$+\frac{\hat{T}^{(1)}\,\alpha^{(2)}\,\beta_0\,k^{(2)}\,\overline{\lambda}_{v\overline{T}}\,\hat{u}^{(2)}}{\mathrm{Re}_e\,h_1\,h_3}-\frac{i\,\Omega_{\mathrm{Re}}\,\hat{T}^{(1)}\,\beta_0\,h_{3,s}\,k^{(1)}\,\overline{\lambda}_{v\overline{T}}\,\hat{u}^{(2)}}{\mathrm{Re}_e\,h_1\,h_3^2}+\frac{\hat{T}^{(1)}\,\alpha^{(2)}\,\beta_0\,k^{(1)}\,\overline{\lambda}_{v\overline{T}}\,\hat{u}^{(2)}}{\mathrm{Re}_e\,h_1\,h_3}$$
$$+\frac{i\,\hat{T}^{(1)}\,\beta_0\,k^{(2)}\,\hat{\rho}^{(2)}}{{\mathrm{M}_e}^2\,\gamma_e\,h_3}+\frac{i\,\hat{T}^{(1)}\,\beta_0\,k^{(1)}\,\hat{\rho}^{(2)}}{{\mathrm{M}_e}^2\,\gamma_e\,h_3}$$

$$\frac{\mathcal{N}^{\mathrm{quad}}(4)}{A^{(1)}\,A^{(2)}} = -\frac{\mathrm{Ec}_e\,\overline{\mu}\,\hat{w}_y^{(1)}\,\hat{w}_y^{(2)}}{\mathrm{Re}_e} + \frac{2\,\mathrm{Ec}_e\,h_{3,y}\,\overline{\mu}\,\hat{w}^{(1)}\,\hat{w}_y^{(2)}}{\mathrm{Re}_e\,h_3} - \frac{2\,\mathrm{Ec}_e\,\hat{T}^{(1)}\,\overline{\mu}_{\overline{T}}\,\overline{w}_y\,\hat{w}_y^{(2)}}{\mathrm{Re}_e}$$
$$+\frac{2\,\mathrm{Ec}_e\,\hat{T}^{(1)}\,h_{3,y}\,\overline{\mu}_{\overline{T}}\,\overline{w}\,\hat{w}_y^{(2)}}{\mathrm{Re}_e\,h_3} - \frac{2\,i\,\mathrm{Ec}_e\,\beta_0\,k^{(1)}\,\overline{\mu}\,\hat{v}^{(1)}\,\hat{w}_y^{(2)}}{\mathrm{Re}_e\,h_3} - \frac{i\,\mathrm{Ec}_e\,\Omega_{\mathrm{Re}}\,\alpha^{(1)}\,\overline{\mu}\,\hat{w}^{(1)}\,\hat{w}_s^{(2)}}{\mathrm{Re}_e\,h_1^2}$$
$$-\frac{2\,i\,\mathrm{Ec}_e\,\Omega_{\mathrm{Re}}\,\beta_0\,k^{(1)}\,\overline{\mu}\,\hat{u}^{(1)}\,\hat{w}_s^{(2)}}{\mathrm{Re}_e\,h_1\,h_3} - \frac{i\,\mathrm{Ec}_e\,\Omega_{\mathrm{Re}}\,\alpha^{(2)}\,\overline{\mu}\,\hat{w}_s^{(1)}\,\hat{w}^{(2)}}{\mathrm{Re}_e\,h_1^2} + \frac{2\,\mathrm{Ec}_e\,{\beta_0}^2\,k^{(1)}\,k^{(2)}\,\overline{\mu}\,\hat{w}^{(1)}\,\hat{w}^{(2)}}{\mathrm{Re}_e\,h_3^2}$$
$$-\frac{\mathrm{Ec}_e\,\left(h_{3,y}\right)^2\,\overline{\mu}\,\hat{w}^{(1)}\,\hat{w}^{(2)}}{\mathrm{Re}_e\,h_3^2} + \frac{2\,i\,\mathrm{Ec}_e\,\Omega_{\mathrm{Re}}\,\alpha^{(2)}\,h_{3,s}\,\overline{\mu}\,\hat{w}^{(1)}\,\hat{w}^{(2)}}{\mathrm{Re}_e\,h_1^2\,h_3} + \frac{\mathrm{Ec}_e\,\alpha^{(1)}\,\alpha^{(2)}\,\overline{\mu}\,\hat{w}^{(1)}\,\hat{w}^{(2)}}{\mathrm{Re}_e\,h_1^2}$$
$$+\frac{\mathrm{Ec}_e\,{\beta_0}^2\,k^{(1)}\,k^{(2)}\,\overline{\lambda}_v\,\hat{w}^{(1)}\,\hat{w}^{(2)}}{\mathrm{Re}_e\,h_3^2} + \frac{2\,\mathrm{Ec}_e\,\hat{T}^{(1)}\,h_{3,y}\,\overline{\mu}_{\overline{T}}\,\overline{w}_y\,\hat{w}^{(2)}}{\mathrm{Re}_e\,h_3} - \frac{2\,i\,\mathrm{Ec}_e\,\Omega_{\mathrm{Re}}\,\hat{T}^{(1)}\,\alpha^{(2)}\,\overline{\mu}_{\overline{T}}\,\overline{w}_s\,\hat{w}^{(2)}}{\mathrm{Re}_e\,h_1^2}$$
$$-\frac{2\,\mathrm{Ec}_e\,\hat{T}^{(1)}\,\left(h_{3,y}\right)^2\,\overline{\mu}_{\overline{T}}\,\overline{w}\,\hat{w}^{(2)}}{\mathrm{Re}_e\,h_3^2} + \frac{2\,i\,\mathrm{Ec}_e\,\Omega_{\mathrm{Re}}\,\hat{T}^{(1)}\,\alpha^{(2)}\,h_{3,s}\,\overline{\mu}_{\overline{T}}\,\overline{w}\,\hat{w}^{(2)}}{\mathrm{Re}_e\,h_1^2\,h_3} - \frac{2\,i\,\mathrm{Ec}_e\,\beta_0\,k^{(2)}\,\overline{\lambda}_v\,\hat{v}_y^{(1)}\,\hat{w}^{(2)}}{\mathrm{Re}_e\,h_3}$$
$$-\frac{4\,i\,\mathrm{Ec}_e\,\beta_0\,h_{3,y}\,k^{(2)}\,\overline{\mu}\,\hat{v}^{(1)}\,\hat{w}^{(2)}}{\mathrm{Re}_e\,h_3^2} + \frac{2\,i\,\mathrm{Ec}_e\,\beta_0\,h_{3,y}\,k^{(1)}\,\overline{\mu}\,\hat{v}^{(1)}\,\hat{w}^{(2)}}{\mathrm{Re}_e\,h_3^2} - \frac{2\,i\,\mathrm{Ec}_e\,\beta_0\,h_{3,y}\,k^{(2)}\,\overline{\lambda}_v\,\hat{v}^{(1)}\,\hat{w}^{(2)}}{\mathrm{Re}_e\,h_3^2}$$
$$-\frac{2\,i\,\mathrm{Ec}_e\,\beta_0\,h_{1,y}\,k^{(2)}\,\overline{\lambda}_v\,\hat{v}^{(1)}\,\hat{w}^{(2)}}{\mathrm{Re}_e\,h_1\,h_3} - \frac{2\,i\,\mathrm{Ec}_e\,\Omega_{\mathrm{Re}}\,\hat{T}^{(1)}\,\beta_0\,k^{(2)}\,\overline{\lambda}_{v\overline{T}}\,\overline{v}_y\,\hat{w}^{(2)}}{\mathrm{Re}_e\,h_3}$$
$$-\frac{4\,i\,\mathrm{Ec}_e\,\Omega_{\mathrm{Re}}\,\hat{T}^{(1)}\,\beta_0\,h_{3,y}\,k^{(2)}\,\overline{\mu}_{\overline{T}}\,\overline{v}\,\hat{w}^{(2)}}{\mathrm{Re}_e\,h_3^2} - \frac{2\,i\,\mathrm{Ec}_e\,\Omega_{\mathrm{Re}}\,\hat{T}^{(1)}\,\beta_0\,h_{3,y}\,k^{(2)}\,\overline{\lambda}_{v\overline{T}}\,\overline{v}\,\hat{w}^{(2)}}{\mathrm{Re}_e\,h_3^2}$$
$$-\frac{2\,i\,\mathrm{Ec}_e\,\Omega_{\mathrm{Re}}\,\hat{T}^{(1)}\,\beta_0\,h_{1,y}\,k^{(2)}\,\overline{\lambda}_{v\overline{T}}\,\overline{v}\,\hat{w}^{(2)}}{\mathrm{Re}_e\,h_1\,h_3} - \frac{2\,i\,\mathrm{Ec}_e\,\Omega_{\mathrm{Re}}\,\beta_0\,k^{(2)}\,\overline{\lambda}_v\,\hat{u}_s^{(1)}\,\hat{w}^{(2)}}{\mathrm{Re}_e\,h_1\,h_3}$$
$$-\frac{4\,i\,\mathrm{Ec}_e\,\Omega_{\mathrm{Re}}\,\beta_0\,h_{3,s}\,k^{(2)}\,\overline{\mu}\,\hat{u}^{(1)}\,\hat{w}^{(2)}}{\mathrm{Re}_e\,h_1\,h_3^2} + \frac{2\,i\,\mathrm{Ec}_e\,\Omega_{\mathrm{Re}}\,\beta_0\,h_{3,s}\,k^{(1)}\,\overline{\mu}\,\hat{u}^{(1)}\,\hat{w}^{(2)}}{\mathrm{Re}_e\,h_1\,h_3^2}$$
$$+\frac{2\,\mathrm{Ec}_e\,\alpha^{(2)}\,\beta_0\,k^{(1)}\,\overline{\mu}\,\hat{u}^{(1)}\,\hat{w}^{(2)}}{\mathrm{Re}_e\,h_1\,h_3} - \frac{2\,i\,\mathrm{Ec}_e\,\Omega_{\mathrm{Re}}\,\beta_0\,h_{3,s}\,k^{(2)}\,\overline{\lambda}_v\,\hat{u}^{(1)}\,\hat{w}^{(2)}}{\mathrm{Re}_e\,h_1\,h_3^2}$$
$$+\frac{2\,\mathrm{Ec}_e\,\alpha^{(1)}\,\beta_0\,k^{(2)}\,\overline{\lambda}_v\,\hat{u}^{(1)}\,\hat{w}^{(2)}}{\mathrm{Re}_e\,h_1\,h_3} - \frac{2\,i\,\mathrm{Ec}_e\,\Omega_{\mathrm{Re}}\,\hat{T}^{(1)}\,\beta_0\,k^{(2)}\,\overline{\lambda}_{v\overline{T}}\,\overline{u}_s\,\hat{w}^{(2)}}{\mathrm{Re}_e\,h_1\,h_3}$$
$$-\frac{4\,i\,\mathrm{Ec}_e\,\Omega_{\mathrm{Re}}\,\hat{T}^{(1)}\,\beta_0\,h_{3,s}\,k^{(2)}\,\overline{\mu}_{\overline{T}}\,\overline{u}\,\hat{w}^{(2)}}{\mathrm{Re}_e\,h_1\,h_3^2} - \frac{2\,i\,\mathrm{Ec}_e\,\Omega_{\mathrm{Re}}\,\hat{T}^{(1)}\,\beta_0\,h_{3,s}\,k^{(2)}\,\overline{\lambda}_{v\overline{T}}\,\overline{u}\,\hat{w}^{(2)}}{\mathrm{Re}_e\,h_1\,h_3^2}$$
$$-\frac{i\,\mathrm{Ec}_e\,\overline{T}\,\beta_0\,k^{(1)}\,\hat{\rho}^{(1)}\,\hat{w}^{(2)}}{{\mathrm{M}_e}^2\,\gamma_e\,h_3} - \frac{i\,\mathrm{Ec}_e\,\hat{T}^{(1)}\,\beta_0\,k^{(1)}\,\overline{\rho}\,\hat{w}^{(2)}}{{\mathrm{M}_e}^2\,\gamma_e\,h_3} + \frac{i\,\hat{T}^{(1)}\,\beta_0\,k^{(1)}\,\overline{\rho}\,\hat{w}^{(2)}}{h_3}$$
$$-\frac{2\,i\,\mathrm{Ec}_e\,\hat{T}^{(1)}\,\beta_0\,k^{(2)}\,\overline{\mu}_{\overline{T}}\,\hat{v}^{(2)}\,\overline{w}_y}{\mathrm{Re}_e\,h_3} - \frac{2\,i\,\mathrm{Ec}_e\,\Omega_{\mathrm{Re}}\,\hat{T}^{(1)}\,\beta_0\,k^{(2)}\,\overline{\mu}_{\overline{T}}\,\hat{u}^{(2)}\,\overline{w}_s}{\mathrm{Re}_e\,h_1\,h_3}$$
$$+\frac{2\,i\,\mathrm{Ec}_e\,\hat{T}^{(1)}\,\beta_0\,h_{3,y}\,k^{(2)}\,\overline{\mu}_{\overline{T}}\,\hat{v}^{(2)}\,\overline{w}}{\mathrm{Re}_e\,h_3^2} + \frac{2\,i\,\mathrm{Ec}_e\,\Omega_{\mathrm{Re}}\,\hat{T}^{(1)}\,\beta_0\,h_{3,s}\,k^{(2)}\,\overline{\mu}_{\overline{T}}\,\hat{u}^{(2)}\,\overline{w}}{\mathrm{Re}_e\,h_1\,h_3^2}$$

$$-\frac{i\,\mathrm{Ec}_e\,\hat{T}^{(1)}\,\beta_0\,k^{(2)}\,\hat{\rho}^{(2)}\,\overline{w}}{{\mathrm{M}_e}^2\,\gamma_e\,h_3}-\frac{i\,\mathrm{Ec}_e\,\hat{T}^{(1)}\,\beta_0\,k^{(1)}\,\hat{\rho}^{(2)}\,\overline{w}}{{\mathrm{M}_e}^2\,\gamma_e\,h_3}+\frac{i\,\hat{T}^{(1)}\,\beta_0\,k^{(1)}\,\hat{\rho}^{(2)}\,\overline{w}}{h_3}$$
$$-\frac{2\,\mathrm{Ec}_e\,\overline{\mu}\,\hat{v}_y^{(1)}\,\hat{v}_y^{(2)}}{\mathrm{Re}_e}-\frac{\mathrm{Ec}_e\,\overline{\lambda}_v\,\hat{v}_y^{(1)}\,\hat{v}_y^{(2)}}{\mathrm{Re}_e}-\frac{2\,\mathrm{Ec}_e\,h_{3,y}\,\overline{\lambda}_v\,\hat{v}^{(1)}\,\hat{v}_y^{(2)}}{\mathrm{Re}_e\,h_3}-\frac{2\,\mathrm{Ec}_e\,h_{1,y}\,\overline{\lambda}_v\,\hat{v}^{(1)}\,\hat{v}_y^{(2)}}{\mathrm{Re}_e\,h_1}$$
$$-\frac{4\,\mathrm{Ec}_e\,\Omega_{\mathrm{Re}}\,\hat{T}^{(1)}\,\overline{\mu}_{\overline{T}}\,\overline{v}_y\,\hat{v}_y^{(2)}}{\mathrm{Re}_e}-\frac{2\,\mathrm{Ec}_e\,\Omega_{\mathrm{Re}}\,\hat{T}^{(1)}\,\overline{\lambda}_{v\overline{T}}\,\overline{v}_y\,\hat{v}_y^{(2)}}{\mathrm{Re}_e}-\frac{2\,\mathrm{Ec}_e\,\Omega_{\mathrm{Re}}\,\hat{T}^{(1)}\,h_{3,y}\,\overline{\lambda}_{v\overline{T}}\,\overline{v}\,\hat{v}_y^{(2)}}{\mathrm{Re}_e\,h_3}$$
$$-\frac{2\,\mathrm{Ec}_e\,\Omega_{\mathrm{Re}}\,\hat{T}^{(1)}\,h_{1,y}\,\overline{\lambda}_{v\overline{T}}\,\overline{v}\,\hat{v}_y^{(2)}}{\mathrm{Re}_e\,h_1}-\frac{2\,\mathrm{Ec}_e\,\Omega_{\mathrm{Re}}\,\overline{\lambda}_v\,\hat{u}_s^{(1)}\,\hat{v}_y^{(2)}}{\mathrm{Re}_e\,h_1}-\frac{2\,\mathrm{Ec}_e\,\Omega_{\mathrm{Re}}\,h_{3,s}\,\overline{\lambda}_v\,\hat{u}^{(1)}\,\hat{v}_y^{(2)}}{\mathrm{Re}_e\,h_1\,h_3}$$
$$-\frac{2\,i\,\mathrm{Ec}_e\,\alpha^{(1)}\,\overline{\lambda}_v\,\hat{u}^{(1)}\,\hat{v}_y^{(2)}}{\mathrm{Re}_e\,h_1}-\frac{2\,\mathrm{Ec}_e\,\Omega_{\mathrm{Re}}\,\hat{T}^{(1)}\,\overline{\lambda}_{v\overline{T}}\,\overline{u}_s\,\hat{v}_y^{(2)}}{\mathrm{Re}_e\,h_1}-\frac{2\,\mathrm{Ec}_e\,\Omega_{\mathrm{Re}}\,\hat{T}^{(1)}\,h_{3,s}\,\overline{\lambda}_{v\overline{T}}\,\overline{u}\,\hat{v}_y^{(2)}}{\mathrm{Re}_e\,h_1\,h_3}$$
$$-\frac{i\,\mathrm{Ec}_e\,\Omega_{\mathrm{Re}}\,\alpha^{(1)}\,\overline{\mu}\,\hat{v}^{(1)}\,\hat{v}_s^{(2)}}{\mathrm{Re}_e\,h_1^2}-\frac{2\,\mathrm{Ec}_e\,\Omega_{\mathrm{Re}}\,\overline{\mu}\,\hat{u}_y^{(1)}\,\hat{v}_s^{(2)}}{\mathrm{Re}_e\,h_1}+\frac{2\,\mathrm{Ec}_e\,\Omega_{\mathrm{Re}}\,h_{1,y}\,\overline{\mu}\,\hat{u}^{(1)}\,\hat{v}_s^{(2)}}{\mathrm{Re}_e\,h_1^2}$$
$$-\frac{2\,\mathrm{Ec}_e\,\Omega_{\mathrm{Re}}\,\hat{T}^{(1)}\,\overline{\mu}_{\overline{T}}\,\overline{u}_y\,\hat{v}_s^{(2)}}{\mathrm{Re}_e\,h_1}+\frac{2\,\mathrm{Ec}_e\,\Omega_{\mathrm{Re}}\,\hat{T}^{(1)}\,h_{1,y}\,\overline{\mu}_{\overline{T}}\,\overline{u}\,\hat{v}_s^{(2)}}{\mathrm{Re}_e\,h_1^2}-\frac{i\,\mathrm{Ec}_e\,\Omega_{\mathrm{Re}}\,\alpha^{(2)}\,\overline{\mu}\,\hat{v}_s^{(1)}\,\hat{v}^{(2)}}{\mathrm{Re}_e\,h_1^2}$$
$$+\frac{\mathrm{Ec}_e\,{\beta_0}^2\,k^{(1)}\,k^{(2)}\,\overline{\mu}\,\hat{v}^{(1)}\,\hat{v}^{(2)}}{\mathrm{Re}_e\,h_3^2}-\frac{2\,\mathrm{Ec}_e\,\left(h_{3,y}\right)^2\,\overline{\mu}\,\hat{v}^{(1)}\,\hat{v}^{(2)}}{\mathrm{Re}_e\,h_3^2}-\frac{2\,\mathrm{Ec}_e\,\left(h_{1,y}\right)^2\,\overline{\mu}\,\hat{v}^{(1)}\,\hat{v}^{(2)}}{\mathrm{Re}_e\,h_1^2}$$
$$+\frac{\mathrm{Ec}_e\,\alpha^{(1)}\,\alpha^{(2)}\,\overline{\mu}\,\hat{v}^{(1)}\,\hat{v}^{(2)}}{\mathrm{Re}_e\,h_1^2}-\frac{\mathrm{Ec}_e\,\left(h_{3,y}\right)^2\,\overline{\lambda}_v\,\hat{v}^{(1)}\,\hat{v}^{(2)}}{\mathrm{Re}_e\,h_3^2}-\frac{2\,\mathrm{Ec}_e\,h_{1,y}\,h_{3,y}\,\overline{\lambda}_v\,\hat{v}^{(1)}\,\hat{v}^{(2)}}{\mathrm{Re}_e\,h_1\,h_3}$$
$$-\frac{\mathrm{Ec}_e\,\left(h_{1,y}\right)^2\,\overline{\lambda}_v\,\hat{v}^{(1)}\,\hat{v}^{(2)}}{\mathrm{Re}_e\,h_1^2}-\frac{2\,\mathrm{Ec}_e\,\Omega_{\mathrm{Re}}\,\hat{T}^{(1)}\,h_{3,y}\,\overline{\lambda}_{v\overline{T}}\,\overline{v}_y\,\hat{v}^{(2)}}{\mathrm{Re}_e\,h_3}-\frac{2\,\mathrm{Ec}_e\,\Omega_{\mathrm{Re}}\,\hat{T}^{(1)}\,h_{1,y}\,\overline{\lambda}_{v\overline{T}}\,\overline{v}_y\,\hat{v}^{(2)}}{\mathrm{Re}_e\,h_1}$$
$$-\frac{4\,\mathrm{Ec}_e\,\Omega_{\mathrm{Re}}\,\hat{T}^{(1)}\,\left(h_{3,y}\right)^2\,\overline{\mu}_{\overline{T}}\,\overline{v}\,\hat{v}^{(2)}}{\mathrm{Re}_e\,h_3^2}-\frac{4\,\mathrm{Ec}_e\,\Omega_{\mathrm{Re}}\,\hat{T}^{(1)}\,\left(h_{1,y}\right)^2\,\overline{\mu}_{\overline{T}}\,\overline{v}\,\hat{v}^{(2)}}{\mathrm{Re}_e\,h_1^2}$$
$$-\frac{2\,\mathrm{Ec}_e\,\Omega_{\mathrm{Re}}\,\hat{T}^{(1)}\,\left(h_{3,y}\right)^2\,\overline{\lambda}_{v\overline{T}}\,\overline{v}\,\hat{v}^{(2)}}{\mathrm{Re}_e\,h_3^2}-\frac{4\,\mathrm{Ec}_e\,\Omega_{\mathrm{Re}}\,\hat{T}^{(1)}\,h_{1,y}\,h_{3,y}\,\overline{\lambda}_{v\overline{T}}\,\overline{v}\,\hat{v}^{(2)}}{\mathrm{Re}_e\,h_1\,h_3}$$
$$-\frac{2\,\mathrm{Ec}_e\,\Omega_{\mathrm{Re}}\,\hat{T}^{(1)}\,\left(h_{1,y}\right)^2\,\overline{\lambda}_{v\overline{T}}\,\overline{v}\,\hat{v}^{(2)}}{\mathrm{Re}_e\,h_1^2}-\frac{2\,i\,\mathrm{Ec}_e\,\alpha^{(2)}\,\overline{\mu}\,\hat{u}_y^{(1)}\,\hat{v}^{(2)}}{\mathrm{Re}_e\,h_1}$$
$$-\frac{4\,\mathrm{Ec}_e\,\Omega_{\mathrm{Re}}\,h_{1,y}\,\overline{\mu}\,\hat{u}_s^{(1)}\,\hat{v}^{(2)}}{\mathrm{Re}_e\,h_1^2}-\frac{2\,\mathrm{Ec}_e\,\Omega_{\mathrm{Re}}\,h_{3,y}\,\overline{\lambda}_v\,\hat{u}_s^{(1)}\,\hat{v}^{(2)}}{\mathrm{Re}_e\,h_1\,h_3}-\frac{2\,\mathrm{Ec}_e\,\Omega_{\mathrm{Re}}\,h_{1,y}\,\overline{\lambda}_v\,\hat{u}_s^{(1)}\,\hat{v}^{(2)}}{\mathrm{Re}_e\,h_1^2}$$
$$-\frac{4\,\mathrm{Ec}_e\,\Omega_{\mathrm{Re}}\,h_{3,s}\,h_{3,y}\,\overline{\mu}\,\hat{u}^{(1)}\,\hat{v}^{(2)}}{\mathrm{Re}_e\,h_1\,h_3^2}+\frac{2\,i\,\mathrm{Ec}_e\,\alpha^{(2)}\,h_{1,y}\,\overline{\mu}\,\hat{u}^{(1)}\,\hat{v}^{(2)}}{\mathrm{Re}_e\,h_1^2}-\frac{4\,i\,\mathrm{Ec}_e\,\alpha^{(1)}\,h_{1,y}\,\overline{\mu}\,\hat{u}^{(1)}\,\hat{v}^{(2)}}{\mathrm{Re}_e\,h_1^2}$$
$$-\frac{2\,\mathrm{Ec}_e\,\Omega_{\mathrm{Re}}\,h_{3,s}\,h_{3,y}\,\overline{\lambda}_v\,\hat{u}^{(1)}\,\hat{v}^{(2)}}{\mathrm{Re}_e\,h_1\,h_3^2}-\frac{2\,i\,\mathrm{Ec}_e\,\alpha^{(1)}\,h_{3,y}\,\overline{\lambda}_v\,\hat{u}^{(1)}\,\hat{v}^{(2)}}{\mathrm{Re}_e\,h_1\,h_3}-\frac{2\,\mathrm{Ec}_e\,\Omega_{\mathrm{Re}}\,h_{1,y}\,h_{3,s}\,\overline{\lambda}_v\,\hat{u}^{(1)}\,\hat{v}^{(2)}}{\mathrm{Re}_e\,h_1^2\,h_3}$$
$$-\frac{2\,i\,\mathrm{Ec}_e\,\alpha^{(1)}\,h_{1,y}\,\overline{\lambda}_v\,\hat{u}^{(1)}\,\hat{v}^{(2)}}{\mathrm{Re}_e\,h_1^2}-\frac{2\,i\,\mathrm{Ec}_e\,\hat{T}^{(1)}\,\alpha^{(2)}\,\overline{\mu}_{\overline{T}}\,\overline{u}_y\,\hat{v}^{(2)}}{\mathrm{Re}_e\,h_1}-\frac{4\,\mathrm{Ec}_e\,\Omega_{\mathrm{Re}}\,\hat{T}^{(1)}\,h_{1,y}\,\overline{\mu}_{\overline{T}}\,\overline{u}_s\,\hat{v}^{(2)}}{\mathrm{Re}_e\,h_1^2}$$
$$-\frac{2\,\mathrm{Ec}_e\,\Omega_{\mathrm{Re}}\,\hat{T}^{(1)}\,h_{3,y}\,\overline{\lambda}_{v\overline{T}}\,\overline{u}_s\,\hat{v}^{(2)}}{\mathrm{Re}_e\,h_1\,h_3}-\frac{2\,\mathrm{Ec}_e\,\Omega_{\mathrm{Re}}\,\hat{T}^{(1)}\,h_{1,y}\,\overline{\lambda}_{v\overline{T}}\,\overline{u}_s\,\hat{v}^{(2)}}{\mathrm{Re}_e\,h_1^2}$$

$$-\frac{4\,\mathrm{Ec}_e\,\Omega_{\mathrm{Re}}\,\hat{T}^{(1)}\,h_{3,s}\,h_{3,y}\,\overline{\mu}_{\overline{T}}\,\overline{u}\,\hat{v}^{(2)}}{\mathrm{Re}_e\,h_1\,h_3^2}+\frac{2\,i\,\mathrm{Ec}_e\,\hat{T}^{(1)}\,\alpha^{(2)}\,h_{1,y}\,\overline{\mu}_{\overline{T}}\,\overline{u}\,\hat{v}^{(2)}}{\mathrm{Re}_e\,h_1^2}$$
$$-\frac{2\,\mathrm{Ec}_e\,\Omega_{\mathrm{Re}}\,\hat{T}^{(1)}\,h_{3,s}\,h_{3,y}\,\overline{\lambda}_{v\overline{T}}\,\overline{u}\,\hat{v}^{(2)}}{\mathrm{Re}_e\,h_1\,h_3^2}-\frac{2\,\mathrm{Ec}_e\,\Omega_{\mathrm{Re}}\,\hat{T}^{(1)}\,h_{1,y}\,h_{3,s}\,\overline{\lambda}_{v\overline{T}}\,\overline{u}\,\hat{v}^{(2)}}{\mathrm{Re}_e\,h_1^2\,h_3}$$
$$-\frac{\mathrm{Ec}_e\,\overline{T}\,\hat{\rho}_y^{(1)}\,\hat{v}^{(2)}}{{\mathrm{M}_e}^2\,\gamma_e}-\frac{\mathrm{Ec}_e\,\overline{T}_y\,\hat{\rho}^{(1)}\,\hat{v}^{(2)}}{{\mathrm{M}_e}^2\,\gamma_e}+\overline{T}_y\,\hat{\rho}^{(1)}\,\hat{v}^{(2)}-\frac{\mathrm{Ec}_e\,\hat{T}^{(1)}\,\overline{\rho}_y\,\hat{v}^{(2)}}{{\mathrm{M}_e}^2\,\gamma_e}$$
$$-\frac{\mathrm{Ec}_e\,\hat{T}_y^{(1)}\,\overline{\rho}\,\hat{v}^{(2)}}{{\mathrm{M}_e}^2\,\gamma_e}+\hat{T}_y^{(1)}\,\overline{\rho}\,\hat{v}^{(2)}-\frac{2\,i\,\mathrm{Ec}_e\,\Omega_{\mathrm{Re}}\,\hat{T}^{(1)}\,\alpha^{(2)}\,\overline{\lambda}_{v\overline{T}}\,\hat{u}^{(2)}\,\overline{v}_y}{\mathrm{Re}_e\,h_1}$$
$$-\frac{4\,i\,\mathrm{Ec}_e\,\Omega_{\mathrm{Re}}\,\hat{T}^{(1)}\,\alpha^{(2)}\,h_{1,y}\,\overline{\mu}_{\overline{T}}\,\hat{u}^{(2)}\,\overline{v}}{\mathrm{Re}_e\,h_1^2}-\frac{2\,i\,\mathrm{Ec}_e\,\Omega_{\mathrm{Re}}\,\hat{T}^{(1)}\,\alpha^{(2)}\,h_{3,y}\,\overline{\lambda}_{v\overline{T}}\,\hat{u}^{(2)}\,\overline{v}}{\mathrm{Re}_e\,h_1\,h_3}$$
$$-\frac{2\,i\,\mathrm{Ec}_e\,\Omega_{\mathrm{Re}}\,\hat{T}^{(1)}\,\alpha^{(2)}\,h_{1,y}\,\overline{\lambda}_{v\overline{T}}\,\hat{u}^{(2)}\,\overline{v}}{\mathrm{Re}_e\,h_1^2}-\frac{\mathrm{Ec}_e\,\hat{T}^{(1)}\,\hat{\rho}_y^{(2)}\,\overline{v}}{{\mathrm{M}_e}^2\,\gamma_e}-\frac{\mathrm{Ec}_e\,\hat{T}_y^{(1)}\,\hat{\rho}^{(2)}\,\overline{v}}{{\mathrm{M}_e}^2\,\gamma_e}$$
$$+\hat{T}_y^{(1)}\,\hat{\rho}^{(2)}\,\overline{v}-\frac{\mathrm{Ec}_e\,\overline{\mu}\,\hat{u}_y^{(1)}\,\hat{u}_y^{(2)}}{\mathrm{Re}_e}+\frac{2\,\mathrm{Ec}_e\,h_{1,y}\,\overline{\mu}\,\hat{u}^{(1)}\,\hat{u}_y^{(2)}}{\mathrm{Re}_e\,h_1}-\frac{2\,\mathrm{Ec}_e\,\hat{T}^{(1)}\,\overline{\mu}_{\overline{T}}\,\overline{u}_y\,\hat{u}_y^{(2)}}{\mathrm{Re}_e}$$
$$+\frac{2\,\mathrm{Ec}_e\,\hat{T}^{(1)}\,h_{1,y}\,\overline{\mu}_{\overline{T}}\,\overline{u}\,\hat{u}_y^{(2)}}{\mathrm{Re}_e\,h_1}-\frac{2\,i\,\mathrm{Ec}_e\,\Omega_{\mathrm{Re}}\,\alpha^{(1)}\,\overline{\mu}\,\hat{u}^{(1)}\,\hat{u}_s^{(2)}}{\mathrm{Re}_e\,h_1^2}-\frac{i\,\mathrm{Ec}_e\,\Omega_{\mathrm{Re}}\,\alpha^{(1)}\,\overline{\lambda}_v\,\hat{u}^{(1)}\,\hat{u}_s^{(2)}}{\mathrm{Re}_e\,h_1^2}$$
$$-\frac{2\,i\,\mathrm{Ec}_e\,\Omega_{\mathrm{Re}}\,\alpha^{(2)}\,\overline{\mu}\,\hat{u}_s^{(1)}\,\hat{u}^{(2)}}{\mathrm{Re}_e\,h_1^2}-\frac{i\,\mathrm{Ec}_e\,\Omega_{\mathrm{Re}}\,\alpha^{(2)}\,\overline{\lambda}_v\,\hat{u}_s^{(1)}\,\hat{u}^{(2)}}{\mathrm{Re}_e\,h_1^2}+\frac{\mathrm{Ec}_e\,{\beta_0}^2\,k^{(1)}\,k^{(2)}\,\overline{\mu}\,\hat{u}^{(1)}\,\hat{u}^{(2)}}{\mathrm{Re}_e\,h_3^2}$$
$$-\frac{\mathrm{Ec}_e\,\left(h_{1,y}\right)^2\,\overline{\mu}\,\hat{u}^{(1)}\,\hat{u}^{(2)}}{\mathrm{Re}_e\,h_1^2}+\frac{2\,\mathrm{Ec}_e\,\alpha^{(1)}\,\alpha^{(2)}\,\overline{\mu}\,\hat{u}^{(1)}\,\hat{u}^{(2)}}{\mathrm{Re}_e\,h_1^2}-\frac{2\,i\,\mathrm{Ec}_e\,\Omega_{\mathrm{Re}}\,\alpha^{(2)}\,h_{3,s}\,\overline{\lambda}_v\,\hat{u}^{(1)}\,\hat{u}^{(2)}}{\mathrm{Re}_e\,h_1^2\,h_3}$$
$$+\frac{\mathrm{Ec}_e\,\alpha^{(1)}\,\alpha^{(2)}\,\overline{\lambda}_v\,\hat{u}^{(1)}\,\hat{u}^{(2)}}{\mathrm{Re}_e\,h_1^2}+\frac{2\,\mathrm{Ec}_e\,\hat{T}^{(1)}\,h_{1,y}\,\overline{\mu}_{\overline{T}}\,\overline{u}_y\,\hat{u}^{(2)}}{\mathrm{Re}_e\,h_1}-\frac{4\,i\,\mathrm{Ec}_e\,\Omega_{\mathrm{Re}}\,\hat{T}^{(1)}\,\alpha^{(2)}\,\overline{\mu}_{\overline{T}}\,\overline{u}_s\,\hat{u}^{(2)}}{\mathrm{Re}_e\,h_1^2}$$
$$-\frac{2\,i\,\mathrm{Ec}_e\,\Omega_{\mathrm{Re}}\,\hat{T}^{(1)}\,\alpha^{(2)}\,\overline{\lambda}_{v\overline{T}}\,\overline{u}_s\,\hat{u}^{(2)}}{\mathrm{Re}_e\,h_1^2}-\frac{2\,\mathrm{Ec}_e\,\hat{T}^{(1)}\,\left(h_{1,y}\right)^2\,\overline{\mu}_{\overline{T}}\,\overline{u}\,\hat{u}^{(2)}}{\mathrm{Re}_e\,h_1^2}$$
$$-\frac{2\,i\,\mathrm{Ec}_e\,\Omega_{\mathrm{Re}}\,\hat{T}^{(1)}\,\alpha^{(2)}\,h_{3,s}\,\overline{\lambda}_{v\overline{T}}\,\overline{u}\,\hat{u}^{(2)}}{\mathrm{Re}_e\,h_1^2\,h_3}-\frac{\mathrm{Ec}_e\,\overline{T}\,\hat{\rho}_s^{(1)}\,\hat{u}^{(2)}}{{\mathrm{M}_e}^2\,\gamma_e\,h_1}-\frac{i\,\mathrm{Ec}_e\,\overline{T}\,\alpha^{(1)}\,\hat{\rho}^{(1)}\,\hat{u}^{(2)}}{{\mathrm{M}_e}^2\,\gamma_e\,h_1}$$
$$-\frac{\mathrm{Ec}_e\,\overline{T}_s\,\hat{\rho}^{(1)}\,\hat{u}^{(2)}}{{\mathrm{M}_e}^2\,\gamma_e\,h_1}+\frac{\overline{T}_s\,\hat{\rho}^{(1)}\,\hat{u}^{(2)}}{h_1}-\frac{\mathrm{Ec}_e\,\hat{T}^{(1)}\,\overline{\rho}_s\,\hat{u}^{(2)}}{{\mathrm{M}_e}^2\,\gamma_e\,h_1}-\frac{i\,\mathrm{Ec}_e\,\hat{T}^{(1)}\,\alpha^{(1)}\,\overline{\rho}\,\hat{u}^{(2)}}{{\mathrm{M}_e}^2\,\gamma_e\,h_1}$$
$$-\frac{\mathrm{Ec}_e\,\hat{T}_s^{(1)}\,\overline{\rho}\,\hat{u}^{(2)}}{{\mathrm{M}_e}^2\,\gamma_e\,h_1}+\frac{i\,\hat{T}^{(1)}\,\alpha^{(1)}\,\overline{\rho}\,\hat{u}^{(2)}}{h_1}+\frac{\hat{T}_s^{(1)}\,\overline{\rho}\,\hat{u}^{(2)}}{h_1}-\frac{\mathrm{Ec}_e\,\hat{T}^{(1)}\,\hat{\rho}_s^{(2)}\,\overline{u}}{{\mathrm{M}_e}^2\,\gamma_e\,h_1}$$
$$-\frac{i\,\mathrm{Ec}_e\,\hat{T}^{(1)}\,\alpha^{(2)}\,\hat{\rho}^{(2)}\,\overline{u}}{{\mathrm{M}_e}^2\,\gamma_e\,h_1}-\frac{i\,\mathrm{Ec}_e\,\hat{T}^{(1)}\,\alpha^{(1)}\,\hat{\rho}^{(2)}\,\overline{u}}{{\mathrm{M}_e}^2\,\gamma_e\,h_1}-\frac{\mathrm{Ec}_e\,\hat{T}_s^{(1)}\,\hat{\rho}^{(2)}\,\overline{u}}{{\mathrm{M}_e}^2\,\gamma_e\,h_1}+\frac{i\,\hat{T}^{(1)}\,\alpha^{(1)}\,\hat{\rho}^{(2)}\,\overline{u}}{h_1}$$
$$+\frac{\hat{T}_s^{(1)}\,\hat{\rho}^{(2)}\,\overline{u}}{h_1}+\frac{i\,\mathrm{Ec}_e\,\hat{T}^{(1)}\,n^{(2)}\,\omega_0\,\hat{\rho}^{(2)}}{{\mathrm{M}_e}^2\,\gamma_e}+\frac{i\,\mathrm{Ec}_e\,\hat{T}^{(1)}\,n^{(1)}\,\omega_0\,\hat{\rho}^{(2)}}{{\mathrm{M}_e}^2\,\gamma_e}-i\,\hat{T}^{(1)}\,n^{(1)}\,\omega_0\,\hat{\rho}^{(2)}$$
$$+\frac{\hat{T}^{(1)}\,\hat{T}^{(2)}\,{\beta_0}^2\,\overline{\kappa}_{\overline{T}}\,\left(k^{(2)}\right)^2}{\mathrm{Pr}_e\,\mathrm{Re}_e\,h_3^2}+\frac{\hat{T}^{(1)}\,\hat{T}^{(2)}\,{\beta_0}^2\,\overline{\kappa}_{\overline{T}}\,k^{(1)}\,k^{(2)}}{\mathrm{Pr}_e\,\mathrm{Re}_e\,h_3^2}-\frac{i\,\Omega_{\mathrm{Re}}\,\overline{T}_s\,\hat{T}^{(1)}\,\hat{T}^{(2)}\,\alpha^{(2)}\,\overline{\kappa}_{\overline{T}\,\overline{T}}}{\mathrm{Pr}_e\,\mathrm{Re}_e\,h_1^2}$$

$$
\begin{aligned}
&-\frac{\overline{T}_y\,\hat{T}^{(1)}\,\hat{T}_y^{(2)}\,\overline{\kappa}_{\overline{T}\,\overline{T}}}{\mathrm{Pr}_e\,\mathrm{Re}_e} - \frac{\hat{T}^{(1)}\,\hat{T}_y^{(2)}\,h_{3,y}\,\overline{\kappa}_{\overline{T}}}{\mathrm{Pr}_e\,\mathrm{Re}_e\,h_3} - \frac{i\,\Omega_{\mathrm{Re}}\,\hat{T}^{(1)}\,\hat{T}^{(2)}\,\alpha^{(2)}\,h_{3,s}\,\overline{\kappa}_{\overline{T}}}{\mathrm{Pr}_e\,\mathrm{Re}_e\,h_1^2\,h_3} \\
&-\frac{\hat{T}^{(1)}\,\hat{T}_y^{(2)}\,h_{1,y}\,\overline{\kappa}_{\overline{T}}}{\mathrm{Pr}_e\,\mathrm{Re}_e\,h_1} + \frac{i\,\Omega_{\mathrm{Re}}\,\hat{T}^{(1)}\,\hat{T}^{(2)}\,\alpha^{(2)}\,h_{1,s}\,\overline{\kappa}_{\overline{T}}}{\mathrm{Pr}_e\,\mathrm{Re}_e\,h_1^3} - \frac{i\,\Omega_{\mathrm{Re}}\,\hat{T}^{(1)}\,\hat{T}^{(2)}\,\alpha_s^{(2)}\,\overline{\kappa}_{\overline{T}}}{\mathrm{Pr}_e\,\mathrm{Re}_e\,h_1^2} \\
&+\frac{\hat{T}^{(1)}\,\hat{T}^{(2)}\,\left(\alpha^{(2)}\right)^2\,\overline{\kappa}_{\overline{T}}}{\mathrm{Pr}_e\,\mathrm{Re}_e\,h_1^2} + \frac{\hat{T}^{(1)}\,\hat{T}^{(2)}\,\alpha^{(1)}\,\alpha^{(2)}\,\overline{\kappa}_{\overline{T}}}{\mathrm{Pr}_e\,\mathrm{Re}_e\,h_1^2} - \frac{2\,i\,\Omega_{\mathrm{Re}}\,\hat{T}^{(1)}\,\hat{T}_s^{(2)}\,\alpha^{(2)}\,\overline{\kappa}_{\overline{T}}}{\mathrm{Pr}_e\,\mathrm{Re}_e\,h_1^2} \\
&-\frac{i\,\Omega_{\mathrm{Re}}\,\hat{T}_s^{(1)}\,\hat{T}^{(2)}\,\alpha^{(2)}\,\overline{\kappa}_{\overline{T}}}{\mathrm{Pr}_e\,\mathrm{Re}_e\,h_1^2} - \frac{i\,\Omega_{\mathrm{Re}}\,\hat{T}^{(1)}\,\hat{T}_s^{(2)}\,\alpha^{(1)}\,\overline{\kappa}_{\overline{T}}}{\mathrm{Pr}_e\,\mathrm{Re}_e\,h_1^2} - \frac{\hat{T}^{(1)}\,\hat{T}_{y\,y}^{(2)}\,\overline{\kappa}_{\overline{T}}}{\mathrm{Pr}_e\,\mathrm{Re}_e} - \frac{\hat{T}_y^{(1)}\,\hat{T}_y^{(2)}\,\overline{\kappa}_{\overline{T}}}{\mathrm{Pr}_e\,\mathrm{Re}_e}
\end{aligned}
$$

$$\frac{\mathcal{N}^{\mathrm{quad}}(5)}{A^{(1)}\,A^{(2)}} = \frac{i\,\beta_0\,k^{(2)}\,\hat{\rho}^{(1)}\,\hat{w}^{(2)}}{h_3} + \frac{i\,\beta_0\,k^{(1)}\,\hat{\rho}^{(1)}\,\hat{w}^{(2)}}{h_3} + \hat{\rho}^{(1)}\,\hat{v}_y^{(2)} + \hat{\rho}_y^{(1)}\,\hat{v}^{(2)} + \frac{h_{3,y}\,\hat{\rho}^{(1)}\,\hat{v}^{(2)}}{h_3}$$
$$+\frac{h_{1,y}\,\hat{\rho}^{(1)}\,\hat{v}^{(2)}}{h_1} + \frac{\hat{\rho}^{(1)}\,\hat{u}_s^{(2)}}{h_1} + \frac{\hat{\rho}_s^{(1)}\,\hat{u}^{(2)}}{h_1} + \frac{h_{3,s}\,\hat{\rho}^{(1)}\,\hat{u}^{(2)}}{h_1\,h_3} + \frac{i\,\alpha^{(2)}\,\hat{\rho}^{(1)}\,\hat{u}^{(2)}}{h_1} + \frac{i\,\alpha^{(1)}\,\hat{\rho}^{(1)}\,\hat{u}^{(2)}}{h_1}$$

C.7 Cubic Nonlinear Forcing Vector

$$\frac{\mathcal{N}^{\mathrm{cub}}(1)}{A^{(1)}\,A^{(2)}\,A^{(3)}} = -\frac{h_{3,s}\,\hat{\rho}^{(1)}\,\hat{w}^{(2)}\,\hat{w}^{(3)}}{h_1\,h_3} + \frac{i\,\beta_0\,k^{(2)}\,\hat{\rho}^{(1)}\,\hat{u}^{(2)}\,\hat{w}^{(3)}}{h_3} + \hat{\rho}^{(1)}\,\hat{u}_y^{(2)}\,\hat{v}^{(3)} + \frac{h_{1,y}\,\hat{\rho}^{(1)}\,\hat{u}^{(2)}\,\hat{v}^{(3)}}{h_1} + \frac{\hat{\rho}^{(1)}\,\hat{u}^{(2)}\,\hat{u}_s^{(3)}}{h_1} + \frac{i\,\alpha^{(3)}\,\hat{\rho}^{(1)}\,\hat{u}^{(2)}\,\hat{u}^{(3)}}{h_1}$$

$$\frac{\mathcal{N}^{\mathrm{cub}}(2)}{A^{(1)}\,A^{(2)}\,A^{(3)}} = -\frac{h_{3,y}\,\hat{\rho}^{(1)}\,\hat{w}^{(2)}\,\hat{w}^{(3)}}{h_3} + \frac{i\,\beta_0\,k^{(2)}\,\hat{\rho}^{(1)}\,\hat{v}^{(2)}\,\hat{w}^{(3)}}{h_3} + \hat{\rho}^{(1)}\,\hat{v}^{(2)}\,\hat{v}_y^{(3)} + \frac{\hat{\rho}^{(1)}\,\hat{u}^{(2)}\,\hat{v}_s^{(3)}}{h_1} + \frac{i\,\alpha^{(3)}\,\hat{\rho}^{(1)}\,\hat{u}^{(2)}\,\hat{v}^{(3)}}{h_1} - \frac{h_{1,y}\,\hat{\rho}^{(1)}\,\hat{u}^{(2)}\,\hat{u}^{(3)}}{h_1}$$

$$\frac{\mathcal{N}^{\mathrm{cub}}(3)}{A^{(1)}\,A^{(2)}\,A^{(3)}} = \hat{\rho}^{(1)}\,\hat{v}^{(2)}\,\hat{w}_y^{(3)} + \frac{\hat{\rho}^{(1)}\,\hat{u}^{(2)}\,\hat{w}_s^{(3)}}{h_1} + \frac{i\,\beta_0\,k^{(3)}\,\hat{\rho}^{(1)}\,\hat{w}^{(2)}\,\hat{w}^{(3)}}{h_3} + \frac{h_{3,y}\,\hat{\rho}^{(1)}\,\hat{v}^{(2)}\,\hat{w}^{(3)}}{h_3} + \frac{h_{3,s}\,\hat{\rho}^{(1)}\,\hat{u}^{(2)}\,\hat{w}^{(3)}}{h_1\,h_3} + \frac{i\,\alpha^{(3)}\,\hat{\rho}^{(1)}\,\hat{u}^{(2)}\,\hat{w}^{(3)}}{h_1}$$

$$
\begin{aligned}
\frac{\mathcal{N}^{\mathrm{cub}}(4)}{A^{(1)}\,A^{(2)}\,A^{(3)}} &= -\frac{\mathrm{Ec}_e\,\hat{T}^{(1)}\,\overline{\mu}_{\overline{T}}\,\hat{w}_y^{(2)}\,\hat{w}_y^{(3)}}{\mathrm{Re}_e} \\
&+\frac{2\,\mathrm{Ec}_e\,\hat{T}^{(1)}\,h_{3,y}\,\overline{\mu}_{\overline{T}}\,\hat{w}^{(2)}\,\hat{w}_y^{(3)}}{\mathrm{Re}_e\,h_3} - \frac{2\,i\,\mathrm{Ec}_e\,\hat{T}^{(1)}\,\beta_0\,k^{(2)}\,\overline{\mu}_{\overline{T}}\,\hat{v}^{(2)}\,\hat{w}_y^{(3)}}{\mathrm{Re}_e\,h_3} \\
&-\frac{i\,\mathrm{Ec}_e\,\Omega_{\mathrm{Re}}\,\hat{T}^{(1)}\,\alpha^{(2)}\,\overline{\mu}_{\overline{T}}\,\hat{w}^{(2)}\,\hat{w}_s^{(3)}}{\mathrm{Re}_e\,h_1^2} - \frac{2\,i\,\mathrm{Ec}_e\,\Omega_{\mathrm{Re}}\,\hat{T}^{(1)}\,\beta_0\,k^{(2)}\,\overline{\mu}_{\overline{T}}\,\hat{u}^{(2)}\,\hat{w}_s^{(3)}}{\mathrm{Re}_e\,h_1\,h_3} \\
&-\frac{i\,\mathrm{Ec}_e\,\Omega_{\mathrm{Re}}\,\hat{T}^{(1)}\,\alpha^{(3)}\,\overline{\mu}_{\overline{T}}\,\hat{w}_s^{(2)}\,\hat{w}^{(3)}}{\mathrm{Re}_e\,h_1^2} + \frac{2\,\mathrm{Ec}_e\,\hat{T}^{(1)}\,{\beta_0}^2\,k^{(2)}\,k^{(3)}\,\overline{\mu}_{\overline{T}}\,\hat{w}^{(2)}\,\hat{w}^{(3)}}{\mathrm{Re}_e\,h_3^2} \\
&-\frac{\mathrm{Ec}_e\,\hat{T}^{(1)}\,\left(h_{3,y}\right)^2\,\overline{\mu}_{\overline{T}}\,\hat{w}^{(2)}\,\hat{w}^{(3)}}{\mathrm{Re}_e\,h_3^2} + \frac{2\,i\,\mathrm{Ec}_e\,\Omega_{\mathrm{Re}}\,\hat{T}^{(1)}\,\alpha^{(3)}\,h_{3,s}\,\overline{\mu}_{\overline{T}}\,\hat{w}^{(2)}\,\hat{w}^{(3)}}{\mathrm{Re}_e\,h_1^2\,h_3} \\
&+\frac{\mathrm{Ec}_e\,\hat{T}^{(1)}\,\alpha^{(2)}\,\alpha^{(3)}\,\overline{\mu}_{\overline{T}}\,\hat{w}^{(2)}\,\hat{w}^{(3)}}{\mathrm{Re}_e\,h_1^2} + \frac{\mathrm{Ec}_e\,\hat{T}^{(1)}\,{\beta_0}^2\,k^{(2)}\,k^{(3)}\,\overline{\lambda}_{v\overline{T}}\,\hat{w}^{(2)}\,\hat{w}^{(3)}}{\mathrm{Re}_e\,h_3^2} \\
&-\frac{2\,i\,\mathrm{Ec}_e\,\hat{T}^{(1)}\,\beta_0\,k^{(3)}\,\overline{\lambda}_{v\overline{T}}\,\hat{v}_y^{(2)}\,\hat{w}^{(3)}}{\mathrm{Re}_e\,h_3} - \frac{4\,i\,\mathrm{Ec}_e\,\hat{T}^{(1)}\,\beta_0\,h_{3,y}\,k^{(3)}\,\overline{\mu}_{\overline{T}}\,\hat{v}^{(2)}\,\hat{w}^{(3)}}{\mathrm{Re}_e\,h_3^2} \\
&+\frac{2\,i\,\mathrm{Ec}_e\,\hat{T}^{(1)}\,\beta_0\,h_{3,y}\,k^{(2)}\,\overline{\mu}_{\overline{T}}\,\hat{v}^{(2)}\,\hat{w}^{(3)}}{\mathrm{Re}_e\,h_3^2} - \frac{2\,i\,\mathrm{Ec}_e\,\hat{T}^{(1)}\,\beta_0\,h_{3,y}\,k^{(3)}\,\overline{\lambda}_{v\overline{T}}\,\hat{v}^{(2)}\,\hat{w}^{(3)}}{\mathrm{Re}_e\,h_3^2} \\
&-\frac{2\,i\,\mathrm{Ec}_e\,\hat{T}^{(1)}\,\beta_0\,h_{1,y}\,k^{(3)}\,\overline{\lambda}_{v\overline{T}}\,\hat{v}^{(2)}\,\hat{w}^{(3)}}{\mathrm{Re}_e\,h_1\,h_3} - \frac{2\,i\,\mathrm{Ec}_e\,\Omega_{\mathrm{Re}}\,\hat{T}^{(1)}\,\beta_0\,k^{(3)}\,\overline{\lambda}_{v\overline{T}}\,\hat{u}_s^{(2)}\,\hat{w}^{(3)}}{\mathrm{Re}_e\,h_1\,h_3} \\
&-\frac{4\,i\,\mathrm{Ec}_e\,\Omega_{\mathrm{Re}}\,\hat{T}^{(1)}\,\beta_0\,h_{3,s}\,k^{(3)}\,\overline{\mu}_{\overline{T}}\,\hat{u}^{(2)}\,\hat{w}^{(3)}}{\mathrm{Re}_e\,h_1\,h_3^2} + \frac{2\,i\,\mathrm{Ec}_e\,\Omega_{\mathrm{Re}}\,\hat{T}^{(1)}\,\beta_0\,h_{3,s}\,k^{(2)}\,\overline{\mu}_{\overline{T}}\,\hat{u}^{(2)}\,\hat{w}^{(3)}}{\mathrm{Re}_e\,h_1\,h_3^2} \\
&+\frac{2\,\mathrm{Ec}_e\,\hat{T}^{(1)}\,\alpha^{(3)}\,\beta_0\,k^{(2)}\,\overline{\mu}_{\overline{T}}\,\hat{u}^{(2)}\,\hat{w}^{(3)}}{\mathrm{Re}_e\,h_1\,h_3} - \frac{2\,i\,\mathrm{Ec}_e\,\Omega_{\mathrm{Re}}\,\hat{T}^{(1)}\,\beta_0\,h_{3,s}\,k^{(3)}\,\overline{\lambda}_{v\overline{T}}\,\hat{u}^{(2)}\,\hat{w}^{(3)}}{\mathrm{Re}_e\,h_1\,h_3^2} \\
&+\frac{2\,\mathrm{Ec}_e\,\hat{T}^{(1)}\,\alpha^{(2)}\,\beta_0\,k^{(3)}\,\overline{\lambda}_{v\overline{T}}\,\hat{u}^{(2)}\,\hat{w}^{(3)}}{\mathrm{Re}_e\,h_1\,h_3} - \frac{i\,\mathrm{Ec}_e\,\hat{T}^{(1)}\,\beta_0\,k^{(2)}\,\hat{\rho}^{(2)}\,\hat{w}^{(3)}}{{\mathrm{M}_e}^2\,\gamma_e\,h_3} \\
&-\frac{i\,\mathrm{Ec}_e\,\hat{T}^{(1)}\,\beta_0\,k^{(1)}\,\hat{\rho}^{(2)}\,\hat{w}^{(3)}}{{\mathrm{M}_e}^2\,\gamma_e\,h_3} + \frac{i\,\hat{T}^{(1)}\,\beta_0\,k^{(1)}\,\hat{\rho}^{(2)}\,\hat{w}^{(3)}}{h_3} - \frac{2\,\mathrm{Ec}_e\,\hat{T}^{(1)}\,\overline{\mu}_{\overline{T}}\,\hat{v}_y^{(2)}\,\hat{v}_y^{(3)}}{\mathrm{Re}_e} \\
&-\frac{\mathrm{Ec}_e\,\hat{T}^{(1)}\,\overline{\lambda}_{v\overline{T}}\,\hat{v}_y^{(2)}\,\hat{v}_y^{(3)}}{\mathrm{Re}_e} - \frac{2\,\mathrm{Ec}_e\,\hat{T}^{(1)}\,h_{3,y}\,\overline{\lambda}_{v\overline{T}}\,\hat{v}^{(2)}\,\hat{v}_y^{(3)}}{\mathrm{Re}_e\,h_3} - \frac{2\,\mathrm{Ec}_e\,\hat{T}^{(1)}\,h_{1,y}\,\overline{\lambda}_{v\overline{T}}\,\hat{v}^{(2)}\,\hat{v}_y^{(3)}}{\mathrm{Re}_e\,h_1} \\
&-\frac{2\,\mathrm{Ec}_e\,\Omega_{\mathrm{Re}}\,\hat{T}^{(1)}\,\overline{\lambda}_{v\overline{T}}\,\hat{u}_s^{(2)}\,\hat{v}_y^{(3)}}{\mathrm{Re}_e\,h_1} - \frac{2\,\mathrm{Ec}_e\,\Omega_{\mathrm{Re}}\,\hat{T}^{(1)}\,h_{3,s}\,\overline{\lambda}_{v\overline{T}}\,\hat{u}^{(2)}\,\hat{v}_y^{(3)}}{\mathrm{Re}_e\,h_1\,h_3} \\
&-\frac{2\,i\,\mathrm{Ec}_e\,\hat{T}^{(1)}\,\alpha^{(2)}\,\overline{\lambda}_{v\overline{T}}\,\hat{u}^{(2)}\,\hat{v}_y^{(3)}}{\mathrm{Re}_e\,h_1} - \frac{i\,\mathrm{Ec}_e\,\Omega_{\mathrm{Re}}\,\hat{T}^{(1)}\,\alpha^{(2)}\,\overline{\mu}_{\overline{T}}\,\hat{v}^{(2)}\,\hat{v}_s^{(3)}}{\mathrm{Re}_e\,h_1^2} \\
&-\frac{2\,\mathrm{Ec}_e\,\Omega_{\mathrm{Re}}\,\hat{T}^{(1)}\,\overline{\mu}_{\overline{T}}\,\hat{u}_y^{(2)}\,\hat{v}_s^{(3)}}{\mathrm{Re}_e\,h_1} + \frac{2\,\mathrm{Ec}_e\,\Omega_{\mathrm{Re}}\,\hat{T}^{(1)}\,h_{1,y}\,\overline{\mu}_{\overline{T}}\,\hat{u}^{(2)}\,\hat{v}_s^{(3)}}{\mathrm{Re}_e\,h_1^2} - \frac{i\,\mathrm{Ec}_e\,\Omega_{\mathrm{Re}}\,\hat{T}^{(1)}\,\alpha^{(3)}\,\overline{\mu}_{\overline{T}}\,\hat{v}_s^{(2)}\,\hat{v}^{(3)}}{\mathrm{Re}_e\,h_1^2}
\end{aligned}
$$

$$+\frac{\mathrm{Ec}_e\,\hat{T}^{(1)}\,{\beta_0}^2\,k^{(2)}\,k^{(3)}\,\overline{\mu}_{\overline{T}}\,\hat{v}^{(2)}\,\hat{v}^{(3)}}{\mathrm{Re}_e\,h_3^2}-\frac{2\,\mathrm{Ec}_e\,\hat{T}^{(1)}\,\left(h_{3,y}\right)^2\,\overline{\mu}_{\overline{T}}\,\hat{v}^{(2)}\,\hat{v}^{(3)}}{\mathrm{Re}_e\,h_3^2}$$
$$-\frac{2\,\mathrm{Ec}_e\,\hat{T}^{(1)}\,\left(h_{1,y}\right)^2\,\overline{\mu}_{\overline{T}}\,\hat{v}^{(2)}\,\hat{v}^{(3)}}{\mathrm{Re}_e\,h_1^2}+\frac{\mathrm{Ec}_e\,\hat{T}^{(1)}\,\alpha^{(2)}\,\alpha^{(3)}\,\overline{\mu}_{\overline{T}}\,\hat{v}^{(2)}\,\hat{v}^{(3)}}{\mathrm{Re}_e\,h_1^2}$$
$$-\frac{\mathrm{Ec}_e\,\hat{T}^{(1)}\,\left(h_{3,y}\right)^2\,\overline{\lambda}_{v\overline{T}}\,\hat{v}^{(2)}\,\hat{v}^{(3)}}{\mathrm{Re}_e\,h_3^2}-\frac{2\,\mathrm{Ec}_e\,\hat{T}^{(1)}\,h_{1,y}\,h_{3,y}\,\overline{\lambda}_{v\overline{T}}\,\hat{v}^{(2)}\,\hat{v}^{(3)}}{\mathrm{Re}_e\,h_1\,h_3}$$
$$-\frac{\mathrm{Ec}_e\,\hat{T}^{(1)}\,\left(h_{1,y}\right)^2\,\overline{\lambda}_{v\overline{T}}\,\hat{v}^{(2)}\,\hat{v}^{(3)}}{\mathrm{Re}_e\,h_1^2}-\frac{2\,i\,\mathrm{Ec}_e\,\hat{T}^{(1)}\,\alpha^{(3)}\,\overline{\mu}_{\overline{T}}\,\hat{u}_y^{(2)}\,\hat{v}^{(3)}}{\mathrm{Re}_e\,h_1}$$
$$-\frac{4\,\mathrm{Ec}_e\,\Omega_{\mathrm{Re}}\,\hat{T}^{(1)}\,h_{1,y}\,\overline{\mu}_{\overline{T}}\,\hat{u}_s^{(2)}\,\hat{v}^{(3)}}{\mathrm{Re}_e\,h_1^2}-\frac{2\,\mathrm{Ec}_e\,\Omega_{\mathrm{Re}}\,\hat{T}^{(1)}\,h_{3,y}\,\overline{\lambda}_{v\overline{T}}\,\hat{u}_s^{(2)}\,\hat{v}^{(3)}}{\mathrm{Re}_e\,h_1\,h_3}$$
$$-\frac{2\,\mathrm{Ec}_e\,\Omega_{\mathrm{Re}}\,\hat{T}^{(1)}\,h_{1,y}\,\overline{\lambda}_{v\overline{T}}\,\hat{u}_s^{(2)}\,\hat{v}^{(3)}}{\mathrm{Re}_e\,h_1^2}-\frac{4\,\mathrm{Ec}_e\,\Omega_{\mathrm{Re}}\,\hat{T}^{(1)}\,h_{3,s}\,h_{3,y}\,\overline{\mu}_{\overline{T}}\,\hat{u}^{(2)}\,\hat{v}^{(3)}}{\mathrm{Re}_e\,h_1\,h_3^2}$$
$$+\frac{2\,i\,\mathrm{Ec}_e\,\hat{T}^{(1)}\,\alpha^{(3)}\,h_{1,y}\,\overline{\mu}_{\overline{T}}\,\hat{u}^{(2)}\,\hat{v}^{(3)}}{\mathrm{Re}_e\,h_1^2}-\frac{4\,i\,\mathrm{Ec}_e\,\hat{T}^{(1)}\,\alpha^{(2)}\,h_{1,y}\,\overline{\mu}_{\overline{T}}\,\hat{u}^{(2)}\,\hat{v}^{(3)}}{\mathrm{Re}_e\,h_1^2}$$
$$-\frac{2\,\mathrm{Ec}_e\,\Omega_{\mathrm{Re}}\,\hat{T}^{(1)}\,h_{3,s}\,h_{3,y}\,\overline{\lambda}_{v\overline{T}}\,\hat{u}^{(2)}\,\hat{v}^{(3)}}{\mathrm{Re}_e\,h_1\,h_3^2}-\frac{2\,i\,\mathrm{Ec}_e\,\hat{T}^{(1)}\,\alpha^{(2)}\,h_{3,y}\,\overline{\lambda}_{v\overline{T}}\,\hat{u}^{(2)}\,\hat{v}^{(3)}}{\mathrm{Re}_e\,h_1\,h_3}$$
$$-\frac{2\,\mathrm{Ec}_e\,\Omega_{\mathrm{Re}}\,\hat{T}^{(1)}\,h_{1,y}\,h_{3,s}\,\overline{\lambda}_{v\overline{T}}\,\hat{u}^{(2)}\,\hat{v}^{(3)}}{\mathrm{Re}_e\,h_1^2\,h_3}-\frac{2\,i\,\mathrm{Ec}_e\,\hat{T}^{(1)}\,\alpha^{(2)}\,h_{1,y}\,\overline{\lambda}_{v\overline{T}}\,\hat{u}^{(2)}\,\hat{v}^{(3)}}{\mathrm{Re}_e\,h_1^2}$$
$$-\frac{\mathrm{Ec}_e\,\hat{T}^{(1)}\,\hat{\rho}_y^{(2)}\,\hat{v}^{(3)}}{{\mathrm{M}_e}^2\,\gamma_e}-\frac{\mathrm{Ec}_e\,\hat{T}_y^{(1)}\,\hat{\rho}^{(2)}\,\hat{v}^{(3)}}{{\mathrm{M}_e}^2\,\gamma_e}+\hat{T}_y^{(1)}\,\hat{\rho}^{(2)}\,\hat{v}^{(3)}-\frac{\mathrm{Ec}_e\,\hat{T}^{(1)}\,\overline{\mu}_{\overline{T}}\,\hat{u}_y^{(2)}\,\hat{u}_y^{(3)}}{\mathrm{Re}_e}$$
$$+\frac{2\,\mathrm{Ec}_e\,\hat{T}^{(1)}\,h_{1,y}\,\overline{\mu}_{\overline{T}}\,\hat{u}^{(2)}\,\hat{u}_y^{(3)}}{\mathrm{Re}_e\,h_1}-\frac{2\,i\,\mathrm{Ec}_e\,\Omega_{\mathrm{Re}}\,\hat{T}^{(1)}\,\alpha^{(2)}\,\overline{\mu}_{\overline{T}}\,\hat{u}^{(2)}\,\hat{u}_s^{(3)}}{\mathrm{Re}_e\,h_1^2}$$
$$-\frac{i\,\mathrm{Ec}_e\,\Omega_{\mathrm{Re}}\,\hat{T}^{(1)}\,\alpha^{(2)}\,\overline{\lambda}_{v\overline{T}}\,\hat{u}^{(2)}\,\hat{u}_s^{(3)}}{\mathrm{Re}_e\,h_1^2}-\frac{2\,i\,\mathrm{Ec}_e\,\Omega_{\mathrm{Re}}\,\hat{T}^{(1)}\,\alpha^{(3)}\,\overline{\mu}_{\overline{T}}\,\hat{u}_s^{(2)}\,\hat{u}^{(3)}}{\mathrm{Re}_e\,h_1^2}$$
$$-\frac{i\,\mathrm{Ec}_e\,\Omega_{\mathrm{Re}}\,\hat{T}^{(1)}\,\alpha^{(3)}\,\overline{\lambda}_{v\overline{T}}\,\hat{u}_s^{(2)}\,\hat{u}^{(3)}}{\mathrm{Re}_e\,h_1^2}+\frac{\mathrm{Ec}_e\,\hat{T}^{(1)}\,{\beta_0}^2\,k^{(2)}\,k^{(3)}\,\overline{\mu}_{\overline{T}}\,\hat{u}^{(2)}\,\hat{u}^{(3)}}{\mathrm{Re}_e\,h_3^2}$$
$$-\frac{\mathrm{Ec}_e\,\hat{T}^{(1)}\,\left(h_{1,y}\right)^2\,\overline{\mu}_{\overline{T}}\,\hat{u}^{(2)}\,\hat{u}^{(3)}}{\mathrm{Re}_e\,h_1^2}+\frac{2\,\mathrm{Ec}_e\,\hat{T}^{(1)}\,\alpha^{(2)}\,\alpha^{(3)}\,\overline{\mu}_{\overline{T}}\,\hat{u}^{(2)}\,\hat{u}^{(3)}}{\mathrm{Re}_e\,h_1^2}$$
$$-\frac{2\,i\,\mathrm{Ec}_e\,\Omega_{\mathrm{Re}}\,\hat{T}^{(1)}\,\alpha^{(3)}\,h_{3,s}\,\overline{\lambda}_{v\overline{T}}\,\hat{u}^{(2)}\,\hat{u}^{(3)}}{\mathrm{Re}_e\,h_1^2\,h_3}+\frac{\mathrm{Ec}_e\,\hat{T}^{(1)}\,\alpha^{(2)}\,\alpha^{(3)}\,\overline{\lambda}_{v\overline{T}}\,\hat{u}^{(2)}\,\hat{u}^{(3)}}{\mathrm{Re}_e\,h_1^2}$$
$$-\frac{\mathrm{Ec}_e\,\hat{T}^{(1)}\,\hat{\rho}_s^{(2)}\,\hat{u}^{(3)}}{{\mathrm{M}_e}^2\,\gamma_e\,h_1}-\frac{i\,\mathrm{Ec}_e\,\hat{T}^{(1)}\,\alpha^{(2)}\,\hat{\rho}^{(2)}\,\hat{u}^{(3)}}{{\mathrm{M}_e}^2\,\gamma_e\,h_1}-\frac{i\,\mathrm{Ec}_e\,\hat{T}^{(1)}\,\alpha^{(1)}\,\hat{\rho}^{(2)}\,\hat{u}^{(3)}}{{\mathrm{M}_e}^2\,\gamma_e\,h_1}-\frac{\mathrm{Ec}_e\,\hat{T}_s^{(1)}\,\hat{\rho}^{(2)}\,\hat{u}^{(3)}}{{\mathrm{M}_e}^2\,\gamma_e\,h_1}$$
$$+\frac{i\,\hat{T}^{(1)}\,\alpha^{(1)}\,\hat{\rho}^{(2)}\,\hat{u}^{(3)}}{h_1}+\frac{\hat{T}_s^{(1)}\,\hat{\rho}^{(2)}\,\hat{u}^{(3)}}{h_1}$$

$$\frac{\mathcal{N}^{\mathrm{cub}}(5)}{A^{(1)}\,A^{(2)}\,A^{(3)}} = 0$$